

**Elucidating the structure function relationship of dietary plant  
flavonoids on adipogenesis.**

Thesis submitted to the University of Staffordshire for the degree of Doctor of Philosophy  
February 2023

# List of Contents

<b>Declaration</b> .....	<b>viii</b>
<b>Acknowledgements</b> .....	<b>viii</b>
<b>Dedication:</b> .....	<b>viii</b>
<b>Abstract</b> .....	<b>ix</b>
<b>List of tables</b> .....	<b>xi</b>
<b>List of figures</b> .....	<b>xi</b>
<b>List of abbreviations</b> .....	<b>xiv</b>
<b>1 Introduction</b> .....	<b>1</b>
1.1 A global health pandemic .....	1
1.2 Defining obesity .....	3
1.3 Adipocytes.....	5
1.3.1 White adipocytes .....	6
1.3.2 Brown adipocytes.....	7
1.3.3 Beige (brite) adipocytes .....	8
1.3.4 Adipocyte proliferation and differentiation.....	9
1.4 Preadipocyte models .....	10
1.5 Mediterranean paradox.....	11
1.6 Flavonoids: .....	13
1.7 Aims and objectives of the study.....	15
1.7.1 Specific objectives:.....	16
1.7.2 Hypothesis.....	16
<b>2 General methods</b> .....	<b>17</b>
2.1 Cell culture .....	17
2.1.1 Materials and equipment.....	17
2.1.2 SGBS Cell culture .....	19
2.1.3 Cryopreserving SGBS cells.....	19
2.1.4 Thawing SGBS cells from cryopreservation .....	20
2.1.5 Cell counting .....	20
2.1.6 Trypan blue cell viability counts.....	20
2.1.7 Differentiation of SGBS cells .....	21
2.1.8 Dedifferentiation of SGBS cells .....	21
2.1.9 Differential cell counts .....	22
2.1.10 3-(4,5-dimethylthiazol-2-yl)-2,5-diphenyltetrazolium bromide (MTT) Assay.....	22

2.2	HPLC .....	22
2.3	Oil red “O” staining for lipid quantification. ....	22
2.4	Triglycerides extraction quantification .....	24
2.4.1.	Triglycerides extraction.....	24
2.4.2.	Triglycerides quantification.....	24
2.5	Protein harvesting, purification, and quantification.....	24
2.6	Western Blotting .....	25
2.7	RNA harvesting, extraction, purification and quantification. ....	25
2.8	Conversion of RNA to cDNA .....	26
2.9	qPCR .....	26
2.10	Statistical analysis .....	27
<b>3</b>	<b>Adipocyte Proliferation.....</b>	<b>28</b>
3.1	Introduction .....	28
3.1.1	Aim .....	32
3.1.2	Objectives.....	33
3.2	Method .....	33
3.2.1	Cell culture .....	33
3.2.2	MTT assays .....	33
3.2.3	Solvent Choice.....	34
3.2.4	Growth Curves .....	34
3.2.5	Microscopic counts .....	35
3.2.6	Single flavonoid treatment .....	35
3.2.7	Combined flavonoid treatment .....	36
3.2.8	Comparative treatments with 3T3-L1 cells.....	37
3.2.9	Statistical analysis .....	37
3.3	Results.....	38
3.3.1	Standard curves .....	38
3.3.2	Choice of flavonoid solvent.....	39
3.3.3	Correlation between MTT assays and microscopic counts.....	41
3.3.4	Single flavonoid treatments.....	42
3.3.5	Combined flavonoid treatments.....	47
3.3.6	Comparative 3T3-L1 flavonoid treated cells .....	53
3.3.7	Cell recovery after treatment .....	53
3.4	Discussion.....	55
3.4.1	Main findings.....	55
3.4.2	MTT assays and microscopic counts .....	55

3.4.3	Single flavonoid treatments.....	56
3.4.4	Flavonoid combinations.....	59
3.4.5	Bioavailability.....	60
3.5	Conclusion.....	61
<b>4</b>	<b>Adipocyte Differentiation .....</b>	<b>63</b>
4.1	Introduction .....	63
4.1.1	Aim .....	66
4.1.2	Objectives.....	66
4.2	Methods.....	66
4.2.1	SGBS cell culture .....	66
4.2.2	3T3-L1 cell culture.....	67
4.2.3	Flavonoid treatment .....	68
4.2.4	Microscopic counts .....	69
4.2.5	Oil red O staining for lipid quantification.....	70
4.2.6	Triglycerides extraction and quantification .....	71
4.2.7	Statistical analysis .....	72
4.3	Results.....	72
4.3.1	Qualitative analysis .....	72
4.3.2	Differentiation proof of concept and quality assurance.....	76
4.3.3	Comparison of flavonoid treatments on rate of differentiation.....	79
4.3.4	Comparison of time of treatment on rate of differentiation.....	84
4.3.5	Triglycerides quantification.....	87
4.4	Discussion: .....	89
4.4.1	Scope.....	89
4.4.2	Stimulation of differentiation. ....	89
4.4.3	Cell morphology.....	90
4.4.4	Single flavonoid treatments.....	91
4.4.5	Flavonoid combination treatments .....	92
4.4.6	Triglyceride accumulation.....	92
4.4.7	Proliferation during differentiation. ....	93
4.4.8	Loss of adherence after differentiation. ....	93
4.5	Conclusion.....	94
<b>5</b>	<b>Molecular Pathways .....</b>	<b>96</b>
5.1	Introduction .....	96
5.1.1	Chapter overview.....	96
5.1.2	Proliferation .....	96

5.1.3.	Cell death .....	97
5.1.4.	Differentiation.....	100
5.1.5.	Transcription factors and cellular pathways.....	104
5.1.6.	Methods for elucidating molecular processes.....	107
5.1.7.	Chapter aims. ....	108
5.2.	Method .....	108
5.2.1.	Cell culture .....	108
5.2.2.	RNA extraction and quantification.....	109
5.2.3.	cDNA synthesis.....	109
5.2.4.	qPCR procedure .....	110
5.2.5.	Protein analysis .....	111
5.2.6.	Statistical analysis .....	113
5.3.	Results.....	114
5.3.1.	Gene expression; general.....	114
5.3.2.	Gene expression; Proliferation .....	116
5.3.2.1.	<i>Ki67</i> gene.....	116
5.3.2.2.	<i>TPX2</i> gene.....	116
5.3.2.3.	<i>BIM</i> gene .....	117
5.3.2.4.	<i>BAD</i> gene.....	118
5.3.2.5.	<i>Adiponectin</i> gene .....	118
5.3.2.6.	<i>GLUT4</i> gene .....	119
5.3.2.7.	PPAR $\gamma$ gene .....	120
5.3.2.8.	<i>SREBP1c</i> gene on quercetin .....	120
5.3.3.	Gene expression; Differentiation.....	121
5.3.3.1.	PPAR $\gamma$ gene .....	121
5.3.3.2.	<i>Adiponectin</i> gene .....	122
5.3.3.3.	<i>GLUT4</i> gene .....	123
5.3.3.4.	<i>SREBP1c</i> gene.....	124
5.3.3.5.	<i>UCP1</i> gene .....	125
5.3.3.6.	<i>C/EBP-beta</i> gene .....	125
5.3.4.	Protein expression; Proliferation.....	126
5.3.4.1.	<i>SREBP1c</i> protein.....	126
5.3.4.2.	C/EBP $\beta$ protein.....	127
5.3.4.3.	Erk and pErk .....	128
5.3.4.4.	Leptin protein.....	129
5.3.4.5.	Akt and pAkt proteins .....	130
5.3.5.	Protein expression; Differentiation.....	131

5.3.5.1.	SREBP1c protein.....	131
5.3.5.2.	C/EBP $\beta$ protein.....	132
5.3.5.3.	PPAR $\gamma$ protein .....	133
5.3.5.4.	UCP1 protein .....	134
5.3.5.5.	Akt and pAkt proteins .....	135
5.3.5.6.	Leptin protein.....	136
5.3.5.7.	Erk and pErk .....	137
5.4.	Discussion.....	138
5.4.1.	Context.....	138
5.4.2.	Gene expression during preadipocyte proliferation.....	138
5.4.2.1.	<i>Ki67</i> .....	138
5.4.2.2.	<i>TPX2</i> .....	139
5.4.2.3.	Proliferation markers summary .....	139
5.4.2.4.	<i>BIM</i> gene .....	140
5.4.2.5.	<i>BAD</i> Gene .....	141
5.4.2.6.	Apoptotic markers summary .....	142
5.4.2.7.	<i>Adiponectin</i> gene .....	142
5.4.2.8.	<i>GLUT4</i> .....	142
5.4.2.9.	<i>PPAR gamma</i> gene.....	143
5.4.2.10.	Differentiation markers summary.....	144
5.4.2.11.	<i>SREBF1</i> gene.....	144
5.4.3.	Adipocyte differentiation.....	145
5.4.3.1.	<i>PPAR gamma</i> .....	145
5.4.3.2.	<i>Adiponectin</i> .....	147
5.4.3.3.	<i>GLUT4</i> .....	148
5.4.3.4.	<i>SREBP1c</i> .....	149
5.4.3.5.	<i>UCP1</i> .....	150
5.4.3.6.	C/EBP beta .....	152
5.4.4.	Protein analysis .....	153
5.4.4.1.	C/EBP beta during proliferation.....	153
5.4.5.	SREBP1c during proliferation .....	154
5.4.5.1.	Erk and pErk during proliferation.....	155
5.4.5.2.	Leptin during proliferation.....	157
5.4.5.3.	Akt and pAkt during proliferation .....	158
5.4.5.4.	SREBP1c protein during differentiation .....	159
5.4.5.5.	C/EBP beta protein during differentiation .....	160
5.4.5.6.	PPAR gamma protein during differentiation .....	162

5.4.5.7.	UCP1 protein during differentiation .....	163
5.4.5.8.	Akt phosphorylation during differentiation.....	165
5.4.5.9.	Leptin protein during differentiation.....	166
5.4.5.10.	Erk phosphorylation during differentiation .....	168
5.4.6.	Conclusion.....	168
<b>6.</b>	<b>Discussion .....</b>	<b>170</b>
6.1.	Preadipocyte proliferation.....	171
6.2.	Adipocyte differentiation.....	174
6.3.	Gene expressions and molecular pathways.....	176
6.4.	Future work.....	179
6.5.	Conclusion.....	180
<b>7</b>	<b>References: .....</b>	<b>182</b>

## **Declaration**

I declare that the thesis is the result of my own work based on research that was undertaken at the Biological Science Department at University of Staffordshire and at the Division of Pediatric Endocrinology and Diabetes, Endocrine Research Lab, University Medical Centre Ulm, Germany.

Trust Diya

28<sup>th</sup> February 2023

## **Acknowledgements**

I want to express my most sincere gratitude to my team of supervisors without whose excellent support, this work would not have been completed. They are Dr Arthur Hosie (principal), Dr Stephen Merry, Dr Gavin McStay, Dr Peter Gowland, Dr Angela Priestman and Dr David Cadagan. Thank you.

I also want to thank my family, friends, colleagues, pastors and everyone else who stood with me on this grand journey.

## **Dedication:**

This work is dedicated to my late mother who always said, “Eat your broccoli and fruit, otherwise you won’t be fit”, I finally got your message mom, although it took me this long. You wanted me to benefit from flavonoids, didn’t you?



## Abstract

Obesity and associated comorbidities such as cardiac diseases have become a major public health problem for today's societies. There has been an increased focus on the use of natural compounds to combat this growing pandemic. Many studies have concluded that dietary polyphenolic flavonoids can reduce the development of mature adipocytes, a prerequisite for obesity, but little is known about the precise mechanisms and stages of flavonoid action. Furthermore, there is a scarcity of literature on the effect of flavonoids on adipogenesis using human cell strains.

Human preadipocytes (SGBS cells), a novel adipogenesis model, were treated with a range of concentrations of quercetin, kaempferol, galangin, chrysin, luteolin and apigenin representing the flavonoid classes of flavanols and flavones. Treated preadipocytes were tested for viability, proliferation, differentiation and dedifferentiation. Assessment protocols used included MTT assays, microscopic cell counts, oil red O assays, morphological analysis, qPCR analysis and western blots. Finally, to simulate the effects of dietary metabolism to glucuronides, culture medium from quercetin treated human Caco2-TC7 colorectal cancer cells was analysed by HPLC.

Results showed a relationship between the number of hydroxyl groups present in flavonoids and their effect on both preadipocyte proliferation and conversion to committed adipocytes. A selection of flavone and flavanol combinations showed synergistic effect on proliferation and an additive effect on differentiation. Genes related to the apoptotic pathway (*BIM* and *BAD*) were significantly upregulated ( $p < 0.05$ ) whereas proliferation genes (*Ki67* and *TPX2*) were downregulated on cells treated with supra-physiological concentrations of selected flavonoids. Insulin regulating genes, *PPAR gamma*, *Leptin* and *Adiponectin* were significantly upregulated ( $p < 0.05$ ) in differentiated cells treated with selected flavonoids. Whilst physiological concentrations of flavonoids appeared to increase preadipocyte proliferation ( $p < 0.05$ ), the increase was not sustained during differentiation.

It was also shown that the impact of flavonoids on differentiation was independent of the stage at which the flavonoid was introduced during the course of differentiation. Flavonoid conversion to glucuronides was shown to be inefficient (< 5%) and so did not warrant further investigation. More specifically, protein and gene analysis suggested that flavonoids reduce both preadipocyte proliferation and differentiation through Akt, Erk, *SREBP1c* and *CEBP- $\beta$*

associated pathways. There were suggestions of increased browning of cells treated with sub-physiological flavonoid concentrations through the upregulation of the uncoupling protein 1 (UCP1), a mitochondrial protein associated with adaptive thermogenesis.

In sum, the study points to great potential of flavonoids being used to reduce fat mass through insulin regulation, browning and dedifferentiation.

## List of tables

Table number	Description
Table 1.1	BMI range
Table 1.2	Flavonoid subclasses
Table 2.1	Seeding densities for SGBS cells
Table 2.2.	Vessel dependent volumes
Table 3.1	Flavonoid combinations
Table 4.3.1a	Effects of the flavanols quercetin, galangin and kaempferol
Table 4.3.1b	Effects of the flavones chrysin, luteolin and apigenin
Table 4.2.3 (a-d)	Comparison between differentiation treatment regimens of proliferation phase only against both proliferation and induction of differentiation
Table 5.1	Preparation of assay tube for quantification of standards and samples using the Quant-it Assay
Table 5.2	cDNA synthesis cycle temperatures and duration
Table 5.3	List of primers used for qPCR gene analysis
Table 5.4	Primary antibodies used and dilutions levels

## List of figures

Figure number	Description
Figure 1.1	Disorders associated with obesity
Figure 1.3.1	Triglycerides are made from a glycerol molecule joined with 3 fatty acids
Figure 1.3.2	Lineage of the brite adipocyte
Figure 1.3.2	The three classes of adipocytes
Figure 1.6.1	Flavonols galangin, kaempferol and quercetin
Figure 1.6.2	Flavones chrysin, apigenin and luteolin
Figure 3.3.1.1	Time course growth curve
Figure 3.3.1.2	SGBS viability curve after 24 hours of incubation
Figure 3.3.2.1	Effects of solvents DMSO, DMF and EtOH at 1%
Figure 3.3.2.2	Comparison of controls, with and without DMSO at (0.5%)
Figure 3.4.3a.	The skeleton structure of flavonoids in general
Figure 3.3.3.2	Correlation plot of cell counts and MTT assays for seeding densities
Figure 3.4.3b.	Chemical Structures of the flavones luteolin, apigenin & chrysin, & the flavonols quercetin, kaempferol & galangin
Figure 3.3.4.1a	Relative cell counts and absorbance of SGBS cells treated with quercetin for 72 hrs
Figure 3.3.4.1b	Relative cell counts and absorbance of SGBS cells treated with kaempferol for 72 hrs
Figure 3.3.4.1c	Relative cell counts and absorbance of SGBS cells treated with galangin and incubated for 72hrs
Figure 3.3.4.1d	Comparison of the potency of the flavanols quercetin, kaempferol and galangin.

Figure 3.3.4.1e	Relative cell counts and absorbance of SGBS cells treated with chrysin for 72hrs
Figure 3.3.4. 1f	Relative cell counts and absorbance of SGBS cells treated with apigenin for 72hrs
Figure 3.3.4.1g	Relative cell counts and absorbance of SGBS cells treated with luteolin for 72hrs
Figure 3.3.5.1	Combined flavonoids appeared to form aggregates with MTT
Figure 3.3.5a	Relative cell counts of SGBS cells treated with chrysin for 72hrs
Figure 3.3.5b	Relative cell counts of SGBS cells treated with combined chrysin and kaempferol for 72hrs
Figure 3.3.5c	Relative cell counts of SGBS cells treated with of combined chrysin and galangin for 72hrs
Figure 3.3.5d	Relative cell counts of SGBS cells treated with of combined quercetin and apigenin for 72hrs
Figure 3.3.5d	Relative cell counts of SGBS cells treated with combined quercetin and apigenin for 72hrs
Figure 3.3.5e	Relative cell counts of SGBS cells treated with quercetin and luteolin for 72hrs
Figure 3.3.5f	Relative cell counts of SGBS cells treated with combined luteolin and galangin for 72hrs
Figure 3.3.5h	Relative cell counts of SGBS cells treated with combined apigenin and galangin for 72 hrs
Figure 3.3.5i	Relative cell counts of SGBS cells treated with combined apigenin and kaempferol for 72hrs
Figure 3.3.5j	Comparative view of the combined flavonoids IC50 values
Figure 3.3.5k	Comparative view of the single and combined flavonoids
Figure 3.3.4.1e	Relative cell counts and absorbance of 3T3 cells treated with quercetin for 72hrs
Figure 3.3.7	Cell recovery after a single treatment with quercetin
Figure 4.2.1	Differentiation treatment schedule
Figure 4.2.3a.	Differentiation stages of SGBS cells treated with flavonoids and flavonoid
4.2.3b.	Differentiation stages of SGBS cells treated with flavonoids and flavonoid combinations on adipocyte differentiation
Figure 4.23	Sampling points for microscopic counts being 6 cardinal points selected from a single well
Figure 4.3.2b	Photomicrographs comparing spontaneous and stimulated mature SGBS adipocytes stained with oil red O
Figure 4.3.2c	Photomicrographs comparing spontaneous and stimulated mature 3T3-L1 adipocytes stained with oil red O
Figure 4.3.2d.	Validation curve showing the correlation between the oil red O absorbance
Figure 4.3.7.	Photomicrographs of differentiated SGBS cells after treatment with 0, 10 and 100 $\mu$ M quercetin for 21 days
Figure 4.3.2e.	Comparison of oil red O absorbance values for SGBS cells treated with differentiation media containing 0.5% DMSO
Figure 4.3.3a.	Comparison of the effectiveness of the flavanols quercetin, galangin and kaempferol on the differentiation of SGBS preadipocytes
Figure 4.3.3b	Comparison of the effectiveness of the flavones chrysin, apigenin and luteolin on the differentiation of SGBS preadipocytes
Figure 4.3.3c	Comparison of the effectiveness of the flavanol quercetin when combined with the flavones chrysin, apigenin and luteolin on the differentiation of SGBS preadipocytes

Figure 4.3.3d	Comparison of the effectiveness of the flavone chrysin when combined with the flavanols quercetin, galangin and kaempferol on the differentiation of SGBS preadipocytes
Figure 4.3.3e	Single and combined flavonoid treatments as ranked by IC50 values
Figure 4.3.4	SGBS preadipocytes were treated with the flavanol quercetin
Figure 4.3.5a	Calibration curve routinely used to quantify triglycerides
Figure 4.3.5b	Comparison of triglyceride presence on cells treated with flavonoids
Figure 4.3.16	Galangin, kaempferol and quercetin molecules showing the locations of hydrogen and hydroxyl molecules
Figure 4.3.17	Flavones a) chrysin, b) apigenin and c) luteolin showing the increasing number of hydroxyl groups
Figure 5.2.1	Treatment and RNA extraction regime for cells treated with quercetin and chrysin
Figure 5.1	BIM gene on a chrysin melt curve
Figure 5.2	A typical gel electrophoresis run of qPCR products showing single bands
Figure 5.3	A screen shot of a typical qPCR run of the PPAR gamma gene expressed on chrysin treated SGBS cells
Figure 5.3.3a&b	Effect of flavonoid concentration on the relative expression of the BIM gene in quercetin and chrysin
Figure 5.3.7a&b	Expression of the PPAR $\gamma$ gene in quercetin and chrysin treated SGBS cells
Figure 5.3.8	All treatments significantly reduced the expression of SREBP1c
Figure 5.3.9a&b	Expression of the PPAR $\gamma$ gene in quercetin and chrysin treated SGBS cells
Figure 5.3.10b	Expression of the adiponectin gene in quercetin and chrysin treated SGBS cells
Figure 5.3.11 a&b	Expression of the GLUT4 gene in quercetin and chrysin treated SGBS cells
Figure 5.3.12 a&b	Expression of the Erk and pErk proteins in quercetin treated SGBS preadipocytes
Figure 5.3.13 a&b	Expression of the Akt and pAkt proteins in quercetin treated SGBS preadipocytes
Figure 5.3.14 a&b	Expression of the Akt and pAkt proteins in quercetin treated SGBS preadipocytes
Figure 5.3.15 a and b	Expression of the Erk and pErk proteins in quercetin treated SGBS preadipocytes
Figure 6.1	Chemical Structures of the generic flavonoid, the flavones luteolin, apigenin and chrysin, and the flavanols quercetin, kaempferol and galangin

## List of abbreviations

Abbreviation	Full Term
ACC1	Acetyl-CoA carboxylase 1
Akt	Akt kinase (Protein kinase B)
ALBP/aP2	Adipocyte lipid binding protein
AMPK	AMP-activated protein kinase
ANOVA	Analysis of Variance
AP	Apical compartment
ATP	Adenosine triphosphate
<i>BAD</i>	BCL-2 associated agonist of cell death
BAK	BCL-2 homologous antagonist/killer
BAX	BCL-2-like protein 4
BCA	Bicinchoninic acid
BCL-2	B-cell lymphoma 2
BCL-xL	Anti-apoptotic proteins B-cell lymphoma-extra-large
BFL-1/A1	BCL-2 homolog Bfl-1/A1
BH3	BCL-2 homology domain 3
<i>BIM</i>	BCL-2-like protein 11
BL	Basolateral
BMI	Body Mass Index
BSA	Bovine serum albumin
<i>CEBP-β</i>	CCAAT enhancer binding protein beta
CHD	Coronary heart diseases
CuSO <sub>4</sub>	Copper Sulphate
DEX	Dexamethasone
DIK1	Delta-like 1 homolog
DMEM/F12	Dulbecco's Modified Essential Medium and Ham's F-12
DMF	Dimethylformamide
DMSO	Dimethylsulfoxide
EDTA	Ethylenediaminetetraacetic acid
Erk	Extracellular signal-regulated kinases
EtOH	Ethanol
FABP4	Fatty acid binding protein 4
FAS	Fatty acid synthase
FBS	Foetal bovine serum
<i>GLUT4</i>	Glucose transporter type 4
HPLC	High-performance liquid chromatography
HPRT	Hypoxanthine Phosphoribosyl transferase
INSIG1	Insulin-induced gene 1 protein
IUPAC	International Union of Pure and Applied Chemistry
MAPK	Mitogen activated protein kinase

MCE	Mitotic clonal expansion
MCM	Mini chromosome maintenance
MIX	Methylisobutylxantine
mTOR	Mechanistic target of rapamycin
NF- $\kappa$ B	Nuclear factor kappa-light-chain-enhancer of activated B cells
NO	Nitric oxide
PBS	Phosphate buffered saline
PCNA	Proliferating cell nuclear antigen
PFA	Paraformaldehyde
PGE2	Prostaglandin E2
PI3K/Akt-FOXO1	Phosphatidylinositol 3-kinase
<i>PPAR gamma</i>	Peroxisome proliferator- activated receptor gamma
Pref-1	Preadipocyte factor 1
qPCR	Quantitative Polymerase Chain Reaction
ROS	Reactive oxygen species
RPMI	Growth medium developed by Roswell Park Memorial Institute
SCAP	SREBP cleavage-activating protein
SCD	Stearoyl-CoA desaturase
SDS-PAGE	Sodium Dodecyl Sulphate Polyacrylamide Gel Electrophoresis
SGBS cells	Simpson-Golabi-Behmel syndrome
<i>SREBP1c</i>	Sterol regulatory element binding transcription factor 1
SVF	Stromal vascular fraction
TAZ	Transcriptional coactivator with PDZ-binding motif
TFA	Trifluoroacetic acid
TNF	Tumor necrosis factor
TPX-2	Targeting protein for Xklp2
TP53	Tumour protein 53
TZDs	Thiazolidinediones
UCP1	Uncoupling protein 1
YAP	Yes-associated protein
Xklp2	Xenopus centrosomal kinesin-like protein 2
3T3-L1	Fibroblast that was isolated from the embryo of a mouse

# 1 Introduction

## 1.1 A global health pandemic

In the UK in 2020, 27% of adults were obese (Keaver et al., 2020). Alongside this, Public Health England (2022) revealed that 67.8% of females and 58.1% of males over 15 years old were classified as overweight or obese. It is estimated that about £6 billion a year is spent on direct medical costs related to being overweight or obese (McKinsey Global Institute, 2019) and recently as much as £3.23 billion per year has been spent on direct obesity costs in the NHS (Aljunid, 2021). A further £10 billion was estimated to cover obesity related disorders. Globally, about 2 billion people are overweight and one third of them obese (Ataey et al., 2020; -Mohajan and Mohajan, 2023). In the last quarter of the century, the obesity burden has more than doubled and it is estimated that a 33% increase in obesity prevalence and a 130% increase in severe obesity prevalence is expected over the next 2 decades (Ryan et al., 2021 ). Forecasts by Hojjat and Hojjatt (2021) suggest that if global obesity were to be contained at current levels, the combined savings in medical expenditures over the next ten years would be more than a trillion dollars.

Obesity does not always exist as a single disorder (Figure 1.1), it brings along increased risks that include high blood pressure, heart diseases, diabetes mellitus type 2 (DM2), some types of cancer, liver diseases, reproductive disorders, behavioural disorders, and dyslipidaemia (Dwivedi et al., 2020; Kyrou et al., 2018) making it into the top 5 mortality risk factors globally (Delfiner., 2023). There is a greater likelihood for an overweight or obese individual to suffer from a host of other metabolic syndrome disorders compared to individuals of normal weight ranges. Hojjat and Hojjatt (2021) assert that individuals who are obese may have 25% more medical expenses compared to their peers of normal weight with this increased cost forecast on treatment expenditure only and not loss of production due to obesity comorbidities. Put together, obesity has a huge health and economic burden to humanity.





Figure 1.1. Different disorders associated with obesity (Kyrou et al., 2018)

It has been estimated that obesity reduces life expectancy by up to 17% and negatively impacts on the quality of life and productivity for individuals with the disorder. Except for sub-Saharan Africa, overweight and obesity are linked to more deaths worldwide than underweight (WHO, 2022). This holds fast despite the fact that the epidemiology of obesity has for a long time been difficult to study because of different classification criteria for the different degrees of overweight across many countries. After hypertension, smoking, and high cholesterol, obesity is estimated to be the fourth largest risk factor contributing to deaths in England (WHO, 2022).

Overweight and obesity mechanically affects the body, it is a weight burden on the skeleton that exacerbates osteoarthritis and back pain (Perera et al., 2022 ). Most obese people are reported to have low self-esteem and often become victims of body shaming (Iannaccone et al., 2016). Bullying in schools has more obese victims than any other group (Jeong et al., 2016) and in women there is an increased risk of suicides in obese individuals compared to their normal weight peers (Branco et al., 2017).

Overall, this weight pandemic affects the mechanics of the body, increases chronic disease susceptibility and increases mortality rate. It affects all countries of the world and has since moved from being a disease predominantly affecting the developed countries to one that impacts the developing and lately the underdeveloped countries (Bosdou et al., 2016; WHO, 2022). There is a financial burden to individuals, families and national health services which calls for the understanding of obesity, its mechanism, and solutions to this pandemic.

## 1.2 Defining obesity

Apovian, (2016) defines obesity as product of complex interactions between genetic, socioeconomic, and cultural influences. He postulates a connection between consumption patterns, urbanisation, and lifestyle as drivers of the obesity pandemic. Metabolically, obesity can be defined as an imbalance in energy consumed in relation to energy expended (WHO, 2016). This echoes Formiguera & Canton, (2004) who saw obesity as a metabolic disorder where energy expenditure lags storage. Garrow (1988) on the other hand defines obesity in light of fat accumulation, he portrays the disorder as an abnormal condition of excessive fat accumulation in adipose tissue so that health is impaired. Close to this definition Romieu et al., (2017) sees obesity as a state of excess adiposity predisposing an individual to risk to health in the form of chronic diseases. He concurs with Apovian, (2016) that there is a complex interplay between behaviour, genetics, and the environment. All these definitions bring in line the notion of net gain of energy which is stored as fat in adipose tissue to a level of pathology. Therefore, obesity is a phenotypic presentation of aberrant or surplus accrual of adipose tissue which is detrimental to health and wellbeing.

Body mass index (BMI) is commonly utilised as an easy and dependable method to determine if a person's weight is appropriate for their height, and to identify potential obesity (Khanna et al., 2022). BMI is calculated by dividing a person's weight in kilograms by the square of their heights in metres ( $\text{kg}/\text{m}^2$ ). BMI's of  $30 \text{ kg}/\text{m}^2$  and above are considered as obese. Within the obese range, there are subcategories (Table 1.1).

Table 1.1. BMI range showing the subcategories of the obesity range. (Freedman et al., 2017).

Category	BMI ( $\text{kg}/\text{m}^2$ )
Very severely underweight	Less than 15
Severely underweight	15 to 16
Underweight	16 to 18.5
Normal health weight	18.5 to 25
Overweight	25 to 30
Moderately obese class 1	30 to 35
Severely obese class 2	35 to 40
Very severely obese class 3	Over 40

BMI as a measure of obesity in itself has many challenges. The CDC (2022) maintain that BMI is a surrogate measure of body fat as its focus is on relative body weight and not excess fat. Furthermore, it does not make a distinction between excess fat, muscle, or bone mass and, with BMI, there is no indication of the distribution of fat among individuals; the canonical pear, apple, rectangle, and hourglass shapes are not captured in BMI measures, yet they are determinants of the risks associated with excess adipose tissue.

Besides BMI, there are other measures that can approximate the level of body fat and hence levels of obesity in an individual. Ortega et al. (2016) compared BMI values with skinfold thicknesses, bioelectrical impedance, underwater weighing, and dual energy x-ray absorption and concluded that these are better measures of fat in the body. A closer measure to BMI is the waist circumference to height ratio, and together with the skinfold thickness, they constitute cheaper and non-invasive measures of excess fat. The incongruence of BMI as a measure of obesity is evidenced by older adults tend to have more body fat than younger adults for an equivalent BMI; females have greater amounts of total body fat than men of the same BMI; and athletic or muscular individuals have a higher muscle mass induced BMI.

Whilst it has its limitations, BMI is considered an evidence based satisfactory proxy for the measure of excess fat and obesity. There exists a correlation between BMI values and obesity related health risks, and other more expensive, time consuming and invasive measures of body fat are not recommended for routine practice (Batsis et al., 2016). For children, a correction factor must be introduced to normalise BMI readings.

As all definitions of obesity anchor on the disparity between calorie intake and energy expenditure, the worldwide distribution of obesity should naturally depend on geographical food supply and genetic variation. Besides genetic predisposition, there is an assumption that the consumption of energy dense foods that are high in fat translates to greater levels of obesity (Romieu et al., 2017). It is easy to relate high fat consumption to obesity but recently it has been made clear that carbohydrates are “new fat” through de novo lipogenesis (Song et al., 2018 ). Furthermore, there have been some views that suggest high fat diets can have a weight reducing effect, but this has not as yet been conclusively agreed (Wali et al., 2020). World over, patterns which link energy dense foods that are high in fat and obesity continue to emerge with some fascinating exceptions.

### 1.3 Adipocytes

Central to obesity is the fat cell, i.e., the adipocyte, because excess calories in the body are stored as either glycogen (glucogenesis) or fat (lipogenesis). Even more interesting, dietary fat is not the major determinant of body fat (Schwingshackl et al., 2021) because studies show an increase in adiposity in cohorts who had reduced their dietary fat intake. Excess calories are stored in adipocytes as triglycerides, which are esters made from glycerol and fatty acids (Figure 1.3.1).

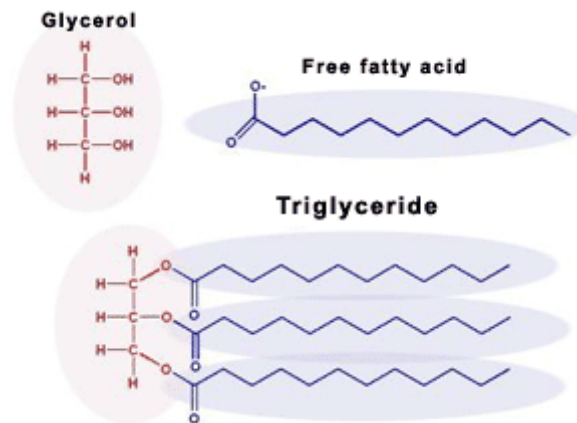


Figure 1.3.1. Triglycerides are made from a glycerol molecule joined with 3 fatty acids (Cardiodiabetes, 2023).

Adipocytes are part of the stromal vascular fraction (SVF) of adipose tissue which includes cells such as adipocytes, preadipocytes, fibroblasts, vascular endothelial cells and some adipose specific immune cells like adipose tissue macrophages. Adipocytes make up to one third of adipose tissue and, besides their role in glucose and lipid metabolism, they function as an endocrine organ, regulate thermogenesis and provide a supportive cushion for internal organs (Giroud, 2022). These functions are made clearer because there are two families of adipose tissue: visceral which surround the internal organs; and subcutaneous which lies beneath the skin (Mittal, 2019). Excess calories can result in an increased number of adipocytes (i.e., hyperplasia) or increased adipocyte size (i.e., hypertrophy) or both (Ghaben et al., 2019) and, while increase in adipocyte size and number is part of the growth of an organism, unregulated increases may alter the normal function of the cells leading to chronic diseases.

Adipocytes themselves have, for many years, been divided into 2 groups; white and brown adipocytes which differ in appearance, physiology and function (Xu et al., 2020 ). In recent

years however the narrative has embraced a third phenotype, the brite (brown-in-white) or beige adipocyte (Rosenwald and Wolfrum, 2014). Whilst it was believed that beige adipocytes are a result of trans-differentiation from the white phenotype (Maurer et al., 2021), some studies suggest that they have their own distinct lineage (Figure 1.3.2).

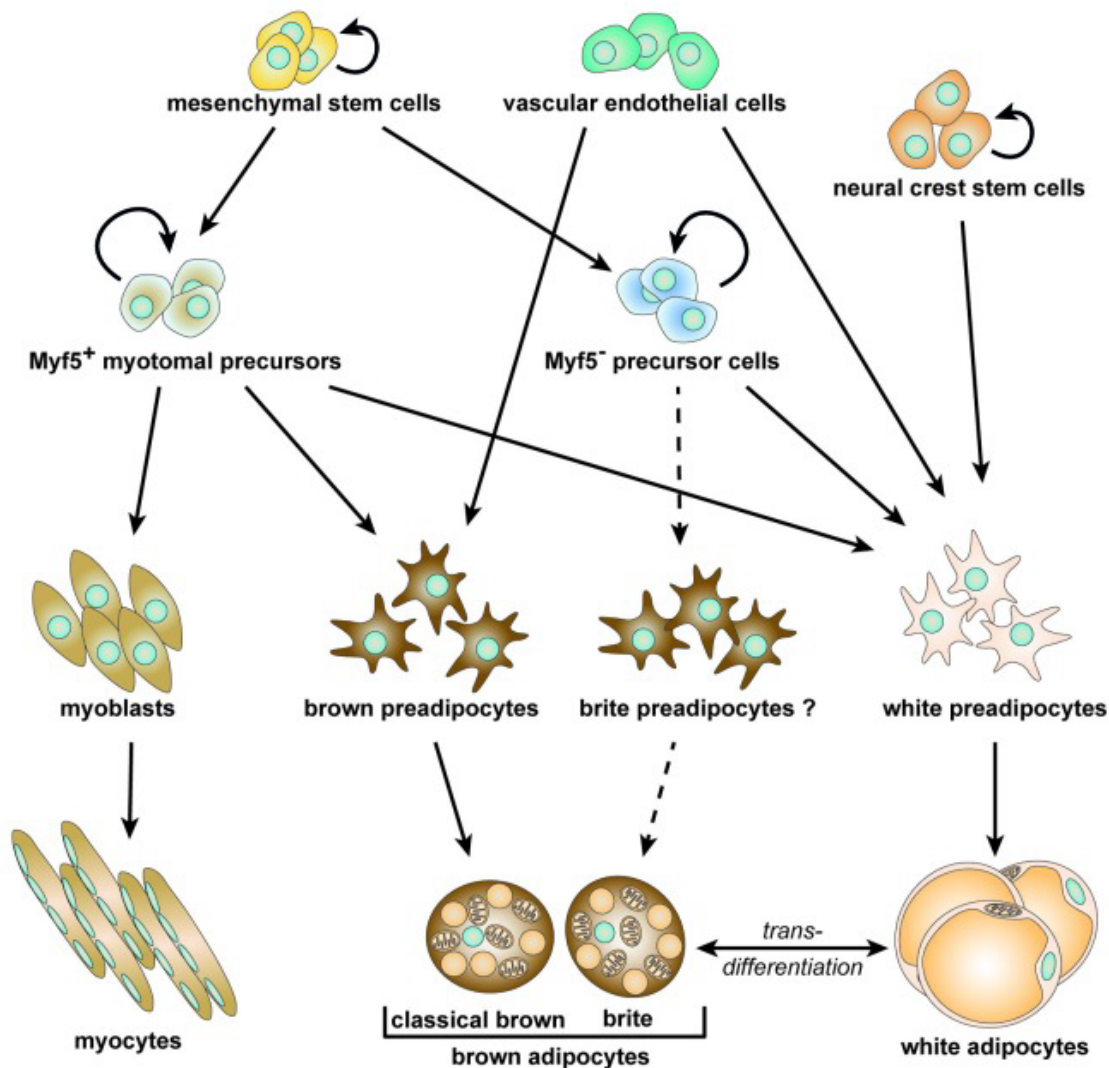


Figure 1.3.2. Depiction of possible lineage of the brite adipocyte with dotted lines suggesting possible independent lineage of the cells besides trans-differentiation from white adipocytes (Rosenwald and Wolfrum, 2014).

### 1.3.1 White adipocytes

White adipocytes play a key role in storing excess energy as fatty molecules such as triglycerides. Structurally, the white adipocyte is a simple cell comprising of a single lipid droplet and standard cell organelles, but with, most significantly, fewer mitochondria. This

reduced mitochondrial density together with the large fat droplet translates into the adipocyte's pale colour. Furthermore, the cell's storage of fatty molecules is tightly regulated by hormones such as insulin, cortisol, glucagon and catecholamines. These hormones control the homeostatic balance of lipogenesis and lipolysis which are the build-up and release of fat respectively.

White adipose tissue also contains other biologically active molecules that are responsible for diverse metabolic functions. These include hormones involved in energy balance, satiety, hunger, and metabolism together with protein molecules involved in inflammatory responses. Visceral white adipose tissue also plays a major role in cushioning internal organs whereas subcutaneous white adipose tissue is associated with insulation of the body from extreme temperatures. It is the visceral white adipose tissue that is implicated in most dyslipidaemia disorders (Chait and Den-Hartigh, 2020).

### 1.3.2 Brown adipocytes

Brown adipocytes are morphologically and functionally distinct from their white kindred. They are multilocular with small lipid droplets, and their mitochondria are dense and darker (i.e., brown) because of their high iron content. Like white adipose tissue, the brown phenotype acts as an endocrine organ whilst also producing heat through non-shivering thermogenesis (Jung et al., 2019). At the molecular level, brown adipocytes have a key uncoupling protein (UCP1) which is coded by the Uncoupling Protein 1 (UCP1) gene and found in their high-density mitochondria. When brown adipocytes are stimulated by the hormone noradrenaline, a signalling cascade triggers UCP1 to release the inter-membrane proton-motive force and so uncouple aerobic respiration resulting in heat energy generation rather than ATP production (Roesler and Kazak, 2020 ).

In humans, brown adipocytes are located on the upper back, lower neck, above the collarbone, around the abdomen, and along the spine (Goossens, 2017). Brown adipose tissue has been thought to be more prevalent in infants and reducing in abundance as humans mature, but recent studies are showing that it can be found within pockets of subcutaneous white adipose tissue and can increase in volume under favourable conditions (Chait and Den-Hartigh, 2020; Sarjeant and Stephens, 2012). Whether dietary interventions or lifestyle changes can increase brown adipose tissue abundance is not yet known (Heenan et al., 2020).

### 1.3.3 Beige (brite) adipocytes

The third phenotype which has gained much traction over the past 20 years is the brite or beige adipocyte. This too is morphologically distinct and has some attributes of both white and brown adipocytes. Brite adipocytes have multilocular lipid droplets (LD) with dense mitochondria, but less so than brown adipocytes. They are found in white adipose tissue pockets and can exhibit both an energy storage and thermogenesis role besides having an endocrine function. An exciting attribute of these cells is their ability to be converted into expressing UCP1 like brown adipocytes when there is  $\beta$ -adrenergic stimulation (Roesler and Kazak, 2020; Waldén et al., 2012). This means brite adipocytes have the capacity to be manipulated to meet desired outcomes and, in the face of obesity and other metabolic syndrome disorders, brite cells are thus candidates for studies on energy regulation.

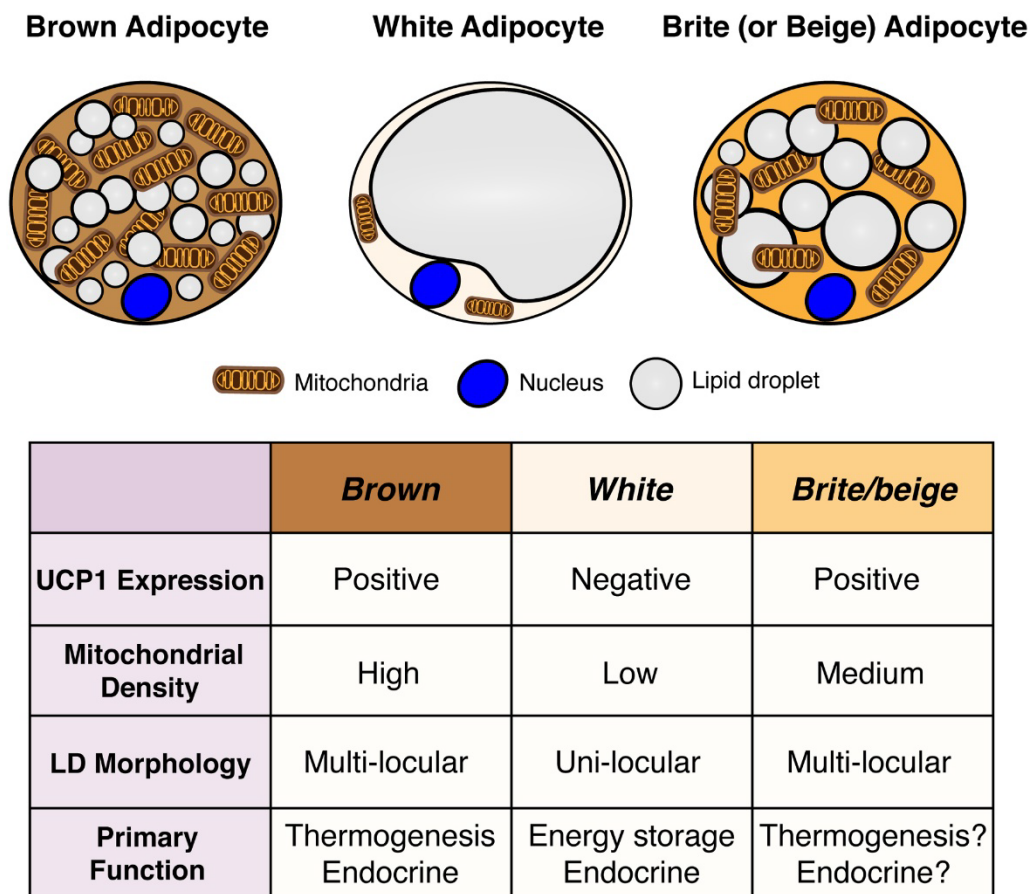


Figure 1.3.2. Illustration of the three classes of adipocytes showing the intermediary aspects of brite adipocytes (Jung et al., 2019).

#### 1.3.4 Adipocyte proliferation and differentiation.

Cell proliferation results in the increase of cell numbers as a result of cell division through mitosis. This process is complex and tightly regulated by many genes and transcription factors in the presence of an enabling environment. Adipocyte proliferation is normal and needed for the growth and sustenance of an organism but it when dysregulation occurs, for example when there is chronic caloric surplus, this process becomes undesirable. Excessive proliferation results in hyperplasia, but the original challenge may be less of a threat than hyperplasia because, when adipocytes outgrow the available space, chronic inflammation occurs because cell death encourages microphages to scavenge the apoptotic bodies and cell remnants (Chan and Hsieh, 2017). Besides cell death, adipose tissue inflammation occurs when hyperplasia results in the induction of pro-inflammatory cytokines and chemokines which attract immune cells. With chronic inflammation, there is the aetiology of obesity, atherosclerosis, cancer, and other chronic multifactorial disorders.

Another challenge is that hypertrophic adipocytes may be subjected to many cytotoxic stressors including lipotoxicity (Trayhurn, 2022). In hypertrophy, insulin action is impaired, and increased lipolysis and release of free fatty acids cause ectopic fat deposition in organs such as the liver and skeletal muscle. Furthermore, when hypertrophy occurs with hyperplasia, the complications are exacerbated. Conversely, however, the downstream disorders can be managed if adipocyte proliferation can be reduced and studying substances that can reduce adipocyte proliferation may be beneficial in the fight against obesity and other disorders.

The reduction of adipocyte proliferation generates a large population of non-dividing cells and is associated with a decrease of cell growth factors and an increase of differentiation factors. This suggests that proliferation and differentiation are mutually exclusive (Olson 1992) with an increase or decrease in proliferation impacting on the availability of cells for differentiation and, consequently, the abundance of differentiation factors.

Differentiation to fully committed adipocytes is a complex process which involves various precursor cells; the chief of which are preadipocytes (Ying and Simmons, 2021; Park et al., 2013). Differentiated adipose tissue has the potential to remodel and conform to the nutritionally derived energy balance of the body with, to avert lipotoxicity, adipocytes assuming the protective role of lipid storage when there is a surplus of calorific supply



(Guilherme, 2008). Mature adipocytes can therefore contribute to energy homeostasis, and in this process, the adipocytes increase their size and incite the production of differentiation factors to recruit more adipocytes from their precursor cells. The production of differentiation factors is believed to occur at the expense of growth factors (Ruijtenberg and van den Heuvel, S, 2016; Gregoire, 1991). Hence, committed adipocytes, although still able to increase in size, withdraw from the cell cycle and are believed not to be able to produce daughter cells (Sarantopoulos et al., 2018; Freytag & Geddes 1992; Freytag 1988). Work on various adipocyte precursor cell lines has been carried out to reveal the underpinning process of preadipocyte differentiation. Such cell lines include 3T3 - L1 and -F442A cells, embryonic fibroblasts, marrow stromal cells and stromal-vascular cells (Aune, 2013). However, because of the complex nature of the preadipocyte conversion, primary cultures have often been chosen for studying the process as they are known to be predisposed to become mature adipocytes with certainty (Carswell, 2012). Work on cell lines therefore benefits from endorsement by primary cell differentiation experiments, but, in the absence of primary cells, human cell lineages such as Simpson-Golabi-Behmel syndrome (SGBS) preadipocyte cells that are neither transformed nor immortalised can be used to produce applicable results on differentiation.

#### 1.4 Preadipocyte models

The 3T3-L1 cells of mouse embryo origin has been the prototypic cell line to represent adipocytes *in vitro*. These cells, like adipose tissue, are not hormonally inert; they are an endocrine organ (Kershaw & Flier 2004) and are sensitive to lipogenic and lipolytic hormones and drugs. Hence, 3T3-L1 cells have been a subject of many adipogenesis studies (Atanasov, 2013), and, whilst many authors have delimited 3T3s as models of visceral adipose tissue (Armani et al., 2010), more recent studies appear to relate 3T3's with attributes of subcutaneous adipose tissue including tight endocrine regulation and involvement in insulin resistance, glucose intolerance, dyslipidemia, hypertension and coronary artery disease (Mori et al., 2014; Ohman, et al., 2008; Kissebah, 1997). *In vivo*, a significant proportion of fat tissue is made up of preadipocytes at various developmental stages (Armani et al., 2010); they have the ability to proliferate and differentiate (Fischer-Posovszky et al., 2008) and they are capable of producing adipokines which are communication hormones that relate to the health or disease state of the organism (MacDougald et al., 2007; Monzillo, 2003; Christiansen et al., 2005). This attribute of preadipocytes at various stages confer 3T3-L1 cells with

constant functional plasticity amenable to exploratory research experiments on substances which affect proliferation and differentiation of preadipocytes.

Posa et al. (2014) chronicles the plasticity of the 3T3-L1 cell line in resistance to insulin, they suggest that hyperinsulinemia impairs insulin sensitivity through the mediation of the TP53 (tumour protein 53) gene whose presence also suggests a tightly regulated apoptosis regime. Hence, insulin sensitivity, growth, differentiation, and apoptosis can essentially be explored using 3T3-L1 cells with the knowledge of the involvement of the Tp53 gene. Other researchers concur that 3T3-L1 cells are amenable to insulin desensitisation and therefore can be used as a model for such metabolic disorders as type 2 diabetes mellitus and obesity (Briones et al., 2012; Thomson et al., 1997), and insulin resistance is believed to be a protective response from lipotoxic damage because of the exclusion of glucose from fat laden cells (Unger, 2003). The propensity for insulin desensitisation is not exclusive to 3T3-L1 cells. Fischer-Posovszky (2010) demonstrated that human SGBS cells can respond favourably to insulin stimulation so there is thus a great aptitude for laboratory modelling of obesity and diabetes mellitus using either murine or human preadipocytes. The mouse 3T3-L1 together with the human SGBS cells become attractive candidates in this pursuit. Ideally, work on 3T3s can be supported by the primary derived SGBS cells.

SGBS cells are a non-transformed nor immortalised human preadipocyte cell strain that gives a sustainable source of homogeneous human preadipocytes which have a high differentiation capacity (Fischer-Posovszky et al., 2008). Easily cultured in 6-96 well plates, the SGBS cells have a high reproducibility level and can reliably be differentiated in the absence of albumin or serum. In their differentiated state, SGBS adipocytes behave in the same way as primary human adipocytes as they give identical responses in key functional assays. Better still, genes related to proliferation, differentiation, apoptosis, and uncoupling are expressed in SGBS cells in the same fashion as they are in primary adipocytes (Tew et al., 2020). Hence, SGBS cells are an attractive tool to validate experiments performed in mouse models and to elucidate the effect of target substances on adipogenesis.

### 1.5 Mediterranean paradox

This paradox has been a subject of great interest over the past three decades (Ghahremani and Salami, 2021; Artaud-Wild et al., 1993). Central to this oddity is the notion that the inhabitants of the Mediterranean region show a relatively low incidence of obesity and

cardiovascular diseases despite a diet which has a high content of dietary cholesterol and saturated fat per capita (Lajous et al., 2014). This is in contrast with epidemiological reports from countries with a lower consumption of fat rich diets that have a greater prevalence of coronary heart diseases (CHD) (Siri-Tarino, 2010). While this observation has seen many challenges and counter theories, interest in the stalemate remains (Doonan et al., 2017; Ferrières, 2004). There are two broad interpretations of this Mediterranean paradox: either the hypothesis linking energy dense foods that are high in fat to obesity related comorbidities is not valid; or that this link is valid, but that some additional factors such as dietary additives or lifestyle behaviours mitigates the risks brought by these foods. If the later interpretation holds, there is scope for finding this mitigating factor and possibly manipulate it across other diets across the world as an anti-obesity drive.

There have been casual observations that communities which subscribe to the paradox are known to consume relatively more wine and vegetables alongside the high fat foods and, in fact, the Mediterranean diet which anchors this paradox is characterized by the abundance of olive oil, fruit, nuts, vegetables and cereals (Santos-Buelga et al., 2021; Willett et al., 1995 cited in Ramón et al., 2013). It has been shown that these foods contain phenolic phytochemicals which are plant aromatic secondary metabolites. Exemplar phytochemicals include resveratrol a natural phenol found in red wine which has enjoyed a great deal of research around its impact on the reduction of a wide range of chronic diseases including obesity and diabetes mellitus (Santos-Buelga et al., 2021; Agouni, 2009). Another example comes from work on blueberries which has demonstrated the presence of phenolic compounds, such as hydroxycinnamic acids, flavonoids, and proanthocyanidines, which positively modulate the development of several chronic disorders (DeFuria, 2009).

Alongside then substantiated claims that link a reduction of obesity and related comorbidities to diets consisting of fruits, vegetables, honey, red wine and other plant derivatives together with the phytochemicals found in these food substances, flavonoids have garnered much interest during the past decade. However, few inroads have been forged in elucidating their mechanism of action in mitigating the obesity pandemic (Vernarelli & Lambert, 2017).

## 1.6 Flavonoids:

Flavonoids are biologically active plant secondary metabolites found in foods and beverages. They are classified by the International Union of Pure and Applied Chemistry (IUPAC) into the following categories or sub classes: chalcones, flavones, flavonols, flavanones, anthocyanins, and isoflavonoids (Table 1.2.; McNaught & Wilkinson, 1997). Within these sub classes, the variability of the side groups (denoted by R<sub>x</sub> in Table 1.2.) results in more than five thousand distinct flavonoid compounds (Kawser Hossain et al., 2016). Many studies have shown the health benefits of flavonoids; some suggest that flavonoids possess anti-inflammatory properties and are capable of inducing apoptosis in dysregulated cells. Hence, they have the potential to combat disease (Erdman, 2007), and epidemiological studies evidence a causal relation between the taking of dietary plant flavonoids and improved health by regulating correct cell progression (Ivey et al., 2017; Hertog et al., 1993; Hertog et al., 1995; Hertog et al., 1997; Knekt et al., 1996).

A flavonoid class of interest is the flavonols which are the most abundant of the flavonoids and the class contains members such as quercetin, kaempferol, myricetin, galangin and isorhamnetin., but the flavonol quercetin (fig 1.6.1.) is the most abundant and makes up the greatest bulk of daily flavonol intake in the Western world (Kelly, 2011) with a typical daily dietary intake of 25 mg (Li et al., 2014). Although they are available as over the counter supplements, flavonols are found in nature in: many fruits such as apples, cherries, grapes, berries and citrus fruits; vegetables such as red onions, asparagus, shallots, capers, kale, pepper, broccoli, fennel, radish, leaves and tomatoes; and beverages including tea and wine (Kelly, 2011; Kawser Hossain et al., 2016). Flavonols, are well studied and important bio-active compounds which act as antioxidants, antimicrobials, hepatoprotective and anti-inflammatory agents. They are also known to reduce the incidence, growth and spread of cancer (Dias et al., 2021).

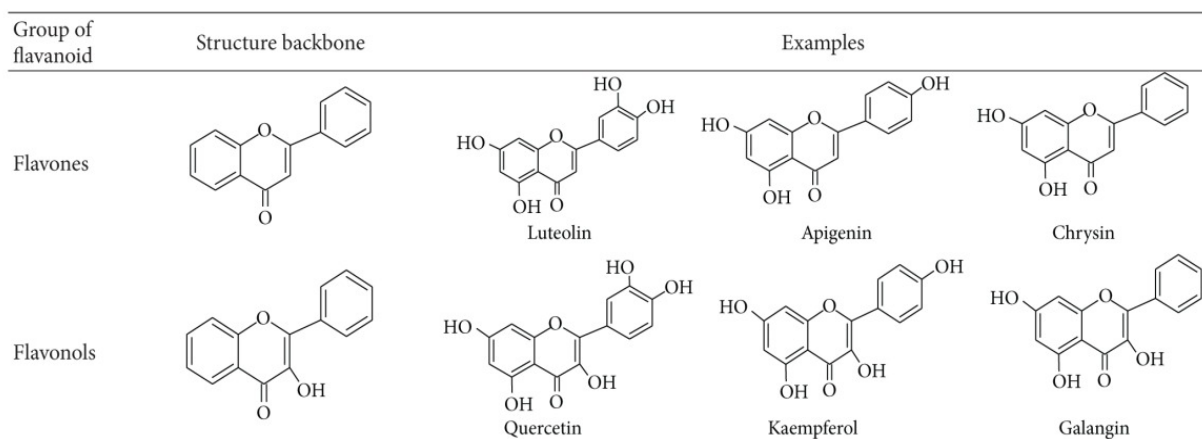
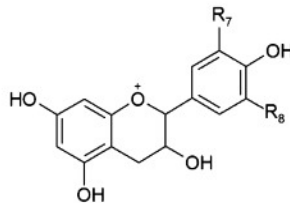
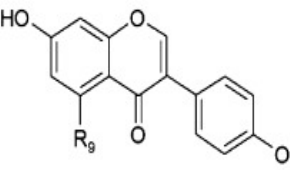


Figure 1.6.1. Flavonols galangin, kaempferol and quercetin showing no hydroxyl, 1 hydroxyl and 2 hydroxyl groups on the determinant carbon ring and flavones chrysin, apigenin and luteolin showing no hydroxyl, 1 hydroxyl and 2 hydroxyl groups on the determinant carbon ring.

Table 1.2. Flavonoid subclasses, examples and chemical structures. Adopted from Kelly, (2011) and Birt and Jeffery (2013).

Subclass	Selected examples	Structure
<b>Flavones</b>	Apigenin, Chrysin, Luteolin and Tangeritin	
<b>Flavonols</b>	Galangin, Kaempferol, Quercetin, Isorhamnetin and Myricetin	
<b>Flavanones</b>	Hesperidin and Naringenin	
<b>Flavanols (Catechins)</b>	Epicatechin and Gallocatechin	

<b>Anthocyanidins</b>	Cyanidin, Malvidin and Pelargonidin	
<b>Isoflavones</b>	Genistein and Daidzein	

Flavones are another category of abundant, widely studied and important flavonoids. Members of this group include apigenin, chrysin, luteolin and tangeritin (Hostetler et al., 2017), and they are found in leaves, flowers and fruits and vegetables including celery, parsley, red peppers, chamomile, mint and ginkgo biloba. Compared to flavanols, however, flavones have lower bioavailability and daily dietary intake with the average daily intake of an adult in the Western world being 2 mg per day, and, worse still, flavones are poorly absorbed and lost in urine. More positively, repeated consumption of flavones can help with bioaccumulation and their daily intake and bioavailability is increased in populations near the Mediterranean region (Hostetler et al., 2017).

Both flavanols and flavones have been implicated in positive health outcomes ranging from cancer reduction, antioxidant, anti-inflammatory effects, and antiviral properties. However, little is known regarding their effects on adipogenesis and whether there is a relationship between the structure of different flavonoids and their biological effects. Studying closely related flavonoids with systematic differences between their side groups (Fig 1.6.1) may be useful in elucidating such structure-function relationships.

### 1.7 Aims and objectives of the study.

The overall aim of this research is to determine the nature of any inhibitory or stimulatory effects of dietary plant flavonoids and their metabolites on the proliferation and differentiation of preadipocytes. In particular, structure-function relationship between and within flavonoid subclasses will be sought together with possible synergy or antagonism and the molecular pathways by which flavonoids exert their effects.

In order to achieve these aims, experiments to measure the effects of a range of concentrations of a select group of flavonoids had on adipocyte viability, differentiation, gene expression and protein levels were conducted. MTT assays were employed to measure cell viability levels and to assess whether flavonoids inhibited or increased preadipocyte cell growth across time and concentrations. Microscopic cell counts were carried out to confirm MTT results. Semi quantitative Oil red O stains were used to measure the effects of flavonoids on preadipocyte differentiation. These were supported by differential cell counts, microscopic morphology observations, and triglyceride quantifications. To assess the molecular changes caused by the flavonoids, RNA was extracted, this was converted to cDNA and candidate genes were probed to see whether flavonoids caused any upregulation or downregulation in comparison to untreated controls. Western blots using candidate antibodies were conducted on extracted proteins to assess levels of presence. These experimental approaches were designed to answer the research question: Do certain classes of flavonoids affect adipogenesis in proliferation and differentiation, if so, what are the molecular mechanisms behind the effects?

#### 1.7.1 Specific objectives:

1. To determine the inhibitory or stimulatory effects, of selected flavonols and flavones alone and in combinations on preadipocytes.
2. To determine the effects of these flavonoids alone and in combinations on the differentiation of preadipocytes.
3. To investigate the expression of selected preadipocyte genes following flavonoid treatment to expose possible pathways of their action on fat cell development.
4. To combine these data to reveal any overall structure-function relationships of the selected flavonoids on adipogenesis.

#### 1.7.2 Hypothesis

There is a hierarchical structure of bioactivity for dietary plant flavonoids on adipogenesis which wanes over time if they are not replenished and can be positively modified by synergistically combining different flavonoid classes.

## 2 General methods

### 2.1 Cell culture

#### 2.1.1 Materials and equipment

Most of the work was carried out at Staffordshire university, Stoke on Trent campus in the science centre. Some work was carried out at the division of Pediatric Endocrinology and Diabetes, Endocrine Research Lab, University Medical Centre Ulm, Germany. Category 2 biological hoods were used throughout the research project. Glassware and distilled water were autoclaved with steam to a temperature of 121°C at pressures of at least 15 p.s.i. for 30 minutes for sterilisation and 70% methylated spirit was used to wipe equipment and vessels used in the hood. Cells were incubated in a Panasonic MCO-18AC-PE incubator. The incubator settings were 37°C with 5% CO<sub>2</sub> and 95% air. All plasticware were acquired from Thermo Fisher scientific (UK).

##### 2.1.1.1 Reagents

A complete list of reagents and the supplier information (including addresses) are listed in appendix 1. Culture media and vessels were purchased from Thermo Fisher scientific (UK). Oil Red 'O' Staining kit was purchased from Bio Vision (CA, USA). Trizol for RNA harvesting was purchased from Cambridge Bioscience. All molecular work reagents including primers were purchased from PrimerDesign. The flavonoids quercetin, chrysin, galangin, kaempferol, apigenin, luteolin as well as penicillin-streptomycin 10,000U/10 mg/ml respectively, biotin/pantothenate, 10x trypsin, 10x EDTA, phosphate buffered saline (PBS) tablets and 12 mM thiazolyl blue tetrazolium bromide were purchased from Sigma Aldrich. DMSO and ethidium bromide were acquired from Alfa Aesar (UK). Gel electrophoresis-Lambda ladder and 100 bp ladder were purchased from Promega (UK). Molecular grade agarose was purchased from Biorline (UK). HPLC reagents were sourced from Sigma-Aldrich (UK) unless specified. Lysis buffer reagents were acquired from Roche (Germany). BCA™ protein assay kit was purchased from Thermo Fisher scientific (UK).

##### 2.1.1.2 Equipment

General spectrophotometers used were the Thermo Scientific *MULTISKAN GO™* model and the rosys™ Anthos 2010. Work was centrifuged using the Sigma 3-16PK ultra acquired from Sigma Aldridge UK. RNA and cDNA were quantified using the "JENWAY" Genova Nano



spectrophotometer. RNA to cDNA conversion was done using a My Cycler™ thermocycler. Gene expression tests were run on an Applied Biosystems StepOne™ Plus PCR machine. HPLC analysis was conducted using a PERKINELMER® 'series 200 autosampler' using a Kinetex C<sub>18</sub> column (5 µm; 250 mm × 4.6 mm i.e., *Kinetex C<sub>18</sub> 100A*) acquired from Phenomenex® and an SPD-10A UV/VIS detector. Cell culture microscopy was carried out using the Nikon TMS microscope with a DS-Fi camera attachment. A Nikon Digital sight DS-LZ screen was used as the camera attachment for grid counting and photomicrograph capture. A Corning™ LSE 6L water bath was used for warming up media.

#### 2.1.1.3 Media

All media were sourced from Thermo Fisher scientific (UK), foetal bovine serum (FBS) was purchased from Seralab (UK). Roswell Park Memorial Institute 1640 (RPMI) media was used for all cell lines except the SGBS cells. This was made of 10% 10xRPMI concentrate, 77.5% distilled, deionised and autoclaved water, 1% 7.5% Sodium Bicarbonate, 1% 200 mM L-Glutamine, 10% Foetal Bovine Serum, 0.1% 50 mg/ml Gentamycin and sufficient 1M NaOH to turn the medium red (approx. pH 7.4). This was kept at 4°C and warmed in a water bath to 37°C before use.

Dulbecco's Modified Essential Medium and Ham's F-12 (DMEM/F12) 1:1 x1 was used to culture the SGBS cells. This was supplemented with 33 mM biotin, 17 mM pantothenate and 1% penicillin/streptomycin this was referred to as 'OF' according to Wabitsch (2001). For general culture 10% foetal bovine serum was added, this is herein referred to as OF+10% FBS. For initiating differentiation, OF media was supplemented with 2 µmol/l rosiglitazone, 25 nmol/l dexamethasone, 0.5 mmol/l methylisobutylxanthine, 0.1 µmol/l cortisol, 0.01 mg/ml transferrin, 0.2 nmol/l triiodothyronine, and 20 nmol/l human insulin. This media was replaced at day 4 with OF supplemented with 0.1 µmol/l cortisol, 0.01 mg/ml transferrin, 0.2 nmol/l triiodothyronine, and 20 nmol/l human insulin.

#### 2.1.1.4 Protein Lysis buffer

Lysis buffer was prepared using 10% Tris-buffered saline (TBS; 10×, pH 7.5), 0.5% 0.5M EDTA, 10% NP-40 (10%) and one EDTA-free complete protease inhibitor cocktail tablet (Roche, Mannheim, Germany) made up to 100% with double distilled water. The lysis buffer was aliquoted into sterile glass universal bottles and stored at 4°C.

### 2.1.2 SGBS Cell culture

SGBS cells were kindly gifted by Professor Martin Wabitsch (Department of Pediatrics and Adolescent Medicine, university of Ulm, Germany). SGBS cells were received at p28 (passage number 28) and sub-cultured first in 25 cm<sup>2</sup> flasks then in 75 cm<sup>2</sup> vessels, containing 0F + 10% FBS. Upon reaching 80-90% confluence cells were passaged following protocol set out by Wabitsch et al. (2001). This involved washing cells three times with 100 µl/cm<sup>2</sup> PBS after discarding spent media. Cells were incubated with 1 ml of trypsin EDTA solution for 3-5 minutes (10% 10xTrypsin, 10% 10xEDTA and 80% 1xPBS). After lifting the cells, the trypsin was neutralised with 9 ml 0F + 10% FBS. The cell suspension was transferred to a 15 ml falcon tube which was centrifuged at 1100 RPM (200 ×g) for 10 minutes at room temperature. The supernatant was removed and replaced with 10 ml of 0F +10%FBS media and mixed by pipetting repeatedly. A haemocytometer was used to count cells which were then seeded according to table 2.1 below.

Table 2.1 Seeding densities of SGBS cells in different vessel sizes for differentiation and routine culture.

<b><u>Vessel</u></b>	Media volume	Quantity of cells unless otherwise stated	
		<b>For differentiation</b>	<b>For routine culture</b>
Jumbo flask -175 ml	24 ml	x	3 - 4.5 x 10 <sup>5</sup>
T 75 flask	15 ml	x	1.35 x 10 <sup>5</sup>
T-25 flask	5 ml	x	4.5 x 10 <sup>4</sup>
10 cm (petri dish)	12 ml	3 x 10 <sup>5</sup>	3.2 x 10 <sup>5</sup>
6 cm dish	5 ml	1 x 10 <sup>5</sup>	1.6 x 10 <sup>5</sup>
6 well plate	2.5 ml	5 x 10 <sup>4</sup>	8 x 10 <sup>4</sup>
12 well plate	1.5 ml	4 x 10 <sup>4</sup>	4 x 10 <sup>4</sup>
24 well plate	1 ml	1 x 10 <sup>4</sup>	2 x 10 <sup>4</sup>
48 well plate	0.5 ml	5 x 10 <sup>3</sup>	1 x 10 <sup>4</sup>
96 well plate	0.2 ml	2.5 x 10 <sup>3</sup>	5 x 10 <sup>3</sup>

### 2.1.3 Cryopreserving SGBS cells

Cells were cryopreserved from 80-90% confluent flasks. This involved washing cells three times with 100 µl/cm<sup>2</sup> warm PBS after discarding spent media. Cells were incubated with 1 ml of trypsin EDTA solution for 3-5 minutes. After suspending the cells, a trypan blue cell

viability count was done before the trypsin was neutralised with 9 ml of growing media (OF plus 10% FBS). Only cells with greater than 95% viability were frozen. The cell suspension was transferred to a 15 ml Falcon tube and centrifuged at 1100 RPM (200 ×g) for 10 minutes at room temperature. The supernatant was removed, and the cells were resuspended at a concentration of  $1-2 \times 10^6$ /ml in OF +10%FBS media supplemented with 10% glycerol. This was mixed by repeated pipetting. The cell suspension in freezing media was aliquoted into 1.5 ml vials which were frozen in -80°C overnight in slow freezing chambers to be transferred to permanent storage in liquid nitrogen.

#### 2.1.4 Thawing SGBS cells from cryopreservation

Cells were thawed according to SGBS cells Protocol (Fischer-Posovszky et al., 2008). A vial of SGBS preadipocyte cells, frozen in liquid nitrogen gas phase was thawed out rapidly in a 37°C in a water bath for no more than 2 minutes. The content of the vial was re-suspended in 10 ml OF + 10% FBS and centrifuged for 5 minutes at 1100 RPM (200×g). The cell pellet was then resuspended in 10 ml OF + 10% FBS and transferred to a T25 flask. These were incubated at 37°C 5% CO<sub>2</sub> until the cells reached 80-90% confluence. The cells were then maintained by sub-culturing in vessels and densities shown in table 2.1 until passage number 50.

#### 2.1.5 Cell counting

The cells were counted microscopically using a Neubauer haemocytometer according to a modified version of the “Counting cells using a haemocytometer” protocol (Abcam, n.d.). A volume of 10 µl of cell suspension was injected under the cover slip of both grids of the haemocytometer in duplicate. A mean count was only accepted if all four counts were within 5 % of the mean.

#### 2.1.6 Trypan blue cell viability counts

Trypan Blue dye exclusion test was used to determine the number of viable cells present in a cell suspension. A volume of cell suspension was mixed with an equal volume of 0.4% trypan blue dye to obtain a 1 to 2 dilution. The mixture was incubated for less than 3 minutes and 10 µl was injected under the cover slips of both sides of a haemocytometer in duplicate. Cells were counted to give the number of clear and total cells. The percentage of viable cells was calculated by dividing the number of clear cells by the number of total cells and multiplying by 100.

### 2.1.7 Differentiation of SGBS cells

Differentiation of SGBS cells was performed according to the Fischer-Posovosky et al. (2008) protocol. SGBS cells were cultured in 6 or 12-well plates and T25 flasks using serum containing medium (OF) for 3 days. To induce differentiation, on day 0, cells were washed twice in warm phosphate buffered saline (PBS) solution and addition of serum free media referred to as quick differentiation (QD) media (DMEM/F12 (1:1) containing 1% penicillin/streptomycin, 1% pantothenate/biotin 0.01 mg/ml transferrin, 20 nM human insulin, 100 nM human cortisol, 0.2 nM triiodothyronine, 25 nM dexamethasone, 250 µM 1-methyl-3-isobutylxanthine and 2 µM rosiglitazone). Cells were cultured in QD media for a further 4 days. On day 4 of adipogenic differentiation QD media was removed, and cells were further cultured in serum free media supplemented with 1% Penicillin/Streptomycin, 1% Pantothenate/Biotin, 0.01 mg/ml transferrin, 20 nM human insulin, 100 nM human cortisol and 0.2 nM triiodothyronine without washing. Cells were cultured in this media for up to 28 days, with media changes every 4 days. The percentage of morphologically differentiated cells was determined after 7, 14, 21 and 28 days of adipogenic differentiation. Oil Red 'O' Staining was performed to visualise differentiation for microscopy and give relative quantification. Microscopic counting of the total number of cells and total number of differentiated cells was achieved by selecting 6 random cardinal points to give a mean well count. Oil Red 'O' was employed to semi-quantitatively measure the differentiation. Oil Red 'O' was extracted from the wells using 100% isopropanol. The extract absorbance was read on a microplate spectrophotometer at 492 nm with 100% isopropanol used as the blank or negative control.

### 2.1.8 Dedifferentiation of SGBS cells

Following 21 days of adipogenic differentiation cells were cultured using the ceiling method as described by Sugihara et al. (1986). To establish ceiling culture of adipocytes, cells were trypsinised, diluted to a volume 10 ml with serum containing media (F0) to 10 ml using a falcon tube and centrifuged at 852 RPM for 3 minutes. The top 2 ml from each tube was then seeded into a 25 cm<sup>2</sup> flask (T25) filled entirely with F0 media. Flasks were double sealed with sterile parafilm and inverted for 2 weeks. Following 14 days of incubation, inverted culture flasks were re-inverted, media was removed and replaced with 5 ml F0 to allow single colonies to grow. Media was then replenished every 4 days.

### 2.1.9 Differential cell counts

Microscope counts of total and differentiated cells were carried out on cells growing in 6, 12 and 24 well plates. An inverted Nikon TMS microscope with a DS-Fi camera attachment was used in conjunction with a Nikon Digital sight DS-LZ display screen. The grid function comprising 10x7 squares was used with a scale of 10 squares = 10000  $\mu\text{m}$ . The microscope was set to x100 magnification for cell counting. Each well was counted 6 times from randomly selected cardinal points and a mean count was derived.

Differentiated adipocytes and total cells were counted in each grid square. Cells with 3 or more lipid droplets per cell were considered to be differentiated. The size or shape of the lipid droplets were not considered.

### 2.1.10 3-(4,5-dimethylthiazol-2-yl)-2,5-diphenyltetrazolium bromide (MTT) Assay

Cells were grown in media volumes of 200  $\mu\text{l}$ /well in 96 well plates. Following periods of incubation (with or without a test substance) the cells were treated with 20  $\mu\text{l}$ /well of 12 mM MTT in PBS and incubated at 37°C, 5% CO<sub>2</sub> and protected from light for 2.5 hours. Following the incubation period, the supernatant media was removed and 100  $\mu\text{l}$  of DMSO was added to each well and the contents were mixed thoroughly by repeatedly pipetting. Using the MANTA Anthos 2010 software or the Thermo Scientific Multiscan GO microplate spectrophotometer, the absorbance of each well was measured at a wavelength of 570 nm with 620 nm background subtraction.

### 2.2 HPLC

Glucuronides from conditioned media were quantified using High-performance liquid chromatography (HPLC). Absorbance was measured at 370 nm. The mobile phases consisted of Acetonitrile (ACN) with 0.1 % trifluoroacetic acid (TFA), and triple distilled water with 0.1 % (TFA) (20:80; v/v) at a flow rate of 1.5 ml/min and a temperature of 40°C. DMSO, which was the solvent used to dissolve the flavonoid, and triple distilled water were used as background subtraction.

### 2.3 Oil red "O" staining for lipid quantification.

Stock solution for oil red "O" was made by dissolving 0.7 g Oil Red O in 200 ml Isopropanol (3.5 mg/ml). This was mixed well by vortexing for 5 minutes and filtered through a 0.2  $\mu\text{m}$  filter. The stock solution was stored at 4°C. Oil red "O" working solution was prepared by diluting 6 parts of Oil Red O Stock with 4 parts of H<sub>2</sub>O. This was mixed by vortexing and allowed

to stand for 20 min. This was then filtered through a 0.2 µm filter using a syringe and syringe filter.

Cell fixation was achieved using paraformaldehyde (PFA). A stock solution of 37% Paraformaldehyde (w/v) was made by dissolving 37 g of PFA in 100 ml of PBS. This was mixed in a water bath at 60°C and cooled to be stored at 4°C. A working solution of 3.7% was made by a 1:10 dilution of the 37% PFA in PBS. After spent media was aspirated and discarded, each well was flooded with the volume of PFA working solution stated in table 2.2. The plates were incubated for 10 mins at room temperature. The PFA was removed and replaced with fresh PFA working solution. The vessel was wrapped in parafilm and aluminum foil and incubated for at least an hour. After incubation, The PFA was completely removed, and wells washed once with 60% isopropanol. Wells were left in the fume hood to dry completely after which oil red “O” working solution was added and incubated for 10 mins at room temperature. After removing the oil red O, water was added immediately. This was followed by 4 washes of a gentle stream of tap water. Photographs were taken whilst the cells were still covered in water. The water was removed, and plates were air dried in a fume hood. The stain was eluted using 100% Isopropanol which was incubated for 10 mins at room temperature. After incubation, the stain was pipetted up and down and transferred to 1.5 ml Eppendorf tubes. Quantification was achieved by adding the eluted stain to 96 well plates in replicates and measuring absorbance at 550 nm. Three controls were used, a blank of 100% isopropanol, a stained empty well and a stained well of Preadipocytes.

Table 2.2. Vessel dependent volumes used for Oil red “O” staining.

<b>Plate</b>	<b>Formalin</b>	<b>60 % Isopropanol</b>	<b>Oil Red O</b>	<b>100 % Isopropanol</b>
24-well	500 µl	500 µl	200 µl	200 - 700 µl
12-well	1 ml	1 ml	400 µl	400 - 1000 µl
6-well	2.4 ml	2.4 ml	1 ml	1000 - 3000 µl

## 2.4 Triglycerides extraction quantification

### 2.4.1. Triglycerides extraction.

Cells growing in 12 well plates had spent media aspirated and discarded in a fume hood. A volume of 500  $\mu$ l of Hexane/Isopropanol (3:2) was added and incubated for 1 minute. This was gently pipetted up and down (without disturbing the adherent cells) and the triglycerides in solvent were transferred to a labelled Eppendorf tube. An additional 500  $\mu$ l of Hexane/Isopropanol (3:2) was added to the same well and incubated for 1 minute and the triglycerides in solvent were added to the same Eppendorf tube. The Eppendorf tubes were evaporated in a vacuum evaporator (Speedvac) at 30°C for 45 minutes.

### 2.4.2. Triglycerides quantification

Quantification was performed according to the ab65336 Colorimetric Triglyceride Quantification Assay Kit (Abcam, Germany). All materials and reagents were equilibrated at room temperature. Reaction wells were set in a 96 well plate such that there were 50  $\mu$ L of standards, and 2 - 50  $\mu$ L of samples which were adjusted to a volume of 50  $\mu$ L/well with Triglyceride Assay Buffer. To sample and standard wells, 2  $\mu$ L of lipase was added followed by agitation and incubation for 20 mins at room temperature to convert any triglyceride to glycerol and fatty acid. A volume of 50  $\mu$ L of Triglyceride Reaction Mix was prepared for each reaction. This was prepared from a master mix for consistency. The master mix was prepared by adding 92% Triglyceride Assay Buffer, 4% Triglyceride Probe and 4% Triglyceride Enzyme Mix. After adding 50  $\mu$ L of the Reaction Mix into each standard and sample, the wells were incubated at room temperature for 60 minutes whilst covered away from light. The absorbance of the wells was read at 570 nm. A calibration curve was made from the standards and used to determine the quantity of triglycerides in the sample.

## 2.5 Protein harvesting, purification, and quantification

Protein quantification was achieved using the Pierce™ BCA Protein Assay Kit. Cells were washed in cold PBS and complete lysis buffer was added (100  $\mu$ l for 6 well plates and 67  $\mu$ l per well in 12 well plates). Cells were retrieved using a plastic scraper and pipetted into labelled Eppendorf tubes. Wells of replicates were pooled into one Eppendorf tube. Tubes were placed in ice for 30 minutes. They were then centrifuged at 14000 rpm in precooled microcentrifuges at 4 °C. Tubes were then stored in -80°C.

Five bovine serum albumin (BSA) protein standards were made with a range of 5 to 100 µg protein. Unknown (test) proteins were diluted so that the resultant concentrations were 5-100 µg protein/30 µl. Test tubes for standards and test samples were labelled and 30 µl each of standard solution or unknown protein sample were added. These were made in duplicates. A volume of 1.5 ml of Bradford reagent was added to each tube and mixed well by vortexing. These were incubated at room temperature for 5 mins. A volume of 200 µl samples and standards were transferred into a 96 well plate and absorbance was measured at 595 nm. A standard curve was plotted using the controls in the inbuilt software to give the derived absolute quantities for the test protein. Further dilutions were made for samples whose values were outside the calibration range.

## 2.6 Western Blotting

Protein levels for treated and control cells were assessed by Western blotting. Cells were washed with ice-cold PBS and total protein was extracted by scraping cells in a lysis buffer (10 mM Tris-HCl at pH 7.5, 150 mM sodium chloride, 2 mM EDTA, 1% TX-100, 10% glycerol, 1X complete Protease Inhibitors (Roche, Mannheim, Germany)). Protein concentrations were determined with the BCA™ protein assay kit (Pierce). For immunodetection, 10–20 µg of protein were separated by SDS-PAGE on Bolt Bis-Tris Plus Gels (ThermoFisher Scientific) and transferred to nitrocellulose membranes by Western Blotting (ThermoFisher Scientific). Membranes were blocked for 1 hour in PBS supplemented with 5% milk powder and 0.1% Tween 20. Membranes were stained overnight at 4°C with the first antibody, followed by 1-hour incubation with the horseradish peroxidase-conjugated second antibody. After antibody incubation steps, band intensity was detected using chemiluminescence (Amersham) according to manufacturer's directions, imaged and quantified using online ImageJ software.

## 2.7 RNA harvesting, extraction, purification and quantification.

Cells were grown and treated in 12 well plates with seeding densities and media volumes described in 2.1.2. Experimental conditions were performed in triplicate (3 wells having the same experimental conditions). Plates were placed on ice and spent media was aspirated. A volume of 500 µl of trizol (phenol) was shared in the 3 wells (approximately 167 µl per well) and left to incubate for 5 minutes at room temperature. After incubation the phenol was pipetted up and down in each well and the 3 wells pooled together into one pre-cooled labelled Eppendorf tube. The tubes were immediately frozen at -80°C ready for extraction, quantification, and cDNA conversion.



RNA was extracted from the frozen cells in trizol using the Primerdesign™ genesig® Easy DNA/RNA Extraction Kit. Purification of the RNA was integral to the extraction process, proteinase K (Tritirachium alkaline proteinase) was used to denature the proteins according to the manufacturer's protocol. Genesig® Carrier RNA was used to optimize RNA yield. Genesig® Easy Binding buffer/magnetic bead mix and a magnetic rack were used as the basis of separation.

The nanodrop, (Genova Nano spectrophotometer) was used to quantify the RNA yield. A volume of 2 µl of the elution buffer was used to zero the spectrophotometer and the same volume of sample was measured. Comparative quantifications were achieved by using UV spectroscopy. Purity was ascertained using the A260/A280 ratio with a ratio of 2<sup>±</sup> 0.5 being acceptable. All procedures were carried out with samples placed on ice.

### 2.8 Conversion of RNA to cDNA

Conversion of RNA to DNA was achieved using Primerdesign Precision™ nanoScript 2 Reverse Transcription kit. The RNA template used ranged from 1 ng to 2 µg. The protocol employed two manual stages, the annealing and extension steps. Thermocyclers and heating blocks were used for the sample heating steps. At the end of the extension step, reactions were heat inactivated by incubating samples at 75°C for 10 minutes. Samples were stored at -20°C until they were used

### 2.9 qPCR

All the primers were designed by Primerdesign™, and gene expression experiments were conducted according to the manufacturer's direction. The SYBR® green gene detection kit was used for all qPCR work. Hypoxanthine Phosphoribosyl transferase (HPRT) primer was used as the reference gene. An equal volume of RNase/DNase free water was used as the negative (no template) control. Gene expression tests were run on the Applied Biosystems StepOne™ Plus PCR machine using Primerdesign™ microplates. All runs were taken through 40 cycles. The temperature settings were 95°C for 2 minutes on the Enzyme Activation step, 95°C for 10 seconds on the denaturation step and 95°C for 1 minute on the data collection step. Reaction microplates were kept at 4 °C after the reaction and results capture in case gel electrophoresis was needed. Relative quantification was calculated using the standard  $2^{-\Delta\Delta Ct}$  formula.

## 2.10 Statistical analysis

Results were expressed as the mean  $\pm$  SD for the number of assays indicated for bar charts and line graphs. Analyses were performed with Microsoft Excel with Daniel's XL Toolbox add-in. For multiple comparisons of groups statistical significance was calculated and evaluated by one-way ANOVA followed by Tukey post-hoc test. To compare two groups, two-tailed paired Student's t-test was used. Logarithms of concentrations were used to derive IC<sub>50</sub> values of flavonoids to enable quantifiable comparisons and ranking. Correlation between comparative measures of differentiation were achieved by calculating the R<sup>2</sup> correlation coefficient in Excel.

### 3 Adipocyte Proliferation

#### 3.1 Introduction

Cell proliferation occurs when a cell population increases as a result of growth and division. It is the net gain from the balance between cell divisions and cell loss through cell death or differentiation. Unlike in single cellular organisms, proliferation of cells in multicellular organisms is tightly regulated by a network of genes, transcription factors and the pericellular microenvironment. Detecting and measuring cell proliferation is necessary and important for monitoring cell vitality and assessing the impact of test substrates on the life cycle of a cell. Decrease in proliferation is often associated with an increase in cell cycle variability and generation of non-dividing cells (Brooks & Riddle, 1988; Granada et al., 2020; Brooks, 2021). The increased variability during compromised proliferation can be a result of the presence of two classes of cells, the dividing and non-dividing siblings. When a greater proportion of cells drop out of cycle in each generation, it will lead to a growth fraction of significantly less than 1.0; growth fraction being the percentage of cells actively dividing in a given population at a given time. Low presence of growth factors leads to a decrease in the proliferation of a cell population. Conversely, high levels of growth factors translate to higher proliferation and shorter doubling times. Cell populations with high growth factors respond better to test substrates such as substances used to inhibit cell growth or chemotherapy for cancer cells for example.

The animal cell cycle has distinct stages whose duration varies with species and the microenvironment of the cell. The basic stages of a cell cycle are; gap one (G1) where the cell increases in size, the synthesis stage (S) where the cell copies its DNA, gap two (G2) where the cell prepares to divide and mitosis (M) where the cell divides into daughter cells. After mitosis, cells can either go into the next round of synthesis or it would go into the quiescence or dormancy stage (G0). The stages G1, S, and G2 are collectively the interphase, which accounts for the span between cell divisions. The commitments to either cell cycle progression or quiescence are thought to be mutually exclusive (Matson and Cook, 2017). It is also known that cells can move away from the G0 stage and continue into the interphase whilst some either terminally differentiate or continue with cellular functions such as producing proteins, until cell death. There are various molecular states that distinguish between quiescent cells and cells committed to S phase entry and these states can be

investigated using gene expression techniques and protein assessment protocols such as Western blots.

It has also been suggested that inhibitory substances to cell proliferation alter the average cycle time by elongating the minimum cell cycle and G0 quiescence (Brooks & Riddle, 1988). This often results in the formation of binucleate cells caused by the increased failure of cytokinesis. Binucleate cells can be visualised through staining and microscopy. Formation of binucleate cells has also been associated with the move from proliferation to differentiation (Windmueller et al., 2020; D'amato, 1989). The presence of binucleate cells in a cell population can sometimes account for the mismatch between reduced cell counts against increased cell component markers. The same can also arise from hypertrophy (increased cell size). Cell population growth can be the result of hypertrophy or hyperplasia (increase in cell number), two distinct processes which can occur simultaneously. This is not always pathological as in cancer but can be normal physiology with such an example as hormonally induced increase in size and number of the cells of the uterus during pregnancy. Hypertrophy in a cell population can be assessed by measuring cell size using microscopes with an eyepiece graticule. Staining cells can also give a visual distinction between normal and hypertrophic cells. In hypertrophy, there is enlargement of the cytoplasm and an increase in organelle number and size. Any test which seeks to quantify cells by measuring proteins or genes associated with the organelles may give an incorrect result due to hyperplasia. An example is the case of megamitochondria where hypertrophy of the mitochondria may give a high reading in an MTT assay which can be misconstrued as an increase in cell number. To distinguish hyperplasia from hypertrophy tests such as MTT, Resazurin, NRU and SRB assays need supporting cell counts or microscopy staining. The challenge however is that the two often occur simultaneously.

A further increase in the population of non-dividing daughter cells can be correlated to the decrease of cell growth factors confirming the reduction in proliferation. The opposite can be argued; an increase in proliferation correlates to an increase in growth factors, reduction in cell cycle variability and increase in dividing cell population. For adipocytes, absence of growth factors gives way to the presence and increase in differentiation factors. This suggests that proliferation and differentiation are mutually exclusive (Olson, 1992). An increase or decrease in proliferation would therefore impact on the available cells for differentiation and the abundance of differentiation factors.

Human preadipocytes, like most mammalian cells are subject to a series of tightly regulated molecular events controlling DNA replication and mitosis. Many proliferation signalling processes are intrinsically linked to the first gap (G1) phase of the cell cycle. This is the phase between the end of mitosis and beginning of the synthesis (S) phase where the cell grows in size and synthesizes mRNA and protein that are required for DNA synthesis. The G1 phase is, among others, controlled by the retinoblastoma (RB) pathway. Work by Duronio and Xiong (2013) identified that Delta-like 1 homolog (Dlk1) (also known as Preadipocyte factor 1 [Pref-1]) inhibits preadipocyte proliferation by regulating their entry into the G1/S-phase of the cell cycle. Many genetic signatures associated with proliferation exist, these depend on the type of cell but include some phylogenetically conserved genes and proteins that can indicate the presence, increase or decrease of proliferation. Marker of proliferation *Ki67*, proliferating cell nuclear antigen (PCNA), and mini chromosome maintenance (MCM) proteins are some of the prototypic markers of proliferation (Juríková *et al.*, 2016). The expression of genes that code for these proteins or the fully formed proteins themselves can be used to compare proliferation levels, but these approaches, whilst accurate, are expensive and often need dedicated equipment for analysis. There are other cheaper assays that can be used to quantify proliferation. Examples are BrdU Assay, EdU Assay, MTT Assay, XTT Assay, WST-1 Assay, Luminescent ATP Assay, *Ki67*, CFSE, Live/Dead Assays and Trypan Blue. These assays though relatively cheap with shorter turnaround times, would need confirmatory tests like microscopy cell counts and cell dimension measurements.

Cell line responses to external factors have been historically measured for viability and proliferation using the reduction of tetrazolium salts (Braicu, 2010). The MTT (3-(4, 5-dimethylthiazolyl-2)-2, 5-diphenyltetrazolium bromide) assay is one where metabolically active cells reduce the salt by dehydrogenase enzymes to produce water insoluble formazan which when dissolved in DMSO can be measured spectrophotometrically with an absorbance maximum near 570 nm (Riss *et al.*, 2016; Petty *et al.*, 1995). This assay measures cell viability in terms of reductive activity as enzymatic conversion of the tetrazolium compound to water insoluble formazan crystals by dehydrogenases occurring in the mitochondria of living cells. Reducing agents and enzymes located in other organelles, such as the endoplasmic reticulum, are also involved (Lu *et al.*, 2012; Stockert *et al.*, 2012). The MTT assay is an example of a semi quantitative cytotoxicity assay because it gives the qualitative attribute of presence of viable cells whilst providing a relative measure of the level of viability in the cell population.

Developed by Mosmann (1983), the MTT assay has become the gold standard for cell viability and proliferation studies (Iqbal and Keshavarz, 2017).

The MTT assay comes with its demerits. Ganapathy-Kanniappan et al. (2010) showed that glycolysis inhibitors, if generated in the assay, will interfere with the MTT assay. Test substances should therefore not be known to induce the production of glycolysis inhibitors such as 3-bromopyruvate. Another limitation of the MTT assay is that tetrazolium-based assays express interactive reactions with phytochemicals (Wang et al., 2010). This may bring artefacts when investigating polyphenols. The basis of the MTT assay is organelle derived enzymes whose volume can increase with an increase in cell number or cell activity. This can therefore give misleading results if it is used to estimate the number of cells in a population. These are a few examples of the limitations of the MTT assay which if known, can lead to mitigating protocols that reduce the impact of the artefacts produced by the limitations. Alternately, there are merits in using MTT as a cytotoxic or viability assay. These include ease and rapidity of performance, result reproducibility and correlation between MTT results and cell counts. Work by Jiao et al. (1992) also demonstrated a clinical correlation between in vitro and in vivo testing. This qualifies the MTT assay as an inexpensive but relevant test protocol to evaluate the effect of flavonoids on adipocyte proliferation especially when the results are backed by cell counts.

Microscopic cell counts are a convenient way of enumerating cells to decide whether a cell population has increased, stayed the same or decreased. Light microscopy is relatively cheap, simple to use and has a rapid result output. With the correct graticules, cell counts can easily be achieved whilst at the same time cell morphology can be seen. By adding some dyes such as the trypan blue stain it also possible to clearly distinguish between live and dead cells. Better still, with phase contrast microscopy, an experienced eye can see dead cells from live ones. Microscopic cell counts can be achieved by using the haemocytometer or by directly observing the cells in their transparent growing vessels. Larger vessels (flasks) benefit from inverted microscopes. The greatest challenge to microscopic cell counts is the variability of counts between users, and this is also correlated to the halo effect bias where the operator will tend to see the cell numbers in the order of their expectations. This can be reduced by blind labelling flasks or slides where possible. Furthermore, microscopic cell counts for cultures which need to continue incubation after counting often demand that flasks or well plates are removed from the incubator for long periods which affects growth patterns for

subsequent protocols and tests. Whilst very expensive, a way around this is to have multiple parallel running plates/flasks to minimise growth disruptions.

MTT assay results can also be confirmed by molecular tests. This stems from the notion that there are some genes which are preferentially expressed during proliferation but suppressed upon induction of differentiation or during cell senescence or death. An example is the peroxisome proliferator-activated receptor gamma (PPAR $\gamma$ ) gene whose expression without ligand modulation promotes proliferation at the expense of differentiation (Desai *et al.*, 2008). Another gene whose expression can be indicative of the stage of preadipocytes is the Glyceraldehyde 3-phosphate dehydrogenase (GAPDH) housekeeping gene which tends to be upregulated during differentiation (Guo *et al.*, 2012). Molecular techniques such as real time qPCR to quantify the resultant transcribed mRNA can be used to validate MTT assay results. They are also important in charting the molecular pathway by which the cells increase/decrease proliferation, meet their committal fate or dies. With the MTT assay, microscopic cell counts, protein assays and molecular protocols, it possible to assess the impact of the flavonoids on the viability of adipocytes.

Dietary flavonoids are known to have a wide range of pharmacological potency which include anti-inflammatory, antitumor, antiviral, antidiabetic, and anti-adipogenic effects on mammalian cells. Whilst a broad spectrum of flavonoid classes which include but not limited to flavonols, flavones, flavan-3-ols, flavanones, anthocyanins and isoflavones, much interest has built around two subclasses; flavonols and flavones because of their dietary significance and bioavailability. Examples of flavonols are quercetin, galangin and kaempferol whilst flavones have examples such as chrysin, luteolin and apigenin. Whilst many studies have looked at these flavonoids, little is known about how each flavonoid impact on the viability and proliferation of Preadipocytes and how the different subclasses and specific flavonoid structures relate to the growth of preadipocytes.

### 3.1.1 Aim

The aim of this chapter is to establish the effect of the flavonoids quercetin, galangin, kaempferol, chrysin, luteolin and apigenin on the growth of Preadipocytes in vitro. The chapter looked at the impact of a range of concentrations for each flavonoid on model preadipocytes. It also investigated the effect of combining a selection of concentrations of flavonoids from the two flavonoid subgroups on the growth and viability of two cell

line/strains representing preadipocytes. MTT assays and supporting microscopic cell counts were used to evaluate and compare the impact.

### 3.1.2 Objectives

- To establish optimal growth time for preadipocytes to induce the greatest flavonoid impact.
- To establish a workable concentration range for flavonoid treatment.
- To test each of the six flavonoids (singular) on pre-adipocyte cells using the MTT assay and supporting cell counts.
- To test flavonoid combinations from flavonol and flavone sub-classes on pre-adipocyte cells using the MTT assay and supporting cell counts.
- To rank the flavonoids according to their efficacy.

## 3.2 Method

### 3.2.1 Cell culture

Cells were cultured according to the protocol mentioned in 2.1.2 and 2.1.7. The passage level range for 3T3 was between 30 and 45 (p30 - p45), they were treated after at least two passage levels from thawing off cryopreservation. The thawed ampule was washed once in 10x the volume of complete media then centrifuged at 150 x g for 5 minutes to remove the freezing medium. SGBS cells ranged from passage 31 to passage number 40 (p31 - p40), they were treated at least one passage level after cryopreservation. SGBS cells were not washed and centrifuged after thawing but were diluted in 10x the volume of media to render the freezing media ineffective.

### 3.2.2 MTT assays

The MTT stock solution was made by dissolving MTT powder in Dulbecco's Phosphate Buffered Saline (pH = 7.4) to 5 mg/ml. The solution was filter sterilised through a 0.2 µM filter into a sterile and light protected medical flasks. This was further aliquoted to light protected universal bottles which were stored at 4°C for frequent use or at -20°C for long term storage.

Cells were seeded at a density of 5000 cells/well in 96 well plates and incubated overnight at 37°C with 5% CO<sub>2</sub> to adhere. Each treatment had eight replicates. Cells were then treated with different concentrations of flavonoid (or flavonoid combination) up to a volume of 200 µl/well and incubated for 72 hours. A volume of 20 µl, 5 mg/ml MTT Solution was added into



each well to achieve a final concentration of 0.45 mg/ml. This was incubated for two and a half hours at 37°C. All the spent media was gently siphoned out using a vacuum pump set at 0.1 bars and 100 µl of DMSO was added to each well and thoroughly mixed using a micropipette. The plates were read on a spectrophotometer at 570 nm. Data was used to plot line graphs and bar charts with values representing the mean relative cell growth as a percentage of control and standard deviation used for error bars. Data was used to calculate the IC<sub>50</sub> for each substance and substance combination. Relative cell growth was calculated using the formula:

$$\text{Relative cell growth (\% of control)} = \frac{\text{Absorbance of treated well} - \text{Absorbance of medium blank well}}{\text{Absorbance of vehicle control well} - \text{Absorbance of medium blank well}} \times 100$$

### 3.2.3 Solvent Choice

The solvents Dimethyl sulfoxide (DMSO), Dimethylformamide (DMF) and ethanol (EtOH) were tested for impact of concentration on the results of MTT assays and flavonoid cell treatments. Serial dilutions of DMSO, DMF and EtOH solvents were made with standard RPMI medium to achieve final concentrations between 50% and 0.02% in two-fold serial dilutions. This solvent in media range was used to culture 3T3-L1, L929, CACO2 and SGBS cells at a density of 5 x 10<sup>3</sup> cells in 96 well plates over a period of 72 hours. The 3-(4,5-dimethylthiazol-2-yl)-2,5-diphenyltetrazolium bromide (MTT) assay was used to measure cell viability. Concentrations which appeared not have any impact on cell viability were tested in the presence of the flavonoid quercetin and compared to solvent free controls. Student t tests were used to ascertain the statistical differences between the compared pairs.

### 3.2.4 Growth Curves

For optimal cell density determination, cells were seeded in 96 well plates in eight-fold replicates on three repeats. Cells were seeded at densities of 2500, 5000, 7500, 10000, 12500, 15000, 17500 and 20000 per well. These were incubated for 18 hours and an MTT assay was performed on the plates. Data was visually presented as line graphs with data points of mean absorbance and error bars were made from standard deviations.

Time course experiments to determine the log phase of cell growth were performed by seeding 5000 cells per well in seven 96 well plates. These were incubated and an MTT assay performed on one plate every 24 hours to give 24, 48, 72, 96, 120, 144 and 168- hour time points. The experiment was performed three times. Data from the absorbance readings were

plotted on a line graph with data points of mean absorbance and error bars being standard deviations.

### 3.2.5 Microscopic counts

Cell counts performed on a Nikon Digital sight DS-LZ screen camera attachment for grid counting and photomicrograph capture. Counts per well for 6 and 12 well plates were performed on a minimum of six cardinal points of the well. These were the; centre, north, east, west, south and the north-east edge of every well. For plates which needed to be further incubated after the counts, counting was done for a period not exceeding 20 minutes before returning to the incubator.

Trypsinised cells were counted using a Neubauer haemocytometer. Cells were diluted appropriately so that a single cell configuration was established. The right side and bottom grid lines were excluded from the counts. The trypan blue assay was used whenever it was necessary to distinguish dead cells from living cells as described in 2.1.4. The percentage of viable cells was calculated by dividing the number of clear cells by the number of total cells and multiplying by 100. Recorded cell counts were derived using the formula below:

$$\text{Total cells/ml} = (\text{Total cells counted} \times \text{Dilution factor} \times 10^4 \text{ cells/ml}) / \text{Number of squares counted}$$

### 3.2.6 Single flavonoid treatment

Flavonols quercetin, galangin and kaempferol and flavones chrysin, luteolin and apigenin were tested for their effect on viability or proliferation of preadipocytes. Flavonoids were dissolved in DMSO to achieve a stock concentration of 50 mM. Aseptic techniques were adhered to for the preservation of sterility throughout the preparation. Dissolution was expediated by warming up the DMSO in water bath to 37°C. These were aliquoted into ampules or Eppendorf tubes of 100 µl and frozen at -20°C. Working concentrations were made fresh on the day by diluting the stock solutions in media to achieve the desired concentration. The final DMSO concentration on the working concentrations was no greater than 1%. Experimental concentrations ranged from 200 µM to 1 µM. Controls of no treatment (0 µM) and DMSO vehicle control were used. Experiments were carried out in triplicate with replicates of 8 wells for every condition in each MTT experiment. Cell count experiments in 12 well plates were performed in triplicate with replicates of 3 wells for every condition of proliferation cell counts.

For MTT assays, 96 well plates were seeded with  $5 \times 10^3$  cells per well and incubated overnight. After cells had adhered, they were washed with warm serum free media. Warm complete medium (F0) containing the right concentration of test flavonoid was added to each well and incubated for 72 hours. A volume of 20  $\mu$ l, 5 mg/ml MTT solution was added into each well and the plate was incubated for two and a half hours at 37°C. A representative of sample photomicrographs was taken before the removal of the MTT treated spent media and addition of 100  $\mu$ l of DMSO. The plates were read on a spectrophotometer at 570 nm.

Cell counts to assess viability and proliferation after treating with single flavonoids were carried out in 12 well plates. Cells were seeded to a density of  $2 \times 10^4$  cells per well in triplicates and incubated in F0 overnight. After the cells had adhered, they were washed with warm serum free media. Warm complete medium containing the right concentration of test flavonoid was added to each well and incubated for 72 hours. Counts per well were performed on a minimum of six cardinal points of the well. These were the; centre, north, east, west, south and the north-east edge of every well. For plates which needed to be further incubated after the counts, counting was done for a period not exceeding 20 minutes before returning to the incubator.

### 3.2.7 Combined flavonoid treatment

The effect of combining flavones and flavanols were tested at similar concentrations as the singular flavonoids. Working solutions were made fresh from frozen flavonoid stocks. Desired final concentrations were made for each flavonoid in combinations shown in the table 3.1. Each flavonoid was made at double the concentration and mixed at half the flavonoid volume to achieve the final flavonoid combination concentration according to Mertens-Talcott (2003). Combination mixtures of flavonoids in media were made in sealable test tubes and vortexed for 1 minute and added to wells containing cells. Remaining flavonoids in media were kept for an hour to make sure there was no precipitation out of solution. Cells were treated with serum free media for 6 hours and then spent media was vacuum syphoned from the wells and immediately replaced with flavonoid treated media at the correct concentrations. Incubation, MTT assays and microscopic cell counts were carried out in the same fashion as described in 3.2.6. above.

Table 3.1 Flavonoid combinations where the flavanols quercetin, galangin and kaempferol were mixed to the flavones chrysin, apigenin and luteolin.

		<b>Flavanols</b>		
		<b>Quercetin</b>	<b>Galangin</b>	<b>Kaempferol</b>
<b>Flavones</b>	<b>Chrysin</b>	X	X	X
	<b>Apigenin</b>	X	X	X
	<b>Luteolin</b>	X	X	X

### 3.2.8 Comparative treatments with 3T3-L1 cells

Effects of flavonoids on non-human preadipocytes were studied using 3T3-L1 cells and compared to SGBS cells. Flavonoids quercetin and chrysin were used to compare 3T3-L1 cells to SGBS cells. Flavonoids were dissolved in DMSO to achieve a stock concentration of 50 mM. Aseptic techniques were adhered to for the preservation of sterility throughout the preparation. Working concentrations used for 3T3-L1 cell lines mirrored those used on SGBS cells for comparison. Experiments were carried out in triplicate with replicates of 8 wells for every condition in each MTT experiment. Cell count experiments in 12 well plates were performed in triplicate with replicates of 3 wells for every condition of proliferation cell count. MTT assays and cell count experiments were carried in a similar fashion as described above in 3.2.5.

### 3.2.9 Statistical analysis

Results were expressed as the mean  $\pm$  SD for the number of assays indicated. Analyses were performed with Microsoft Excel with Daniel's XL Toolbox add-in (<https://www.xltoolbox.net>). For multiple comparisons of groups statistical significance was calculated and evaluated by one-way ANOVA followed by Tukey post-hoc test. To compare two groups, two-tailed paired Student's t-test was used. Logarithms of concentrations were used to derive IC<sub>50</sub> values of flavonoids to enable quantifiable comparisons and ranking. To calculate the IC<sub>50</sub>, flavonoid concentrations were plotted on the x-axis against normalised MTT absorbance percentage readings which formed a sigmoidal curve. The concentration which corresponds to the 50% absorbance value was taken as the IC<sub>50</sub>. For microscopic cell counts, logarithms of flavonoid concentrations were plotted on the x-axis against normalised cell count percentage readings

and a line of best fit was derived. The  $IC_{50}$  was then calculated from the equation of the line by finding the x value when  $y=50$ . The antilogarithm of the X value was taken as the  $IC_{50}$  value. Correlation between measures of differentiation was determined by calculating the  $R^2$  correlation coefficient in Excel.

### 3.3 Results

#### 3.3.1 Standard curves

Time course experiments to determine optimum growth duration using the MTT assay showed that optimal growth at approximately 72 hours. SGBS cells were seeded at a density of  $5 \times 10^3$  cells/well and incubated for periods between 24 and 144 hours. MTT assays were carried out at the end of every time point and the results show a sigmoidal increase. Although showing a marginal increase, there was no significant difference between 120 and 144 hours.

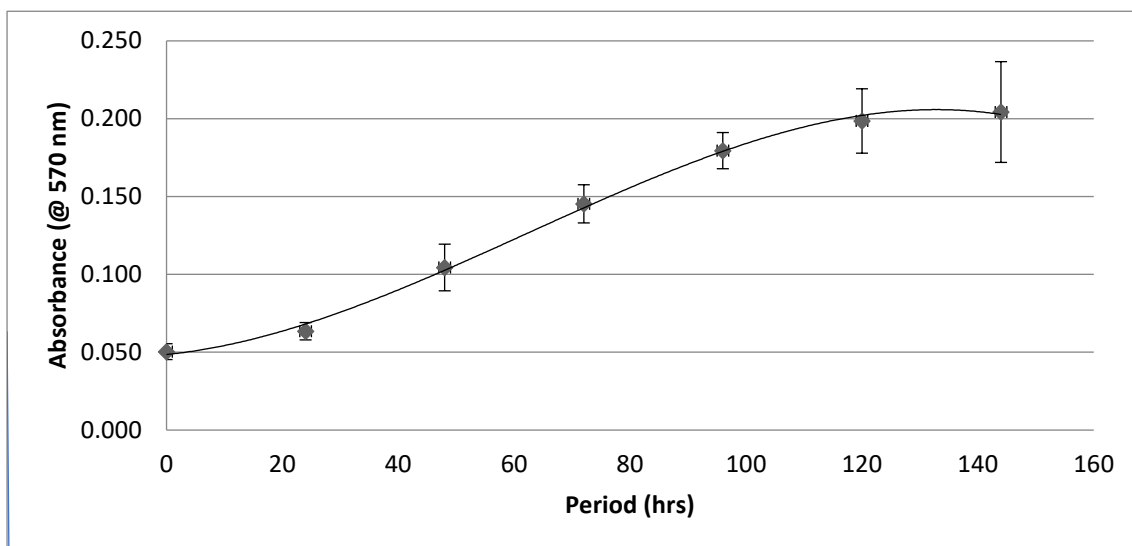


Figure 3.3.1.1 Time course growth curve showing optimal growing time of 72 hours as shown by the point of inflection. Cells were seeded at densities of  $5 \times 10^3$ /well and incubated for periods ranging from 24 to 168 hours. MTT assays were carried out in turn and resultant absorbances were plotted against time. Data points indicate mean ( $n=36$ ) and error bars were standard deviation. The correlation coefficient ( $R^2=0.99$ ) of the sigmoidal growth curve showed a significantly high positive correlation. There was greater variability however at longer periods of incubation as shown by the increase in error bar size.

Multiple viability curves were constructed using SGBS cells with different passage numbers and the passage numbers of the pooled cells used for each curve differing by less than five. Figure 3.2 shows a typical viability curve for seeding densities ranging from 2500 cells to 200 000 cells/well for SGBS cells at passage 36. The absorbances after 24 hours ranged from 0.02 to 0.8 AU. Linearity was strongest between seeding densities of 5000 cells and 20 000 cells/well with a correlation coefficient ( $R^2$ ) value greater than 0.997. Higher densities had greater variability and reduced relative viability. Observations confirmed that at higher seeding densities, cells were less adherent and could be lost during MTT and spent media removal. The results confirmed the viability of SGBS cells at the passage levels and seeding densities used in subsequent experiments.

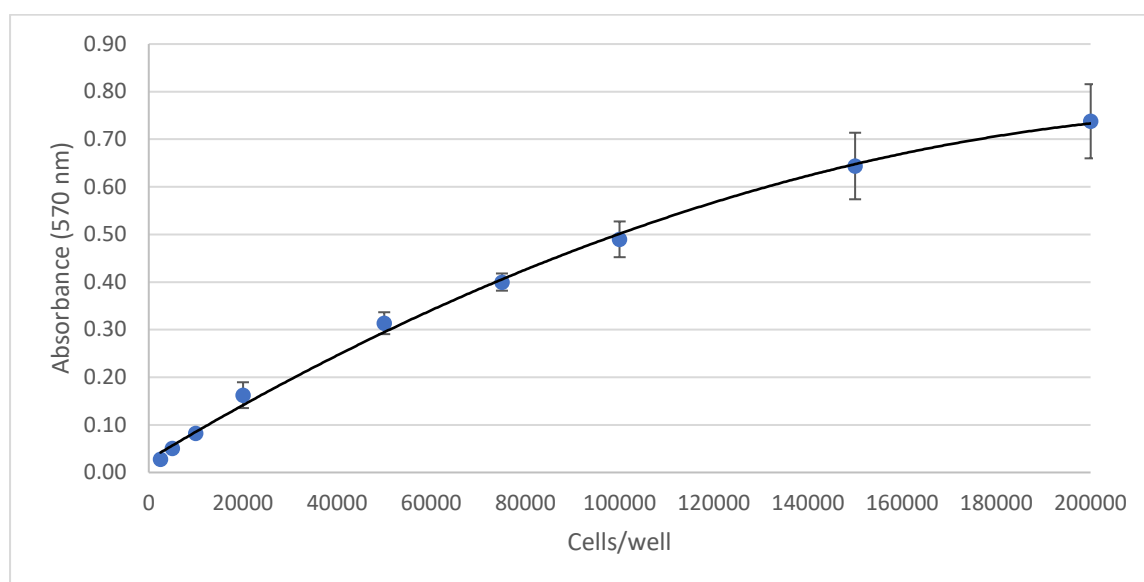


Figure 3.3.1.2 showing a representative SGBS viability curve after 24 hours of incubation. Varying cell densities between 2500 and 200000 cells/well were incubated and the resultant absorbances were plotted against cell densities. Data points indicate mean ( $n=8$ ) and error bars were standard deviation. Above 20 000 cells, the cell count to absorbance relationship gradually reduced in linearity. Linearity was observed between cell densities of 5000 and 20000 cells per well ( $R^2 > 0.997$ ).

### 3.3.2 Choice of flavonoid solvent.

Solvents Dimethyl sulfoxide (DMSO), Dimethylformamide (DMF) and ethanol (EtOH) were assessed for their effect on MTT assays at a range of concentrations (from 50% to 0.02%). Relative absorbances at 1% were compared and it was observed that DMSO and EtOH had no significant difference from the control at 1%. However, DMF affected the MTT assay at that concentration.

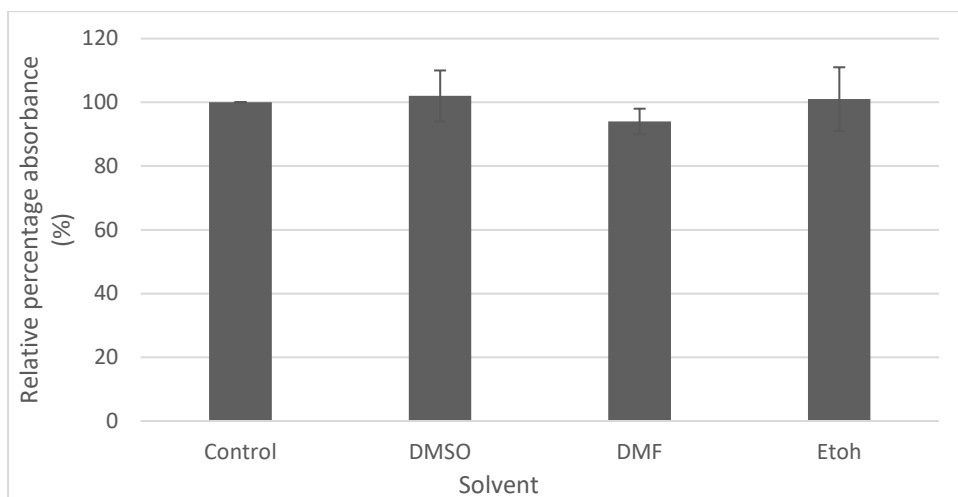


Figure 3.3.2.1. Effects of solvents DMSO, DMF and EtOH at 1% concentration (v/v) on MTT assays. Cells were seeded at densities of  $5 \times 10^3$ /well in media containing 1% solvent and incubated for a period of 24 hours. MTT assays were carried out and resultant absorbances were plotted against the solvent used. Data points indicate mean (n=24), and error bars were standard deviation. DMF had a significant difference in affecting the MTT assay at  $p < 0.05$  (ANOVA followed by Tukey test). At 1% concentration, DMSO and EtOH had no effect on the MTT assay. The control was media without solvent.

Throughout the subsequent experiments, a media only control was used alongside a solvent control (0.5% DMSO) comprising of the solvent concentration at the highest flavonoid dose. There was no significant difference between media only and media containing 0.5% DMSO ( $P < 0.05$ ).

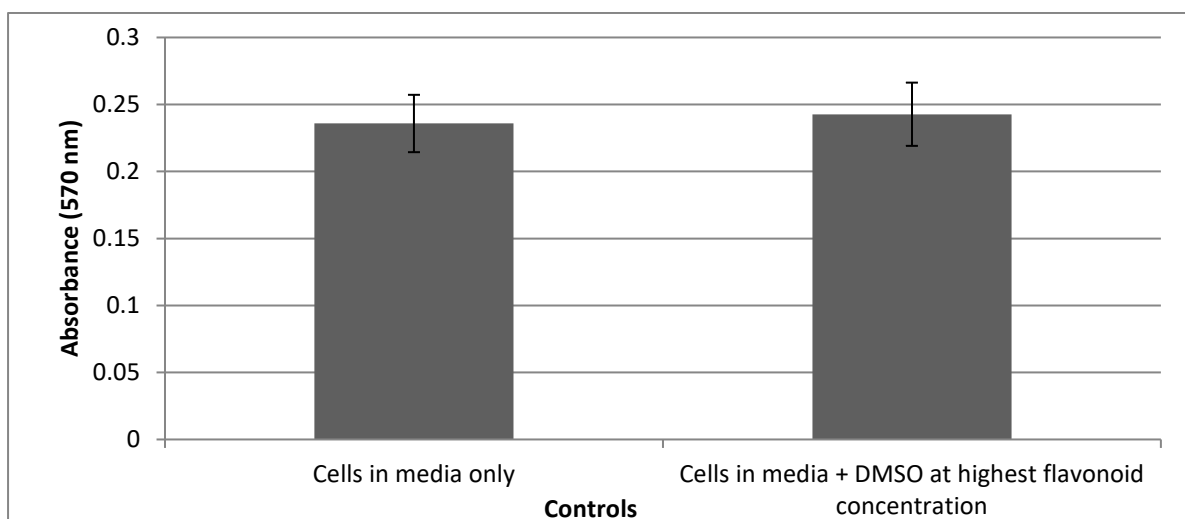


Figure 3.3.2.2. A typical comparison of controls, with and without DMSO at highest experimental concentration (0.5%). Cells were seeded at densities of  $5 \times 10^3$  in media only or media containing DMSO at the highest subsequent experimental concentration and incubated for a period of 72 hours similar to subsequent experiments. MTT assays were carried out and resultant OD readings were plotted against the solvent/control used. Data points indicate mean (n=8) and error bars were made from standard deviations, these were less than 10%. There was no significant difference at  $p < 0.05$  (student t-test).

### 3.3.3 Correlation between MTT assays and microscopic counts

Manual cell counts were employed to confirm MTT absorbance data. The range where linearity of cell counts to absorbances was assessed by running parallel experiments of cell counts and MTT assays at similar seeding densities. There was a moderate correlation ( $R^2 < 0.75$ ) of the two assays for seeding densities in the range of 2500 and 200 000 cells/well (figure 3.3). However, for seeding densities ranging from 5 000 cells to 75 000 cells/well the correlation was very strong ( $R^2 > 0.99$ ) as shown in figure 3.4. Using microscopic cell counts to confirm MTT assay data was therefore reliable when the seeding densities are below 75000 cells per well.

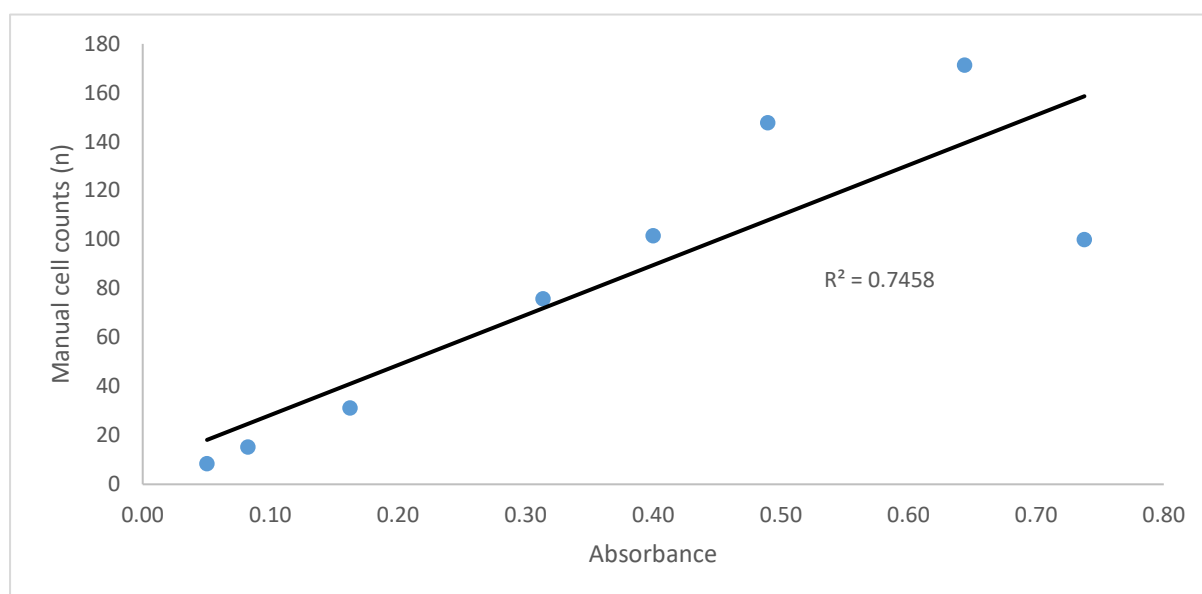


Figure 3.3.3.1. A typical correlation plot of cell counts and MTT assays for seeding densities in the range of 2 500 and 200 000 cells/well and incubated for 72 hours in growth media. Ninety-six well plates were used for MTT assays and 12 well plates for microscopic cell counts. The resultant cell counts were plotted against absorbance. There was a moderate correlation ( $R^2 < 0.75$ ).



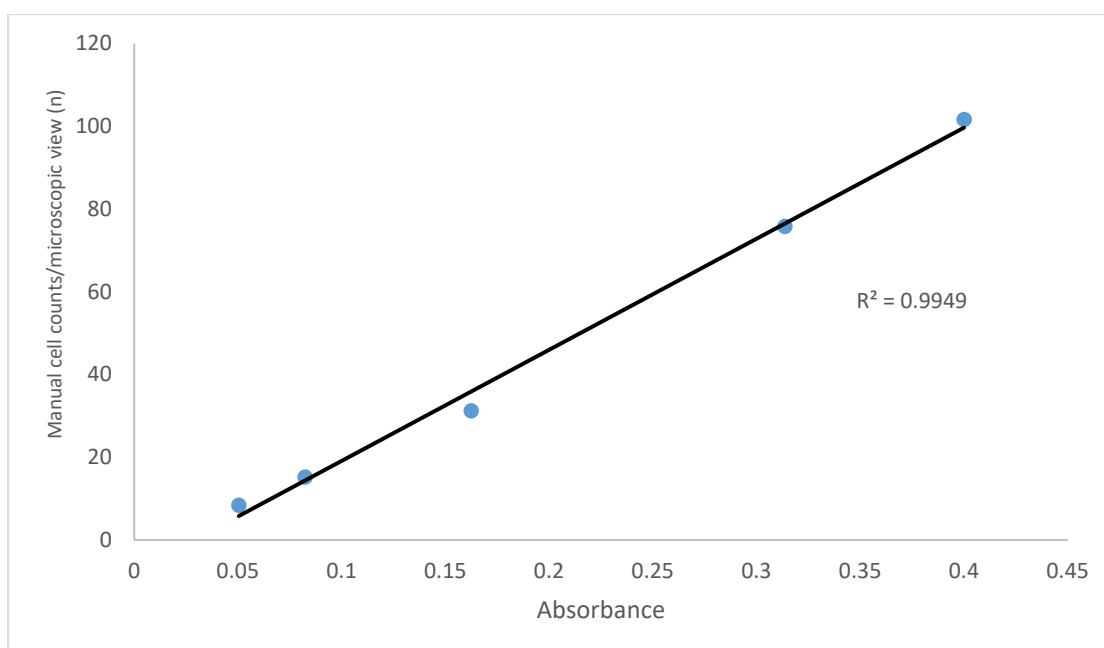


Figure 3.3.3.2. A typical correlation plot of cell counts and MTT assays for seeding densities in the range of 2 500 and 75 000 cells/well and incubated for 72 hours in growth media. Ninety-six well plates were used for MTT assays and 12 well plates for microscopic cell counts. The resultant cell counts were plotted against absorbance. There was a very strong correlation ( $R^2 > 0.99$ ).

### 3.3.4 Single flavonoid treatments.

The flavonoids quercetin, galangin and kaempferol from the flavanol classes, and chrysin apigenin and luteolin from the flavone family were tested for effects on SGBS cell growth. Their effects were assessed by MTT assays and confirmed by cell counts. There was an observed similarity in the result trends between MTT relative absorbance values and relative cell counts and  $IC_{50}$  values from cell counts were used to compare relative effectiveness between flavonoids because MTT assay results are semi quantitative. Cell counts experiments were done with flavonoid concentrations of 1  $\mu\text{M}$  up to 100  $\mu\text{M}$  because preliminary experiments indicated that effects on flavonoid variability was only present within that concentration range. In these assays, quercetin was the most potent flavanol with an  $IC_{50}$  of 84.22  $\mu\text{M}$  followed by kaempferol and galangin with  $IC_{50}$  values of 90.27 and 99.89  $\mu\text{M}$  respectively. Chrysin was the most potent flavone with an  $IC_{50}$  of 62.11  $\mu\text{M}$  followed by apigenin and luteolin with  $IC_{50}$  values of 82.87 and 86.48  $\mu\text{M}$  respectively. For all single flavonoids, peri-physiological concentrations (approx. 5  $\mu\text{M}$ ) often showed an increase in cell

viability suggesting increased proliferation whereas higher concentrations showed significant decrease in viability.

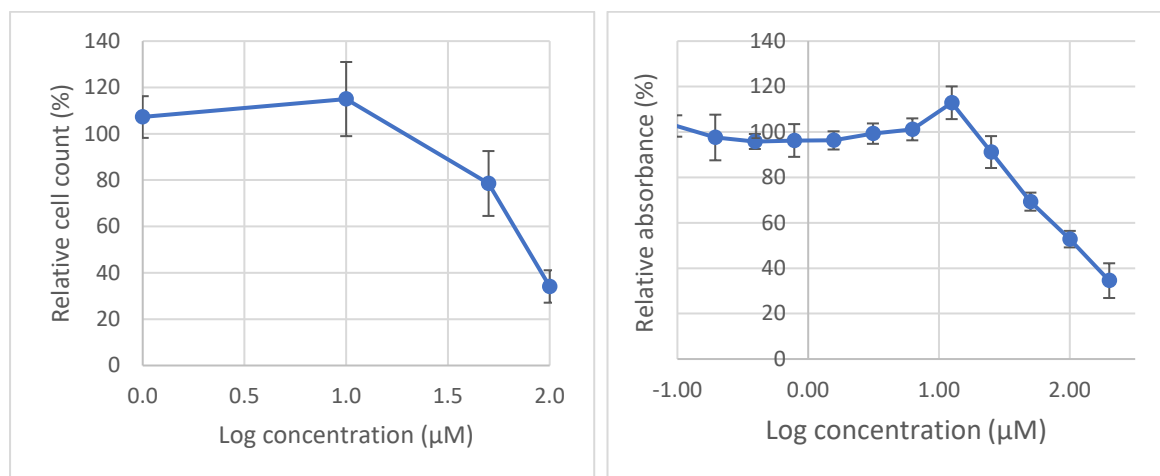


Figure 3.3.4.1a Relative cell counts and absorbance of SGBS cells treated with varying concentrations of quercetin and incubated for 72 hours. MTT assays were carried out and resultant absorbances were plotted against the logarithm of the concentrations to base 10. There was a peak absorbance at 12.5 μM concentration which was 112% relative to the control. There was a significant difference in efficacy ( $p < 0.05$ ) for all concentrations above 25 μM (ANOVA followed by Tukey test). The relative cell counts showed a peak of 114% relative to the control at 10 μM concentration and concentrations above this were significantly lower in efficacy ( $p < 0.05$ ; ANOVA followed by Tukey test). Data points indicate mean ( $n = 24$  for MTT,  $n = 18$  for cell counts) and error bars were standard deviations.

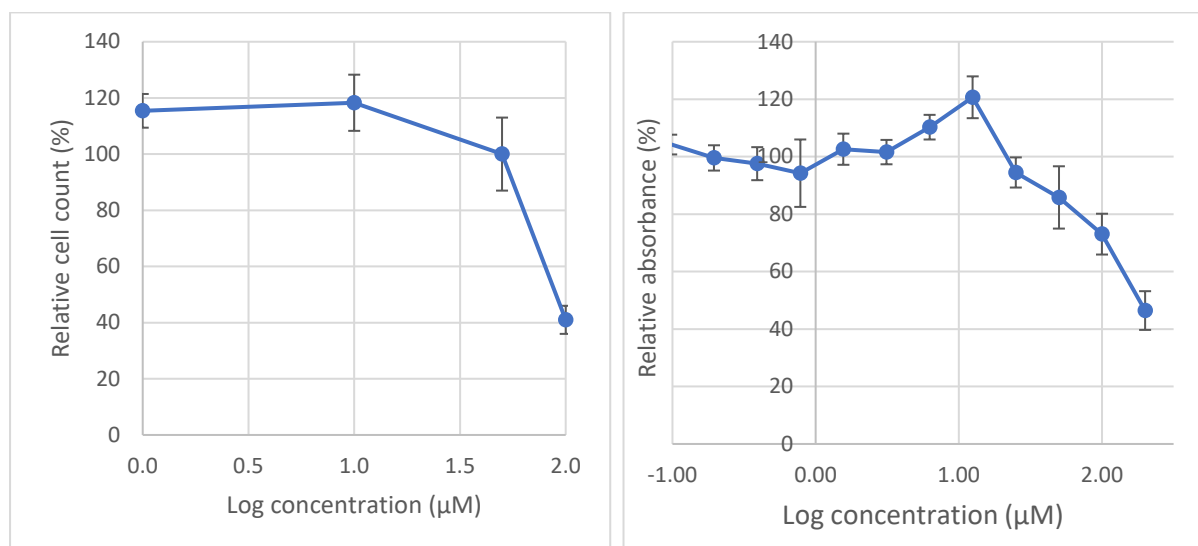


Figure 3.3.4.1b Relative cell counts and absorbance of SGBS cells treated with varying concentrations of kaempferol and incubated for 72 hours. MTT assays were carried out and resultant absorbances were plotted against the logarithm of the concentrations to base 10. There was a peak absorbance at 12.5 μM concentration which was 120% relative to the control. There was a significant difference in

efficacy ( $p < 0.05$ ) for all concentrations above 25  $\mu\text{M}$  (ANOVA followed by Tukey test). The relative cell counts showed a peak of 118% relative to the control at 10  $\mu\text{M}$  concentration and concentrations above this were significantly lower in efficacy ( $p < 0.05$ ; ANOVA followed by Tukey test). Data points indicate mean ( $n = 24$  for MTT,  $n = 18$  for cell counts) and error bars were standard deviations.

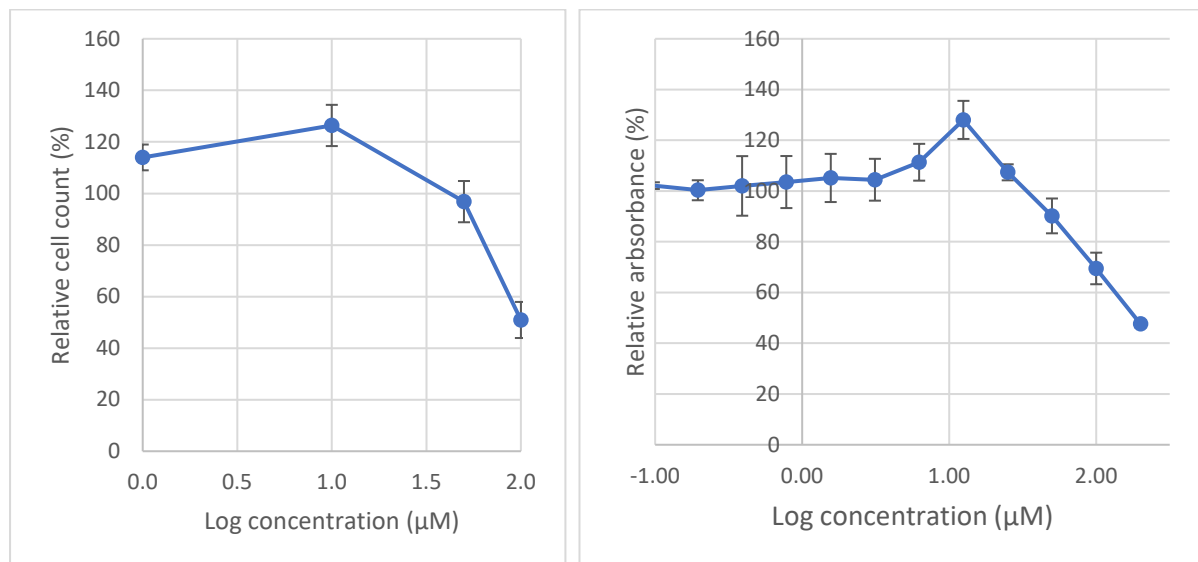


Figure 3.3.4.1c Relative cell counts and absorbance of SGBS cells treated with varying concentrations of galangin and incubated for 72 hours. MTT assays were carried out and resultant absorbances were plotted against the logarithm of the concentrations to base 10. There was a peak absorbance at 12.5  $\mu\text{M}$  concentration which was 128% relative to the control. There was a significant difference in efficacy ( $p < 0.05$ ) for all concentrations above 25  $\mu\text{M}$  (ANOVA followed by Tukey test). The relative cell counts showed a peak of 126% relative to the control at 10  $\mu\text{M}$  concentration and concentrations above this were significantly lower in efficacy ( $p < 0.05$ ; ANOVA followed by Tukey test). Data points indicate mean ( $n = 24$  for MTT,  $n = 18$  for cell counts) and error bars were standard deviations.

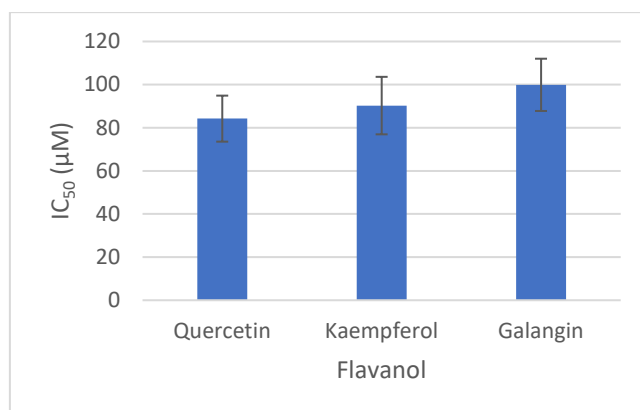


Figure 3.3.4.1d Comparison of the potency of the flavanols quercetin, kaempferol and galangin. IC<sub>50</sub> values were extracted from relative cell counts. Kaempferol was 7% less effective when compared to quercetin, whereas galangin was 17% less effective compared to quercetin.

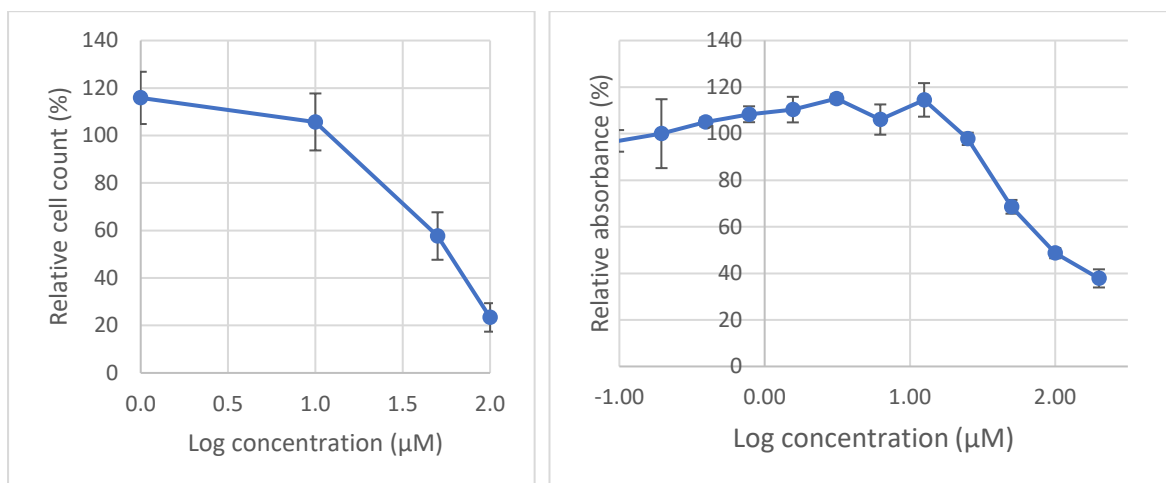


Figure 3.3.4.1e Relative cell counts and absorbance of SGBS cells treated with varying concentrations of chrysin and incubated for 72 hours. MTT assays were carried out and resultant absorbances were plotted against the logarithm of the concentrations to base 10. There was a peak absorbance at 12.5 μM concentration which was 114% relative to the control. There was a significant difference in efficacy ( $p < 0.05$ ) for all concentrations above 25 μM (ANOVA followed by Tukey test). The relative cell counts showed a peak of 115% relative to the control at 1 μM concentration and concentrations above 10 μM were significantly lower in efficacy ( $p < 0.05$ ; ANOVA followed by Tukey test). Data points indicate mean ( $n = 24$  for MTT,  $n = 18$  for cell counts) and error bars were standard deviations.

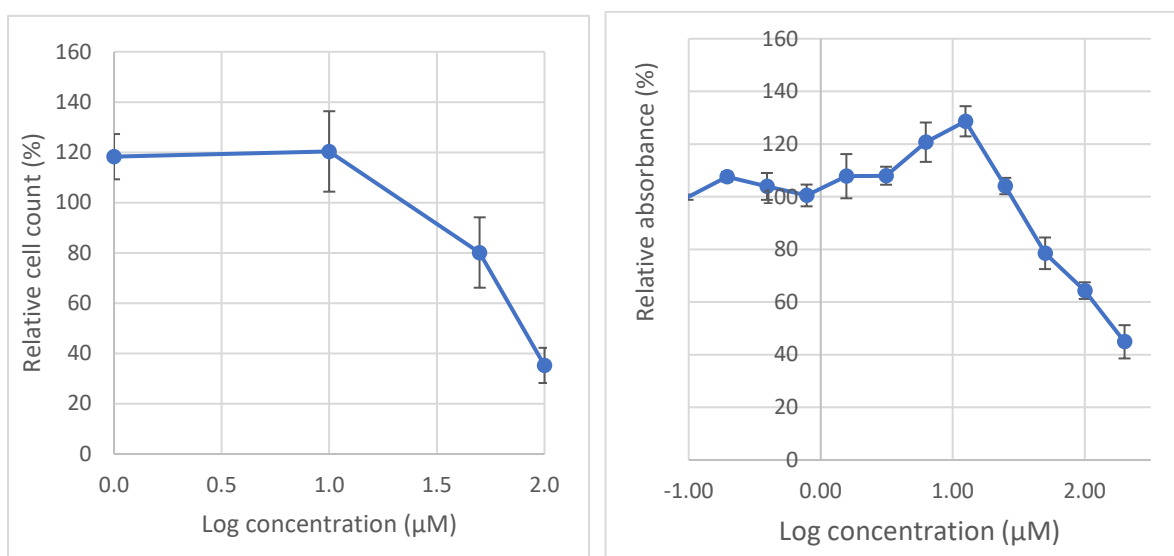


Figure 3.3.4.1f Relative cell counts and absorbance of SGBS cells treated with varying concentrations of apigenin and incubated for 72 hours. MTT assays were carried out and resultant absorbances were plotted against the logarithm of the concentrations to base 10. There was a peak absorbance at 12.5 μM concentration which was greater than 128% relative to the control. There was a significant difference in efficacy ( $p < 0.05$ ) for all concentrations above 25 μM (ANOVA followed by Tukey test). The relative cell counts showed a peak of 120% relative to the control at 10 μM concentration and

concentrations above this were significantly lower in efficacy ( $p < 0.05$ ; ANOVA followed by Tukey test). Data points indicate mean ( $n = 24$  for MTT,  $n = 18$  for cell counts) and error bars were standard deviations

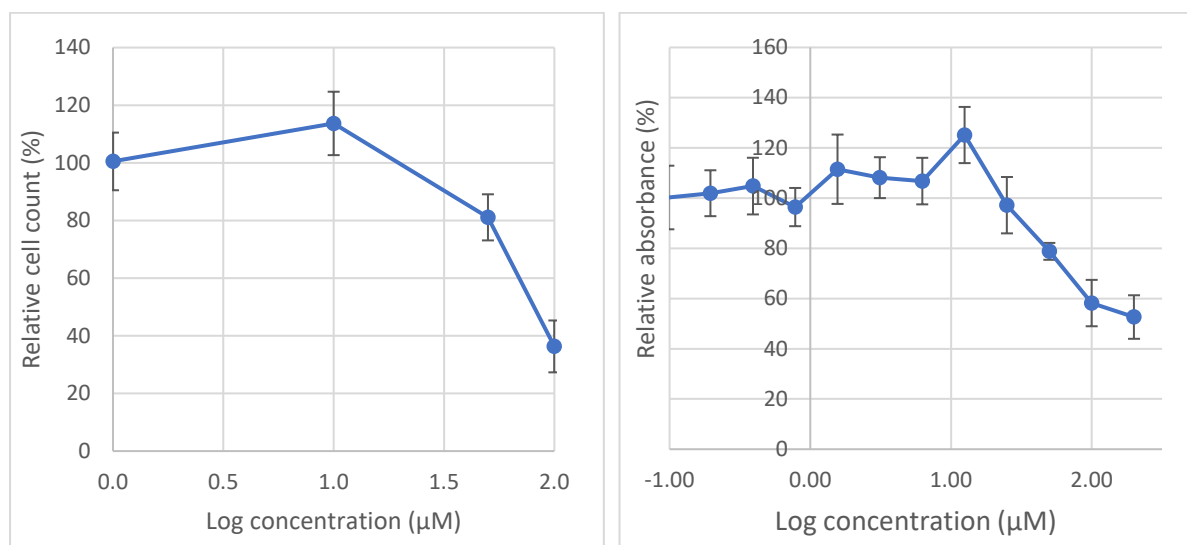


Figure 3.3.4.1g Relative cell counts and absorbance of SGBS cells treated with varying concentrations of luteolin and incubated for 72 hours. MTT assays were carried out and resultant absorbances were plotted against the logarithm of the concentrations to base 10. There was a peak absorbance at 12.5  $\mu\text{M}$  concentration which was greater than 125% relative to the control. There was a significant difference in efficacy ( $p < 0.05$ ) for all concentrations above 25  $\mu\text{M}$  (ANOVA followed by Tukey test). The relative cell counts showed a peak of 113% relative to the control at 10  $\mu\text{M}$  concentration and concentrations above this were significantly lower in efficacy ( $p < 0.05$ ; ANOVA followed by Tukey test). Data points indicate mean ( $n = 24$  for MTT,  $n = 18$  for cell counts) and error bars were standard deviations.

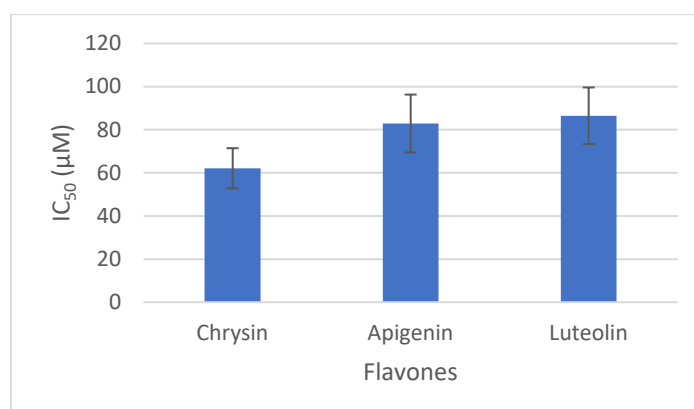


Figure 3.3.4.1h Comparison of the potency of the flavones chrysin, apigenin and luteolin.  $\text{IC}_{50}$  values were extracted from relative cell counts. Apigenin was 33% less effective when compared to chrysin, whereas luteolin was 39% less effective compared to chrysin.

### 3.3.5 Combined flavonoid treatments.

Flavonoid combinations of each flavanol (quercetin, galangin and kaempferol) with all three flavones (chrysin apigenin and luteolin) were tested for effects on SGBS cell growth according to the schedule detailed in figure 3.2.8. Their effects were assessed by MTT assays and confirmed by cell counts. MTT assay results, however, were discordant with the cell count results. Microscopic views showed that the MTT seemed to combine with the flavonoid combinations to form aggregates that gave a false reading (figure 3.3.5.1). Hence, cell counts were used to derive IC<sub>50</sub> values of cell viability. Cell counts experiments were done with flavonoid 50;50 because preliminary experiments had indicated that flavonoid effects occurred within that range. Most flavonoid combinations had a greater potency than their constituents and showed hormetic effects at lower concentrations. The reduction of greater than 50%, is suggestive of synergy between most flavonoid combinations with a few exceptions.

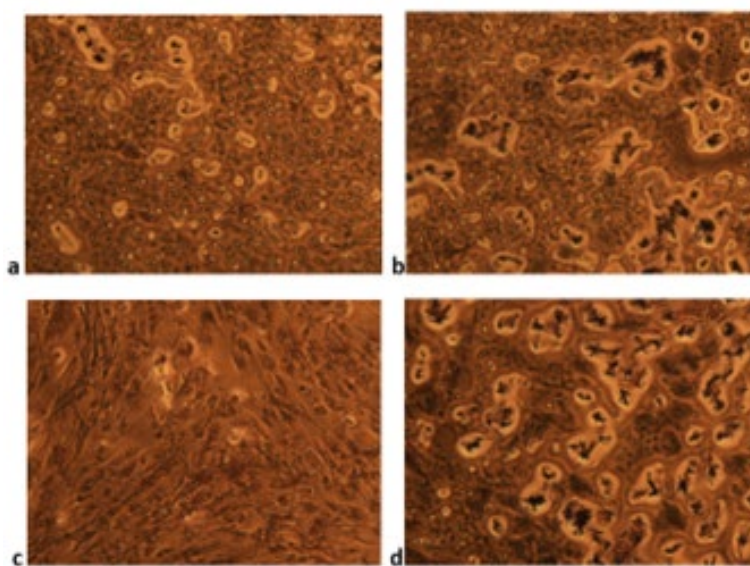


Figure 3.3.5.1 Combined flavonoids appeared to form aggregates with MTT that gave discordant absorbances when compared to microscopic cell counts. Photomicrograph a) is 12.5  $\mu$ M quercetin, b) is 12.5  $\mu$ M quercetin and chrysin combination, c) is 100  $\mu$ M quercetin and d) is 100  $\mu$ M quercetin and Chrysin. Photomicrographs were taken at x100 after MTT incubation and before the removal of spent media.

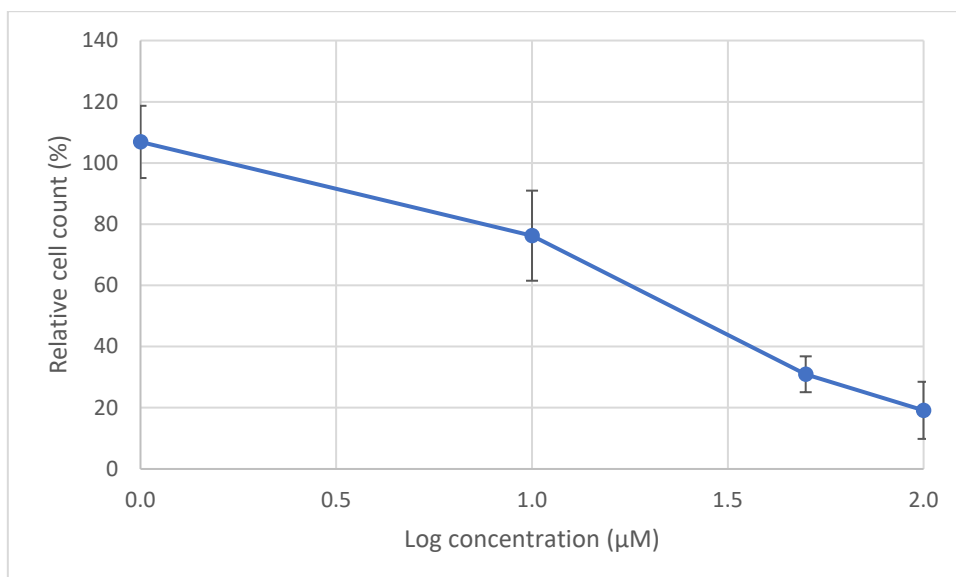


Figure 3.3.5a. Relative cell counts of SGBS cells treated with varying concentrations of combined chrysin and quercetin and incubated for 72 hours. The relative cell counts showed a peak of 106% at 1 µM concentration and greater concentrations were significantly inhibitory ( $p < 0.05$ ; ANOVA followed by Tukey test). The  $IC_{50}$  for this combination was 28.31 µM. Data points indicate mean ( $n = 18$  for cell counts) and error bars were standard deviations.

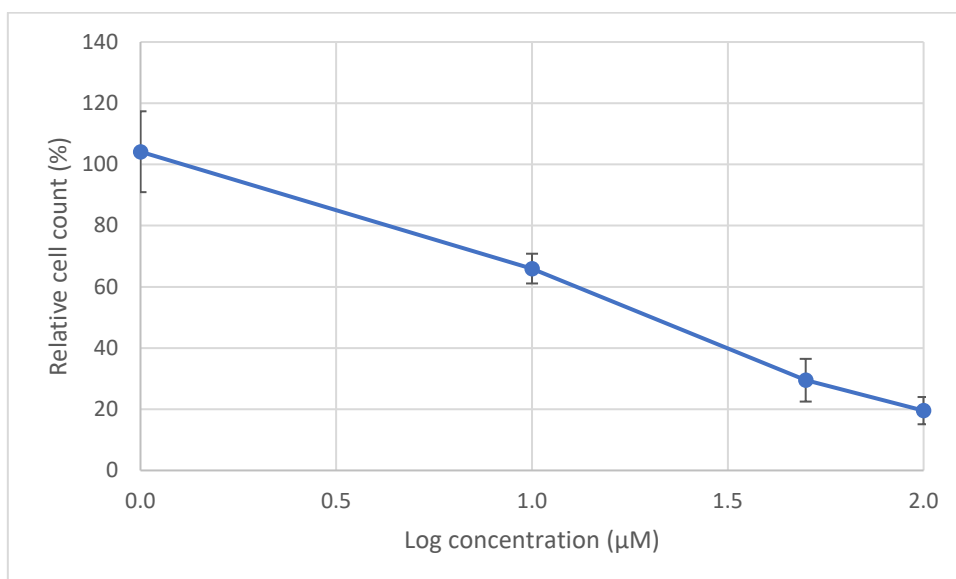


Figure 3.3.5b. Relative cell counts of SGBS cells treated with varying concentrations of combined chrysin and kaempferol and incubated for 72 hours. The relative cell counts showed a peak of 104% at 1 µM concentration and greater concentrations were significantly inhibitory ( $p < 0.05$ ; ANOVA followed by Tukey test). The  $IC_{50}$  for this combination was 23.98 µM. Data points indicate mean ( $n = 18$  for cell counts) and error bars were standard deviations.

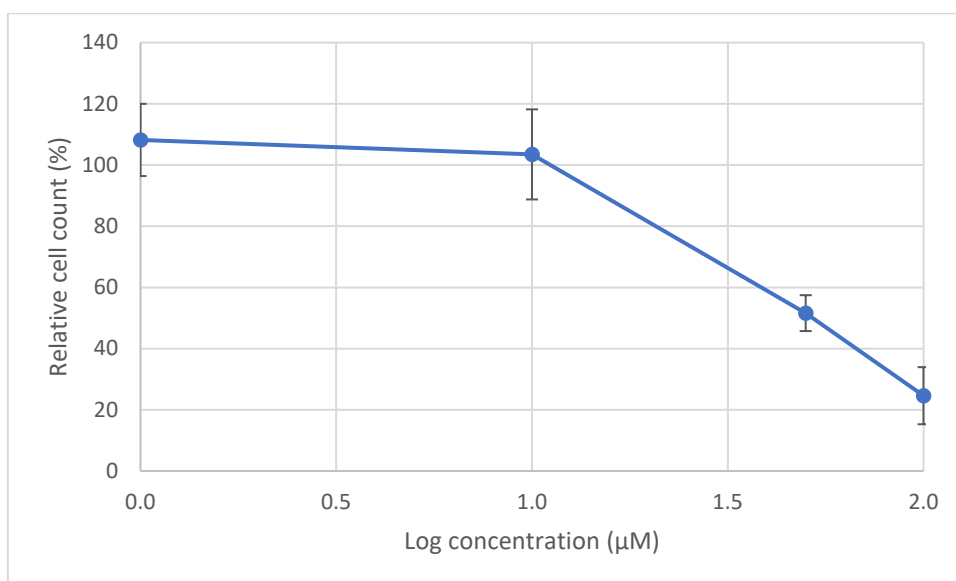


Figure 3.3.5c. Relative cell counts of SGBS cells treated with varying concentrations of combined chrysin and galangin and incubated for 72 hours. The relative cell counts showed a peak of 108% at 1 μM concentration and greater concentrations were significantly inhibitory ( $p < 0.05$ ; ANOVA followed by Tukey test). The  $IC_{50}$  for this combination was 48.40 μM. Data points indicate mean ( $n = 18$  for cell counts) and error bars were standard deviations.

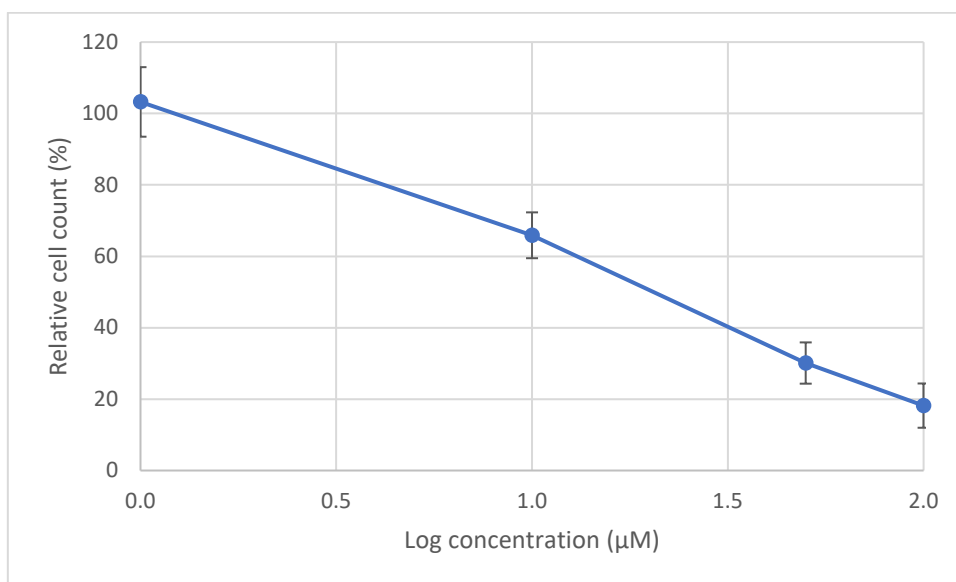


Figure 3.3.5d. Relative cell counts of SGBS cells treated with varying concentrations of combined quercetin and apigenin and incubated for 72 hours. The relative cell counts showed a peak of 103% at 1 μM concentration and greater concentrations were significantly inhibitory ( $p < 0.05$ ; ANOVA followed by Tukey test). The  $IC_{50}$  for this combination was 29.22 μM. Data points indicate mean ( $n = 18$  for cell counts) and error bars were standard deviations.



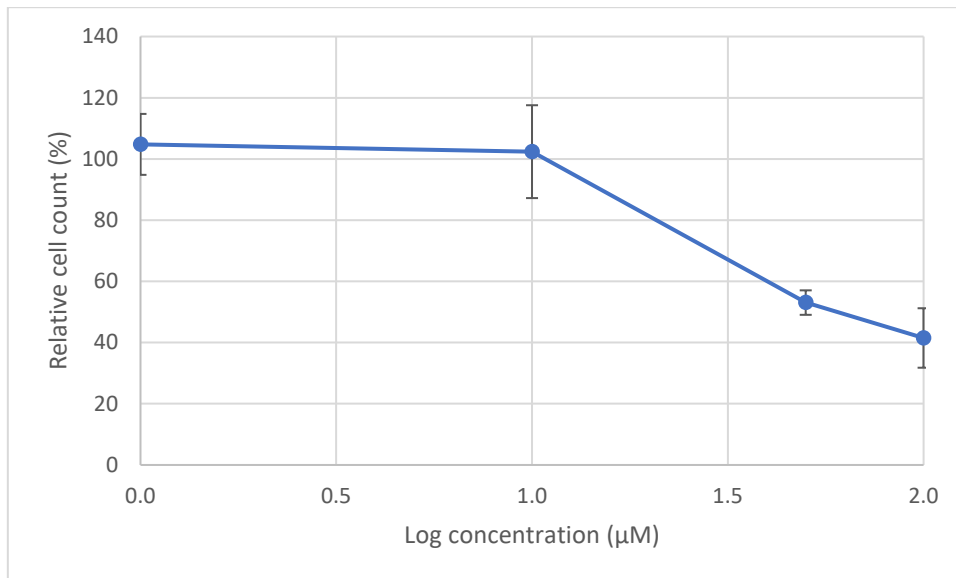


Figure 3.3.5e. Relative cell counts of SGBS cells treated with varying concentrations of combined quercetin and luteolin and incubated for 72 hours. The relative cell counts showed a peak of 104% at 1 μM concentration and greater concentrations were significantly inhibitory ( $p < 0.05$ ; ANOVA followed by Tukey test). The  $IC_{50}$  for this combination was 54.27 μM. Data points indicate mean ( $n = 18$  for cell counts) and error bars were standard deviations.

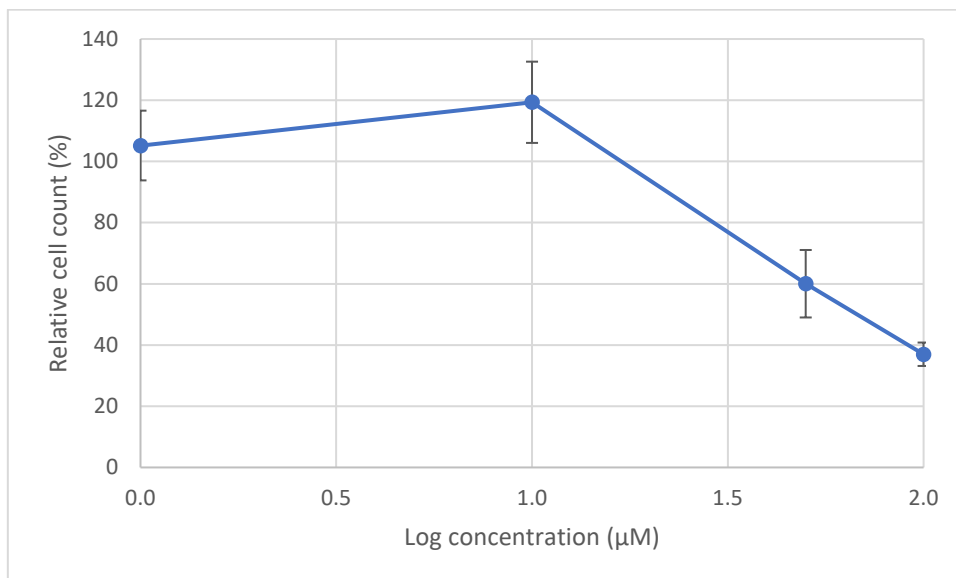


Figure 3.3.5f. Relative cell counts of SGBS cells treated with varying concentrations of combined luteolin and galangin and incubated for 72 hours. The relative cell counts showed a peak of 119% at 1 μM concentration and greater concentrations were significantly inhibitory ( $p < 0.05$ ; ANOVA followed by Tukey test). The  $IC_{50}$  for this combination was 74.96 μM. Data points indicate mean ( $n = 18$  for cell counts) and error bars were standard deviations.

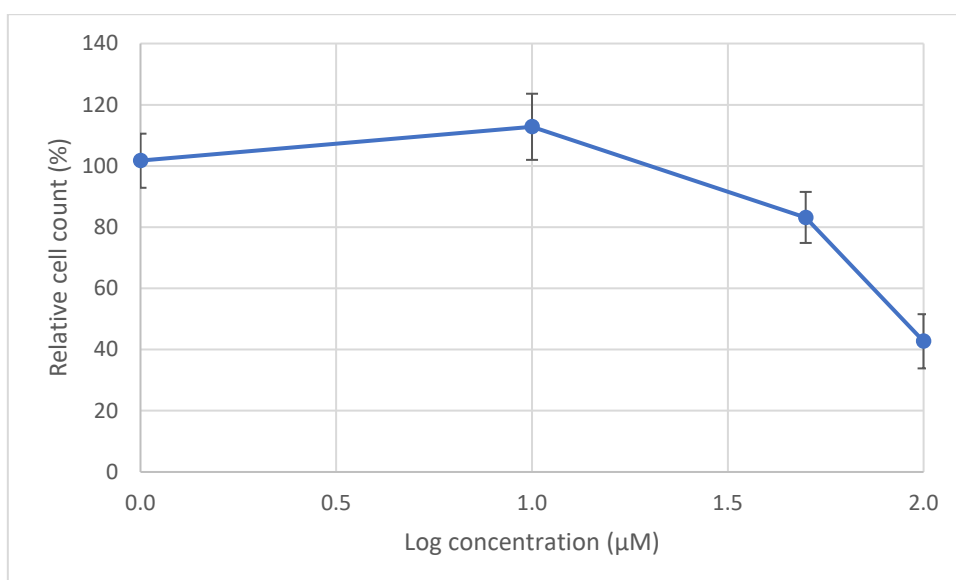


Figure 3.3.5g. Relative cell counts of SGBS cells treated with varying concentrations of combined luteolin and kaempferol and incubated for 72 hours. The relative cell counts showed a peak of 112% at 10 µM concentration and greater concentrations were significantly inhibitory ( $p < 0.05$ ; ANOVA followed by Tukey test). The  $IC_{50}$  for this combination was 98.09 µM. Data points indicate mean ( $n = 18$  for cell counts) and error bars were standard deviations.

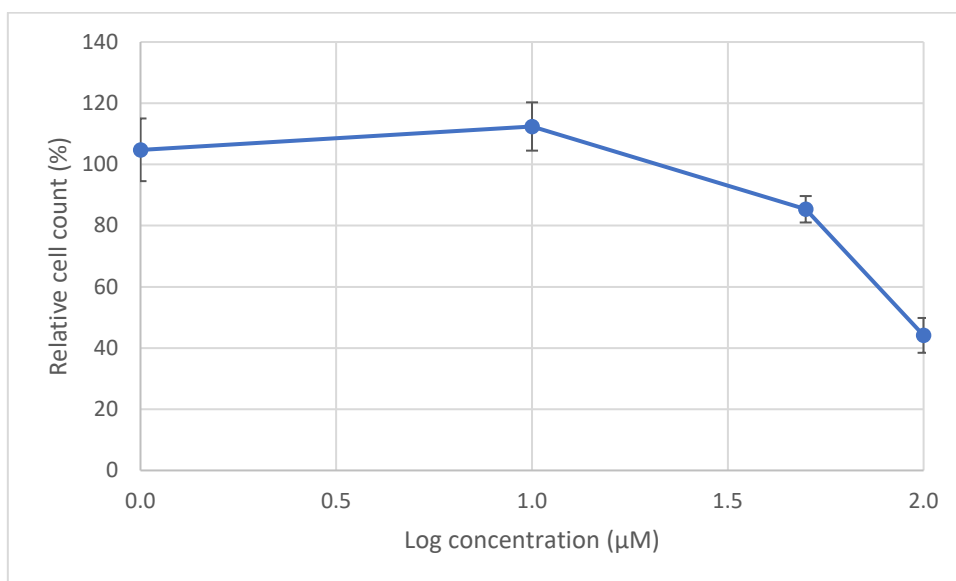


Figure 3.3.5h. Relative cell counts of SGBS cells treated with varying concentrations of combined apigenin and galangin and incubated for 72 hours. The relative cell counts showed a peak of 112% at 10 µM concentration and greater concentrations were significantly inhibitory ( $p < 0.05$ ; ANOVA followed by Tukey test). The  $IC_{50}$  for this combination was 82.28 µM. Data points indicate mean ( $n = 18$  for cell counts) and error bars were standard deviations.

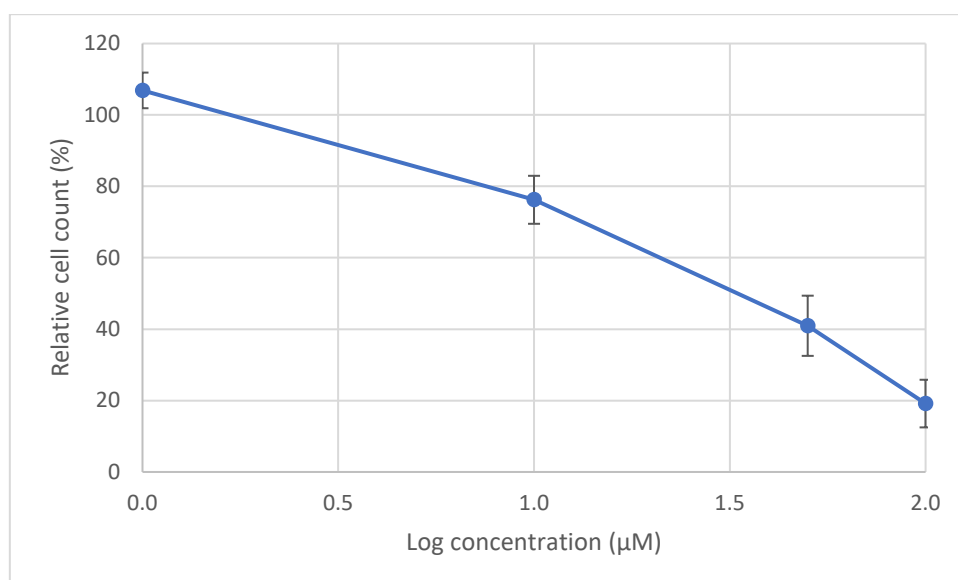


Figure 3.3.5i. Relative cell counts of SGBS cells treated with varying concentrations of combined apigenin and kaempferol and incubated for 72 hours. The relative cell counts showed a peak of 104% at 1 µM concentration and greater concentrations were significantly inhibitory ( $p < 0.05$ ; ANOVA followed by Tukey test). The  $IC_{50}$  for this combination was 27.02 µM. Data points indicate mean ( $n = 18$  for cell counts) and error bars were standard deviations.

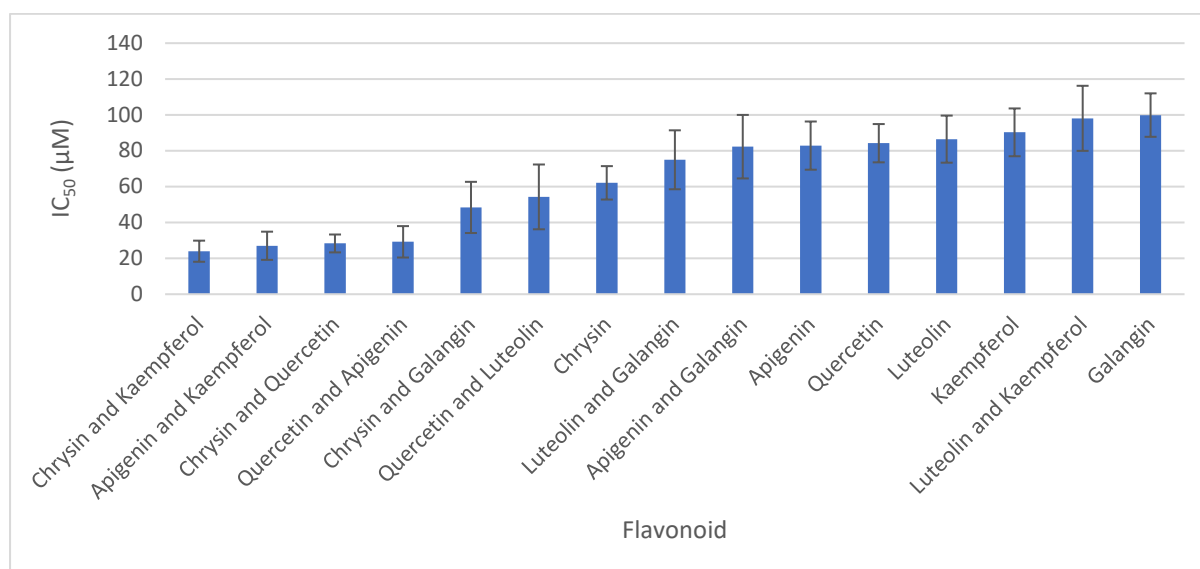


Figure 3.3.5k Comparative view of the single and combined flavonoids. Values were derived from relative cell counts. Except for luteolin and kaempferol combination, all combined flavonoids had more potency than their singular presence.

### 3.3.6 Comparative 3T3-L1 flavonoid treated cells

For comparison, 3T3 cells were treated with quercetin across similar concentrations as SGBS cells. There appears to be some similarities in the outcomes for both MTT assays and cell counts. Like SGBS cells, 3T3 cells show a hormetic effect of flavonoids at peri-physiological concentrations. Higher concentrations show reduction in viability in a dose dependant manner. The  $IC_{50}$  of 3T3 cells treated with quercetin had similar slopes showing comparability between the model preadipocytes.

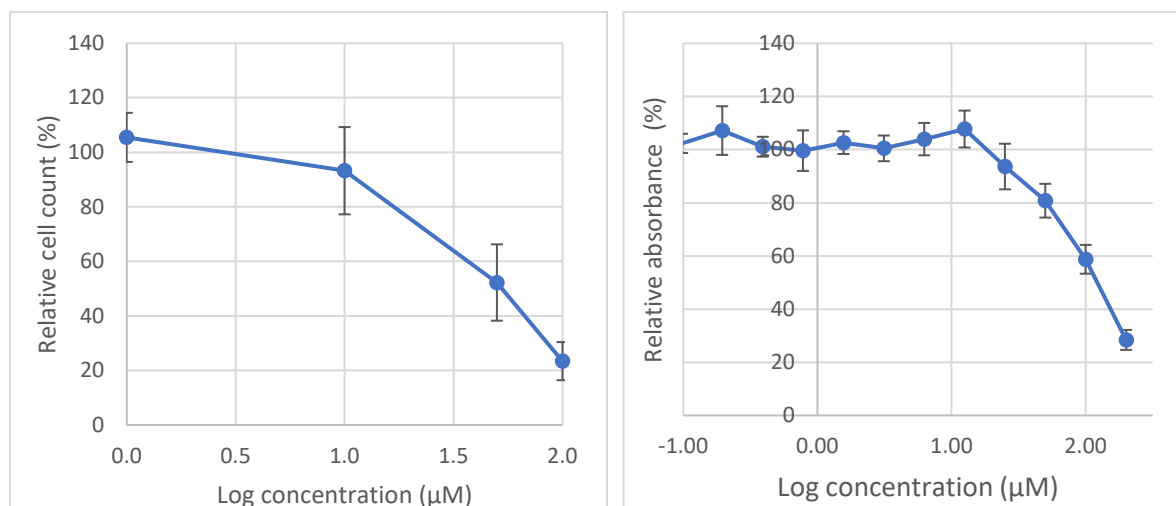


Figure 3.3.4.1e Relative cell counts and absorbance of 3T3 cells treated with varying concentrations of quercetin and incubated for 72 hours. MTT assays were carried out and resultant absorbances were plotted against the logarithm of concentrations to base 10. There was a peak absorbance at 12.5 µM concentration which was greater than 107% relative to the control. There was a significant difference in efficacy ( $p < 0.05$ ) for all concentrations above 25 µM (ANOVA followed by Tukey test). The relative cell counts showed a peak of 105% relative to the control at 1 µM concentration and concentrations above 10 µM were significantly lower in efficacy ( $p < 0.05$ ; ANOVA followed by Tukey test). Data points indicate mean ( $n = 24$  for MTT,  $n = 18$  for cell counts) and error bars were standard deviations.

### 3.3.7 Cell recovery after treatment

SGBS cells were treated with a range of quercetin concentrations and daily microscopic cell counts (for 7 days) were used to monitor cell recovery from the effects of the treatment. Results show that cells did recover after viability was reduced by treatment. The recovery rate seemed inversely proportional to the original quercetin concentration.

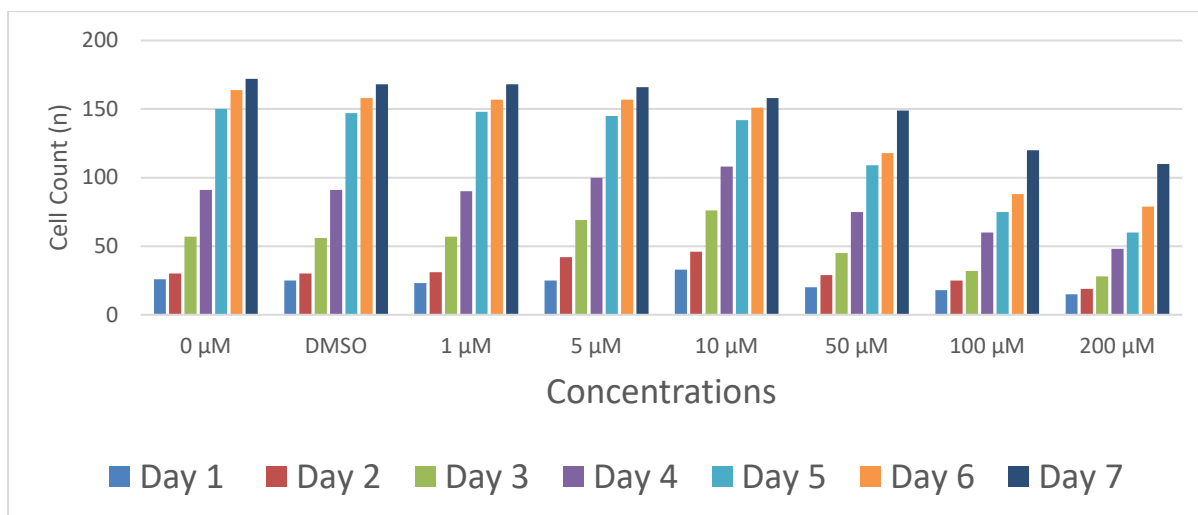


Figure 3.3.7. A representative graph showing cell recovery after a single treatment with quercetin. SGBS cells were treated with different concentrations of quercetin from 0 to 200  $\mu$ M after 12 hours of adherence and microscopic cell counts were made every 24 hours for 7 days. Data points indicate mean ( $n = 6$ ).

### 3.4 Discussion

#### 3.4.1 Main findings.

This chapter considered the effects of 2 classes of flavonoids, the flavones represented by chrysin, apigenin and luteolin and the flavonols which were represented by quercetin kaempferol and galangin on the growth of the SGBS preadipocytes in vitro. These were tested as single flavonoids and in combinations across the classes. Method validation protocols showed that the preadipocyte model used retained consistent viability throughout the experiments. It also showed that microscopic cell counts produced similar results to MTT assay results for singular flavonoids but when flavones were combined, there was discordance in the results. For this reason, ranking of single and combined flavonoids were based on microscopic cell counts. Effectiveness of flavonoids had a relationship to the hydroxyl groups on the determinant side chain. Flavonoid combinations appeared to be more effective than single treatments with a few exceptions. Peri physiological concentrations of single flavonoids appeared to increase cell viability; this was not apparent in flavonoid combinations. Comparative studies with 3T3-L1 showed the same effects of flavonoids on preadipocyte viability and growth. Cells treated once with flavonoids and cultured for 7 days appeared to recover daily to a limit.

#### 3.4.2 MTT assays and microscopic counts

Many assays can be used to assess cell viability, growth, or proliferation. The MTT assay which depends on the conversion of water-soluble yellow dye MTT [3-(4,5-dimethylthiazol-2-yl)-2,5-diphenyltetrazolium bromide] substrate to chromogenic (purple formazan) product by the action of mitochondrial reductase in living cells has been a golden standard for many years (Van Tonder et al., 2015). Whilst good result linearity is preserved in cells up to 1 million cells per well in MTT assays, small variations in metabolic activities can bring large changes in MTT results. For example, cell stress without cell death can reduce MTT readings as much as cell death itself. However, for comparative tests, these variabilities can be cancelled out by setting identical experimental conditions where the unknown variables only can be compared and ranked. MTT assays have been used on experiments with flavonoids (Zhang et al., 2018; Kling et al., 2014) and their results have been validated by parallel experiments. Nevertheless, there are some studies that have claimed that flavonoids can reduce MTT in the absence of living cells (Talorete et al., 2006; Peng et al., 2005), whilst worrying, these findings can be avoided by adopting a method that washes away all non-cell absorbed MTT. Validation of MTT results

can be achieved by other calorimetric assays, microscopic cell counts or molecular methods. Whilst tedious and time consuming, the microscopic cell count means of quantifying cell growth is relatively cheap and reproducible. It measures one thing, that is the available cells, and this removes any contra indications such as stressed or metabolically hyperactive cells. Together with microscopic cell counts, MTT assays, being based on standard laboratory equipment, give more economic outcomes with very high throughputs for single flavonoid assays.

Combined flavonoids are an area which has not been exhaustively studied. Whilst these can stay in solution in media under fridge, room or incubator conditions, nothing is known about how they behave in culture. Xia et al. (2022) for example postulates that in culture and indeed *in vivo*, 2 or more flavonoids form new crystal structures by hydrogen bonding from their hydroxyl groups. These emerging bonds produce a different lattice packing and molecular arrangement (Zhang et al., 2019). It is not known how these new lattice structures fare with MTT assays, but current findings show that MTT results for combined flavonoids lose concordance with microscopic cell counts for some experimental conditions. Results showed that MTT assay outcomes appeared to indicate greater cell viability when actual cell counts showed otherwise. Since MTT assays are semi quantitative measures, microscopic cell counts, being the direct quantification methods were the preferred means of comparing combined flavonoids to their single equivalences. Microscopic cell counts were consistent throughout the experiments.

### 3.4.3 Single flavonoid treatments

The 2 classes of flavonoids within this study produced results that show a bearing on the hydroxyl groups on their determinant benzene ring. Most interesting was the fact that for all tested flavonoids, at physiological concentrations, there was a notable increase in cell viability which is counter intuitive, knowing that flavonoids are associated with a reduction in obesity (García-Barrado et al., 2020). This hormetic phenomenon, which is the biphasic dose/concentration response where low-doses stimulate, and high-doses inhibit the growth of test organisms/cells has been recorded before. Calabrese et al. (2021) for example found that Luteolin had a hormetic effect when they looked at its effects on inflammation, diabetes, and osteoporosis using models. Their conclusion was that it was necessary for the cells to, though counterintuitive, proliferate under treatment by low dose concentrations of the flavonoid because the process upregulated a nuclear factor which significantly reduced the

rate of inflammation (Calabrese et al., 2021). These studies also resonate with earlier work (Son et al., 2008) which termed this phenomenon of flavonoids having biphasic presentations as preconditioning. They concluded that at these sub-physiological concentrations of around 5  $\mu\text{M}$  an evolutionally adaptive cellular stress response pathway is activated. This results in the production of a clone of cells which express genes that encode antioxidant enzymes, protein chaperones, and other cytoprotective proteins. Genes for neurotrophic factors are also said to increase in these clones suggesting an immune-protective advantage as seen in experiments discussed in chapter 3. Some schools of thought suggest that this biphasic response occurs because of overcompensation to a disruption in homeostasis (Calabrese, 2001). It therefore remains to be seen whether concentrations that show a hormetic increase in preadipocyte viability will translate to better differentiation outcomes or not. This thought has been addressed in chapter 4. As the concentrations increased post physiological levels, cell growth significantly reduced on all flavonoid treatments. The effectiveness of the flavonoids had a bearing on the hydroxyl groups of the determinant carbon ring often referred to as the B ring (IUPAC, 2017). Flavonols had a direct correlation whilst flavones had an inverse correlation of hydroxyl groups to effectiveness.

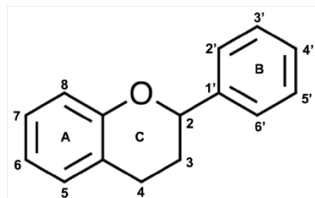


Figure 3.4.3a. The skeleton structure of flavonoids in general showing the nomenclature of the carbon rings (Teixeira et al., 2013). The B ring is the determinant ring.

Group of flavanoid	Structure backbone	Examples		
Flavones				
Flavonols				

Figure 3.4.3b. Chemical Structures of the flavones luteolin, apigenin and chrysin, and the flavonols quercetin, kaempferol and galangin showing the variation in hydroxyl groups on the B ring (Kumar and Pandey, 2013).



### 3.4.3.1 Flavonols

Quercetin, kaempferol and galangin were the test flavonoids representing the flavonol class. When ranked, quercetin was the most effective followed by kaempferol then galangin. Their IC<sub>50</sub> values were 84.22, 90.27 and 99.89  $\mu$ M for quercetin, kaempferol and galangin. This order is consistent with the hydroxyl groups on the determinant B carbon ring (Figure 3.4.3.1.). Hydroxyl groups in flavonoids, in general, are responsible for the generation or removal of free radicals depending on the cellular milieu and the homeostasis needs of the cell. Excess hydroxyl groups can lead to oxidative stress where reactive oxygen species (ROS) including free radicals can cause cell damage or the induction of cell death through apoptosis or autophagy (Chen et al., 2008). The greater the number of hydroxyl groups will predictably increase the potency of the flavonol and reduce the viability of the preadipocytes. It can be predicted that, myricetin, a flavone with 3 hydroxyl groups on the determinant B ring will be more potent than quercetin given the same experimental conditions. It needs to be emphasised however that this oxidative stress happens when there are high flavonol concentrations because at physiological concentrations, the same flavonols will act as antioxidants and mop away the free radicals. As such, flavonols can be viewed as buffers for reactive oxygen species depending on the limits of homeostasis.

Flavonoids because of their carbon rings are poorly soluble in both aqueous and lipidic environments, their solubility becomes better with increasing number of hydroxyl groups (Premathilaka et al., 2022). These hydroxyl groups go on to form hydrogen bonds between the polar head groups of lipids and the more hydrophilic flavonoids hydroxyl ends at the membrane interface. This has a 2-fold benefit, when these polyphenols, at low concentrations, stay bonded at the membrane interface, they reduce the access of deleterious molecules such as free radicals to protect the function of the membrane. This is seen at hormetic concentrations. At higher concentrations, they, adhere and preclude other necessary molecules from entering the cell thus denying the preadipocyte useful nutritional and communication molecules (Oteiza et al., 2005). This observation will favour flavonols with more hydroxyl groups in reducing cell viability at high concentrations. On the other hand, more hydroxyl groups allow the polyphenol to enter the cell and thus increase its bioavailability. Increased bioavailability translates to greater efficacy. The results are therefore predictable by looking at the side chains on the determinant ring because of the

exhibited hierarchy of inhibitory capability. Whether these results can be extrapolated to other flavonols of the same order will need to be confirmed by experimentation.

#### 3.4.3.2 Flavones

The flavones chrysin, apigenin and luteolin were effective in reducing cell viability in a manner that was inversely proportional to the number of hydroxyl groups on the determinant (B) ring. Chrysin has no hydroxyl group on that ring, it was the most effective this was followed by apigenin with 1 and luteolin with 2 hydroxyl groups on the B ring. The IC<sub>50</sub> values were 62.11 μM, 82.87 and 86.48 μM respectively. These IC<sub>50</sub> values were a relatively lower than those of tested flavonols above, suggesting that flavones were more potent in reducing SGBS preadipocyte viability than flavonols. These findings are contrary to those by Zhao et al., (2023) where the hierarchy for these 3 flavones was shown in reverse order. However, their findings, which were conducted on 3T3-L1 murine cells were focusing on differentiation and not proliferation.

The B ring hydroxyl configuration in flavones is the deciding factor for determining the scavenging capacity for reactive oxygen species and reactive nitrogen species since it donates hydrogen and an electron to hydroxyl, peroxy, and peroxy-nitrite radicals, this gives stability and produces a relatively stable flavonoid radical (Kumar and Pandey, 2013). This suggests that the more the hydroxyl groups, the less potent the flavone is in reducing cell. Therefore, chrysin with no hydroxyl group on ring B is more potent. Ingress of flavones into the cell is heavily dependent on its lipophilicity, there is an inverse correlation between the number of hydroxyl groups and the lipophilicity of the flavones (Khalilpourfarshbafi et al., 2019). The fewer the hydroxyl groups the better the lipophilicity and hence chrysin becomes more readily permeable to the lipid membrane compared to apigenin and luteolin.

#### 3.4.4 Flavonoid combinations.

Flavone and flavonol combinations were more potent than the individual treatments except for luteolin and kaempferol combined (fig 3.3.5k.). The decrease can be seen as synergistic basing on the magnitude of decrease, for example, the IC<sub>50</sub> for the combination of the flavone apigenin and flavonol kaempferol is 27.02 μM, yet apigenin alone was 82.27 μM and kaempferol was 90.27 μM. This phenomenon of synergy in combined flavonoids, whilst scarce in literature, has been observed by other researchers. Harasstani et al. (2010) observed

that chrysin and kaempferol were synergetic when assessed for inhibition of nitric oxide (NO), prostaglandin E2 (PGE2) and tumour necrosis factor- $\alpha$ .

It is known that flavonoids have low solubility and cell permeability (Lee et al., 2007), many ways have been used improve solubility and cell permeability challenges include amorphisation and particle size reduction (Khan et al., 2015; Tseng et al., 2011; Kumari et al., 2010). These approaches however produce thermodynamically metastable species which require stabilizers in the form of surfactants or stabilising polymers. Another approach would be to form crystalline salts as solubilisation step, but this is hit by the challenge that a lot of flavonoid molecules contain weakly acidic phenolic hydroxyl groups which are difficult to deprotonate, this is the reason why there is not many flavonoid pharmaceutical salts that have been published (Zhang et al., 2019; Grynkiewicz et al., 2004). A more workable approach is the formation of cocrystals which are multicomponent crystalline complexes that are formed through heteromolecular hydrogen bonds which improve physiochemical properties of molecules such as cell permeability and solubility (Zhang et al., 2019; Yadav et al., 2019). This can be achieved in laboratory settings where the need of co-formers such as diazabicyclooctane are needed, but in nature, 2 or more flavonoids are able to form these and improve the net flavonoid content available to the cell. This can explain the observed synergistic effect of combined flavonoids.

Since it has been suggested that flavones and flavonols utilise different mechanisms that is related to their hydroxyl groups, lipophilicity, and hydrophilicity a combination can confer these merits together and allow the better bioavailability. More work is still needed however, that will show the resultant structure of the combined flavonoids, this will show the possibilities of mechanisms of function in the combined state. A more interesting observation was the fact that the most effective flavonol and the most effective flavone did not produce the most potent combination. The same can be said about the least effective singles (fig 3.3.5k.). This observation may suggest that neither too many available hydroxyl groups nor too few are not the most potent states.

#### 3.4.5 Bioavailability

Cells treated with the flavonol quercetin over a period of 7 days appeared to recover over time (fig 3.3.7). This included very high concentrations above the IC50 value. Studies on bioavailability focus on gut absorption, liver retention and blood levels (Hollman et al., 1997).

There is a scarcity of literature looking at the active life of the flavonoid in culture. The results suggest that flavonoids can be expended, and the initial effect can wear away. Flavonoids under culture are unstable and prone to enzymatic degradation, they can break down to their metabolites such as glucuronides and sulphates (Isika et al., 2022). There is no literature of flavonoid in culture, however, *in vitro*, flavonoids have an elimination half-life ( $T_{1/2}$ ) within the range of 2 to 28 hours (Manach and Donovan, 2004). This accounts for the flavonoids in blood and circulatory fluids but not quite that in cellular matrices.

The fact that cells treated with high concentrations of flavonoids show significant levels of decrease in the first 72 hours but continue to increase in number is interesting. It can be seen to suggest that the mechanism by which viability is reduced by the flavonoid is reversible and cells can recover from the onslaught. A study looking at the effects of flavonoids on cancer cells proposed that flavonoids cause cell cycle arrest at the G2 and M phase interface. This interface has a G2/M checkpoint where genes involved in apoptosis, autophagy and tumour suppression are implicated (Stark and Taylor, 2004). Both autophagy and apoptosis are multi step processes (Al-Odat et al., 2022) which are reversible if the stressor is removed before the decisive step (Fernández et al., 2015). Upon the degradation of the unstable flavonoids and their decay into lower concentrations, the hormetic effect that was seen in low concentrations could be triggered and result in the notable recovery. There is still however, scope for further investigation into the reasons for recovery.

### 3.5 Conclusion

The experiments in this chapter, were meant to investigate the effects of single and combined flavonoids on the viability of SGBS preadipocytes. In the process, method validation protocols have shown that MTT assays are valid and relate to microscopic cell counts for single flavonoids only, for flavonoid combinations, there was a discordance between microscopic cell counts and MTT assay results. This mismatch was believed to be the result of combined flavonoids forming complexes that reacted with the MTT to give false high readings that were not supported by cell counts. These complexes were seen as crystalline structures under the microscope, and they were absent on single flavonoid treatment. This observation has not been recorded elsewhere.

Treatment with low concentrations of flavonoid showed hormetic characteristics which are believed to invoke cellular stress response pathway which produce protective proteins and

reduce inflammation. This biphasic response was seen in both single and combined flavonoids although it was higher in the former. It is yet to be seen whether increased proliferation at these concentrations can be transferred to differentiation and the accumulation of lipid droplets.

Single flavonoids reduced preadipocyte viability in a dose dependant manner. There was a hierarchical relationship between the effectiveness of the single flavonoids and the hydroxyl groups on the determinant (B) carbon ring. However, the hierarchy is counter directional between flavones and flavonols. Effectiveness of flavonols increased with increasing number of hydroxyl groups whereas flavones were less effective when the number of hydroxyl groups increased. This effectiveness was thought to be related hydrophobicity and lipophilicity of the flavonoids. Preadipocyte cell membrane interactions and cell entrance would therefore be the deciding factor on effectiveness.

Combined flavonoids were more effective than the single individuals. The difference suggested a synergistic relationship. This synergy was thought to be brought about by the combined positive attributes of the single flavonoids of interaction with the cell membrane and lipophilicity that allowed more total flavonoid access to the cell. It was also suggested that the formation of secondary cocrystals helped with flavonoid transportation into the cell. More work to characterise the cocrystals and their mutual co-formers is warranted.

Cell recovery after a single treatment was investigated by taking daily cell counts after flavonoid treatment and incubation for 7 days. All concentrations showed recovery across time suggesting that bioavailability of flavonoids decayed with time and that affected cells had cell cycle arrest which could be reversible when the flavonoid stressor is removed. These findings will benefit from cell fraction analysis.

Flavonoids were therefore seen to reduce preadipocyte proliferation of preadipocytes at high concentrations with increased efficacy when they were combined. More work is needed to investigate how these findings translate in adipocyte differentiation.

## 4 Adipocyte Differentiation

### 4.1 Introduction

Differentiation of cells to mature adipocytes is a complex process which involves various precursor cells which are tightly regulated by a variety of intrinsic and extrinsic molecules (Arimochi et al., 2016; Park et al., 2013). Intrinsic factors include genes and transcription factors which are involved in increasing differentiation (Fève, 2005). Besides these, other molecules such as hormones, solutes, and extra cellular signalling help in achieving differentiation *in vivo*. *In vitro*, exogenous additives to the media allow the process of differentiation to mimic *in vivo* processes. There are different additives for making differential media; typical constituents are foetal bovine serum, dexamethasone, insulin, methylisobutylxanthine and triiodothyronine (Ghoniem et al., 2015; Scott et al., 2011; Dani et al., 1997). Upon the introduction of the differentiation media, pre-adipocyte cells change to adopt a spherical adipocyte shape which is evidenced by the accumulation of lipid droplets and the acquisition of the biochemical and morphological characteristics of fully differentiated adipocytes (Richard et al., 2020). The change in biochemistry can easily be correlated to the changes in gene expression which can be evidenced by the presence of bespoke protein markers and mRNA sequences. Whilst it is agreed that most molecular changes are at transcriptional level, there is a growing body of interest in the post transcriptional regulation of adipogenic genes (Lee et al., 2019; Moustaid & Sul, 1991). Indeed, there has been an increase in studies around epigenetic modifications in the process of adipocyte differentiation (Pant et al., 2021). The activation of differentiation genes is on the other hand inversely correlated with the expression of proliferation genes and those genes that are limiting to adipocyte conversion (Goossens et al., 2017; Cornelius, 1994). This feeds to the argument of whether proliferation and differentiation of preadipocytes is mutually exclusive (Victor et al., 2020; Ruijtenberg et al., 2016).

Differentiated adipocytes remodel and conform to the nutritionally derived energy balance of the body, they assume the protective role of lipid storage when there is a surplus of calorific supply to avert lipotoxicity (Guilherme, 2008). Mature adipocytes are an endocrine organ providing energy homeostasis. In this process, the adipocytes increase their size and incite the production of differentiation factors to recruit more adipocytes from their precursor molecules. The production of differentiation factors is believed to occur at the expense of growth factors for proliferation (Gregoire, 1991). Committed adipocytes, although still able

to increase in size, withdraw from the cell cycle and are believed not to be able to produce daughter cells (Goossens et al., 2017; Freytag & Geddes 1992; Freytag 1988). Work on various adipocyte precursor cell lines has been carried out to reveal the underpinning process of preadipocyte differentiation; these include 3T3 - L1 and -F442A cells, embryonic fibroblasts, marrow stromal cells and stromal-vascular cells (Aune, 2013). Recently, SGBS cells have started to emerge in literature but still lack the rigour needed to elucidate their pathway in differentiation. Because of the complex nature of the preadipocyte conversion, primary cultures have typically been the choice vehicle for studying the process as they are known to be predisposed to become mature adipocytes with certainty (Andrea and Enrique, 2021; Galmozzi et al., 2021; Carswell, 2012). Cell lines on the other hand do not ordinarily differentiate spontaneously, they need differentiation enhancing media. Work on cell lines would therefore benefit from endorsement or validation from primary cell differentiation experiments. The SGBS cell strain, whilst not primary, has the attributes to mirror primary cells (Tews et al., 2022; Yeo et al., 2017) and therefore would not necessarily need primary cell authentication. They are good representatives of primary cells because they are neither transformed nor immortalized, they have high proliferation and differentiation capacity, just like primary cells (Fischer-Posovszky et al., 2008).

Preadipocytes, whether primary or sustained cell line, have the morphological identity of fibroblasts. When they become confluent, contact inhibition stops continued growth, and they form mature round fat cells. They move on to accumulate lipid droplets, and progressively acquire the morphological and biochemical characteristics of the mature adipocyte (Gregoire et al., 1998). During culture, when preadipocytes reach confluence, differentiation can be induced by methodically introducing differentiation media. The distinct shapes of preadipocytes and mature adipocytes are easily identifiable under a light microscope. In fact, the rate of differentiation can be quantified by counting the number of differentiated cells relative to the number of cells viewed down the microscope (Fischer-Posovszky et al., 2008). However, it is even easier to distinguish the two states by staining the cells by a dye such as the oil red O stain. Not only does this show the difference between the differentiated and non-differentiated states, it also helps to give a semi-quantification measure of the level of differentiation per cell (Kraus et al., 2016).

Oil red O stains have been used for more than 70 years (Kraus et al., 2016; Green and Kehinde, 1974; Lillie and Ashburn, 1943). It is a dye that strongly stains lipids, a major constituent of

differentiated adipocytes. Oil red O is a low cost, non-hazardous, and time saving stain which when eluted can be read on a spectrophotometer with filters in the range of 490 to 580 nm although the peak absorbance of oil red O in propanol is 518 nm (Kraus et al., 2016). Protocol validation and optimisation for oil red O has traditionally been conducted on 3T3-L1 cells and there is still scarcity of research on oil red O validation and optimisation on SGBS cells. For that reason, it is often prudent to compare oil red O results with microscopic cell counts and triglycerides quantities.

Adipocytes store energy reserves as triglycerides, which are kept in large lipid droplets as highly specialised lipid reservoirs (Varinli et al., 2015). The quantity of available triglycerides in culture are indicative of, but indistinguishable from, the number of cells which have differentiated and the magnitude of lipid droplets accumulation. Like the oil red O stain, triglyceride assays are semi-quantitative and would benefit from confirmatory protocols like direct microscopy counts. There are many variants of triglyceride assays, the majority involve extraction of cellular lipids by heating in an extraction solution and adding lipase which convert triglycerides to glycerol. The glycerol will then convert the probe generator which is measurable by a spectrometer at 570 nm and gauged against a standard curve made from triglyceride standards (Li et al., 2017). Like oil red O, most protocol validations of triglyceride assays on differentiation are on 3T3-L1 cells and experiments on SGBS cells are few (Eseberri et al., 2019; Li et al., 2016). Experimentation on exogenous molecules on adipogenesis can therefore be assessed by triglyceride assays, oil red O stains and microscopic relative differentiation counts.

Natural plant products have been the subject of experimentation for exogenous molecules that can vary adipocyte differentiation (Wong et al., 2014). Of these, flavonoids have had a share of interest (Kim et al., 2020; Khalilpourfarshbafi et al., 2019) and these studies have been predominantly on animal cell lines or models. The need for human cell strains experimentation is therefore huge. Furthermore, existing flavonoid experiments do not make much attempt to rank the flavonoids according to their biochemical structures so that predictions on the effect of those flavonoids not yet tested are possible by studying the structure. Whilst it is not possible to experiment every flavonoid class and type in a meaningful time frame, a careful selection of representative classes and types can help make an informed prediction of structure function relationships of dietary plant flavonoids on adipocyte differentiation. Besides the structure function relationship, not much is known



about the timing of the effectiveness of the flavonoids in the journey of the adipocyte, whether treatment before induction, during induction or past the induction of differentiation give any differences.

#### 4.1.1 Aim

The aim of this chapter is to experiment on the effects of flavonoids on the differentiation of human SGBS cells, the structure function relationship and timing of effectiveness.

#### 4.1.2 Objectives

- To enable preadipocyte differentiation using differentiation induction media.
- To quantify differentiation in adipocytes using microscopic cell counts, oil red O staining and the triglyceride assay.
- To rank the effectiveness of chosen flavones and flavanones using their IC<sub>50</sub> values.
- To determine the effect of treatment stage on magnitude of differentiation
- To investigate whether differentiation and proliferation are mutually exclusive.

### 4.2 Methods

#### 4.2.1 SGBS cell culture

SGBS cells of passage levels between 33 and 38 were seeded in 6, 12 and 24 well plates at seeding densities described in chapter 2. Plates were incubated overnight with complete media (OF+10% FBS) at 37 °C in 5% CO<sub>2</sub> until cells had adhered. Cells that needed pre-differentiation flavonoid treatment were inoculated with the various flavonoid concentrations and combinations and incubated for 4 days. Cells that did not need pre-differentiation flavonoid treatment were incubated in complete (OF+10% FBS) media for 4 days, until they were 80%- 90% confluent. Differentiation was induced on day 4 by removing spent media and washing cells twice with warm PBS and adding F12 media supplemented with 33 μM biotin, 17 μM pantothenic acid, 100 U/ml penicillin/streptomycin, 2 μM rosiglitazone, 10 μg/ml human apo-transferrin, 20 nM human insulin, 25 nM dexamethasone, 500 μM 3-isobutyl-1-methylxantine, 100 nM cortisol and 200 pM triiodothyronine (Fischer-Posovszky, 2008). Cells were cultured in this differentiation induction media for 4 days and spent media was replaced with the same media constituents without rosiglitazone, 3-isobutyl-1-methylxantine and dexamethasone. Subsequent media changes were carried out according to the experiment type. Figure 4.2.1 below shows the treatment stages of the cells.

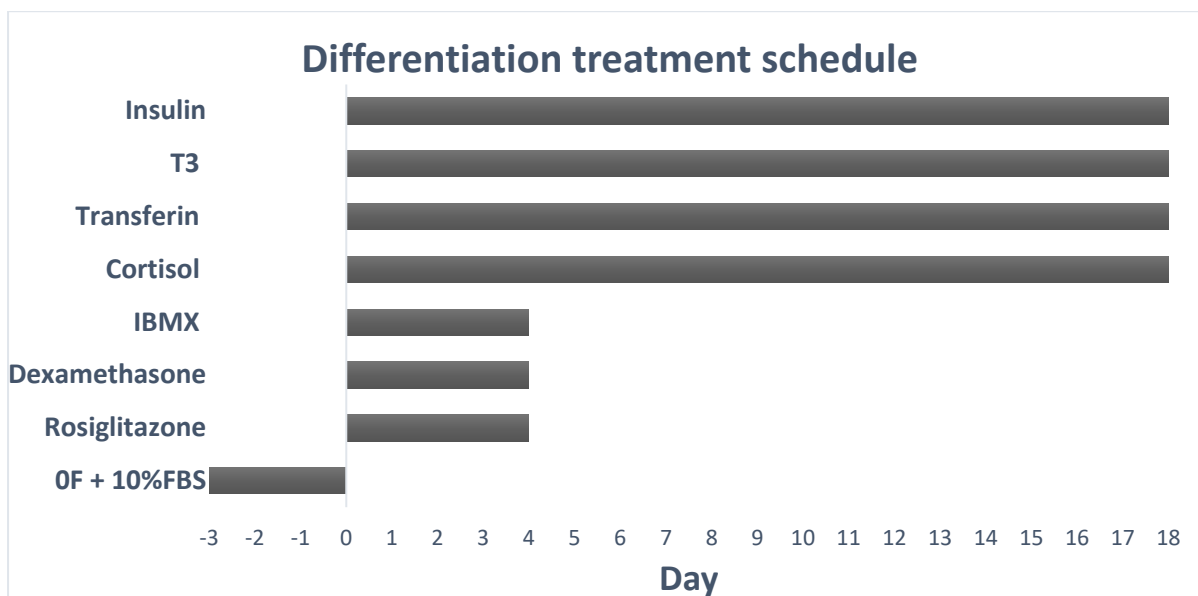


Figure 4.2.1 Differentiation treatment schedule. Cells were incubated in OF + 10% FBS media for 4 days until 80-90% confluent. At differentiation day 0, differentiation stimulation media (quick Diff) containing insulin, triiodothyronine (T3), transferrin, cortisol, isobutyl-methyl-xanthine (IBMX), dexamethasone (Dex) and rosiglitazone was added. Differentiation media containing insulin, T3, transferrin, cortisol was added on differentiation day 4 and on subsequent media changes.

#### 4.2.2 3T3-L1 cell culture

Comparator 3T3-L1 preadipocytes donated by Nottingham University were differentiated to validate SGBS experiments. All cells were grown on standard tissue culture-treated polystyrene T25 culture flasks (Corning, Berlin, Germany). Preadipocytes were kept at 37°C with 5% CO<sub>2</sub> in RPMI with 1% Sodium Bicarbonate, 1% 200 mM L-Glutamine, 10% Foetal Bovine Serum, 0.1% 50 mg/ml Gentamycin and sufficient 1M NaOH to turn the medium red (approx. pH 7.4). Cultures were passaged every 7 days, or when they achieve 70-80% confluence. For differentiation, preadipocytes were seeded on 12-well plates (3.8 cm<sup>2</sup>/well, Corning, Berlin, Germany), and kept in normal growth medium as described above. Differentiation was induced 4 days after confluence by replacing the growth medium with differentiating medium (RPMI, 10% FBS, 1 mmol/l insulin) supplemented with 100 nmol/l dexamethasone, 1 mmol/l rosiglitazone, 500 mmol/l isobutyl methylxanthine, and 250 mmol/l indomethacin. This media was replaced every 4 days. Other experimental timings mirrored those applied to SGBS cells.

### 4.2.3 Flavonoid treatment

Flavonoids were dissolved in DMSO so that the final solvent concentration was 0.5% from stock solutions of 50 mM. Working solutions ranged from 200  $\mu$ M to 1  $\mu$ M. Combination concentrations of flavonoids were achieved by mixing equal volumes of working solution treated media which were vortexed for 30 seconds. The flavonoids quercetin, galangin and kaempferol (flavonols) and chrysin, apigenin and luteolin (flavones) were experimented as single flavonoids or in combinations with a member of the other class. All three flavonols were experimented with each flavone and vice versa. Flavonoid treatments differed with the different experimental schedules as shown in figures 4.2.3a-d.

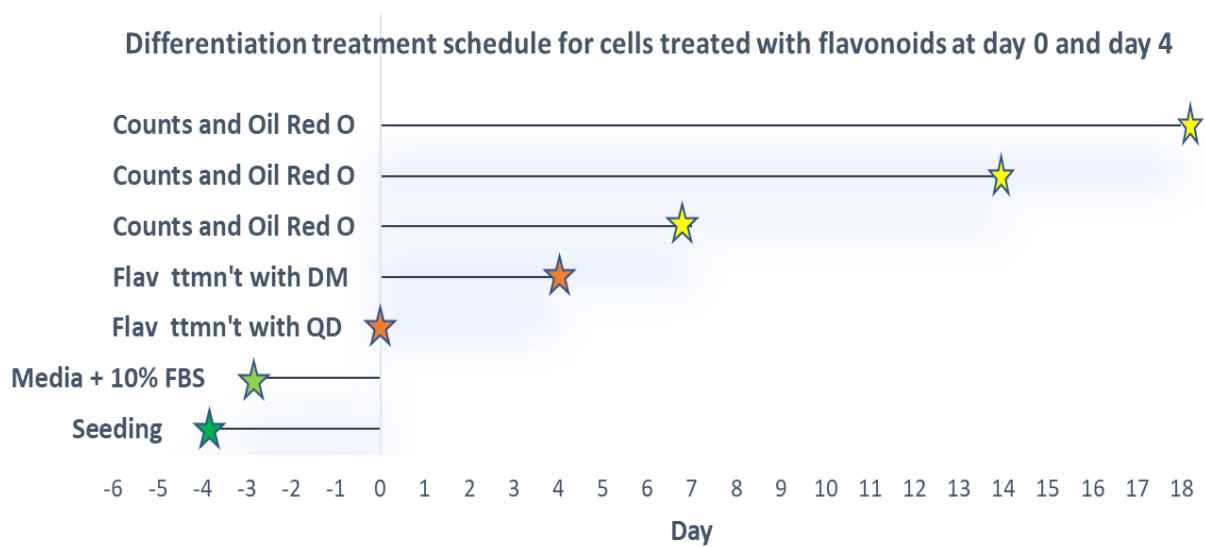


Figure 4.2.3a. Differentiation stages of SGBS cells treated with flavonoids and flavonoid combinations for comparisons on effect of flavonoids on adipocyte differentiation. Cells were seeded on day -4 and media was replaced on day -3 (after adherence) with complete media containing 10% FBS. On day 0 cells were treated with quick differentiation media (QD) containing the different concentration of flavonoids and flavonoid combinations. On day 4 cells were treated with the standard differentiation media containing the different concentrations and flavonoid combinations. Differential counts, oil red O quantification and photomicrographs were taken on days 7, 14 and 18.

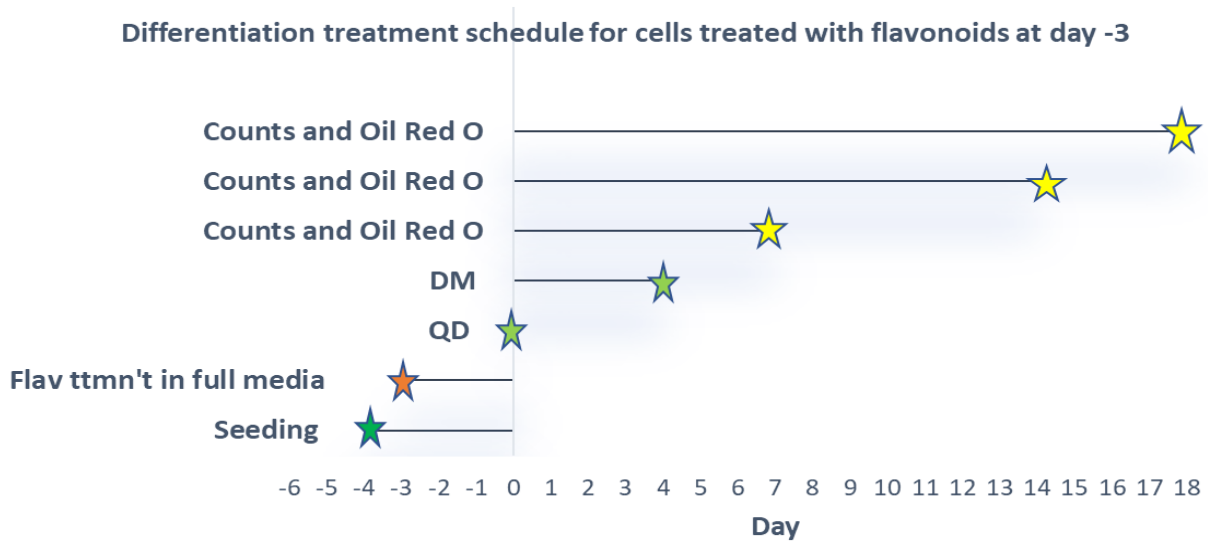


Figure 4.2.3b Figure 4.2.3b. Differentiation stages of SGBS cells treated with flavonoids and flavonoid combinations for comparisons on effect of flavonoids on adipocyte differentiation. Cells were seeded on day -4 and media was replaced on day -3 (after adherence) with complete media containing 10% FBS and the various flavonoid and flavonoid combinations concentrations. On day 0 cells were treated with quick differentiation media (QD). On day 4 cells were treated with the standard differentiation media. Differential counts, oil red O quantification and photomicrographs were taken on days 7, 14 and 18.

#### 4.2.4 Microscopic counts

Microscope counts of total and differentiated cells were carried out in cells growing in 12 well plates for experiments which compared all flavonoids and flavonoid combinations. An inverted Nikon TMS microscope was used for cell counts. A DS-Fi camera attachment was used in conjunction with a Nikon Digital sight DS-LZ display screen to take photomicrographs. The microscope was set to x100 magnification for cell counting. Each well was counted 6 times from randomly selected cardinal points and a mean count was derived as illustrated in figure 4.23 below. Cells with three or more lipid droplets per cell were considered to be differentiated. The size or shape of the lipid droplets was not considered in differential rates experiments.

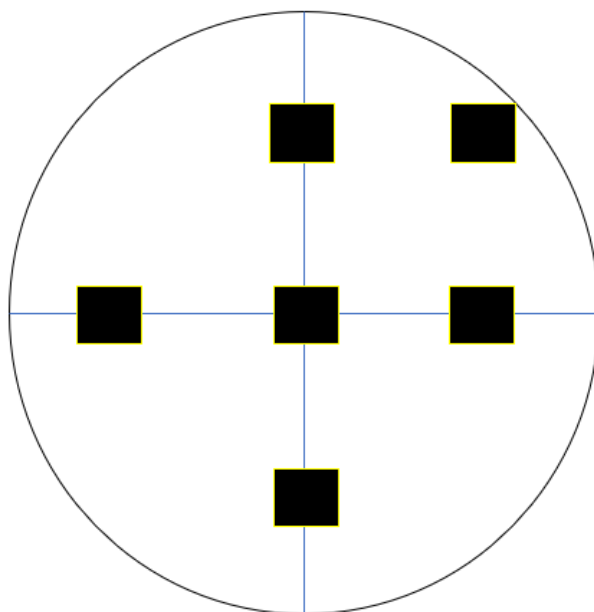


Figure 4.2.4 Sampling points for microscopic counts being 6 cardinal points selected from a single well of a 12 well plate with triplicate wells bearing the same treatment conditions.

#### 4.2.5 Oil red O staining for lipid quantification.

The magnitude of differentiation was quantified by the oil red O stain protocol. Treatment of cells whose differentiation was quantified by oil red O followed the schedule shown in figure 4.2.3a which is treatment at day 0 and day 4. Stock solution for oil red O was made by dissolving 0.7 g Oil Red O in 200 ml Isopropanol (3.5 mg/ml). This was mixed well by vortexing for 5 minutes and filtered through a 0.2  $\mu\text{m}$  filter. The stock solution was stored at 4°C. Oil red O working solution was prepared by diluting 6 parts of Oil Red O Stock with 4 parts of H<sub>2</sub>O. This was mixed by vortexing and allowed to stand for 20 min. This was then filtered through a 0.2  $\mu\text{m}$  filter. Cell fixation was achieved using paraformaldehyde (PFA). A stock solution of 37% Paraformaldehyde (w/v) was made by dissolving 37 g of PFA in 100 ml of PBS. This was mixed in a water bath at 60°C and cooled to be stored at 4°C. A working solution of 3.7% was made by a 1:10 dilution of the 37% PFA in PBS.

Flavonoid comparison experiments were conducted in 12 well plates. After spent media was aspirated and discarded, each well was flooded with the 1 ml of PFA working solution. The plates were incubated for 10 mins at room temperature. The PFA was removed and replaced with 1 ml of fresh PFA working solution. The plate was wrapped in parafilm and aluminum foil and incubated for an hour. After incubation, the PFA was completely aspirated, and wells washed once with 60% isopropanol. Wells were left in the fume hood to dry completely after which 400  $\mu\text{l}$  per well of oil red O working solution was added and incubated for 10 mins at

room temperature. Distilled water was added immediately after removing the oil red O. This was followed by 4 washes of a gentle stream of tap water. Photos were taken whilst the cells were still covered in water. The water was removed, and plates were air dried in a fume hood. The stain was eluted using 1 ml per well of 100% Isopropanol which was incubated for 10 mins at room temperature. After incubation, the stain was pipetted up and down and transferred to 1.5 ml Eppendorf tubes. Quantification was achieved by adding 200  $\mu$ l of the eluted stain to wells of the 96 well plates in duplicates and measuring absorbance at 550 nm. Three controls were used, a blank of 100% isopropanol, a stained empty well and a stained well of preadipocytes.

#### 4.2.6 Triglycerides extraction and quantification

Triglycerides were quantified from differentiated adipocytes that were treated with quercetin alone. 12 well culture plates were placed in a fume hood and the spent media aspirated and discarded. A volume of 500  $\mu$ l of Hexane/Isopropanol (3:2) was added and incubated for 1 min. This was gently pipetted up and down (without disturbing the adherent cells) and the triglycerides in solvent were transferred to a labelled Eppendorf tube. An additional 500  $\mu$ l of Hexane/Isopropanol (3:2) was added to the same well and incubated for 1 minute and the triglycerides in solvent were added to the same Eppendorf tube. The Eppendorf tubes were evaporated in a vacuum evaporator (Speedvac) at 30°C for 45 minutes.

Quantification was performed according the ab65336 Colorimetric Triglyceride Quantification Assay Kit (Abcam, Germany). All materials and reagents were equilibrated at room temperature. Wells were set in a 96 well plate such that there were 50  $\mu$ L of standards, and 2 - 50  $\mu$ L of samples which were adjusted to a volume to 50  $\mu$ L/well with Triglyceride Assay Buffer. To sample and standard wells, 2  $\mu$ L of lipase was added followed by agitation and incubation for 20 mins at room temperature to convert any triglyceride to glycerol and fatty acid. A volume of 50  $\mu$ L of Triglyceride Reaction Mix was prepared for each reaction. This was prepared from a master mix for consistency. The master mix was prepared by adding 92% Triglyceride Assay Buffer, 4% Triglyceride Probe and 4% Triglyceride Enzyme Mix. After adding 50  $\mu$ L of the Reaction Mix into each standard and sample the wells were incubated at room temperature for 60 minutes whilst protected from light. The absorbance of the wells was then read at 570 nm. A calibration curve was made from the standards and used to determine the quantity of triglycerides in the sample.

#### 4.2.7 Statistical analysis

Results were expressed as the mean  $\pm$  SD for the number of assays indicated. Analyses were performed with Microsoft Excel with Daniel's XL Toolbox add-in. For multiple comparisons of groups statistical significance was calculated and evaluated by one-way ANOVA followed by Tukey post-hoc test. To compare two groups, two-tailed paired Student's t-test was used. Logarithms of concentrations were used to derive IC<sub>50</sub> values of flavonoids to enable quantifiable comparisons and ranking. Correlation between comparative measures of differentiation were determined by calculating the R<sup>2</sup> correlation coefficient in Excel.

### 4.3 Results

#### 4.3.1 Qualitative analysis

Cells treated with 10  $\mu$ M and 100  $\mu$ M of flavonoids in 12 well plates and stained with oil red 'O' were observed microscopically for qualitative analysis (table 4.2.1a and b). The results mirrored quantitative spectrophotometric results of oil red O experiments. The general finding was that, after treating the cells with the flavonoids and incubating for 18 days, there was emerging proliferation in the 10  $\mu$ M treated wells across all the flavonoids. There was significantly lower evidence of differentiation compared to the controls. For the 100  $\mu$ M treated cells, there was a decrease in viability and differentiation when compared to the controls. There was a greater range of variability across wells of the same flavonoid and across different flavonoids because most cells were dead and detached. However, the detached cells could take up the stain, resulting in a small variability between counts and oil red O measurements at higher concentrations.

Table 4.3.1a Effects of the flavanols quercetin, galangin and kaempferol at 10 and 100  $\mu\text{M}$  concentrations on SGBS cells during differentiation as viewed under the microscope. Of the three flavanols, quercetin appeared to be more effective at both concentrations and galangin was the least in reducing the level of differentiation.

		Qualitative description	Percentage differentiation
Solvent control	DMSO	Same size and shape as media control. Evenly distributed cells. Greater than 80% differentiation with many big lipid droplets. Minimum presence of classic preadipocytes.	>80%
Media control	0 $\mu\text{M}$ (media)	Same size and shape as solvent control. Evenly distributed cells. Greater than 80% differentiation with many big lipid droplets. Minimum presence of classic preadipocytes.	>80%
Quercetin	10 $\mu\text{M}$	There was presence of more “flat and stretched” cells without any lipid droplets; these had the appearance of undifferentiated preadipocytes. The cell density was significantly greater than observed in the controls. Those cells showing signs of differentiation had very small lipid droplets and the maturity of the emerging adipocytes resembled those of day 7 adipocytes or less.	>15% and <35%
Quercetin	100 $\mu\text{M}$	Few adipocytes appeared to still be adhered. The adhered cells resembled undifferentiated preadipocytes. A large area had a film of detached cells (a curtain membranous film/curtain). These detached cells had emerging features of differentiation. The lipid droplets were small and formed a circular or semi-circular formation which is similar to what is observed in differentiating cells at day 4. There were however some isolated cells which had larger lipid droplets.	>10% and <30%
Kaempferol	10 $\mu\text{M}$	There were more cells which appeared like proliferating preadipocytes. The plates contained cells with small and emerging lipid droplets. These were not as dense as in the quercetin treated cells but were significantly more than those in the untreated controls.	>20% and <35%
Kaempferol	100 $\mu\text{M}$	A few cells showed continued growth which did not take in the stain. The edges of the cell populations did however have trails or remnants of the stain. There were features which appeared like cracks in the cell clusters	>30% and <45%



		and some cells appeared to be shrivelled with debris around the shrivelled cells. There were a significant number of cells showing signs of emerging differentiation with a similarity of day 7 proliferating adipocytes.	
Galangin	10 $\mu$ M	Almost virgin preadipocytes were evident in the plates. There was evidence of proliferation by the shape of the cells and the budding colonies.	>40% and <60%
Galangin	100 $\mu$ M	There were some intact and heavily proliferated preadipocytes without any oil red 'O' stain taken in. Most cells were dead, there were debris and cell fragments. Some pockets of viable cells had evidence of emerging differentiation consistent with day 4 features.	>15% and <30%

Table 4.3.1b Effects of the flavones chrysin, luteolin and apigenin 10 and 100  $\mu$ M concentrations on SGBS cells during differentiation as viewed under the microscope. Of the three flavones, chrysin appeared to be more effective at both concentrations and luteolin was the least in reducing the level of differentiation. A combination of chrysin and the flavanol quercetin appeared to be more effective than either flavonoid.

		Qualitative description	Percentage differentiation
Chrysin	10 $\mu$ M	Most of the cells were "flat and stretched" without any lipid droplets; these had the appearance of undifferentiated preadipocytes. The cell density was significantly greater than the controls. Those cells showing signs of differentiation had very small lipid droplets and the maturity of the emerging adipocytes resembled those of under day 7 adipocytes.	>15% and <40%
Chrysin	100 $\mu$ M	Most cells were dead; there were debris and cell fragments. There was a filament "curtain" of detached cells which made up about 50% of some wells and took up the oil red "O" dye. There were however still some pockets of viable cells which had evidence of emerging differentiation consistent with day 4 features with very small lipid droplets which took up the stain. There was a very low ratio of differentiation to total cell ratio. Many cells appeared disfigured and shrivelled. There were signs of "trauma" and ravaged cells.	>10% and <20%

Apigenin	10 µM	Heavy growth of preadipocytes characterised with fibroblast looking cells without stain uptake. There was evidence of proliferation by the shape of the cells and the budding colonies.	>20% and <40%
Apigenin	100 µM	Most cells were dead; there were debris and cell fragments. Very few pockets of viable cells had evidence of emerging differentiation consistent with day 4 features. However, there were signs of toxicity.	>15% and <30%
Luteolin	10 µM	There were many cells which appeared like proliferating preadipocytes. The plates contained cells with small and emerging lipid droplets. These were not as dense as in the quercetin treated cells but were significantly more than those in the untreated controls.	>35% and <50%
Luteolin	100 µM	There were intact and evidently proliferated preadipocytes without any oil red 'O' stain taken in. There were clusters of stained cell boundaries without lipid droplets. There were features which appeared like cracks in the cell clusters and some cells appeared to be shrivelled with debris around the shrivelled cells. The cells which showed signs of emerging differentiation had a similarity with above day 4 proliferating adipocytes	>20% and <40%
Quercetin and Chrysin	10 µM	More "flat and stretched" cells without any lipid droplets were observed with the appearance of undifferentiated preadipocytes. Those cells showing signs of differentiation were very few and had very small lipid droplets and the maturity of emerging adipocytes resembled those of day 7 or less. There were streaks which resembled crystals in the media.	>10% and <35%
Quercetin and Chrysin	100 µM	Fewer adipocytes appeared attached. Most cells were dead. There were filament "curtains" of detached cells which made up about 50% of some wells; these took up the oil red "O" dye. Differentiated cells had few lipid droplets per cell. There was a very low ratio of differentiation to total cell ratio. Many cells appeared disfigured and shrivelled. There were many crystalline features which suggested flavonoid crystallisation.	>5% and <20%

#### 4.3.2 Differentiation proof of concept and quality assurance.

SGBS and comparator 3T3L1 cells were allowed to differentiate spontaneously for 18 days in comparison with cells differentiated using the differentiation media described in 4.2.1 and 4.2.2. Spontaneously differentiated SGBS and 3T3-L1 cells had significantly lower absorbance readings ( $p < 0.01$ ) compared to the stimulated cells suggesting that the stimulation media was effective in achieving differentiation within the time frame of the experience (figure 4.3.2a). Photomicrographs (figure 4.3.2b and c) also showed the visual differences between cells allowed to differentiate naturally and those assisted using the enhanced differentiation media. A comparison of oil red O stain results as a measure of the magnitude of differentiation with relative differentiation counts indicated a very high level of correlation ( $R^2 > 97\%$ ) suggesting validity in the methods employed (figure 4.3.2d). Presence of the solvent DMSO did not affect the level of differentiation in treated cells (figure 4.3.2e) as there was no statistical significance ( $p < 0.001$ ) between the treatments with or without the solvent.

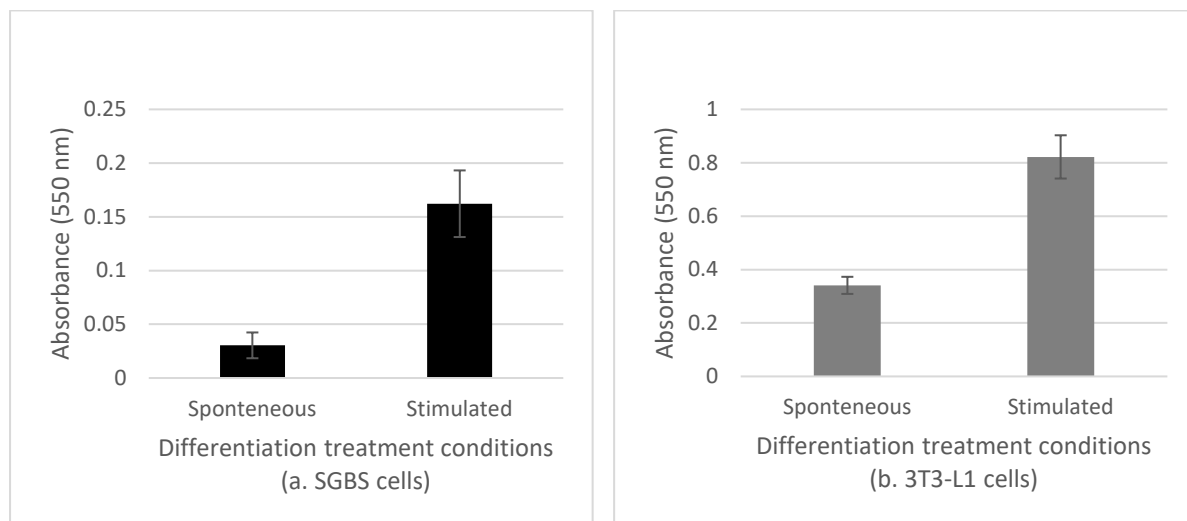


Figure 4.3.2a Comparison between spontaneous and stimulated mature SGBS and 3T3-L1 adipocytes. Spontaneous differentiation was achieved by allowing cells to grow until they were confluent and standard growth media (described in 4.2.1 and 4.2.2) was changed every 4 days until 18 days. Stimulated differentiation was achieved by replacing standard growth media with quick differentiation media on day 4 of growth and routine differentiation media (described in 4.2.1) on day 8 and every subsequent 4th day until day 18. Stimulated adipocytes were significantly more mature than those allowed to differentiate naturally ( $p < 0.01$ ) for both SGBS and 3T3-L1 cells.

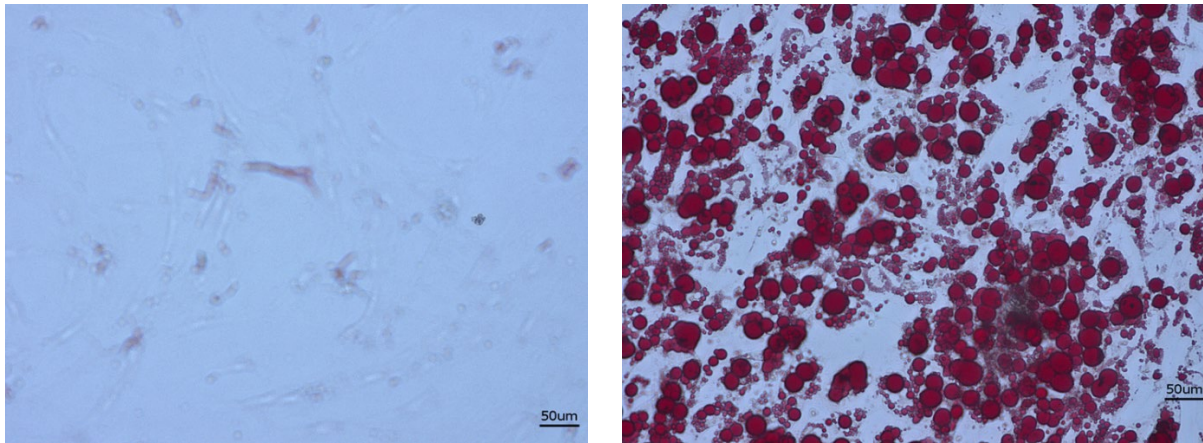


Figure 4.3.2b. Photomicrographs comparing spontaneous and stimulated mature SGBS adipocytes stained with oil red O. Spontaneous differentiation was achieved by allowing cells to grow until they were confluent and standard growth media (described in 4.2.1) was changed every 4 days until 18 days. Stimulated differentiation was achieved by replacing standard growth media with quick differentiation media on day 4 of growth and routine differentiation media (described in 4.2.1) on day 8 and every subsequent 4th day until day 18. Stimulated adipocytes were significantly more mature than those allowed to differentiate naturally ( $p < 0.01$ ).

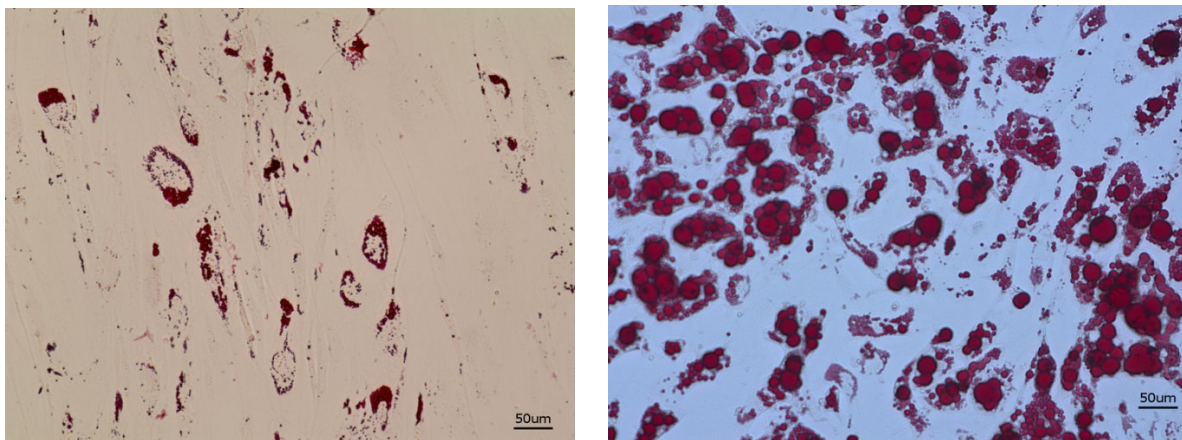


Figure 4.3.2c. Photomicrographs comparing spontaneous and stimulated mature 3T3-L1 adipocytes stained with oil red O. Spontaneous differentiation was achieved by allowing cells to grow until they were confluent and standard growth media (described in 4.2.2) was changed every 4 days until 18 days. Stimulated differentiation was achieved by replacing standard growth media with quick differentiation media on day 4 of growth and routine differentiation media (described in 4.2.2) on day 8 and every subsequent 4th day until day 18. Stimulated adipocytes were significantly more mature than those allowed to differentiate naturally ( $p < 0.01$ ).

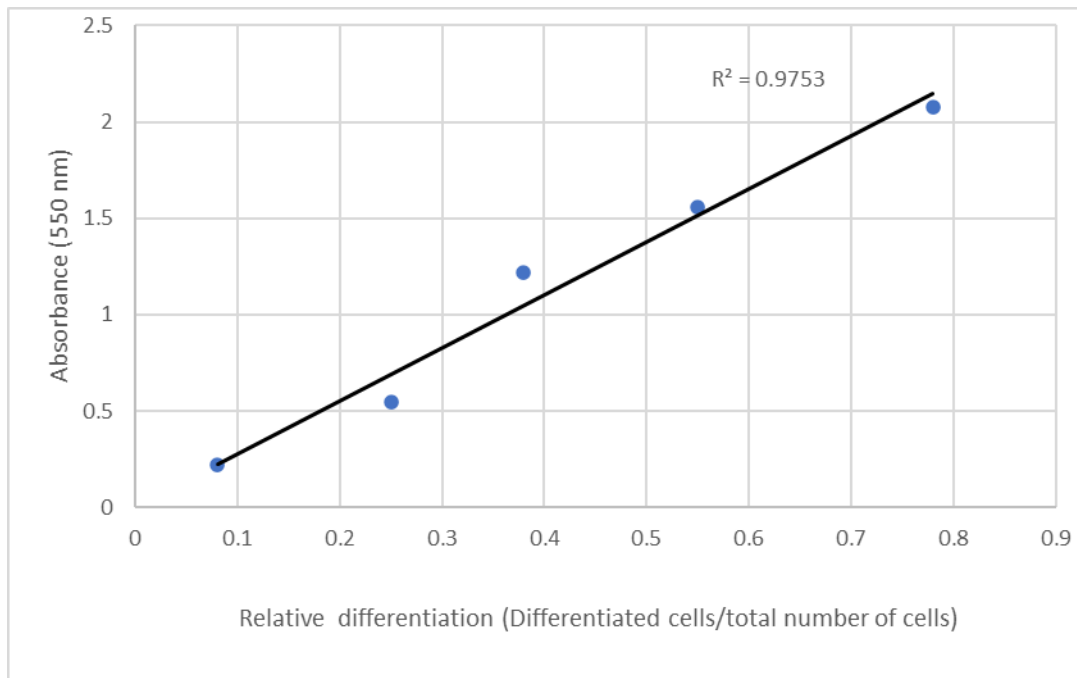


Figure 4.3.2d. Validation curve showing the correlation between the oil red O absorbance reading to the relative differentiation microscopic counts (differentiated cells/total number of available cells). Plates with different differentiation levels were counted and the same plates were taken through the oil red O protocol to compare the 2 approaches to quantifying. There was a very strong correlation ( $R^2=0.9753$ ) between the two measures of differentiation.

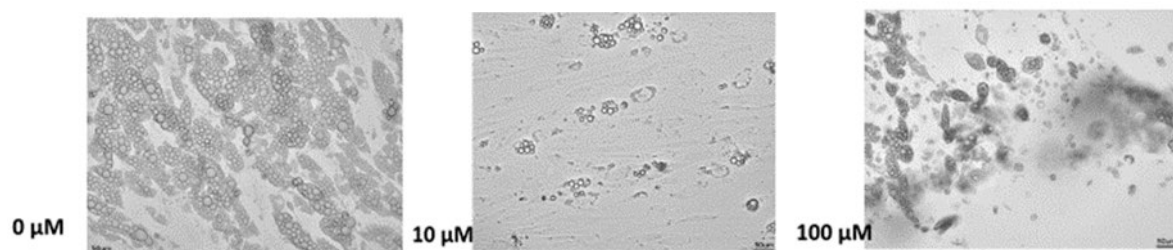


Figure 4.3.7. Photomicrographs of differentiated SGBS cells after treatment with 0, 10 and 100  $\mu\text{M}$  quercetin for 21 days. The untreated control had greater than 80% differentiation, the 10  $\mu\text{M}$  treatment had fewer differentiated cells and of those, they had fewer and smaller lipid droplets. The 100  $\mu\text{M}$  had detached differentiated cells that could easily wash away during the washing stages of oil red O protocol.

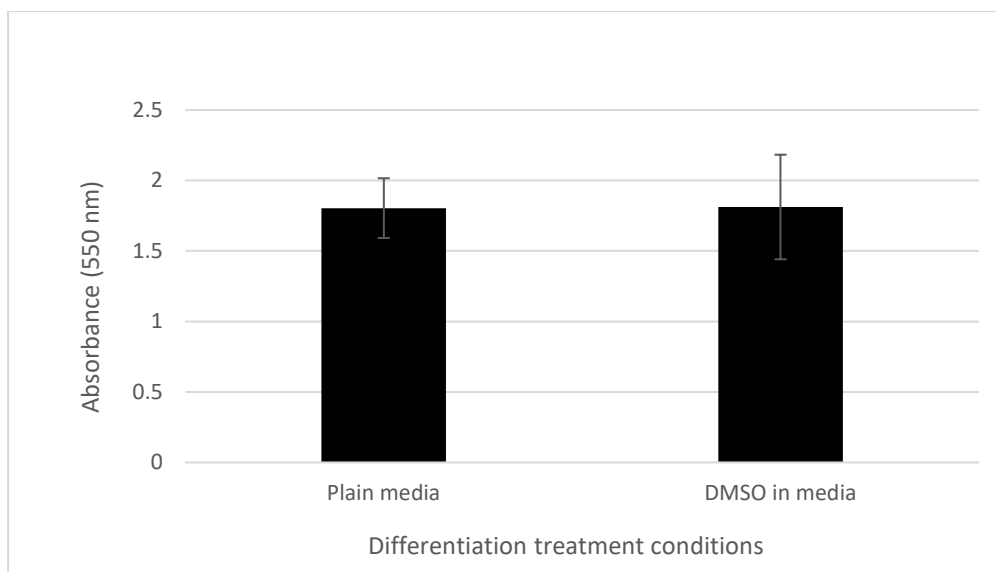
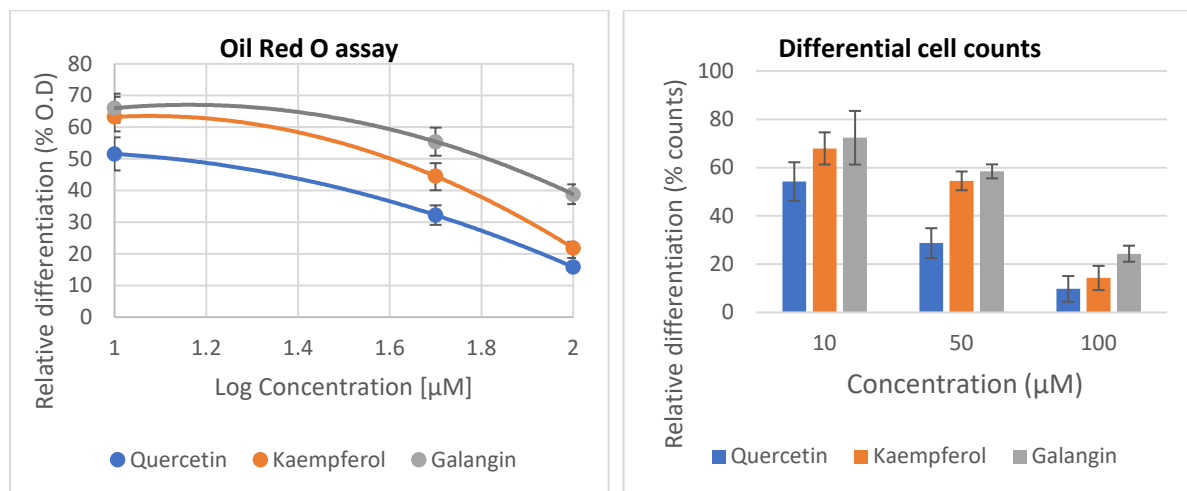


Figure 4.3.2e. Comparison of oil red O absorbance values for SGBS cells in standard differentiation media to cells treated with differentiation media containing 0.5% DMSO (the highest dose found in the 100  $\mu$ M treatment). There was no statistical difference ( $p > 0.001$ ) in the absorbance between the 2 treatments conditions. The presence of the solvent at that concentration had no impact on the rate of differentiation.

#### 4.3.3 Comparison of flavonoid treatments on rate of differentiation.

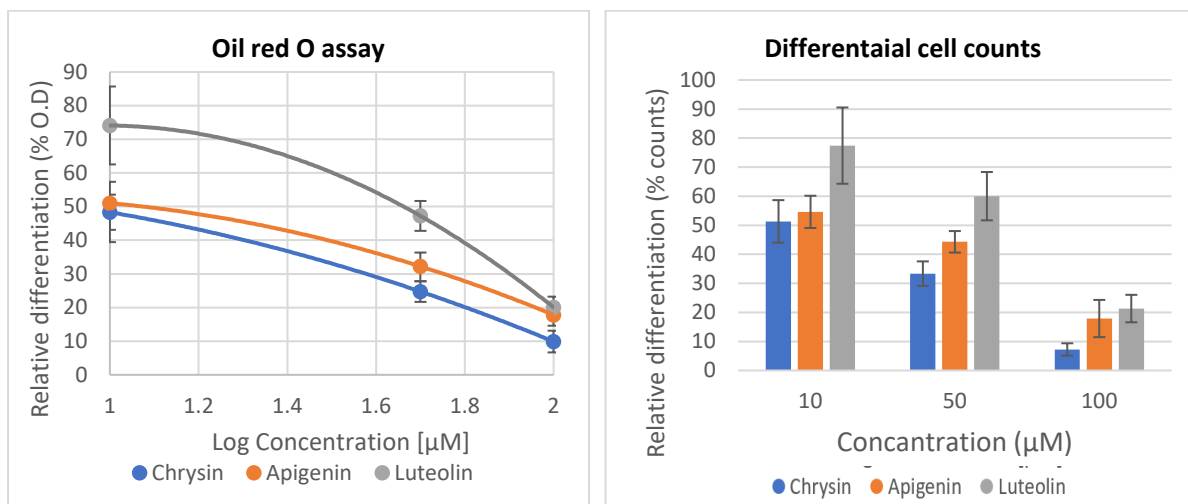
Cells treated twice during differentiation (figure 4.2.3a) with the flavanols quercetin, kaempferol and galangin, and the flavones chrysin, apigenin and luteolin were tested for oil red O absorbance and relative microscope differential counts. Results for oil red O stains as measured by spectrophotometer absorbance were similar to those of microscopic differential counts for single flavonoid treatments, this helped validate the methods. However, for flavonoid combinations, oil red O stain results were elevated compared to the microscopic count results. Further investigation revealed that flavonoid combinations produced crystalline features in cells which absorbed more oil red O dye than the number of cells per well would absorb. The distinction also suggested differences in the way flavonoids reduced differentiation, that is either reduction of the number of cells which differentiated or reduction in the amount of lipid droplets formed per cell. This was further tested by triglyceride assays.

All flavonoids and flavonoid combinations reduced adipocyte differentiation at all concentrations. The effect of the flavonoids was dose dependant, higher doses were more effective in reducing differentiation. When the flavanols were compared, the order of effectiveness was quercetin, galangin and kaempferol, that of flavones was chrysin, apigenin and luteolin. Flavonoid combinations appeared to be additive as some combinations were less effective than the more effective single flavonoid but more effective than the least effective single flavonoid. Flavonoid ranking was achieved by comparing the IC<sub>50</sub> values from the range of concentrations employed. The overall order of effectiveness of all flavonoids and flavonoid combinations experimented was chrysin, quercetin, apigenin, quercetin & chrysin, quercetin & apigenin, chrysin & galangin quercetin & luteolin, galangin, chrysin & kaempferol, luteolin and kaempferol.



	Quercetin	Galangin	Kaempferol
IC <sub>50</sub> (µM)	12	40	65

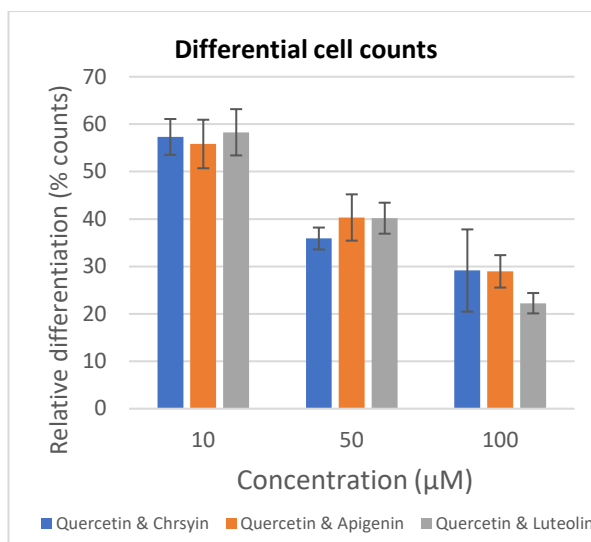
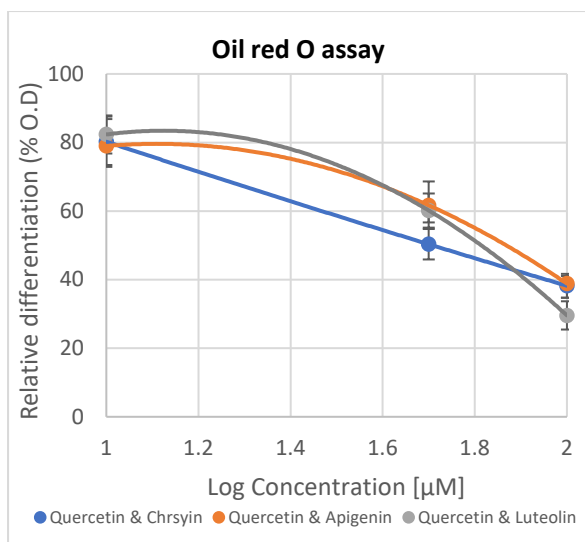
Figure 4.3.3a. comparison of the effectiveness of the flavanols quercetin, galangin and kaempferol on the differentiation of SGBS preadipocytes. Cells were treated twice during differentiation with the flavanols and tested for oil red O absorbance and relative microscope differential counts. Both oil red O absorbance and relative differentiation cell counts showed that quercetin was most effective, followed by galangin then kaempferol. The IC<sub>50</sub> values were 11.98 µM, 39.82 µM and 64.57 µM, respectively. The differences were statistically significant (p<0.05) and results were a mean of three independent experiments each with 8 replicates for the absorbance measurements and 18 replicates for the relative cell counts. Results are presented as mean +/- standard deviation.



	Chrysin	Apigenin	Luteolin
IC <sub>50</sub> (µM)	8	12	46

Figure 4.3.3b. comparison of the effectiveness of the flavones chrysin, apigenin and luteolin on the differentiation of SGBS preadipocytes. Cells were treated twice during differentiation with the flavones and tested for oil red O absorbance and relative microscope differential counts. Both oil red O absorbance and relative differentiation cell counts showed that chrysin was most effective, followed by apigenin then luteolin. The IC<sub>50</sub> values were 7.59 µM, 12.04 µM and 45.71 µM, respectively. The differences were statistically significant ( $p < 0.05$ ) and results were a mean of three independent experiments each with 8 replicates for the absorbance measurements and 18 replicates for the relative cell counts. Results are presented as mean +/- standard deviation.





	Quercetin & Chrysin	Quercetin & Apigenin	Quercetin & Luteolin
IC <sub>50</sub> (µM)	21	25	31

Figure 4.3.3c comparison of the effectiveness of the flavanol quercetin when combined with the flavones chrysin, apigenin and luteolin on the differentiation of SGBS preadipocytes. Cells were treated twice during differentiation with the flavonoid combinations and tested for oil red O absorbance and relative microscope differential counts. Both oil red O absorbance and relative differentiation cell counts showed that the IC<sub>50</sub> of quercetin and chrysin was lowest, followed by that of quercetin and apigenin and finally quercetin and luteolin. The IC<sub>50</sub> values were 21.09 µM, 25.41 µM and 30.76 µM, respectively. Relative cell counts values were generally lower than oil red O absorbance values. The differences between flavonoid combinations were statistically significant ( $p < 0.05$ ) and results were a mean of three independent experiments each with 8 replicates for the absorbance measurements and 18 replicates for the relative cell counts. Results are presented as mean +/- standard deviation.

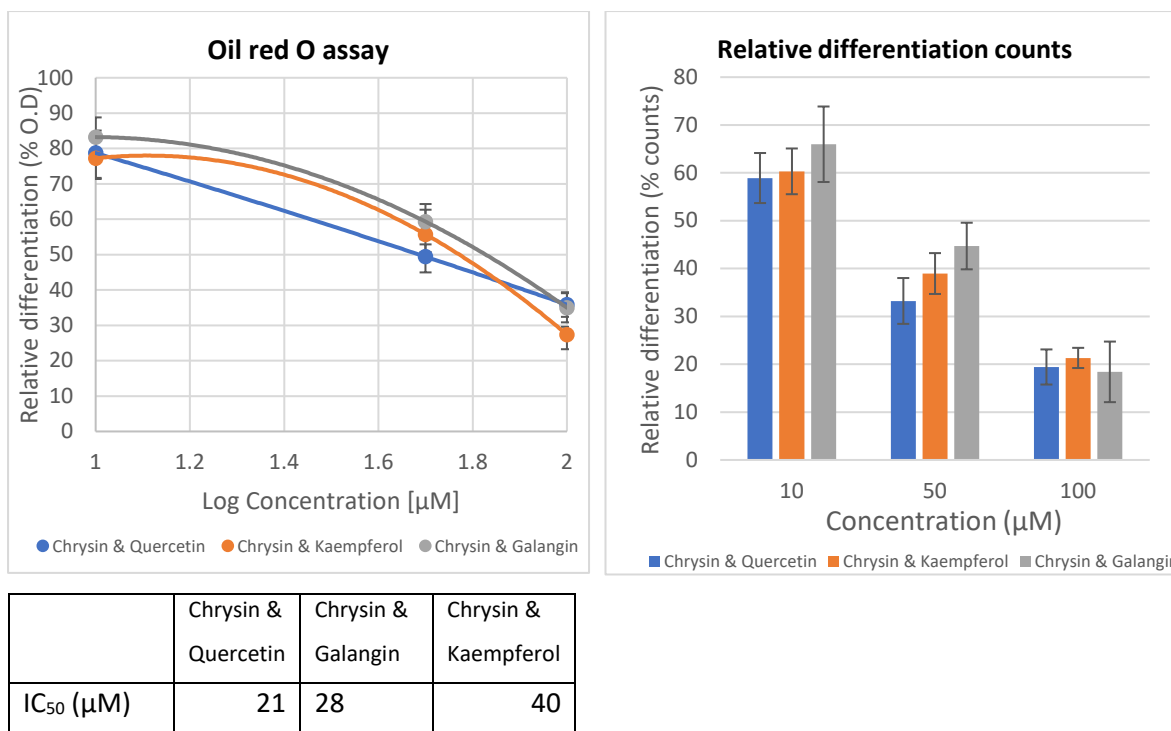


Figure 4.3.3d. comparison of the effectiveness of the flavone chrysin when combined with the flavanols quercetin, galangin and kaempferol on the differentiation of SGBS preadipocytes. Cells were treated twice during differentiation and tested for oil red O absorbance and relative microscope differential counts. Both oil red O absorbance and relative differentiation cell counts showed that the IC<sub>50</sub> of chrysin and quercetin was lowest, followed by that of chrysin and galangin and finally chrysin and kaempferol. The IC<sub>50</sub> values were 21.23 µM, 28.47 µM and 40.21 µM, respectively. Relative cell counts values were generally lower than oil red O absorbance values. The differences between flavonoid combinations were statistically significant ( $p < 0.05$ ) and results were a mean of three independent experiments each with 8 replicates for the absorbance measurements and 18 replicates for the relative cell counts. Results are presented as mean +/- standard deviation.

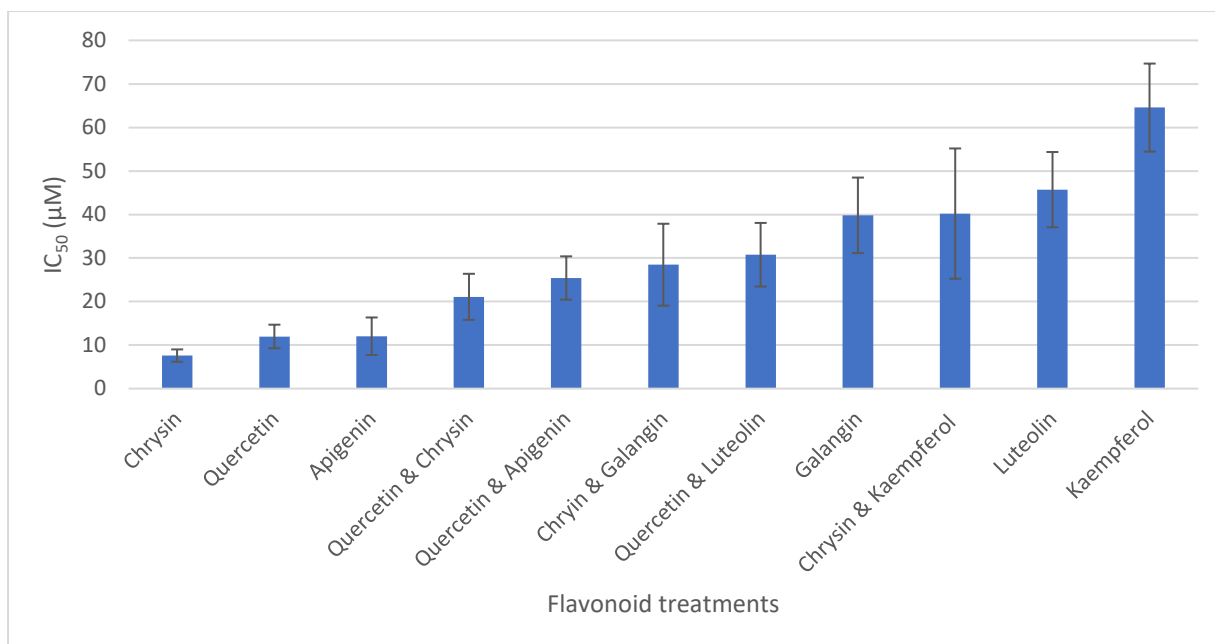


Figure 4.3.3e Single and combined flavonoid treatments as ranked by IC<sub>50</sub> values show that the order of effectiveness in inhibiting differentiation was chrysin, quercetin, apigenin, quercetin & chrysin, quercetin & apigenin, chrysin & galangin quercetin & luteolin, galangin, chrysin & kaempferol, luteolin and kaempferol.

#### 4.3.4 Comparison of time of treatment on rate of differentiation.

The flavanol quercetin was further investigated to find the critical phase of adipogenesis where flavonoids may be effective. SGBS preadipocytes were treated with the flavanol quercetin at concentrations ranging from 1 µM to 100 µM during proliferation before the induction of differentiation, during both proliferation and differentiation, and only part way through differentiation, on day 4. All concentrations reduced differentiation with the higher concentrations with the greatest reduction. Peri-physiological flavonoid concentrations of 1, 5 and 10 µM did not have any intra-range significant difference in effect ( $p > 0.05$ ). All treatment regimens reduced differentiation and therefore it does not seem to matter at what point in the adipogenesis process that a flavonoid is introduced. Multiple flavonoid treatments however had a significantly greater impact in reducing differentiation ( $p < 0.05$ ) across all concentrations. Readings were taken at day 18 of differentiation. There was relatively higher variability in the repeats as seen by larger values of standard deviation values (shown as error bars in figure 4.3.4), this was attributed to the bioaccumulation of the solvent DMSO.

Microscopic cell counts were used to follow the time course for differentiation of cells treated during proliferation only and those which were treated during both differentiation and initiation of differentiation (tables 4.3.4a-d). Results showed that cells treated during proliferation only had significantly lower rates of differentiation compared to those treated in the 2 phases. It was also interesting to note that, when flavonoid treatment stopped, during differentiation, cells recovered from differentiation and reverted to proliferation. This adds to the argument of whether proliferation is mutually exclusive to differentiation. Whilst rate of differentiation percentages may remain similar, recovering cells were seen to have a higher total number of available cells because some continued to replicate during differentiation. Having the differentiation media available, the nascent cells would also have the potential to differentiate.

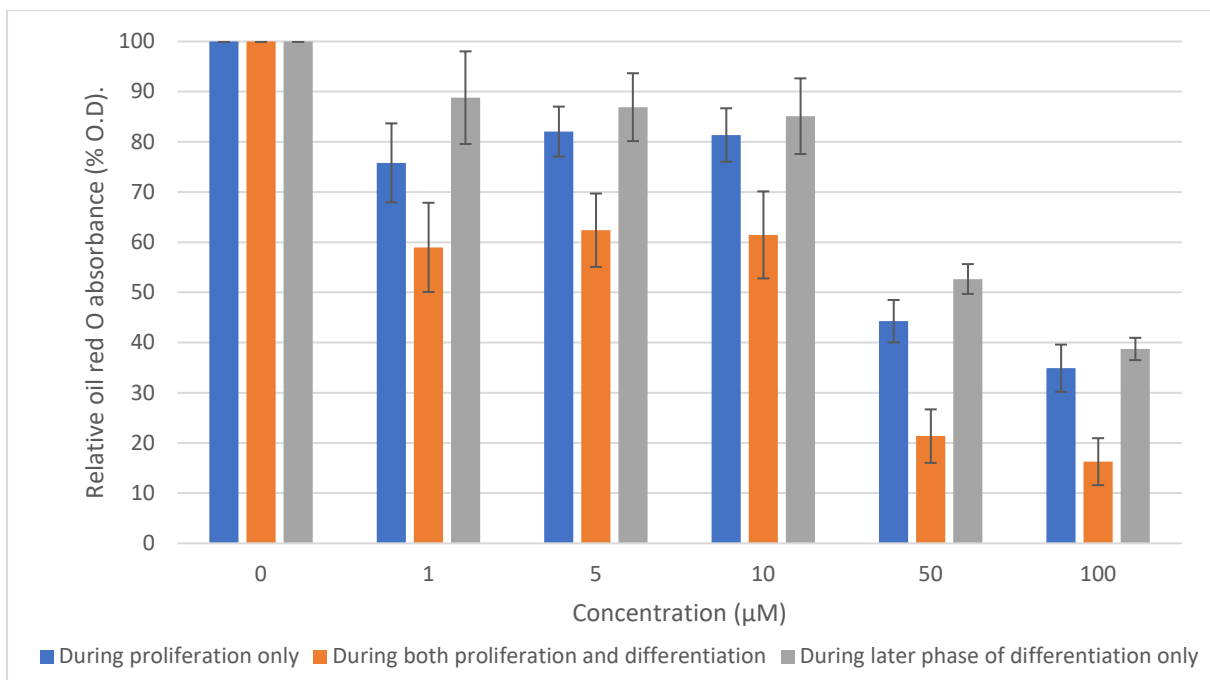


Figure 4.3.4 SGBS preadipocytes were treated with the flavanol quercetin with concentrations ranging from 1 µM to 100 µM during proliferation before the induction of differentiation, during both proliferation and differentiation, and only part way through differentiation, on day 4. All treatments regimens and concentrations reduced the differentiation rate of the SGBS cells. Cells treated with the flavonoid at every media change had the highest effect although it had the highest variation of repeats because of solvent (DMSO) bioaccumulation. Values represent means and error bars are standard deviations from three independent experiments with 8 replicates each.

Table 4.2.3 (a-d) Comparison between differentiation treatment regimens of proliferation phase only against both proliferation and induction of differentiation. Cells treated during proliferation only had significantly lower rates of differentiation compared to those treated during both phases. The total number of cells continued to increase even in treated cells although more differentiated cells were emerging. For the cells treated during both proliferation and differentiation phases, the higher concentrations cause the cells to lose their adherence properties and lipid laden cells were seen floating in the media and hence the low counts. Results are from 3 independent experiments with 18 replicates each.

a) Day 7

	Treated during proliferation only (day -3)					Treated during both proliferation and differentiation (day -3 and day 0)			
Quercetin concentration ( $\mu\text{M}$ )	0	1	10	100		0	1	10	100
Mean mature adipocyte count	156.8	161.33	80.22	14.22		149.33	91.67	38.22	0
Mean total cell count	268.3	260.67	236.33	205.9		314.44	314.4	317.8	183.9

b) Day 10

	Treated during proliferation only (day -3)					Treated during both proliferation and differentiation (day -3 and day 0)			
Quercetin concentration ( $\mu\text{M}$ )	0	1	10	100		0	1	10	100
Mean mature adipocyte count	223.4	203.89	140.56	21.44		140.22	98.11	71	2.56
Mean total cell count	292.1	295.33	273.56	208.9		280.44	295.7	312.8	227.8

c) Day 14

	Treated during proliferation only (day -3 )				Treated during both proliferation and differentiation (day -3 and day 0)			
	0	1	10	100	0	1	10	100
Quercetin concentration ( $\mu\text{M}$ )	0	1	10	100	0	1	10	100
Mean mature adipocyte count	324.1	282.89	231.44	71.78	213.33	112.1	64.89	2.22
Mean total cell count	374.2	360	306	233.2	270.67	261.2	249	238.6

d) Day 18

	Treated during proliferation only (day -3)				Treated during both proliferation and differentiation (day -3 and day 0)			
	0	1	10	100	0	1	10	100
Quercetin concentration ( $\mu\text{M}$ )	0	1	10	100	0	1	10	100
Mean mature adipocyte count	396	376	256	98	294.22	254.1	99	0
Mean total cell count	448	427	389	247	432.44	417.4	474.9	129.8

#### 4.3.5 Triglycerides quantification

Cells treated with 0, 10 and 100  $\mu\text{M}$  of quercetin during proliferation and part way through differentiation were analysed for triglyceride accumulation over a period of 28 days post differentiation induction. Results were taken every 7 days. Cells treated during proliferation had lower triglyceride accumulation compared to cells treated partway through differentiation. Cells treated with 10  $\mu\text{M}$  of quercetin appear to recover when the flavonoid was withdrawn but those treated with 100  $\mu\text{M}$  sustained their reduced triglyceride status.

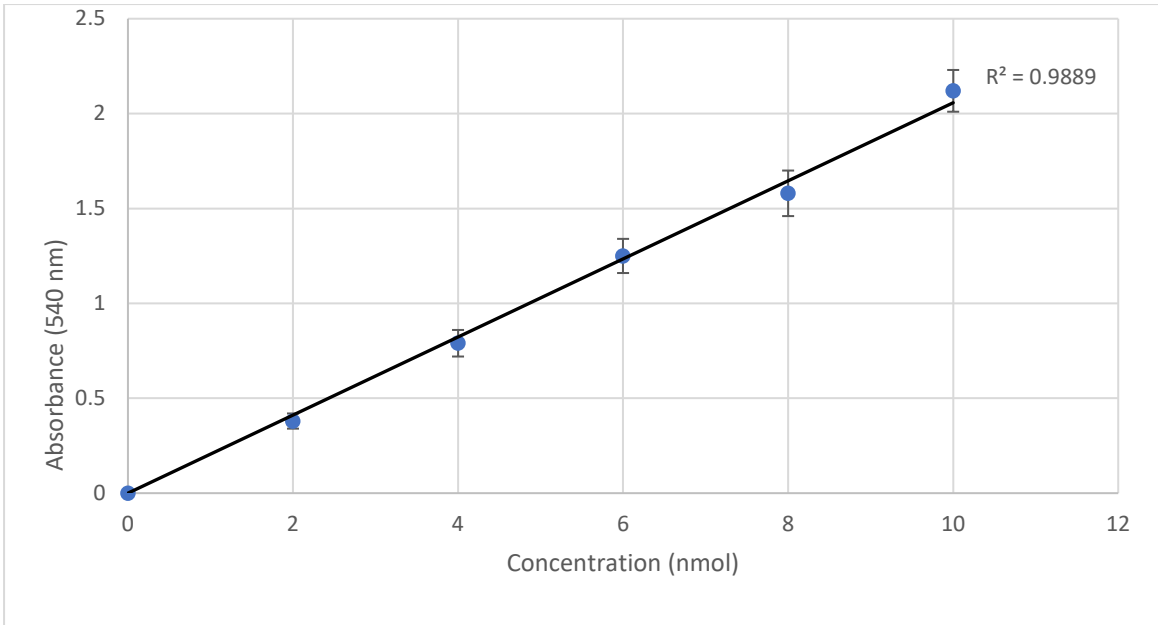


Figure 4.3.5a Calibration curve routinely used to quantify triglycerides. There was a strong correlation ( $R^2 = 0.9889$ ) of calibrator points. All calibrator reagents were supplied by manufacturer.

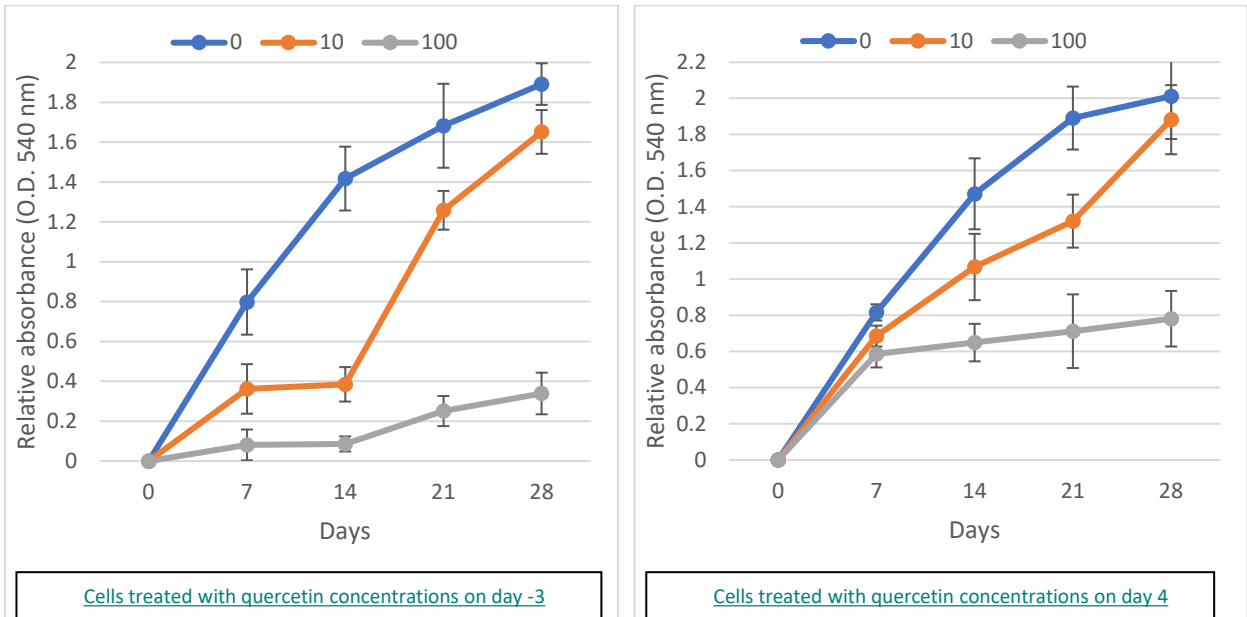


Figure 4.3.5b Comparison of triglyceride presence on cells treated with flavonoids during either proliferation or partway through differentiation (day 4). Proliferation phase treated cells had reduced triglycerides accumulation for the 10 and 100  $\mu\text{M}$  treatments compared to those treated part way through differentiation. However, the 10  $\mu\text{M}$  treated cells appear to recover when the presence of the flavonoid had worn off. Data points are mean values and error bars represent standard deviation. Experiments were repeated 3 times, and each had 6 replicates.

#### 4.4 Discussion:

##### 4.4.1 Scope

This chapter considered experiments designed to find the effects of flavonoids on the differentiation of SGBS preadipocytes. It looked at preadipocyte differentiation by using published protocols and compared the output with spontaneously differentiated cells. SGBS results were in turn compared to those of the 3T3-L1 cell line which stands as a prototypic model of adipogenesis (Roberts et al., 2009). Furthermore, microscopic relative differentiation counts were used in tandem with oil red O stains and triglyceride quantification protocols to determine the relative order of flavonoid effectiveness as seen by  $IC_{50}$  values and the effect of timing on adipocyte treatment. Microscopic counts were used to validate either the oil red O stains or the triglyceride assays whilst assessing levels of cell proliferation during differentiation to establish whether proliferation and differentiation processes are mutually exclusive.

##### 4.4.2 Stimulation of differentiation.

Stimulated preadipocytes differentiated significantly better than those left to differentiate spontaneously for both the SGBS cells and the comparator 3T3-L1 cells (Fig. 4.3. 2a and b). SGBS cells had higher relative differentiation of greater than 400% compared to 3T3-L1 at 200%. Furthermore, the absorbance of stimulated SGBS cells was significantly higher than that of 3T3-L1 cells ( $p < 0.05$ ). The SGBS findings were relatable to those by Yeo et al. (2017) and Fischer-Posovszky et al. (2008) in that differentiation induction media brought significant increase in differentiation. This study further showed that SGBS cells have higher capacity to differentiate relative to the prototype adipocyte cell line 3T3-L1 because the former had a significantly higher absorbance value. This supports the notion that SGBS are a good representative of primary cells because they are neither transformed nor immortalized, they have high proliferation and differentiation capacity, just like primary cells (Tew et al., 2022). While parallel experiments with primary cells are recommended to validate this assertion, subsequent experiments did benefit from the finding that it is possible to stimulate preadipocytes to differentiate in short enough time to allow experimentation with flavonoids.



#### 4.4.3 Cell morphology

Preadipocytes have a signature stretched fibroblast shape and convert to the round and lipid droplet laden phenotype upon differentiation (Audano., 2022; Eckel, 2018; Zhang et al., 2013; Fan et al., 1983). This change was clearly visible under the microscope with or without a stain (Figure 4.3.4a and b and figure 4.3.7) and this made a basis for comparison with the oil red O and triglyceride assays. Whilst the oil red O and triglyceride assays have been in wide use in many experiments, they cannot distinguish between few differentiated cells with many or large lipid droplets per cell and many differentiated cells each with very few or small lipid droplets. Experiments to show the relationship between microscopic relative differentiation cell counts and oil red O assays (figure 4.3.6) showed a very strong correlation ( $R^2 > 0.97$ ) which implied the 2 measures could ordinarily be interchangeable. In this study, the correlation was sustained in all single flavonoid experiments (figure 4.3.3a and figure 4.3.3b), however, when the flavonoids were combined, there was a mismatch between the relative differentiation microscopic counts and the oil red O measures (figure 4.3.3c and figure 4.3.3d). Oil red O results appeared to show reduced flavonoid impact when flavones were mixed with flavanols. There was greater oil red O residue which gave the impression that differentiation was marginally affected yet cell counts showed that even flavonoid combinations significantly reduced the rate of differentiation. This observation highlights the limitations of the semi quantitative oil red O assays and the importance of having confirmatory tests to uphold the quality and meaning of results.

Microscopic morphology views showed two observations; that combined flavonoids crystallised in culture but not in storage (Huang et al., 2019; Zirlin, 1974), and that fewer cells differentiated but those that did, carried larger lipid droplets. Crystallization of combined flavonoids occurs at acidic pH values (Jurasekova et al., 2022; Luo et al., 2012) which is what happens to cells in culture the longer they stay in spent media. This explained the difference in patterns and opened views of a possible alternative pathway by which combined flavones and flavanols impact adipocyte differentiation. Whilst morphology observations did not provide quantitative data, the qualitative information was useful to suggest other possible mechanisms.

Photomicrographs of cells treated with very low concentrations of flavonoids (Figure x) showed reduced size and number of lipid droplets per differentiated cell. This phenotype is

associated with multi-locular beige cells (Jung et al., 2018) and suggests that physiological concentrations of flavonoids encourage the browning of white adipocytes. This feature has been observed in mice that were fed with the flavanol quercetin (Kuipers et al., 2018). The study concluded that mice fed a diet rich in quercetin reduced triglyceride abundance and the adipocytes that resulted had a brown phenotype and showed an increased expression of the UCP1 gene, a marker of adipocyte browning. Zhang et al. (2019) also reviewed many studies of mice and 3T3-L1 cell line models that demonstrated the browning potential of flavonoids with evidence of differentiated cells containing smaller and fewer lipid droplets. In their review, there was no study which demonstrated the same in SGBS cells.

#### 4.4.4 Single flavonoid treatments

All flavonoids reduced adipocyte differentiation at all concentrations (Tables 4.3.1a and 4.3.1b). The effect was dose dependant, higher doses were more effective in reducing differentiation. Comparison of the IC<sub>50</sub> values of the flavonoids showed that flavanols had levels of effectiveness ranked in the order of quercetin, galangin and kaempferol, whereas flavones had chrysin, apigenin and luteolin (figure 4.3.9 and figure 4.3.10). These findings have an interesting association with the number of hydroxyl groups that form the side chains of the 3<sup>rd</sup> carbon ring of the basic flavonoid molecule. For flavanols, the more the hydroxyl groups there are, the more effective the flavanol is on the reduction of differentiation (figure 1.6.1). For flavanols, the number of hydroxyl groups in the 3<sup>rd</sup> carbon ring determine the water solubility which is related to how long the flavonoid stays in solution when culture pH reduces because of metabolism (Song et al., 2019; Wang et al., 2017; Jiménez-Girón et al., 2013).

The flavones chrysin, apigenin and luteolin also share a basic skeleton with varying side groups. On the 3<sup>rd</sup>, the determinant carbon ring, the absence of hydroxyl groups inferred greater effect on the reduction of adipocyte differentiation, thus chrysin without any hydroxyl group on the determinant ring was more effective followed by apigenin with 1 and lastly luteolin with 2 (Figure 1.6.1.). For flavones, it is the decrease of hydrogen ions that increases effectiveness which is the opposite to flavanols. It is known that in some flavonoids, there is a negative correlation between the number of hydroxyl groups and their lipophilicity

(Khalilpourfarshbafi et al., 2019). In the absence of specific transporter mechanisms, cells, by virtue of their lipid membrane, would favour the uptake of molecules with greater lipophilicity. Therefore, it can be assumed that the limiting factor is the quantity of flavonoid taken in by the cell as determined by the number of hydroxyl side chains.

#### 4.4.5 Flavonoid combination treatments

Flavonoid combinations between flavones and flavanols appeared to be additive as some combinations were less effective than the strongest single flavonoid but more effective than the weakest single flavonoid. This was predictable seeing that flavones, became less effective with more hydroxyl groups in contrast to flavanols which were more effective with every increase in hydroxyl groups on the determinant carbon ring. This suggests a cancelling effect. But even more, the presence of hydroxyl groups on flavonoids plays conflicting roles, that of increasing solubility and lipophilicity. Outside adipogenesis, in antibiotic studies, flavonoid combinations have also been seen to give additive results (Amin et al., 2015) and this has been explained by different modes of action that often have conflicting elements which are not necessarily antagonistic. The same additive outcome has been observed in flavonoid combinations in the study of cancer (Zhang et al., 2004), estrogenic activity (Wong et al., 2007), nutrition (Liu, 2003) and malaria studies (Lehane and Saliba, 2008). Other flavonoids do have synergistic effects (Ma et al., 2018; Guo et al., 2008) but this study only pointed to combinations with additive effects.

#### 4.4.6 Triglyceride accumulation

When comparing the triglycerides produced from SGBS cells treated with 0, 10 and 100  $\mu\text{M}$  of quercetin during proliferation alone and partway through differentiation, it was shown that all treatments were effective in reducing triglyceride accumulation relative to the untreated controls, irrespective of when the treatment was given (Figure 4.3.15). However, pre-differentiation induction treatments had a significantly lower triglyceride presence compared to post-induction treated cells. The 10  $\mu\text{M}$  treatment appeared to recover as time progressed suggesting possible exhaustion of available flavonoid for continued depression of triglyceride production. However, cells treated with 10  $\mu\text{M}$  of quercetin appear to recover when the flavonoid was withdrawn but those treated with 100  $\mu\text{M}$  sustained their reduced triglyceride status suggesting either protracted bioavailability at higher concentrations or irreversible biochemical or genetic changes by higher concentrations.

Reduction in fatty acid and triglyceride synthesis in adipocytes treated with flavonoids has been observed before. Nagai et al. (2018) observed a suppression of fatty acid and triglyceride synthesis by the flavonoid orientin. They attributed this decrease to a reduction of C/EBP-delta expression and the inhibition of PI3K/Akt-FOXO1 signalling in adipocytes. Therefore, flavonoids can bring molecular changes that suppress triglyceride synthesis. Another study by Eseberri et al. (2019) looked at the effects of quercetin on 3T3-L1 cells. They found that the quercetin 3S metabolite had delipidating effects which were linked to triglyceride metabolism. Their work showed some biochemical changes in cells that were induced by the flavonoid metabolite. These and other studies have shown the suppression of triglycerides after flavonoid treatment in either 3T3-L1 cell lines or in vivo, however, there is still a void in knowledge on the effect of the same flavonoids on SGBS cells and the effect of changing the times of treatment during the process of adipogenesis.

#### 4.4.7 Proliferation during differentiation.

It has generally been assumed that when differentiation is induced, proliferation is arrested because the two processes are alternative and mutually exclusive (Zhu et al., 2018; Bouraoui et al., 2008; Freytag & Geddes 1992; Freytag, 1988). To assess this, relative differentiation cell counts (number of differentiated cells out of total number of cells) were recorded for quercetin treated cells over a period between 7 and 18 days and undergoing differentiation treatment. This was done for 2 sets of cells, one which was treated during proliferation only and the other treated during both proliferation and differentiation (Table 4.3.1a-d). In both cases, cells recovered, and the total number of cells increased together with cells that had differentiated. There were more new cells on the cells treated during proliferation only, than those treated in both phases. The results could suggest differentiation taking place at the same time as proliferation. This would be in contrast with a recent study which looked at viability of SGBS and 3T3-L1 differentiated cells (Wu et al., 2020). They found out that sphingosine-1-phosphate, a bioactive lipid mediator, increased proliferation of preadipocytes but once they differentiate, cell viability was reduced. This dual process as observed in SGBS cells is new. Further studies would be warranted to elucidate this better.

#### 4.4.8 Loss of adherence after differentiation.

High quercetin presence showed increasing rate of differentiation until day 14, after which it declined (Table 4.2.3 (a-d)). Differentiated cells lost their adherent properties and floated in

media. This was confirmed by microscopic views and differential cell counts. The loss of adherence in cells treated with flavonoids is not new. Grijalva-Guiza et al. (2021) demonstrated the benefits of flavonoids on the progression of atherosclerosis in that flavonoid treated smooth muscle inhibited plaque from adherence. Another study by Abdallah et al., (2020) showed that flavonoids altered the adhesion properties of endothelial cells, they attributed this to changes to calcium and nitric oxide (NO) signalling. However, not many studies explore this phenomenon on adipocytes and least, SGBS cells.

#### 4.5 Conclusion

The experiments in this chapter have shown that the flavanols quercetin, kaempferol and galangin, and the flavones chrysin, apigenin and luteolin at all concentrations reduce the rate of differentiation of human adipocytes in a dose dependant manner. When the flavanols were compared, the order of effectiveness was quercetin, galangin and kaempferol, that of flavones was chrysin, apigenin and luteolin. Flavonoid combinations appeared to be additive as some combinations were less effective than the more effective single flavonoid but more effective than the least effective single flavonoid. Flavonoid ranking was achieved by comparing the  $IC_{50}$  values and the order of effectiveness of all flavonoids and flavonoid combinations experimented was chrysin, quercetin, apigenin, quercetin & chrysin, quercetin & apigenin, chrysin & galangin quercetin & luteolin, galangin, chrysin & kaempferol, luteolin and kaempferol. The effectiveness of flavones was directly proportional to the absence of hydroxyl groups on the third and determinant carbon ring whilst for flavanols, the relationship was inverse.

Microscopic cell counts, oil red O stains and triglyceride assays all confirmed that flavonoids reduce differentiation. Lower concentrations of flavonoids had a higher value of relative differentiation counts but a lower value of oil red O reading, morphology microscopic views showed that the differentiated cells contained fewer and smaller lipid droplets a feature that is associated with browning of adipocytes. It is therefore possible that flavonoids reduce the differentiation of adipocytes whilst increasing the brown phenotype. Reduction of differentiation by presence of flavonoids occurred irrespective of whether the treatment was done before, during or after differentiation induction. However, those that were treated in all phases had the greatest impact. After differentiation was induced, the number of differentiated and undifferentiated cells continued to rise with the number of differentiated

cells rising faster for differentiated cells except for the 100  $\mu\text{M}$  concentration treatment after 14 days. It was clear from the results that differentiation and proliferation were happening at the same time.

## 5. Molecular Pathways

### 5.1 Introduction

#### 5.1.1. Chapter overview

Understanding the pathways by which a substance affects the growth and development of cells is important if the substance is to be used as a therapeutic agent in the event of pathological dysregulation. It has been shown that flavonoids, at supraphysiological concentrations, reduce adipocyte proliferation and differentiation but the molecular pathways by which the flavonoids exert their effects is not fully known. The flavonoids quercetin and chrysin representing flavanols and flavones respectively were used to investigate genes associated with proliferation, apoptosis, differentiation, and insulin regulation pathways. Quercetin was additionally used to elucidate the signal pathways and protein expression involved in adipogenesis. The following genes were investigated; *PPAR gamma*, *adiponectin*, *GLUT4*, *UCP1*, *TPX2*, *Ki67*, *BIM*, *BAD*, *SREBP1c* and *CEBP- $\beta$*  whereas the proteins investigated were *UCP1*, *PPAR gamma*, *SREBP1c*, *C/EBP beta*, *Erk*, *pErk*, *Akt*, *pErk* and *leptin*.

#### 5.1.2. Proliferation

Cell proliferation is the net increase in the number of cells when cell divisions exceed cell loss through cell death or differentiation Sperelakis (2001). There are many genes associated with proliferation and most of this influence the different stages of the cell cycle. Genes that code for the proteins Kiel clone 67 (Ki-67), proliferating cell nuclear antigen (PCNA), minichromosome maintenance (MCM), topoisomerase IIalpha (TOP2A), and Targeting protein for Xklp2 (*TPX2*) are typical genes used to assess levels of proliferation especially in cancer cells. Many studies on adipogenesis have focused on Ki-67 and *TPX2* as markers for proliferation (Anari et al., 2022; Shipp et al., 2016; Miller, 2005) because they are ubiquitously present in adipocytes across many species.

##### 5.1.2.1. *Ki-67*

The Ki-67 protein (pKi-67) is a proliferating cell nuclear antigen (PCNA) and is a standard marker of cell proliferation which is commonly employed to investigate the growth fraction of a cell population. This nuclear protein is encoded by the *Ki67* gene, and it mediates its proliferation role through heterochromatin organisation (Sobecki et al., 2016). As such, pKi-67 is only produced in actively dividing cells irrespective of the rate of division. Proliferating

cells have a relatively higher gene expression index for the *Ki67* gene compared to other thriving cells and for this reason, *Ki67* is a recognised marker for cancer (Li et al., 2015). The canonical view of *Ki-67* transcript as a binary marker of proliferation has recently been challenged. Miller et al. (2018) for example has argued that *Ki-67* transcript exist on a gradient which decays, over time, in quiescent cells. For this reason, a clearer picture can be drawn by assessing the gene transcript level as well as the protein presence. Given a choice from the 2, gene expression levels are more indicative of proliferation activity than protein presence which tends to straddle across multiple phases. The G0 phase for example should not show any mRNA activity for *Ki-67* but will show pKi-67 in graduated magnitudes depending on how long the cell has stayed in quiescence or senescence. Contrary, in the S, G2 and M phases of the cell, there is a high expression of the *Ki-67* transcript and concurrent pKi-67 presence because of heterochromatin organisation demands (Miller et al., 2018). For this reason, carrying a gene expression assay alone for *Ki-67* expression is justified.

#### 5.1.2.2. *TPX2*

A key factor of dividing cells is microtubule assembly. In fact, in dividing cells, there are many spindles assembly factors whose role is to induce microtubule assembly and growth during the M phase. One such factor is the targeting protein for Xenopus centrosomal kinesin-like protein 2 (Xklp2) which in humans is encoded by the *TPX2* gene. *TPX2* is a gene generally associated with microtubule nucleation spindle assembly which is required for normal assembly of mitotic spindles (King and Petry, 2020). Whilst there is a scarcity of studies investigating variations of *TPX2* expression in adipocytes and specifically SGBS, there has been some work on how flavonoids affect the expression of this gene. Moskot et al. (2015) found a significant ( $p < 0.01$ ) reduction in the expression of *TPX2* on human fibroblast cells treated with genistein. Whilst the correlation was established, the pathway was not elucidated. Moreover, the recent entrance of SGBS cells as a close cell strain to primary adipocytes demands an investigation on how flavonoids and in our case, quercetin and chrysin effects adipogenesis.

#### 5.1.3. Cell death

Cell death is a necessary event of a biological cell ceasing to carry out its functions, it can be programmed or a result of trauma or pathology. Of the programmed cell death modes, apoptosis (type I cell death), autophagic cell death (type II), and necrosis (type III) have been



heavily studied. Whilst these three typical pathways are distinct, they have many pathway overlaps (Green and Llambi, 2015). Of the three, necrosis is not always programmed (Yuan and Kroemer 2010), and autophagy is not a universal mode in all cell types (Shen et al. 2012), not all cells undergoing autophagy result in cell death (Kroemer et al. 2010). So, this leaves apoptosis as the ubiquitous mode found in all the cells.

Apoptosis is the form of cell death characterised by chromatin condensation, blebbing of the membrane and cell shrinkage. There are 2 main signalling pathways by which the process is triggered, these are the death receptor (DR) and the mitochondrial pathways. The former employs typical ligand to cell-surface-receptor interaction and therefore it is extrinsic in its induction whereas the mitochondrial pathway is intrinsic, it is primarily initiated in a cell-autonomous manner. Apoptosis of other cells treated flavonoids has been extensively studied, Abotaleb et al. (2018) for example looked at effect of a range of flavonoids on cancer cell lines. They postulated that whether flavonoids induce extrinsic or extrinsic apoptosis was dependant on the cell line and the flavonoid applied. For example, quercetin enhanced extrinsic apoptosis in BT-474 cells but the same flavonoid invokes the intrinsic pathway in HL-60 cell lines by modulating Cox-2, caspase-3, Bax, *BAD*, Bcl-2, cytochrome c, and PARP proteins (Niu et al., 2011). Not much is known whether flavonoids directly initiate apoptosis through classic ligand to cell-surface-receptor interaction or they present as genotoxic agents which invoke the intrinsic pathway in adipocytes and especially SGBS cells. The intrinsic pathway is tightly regulated by two groups of antagonistic proteins, pro apoptotic and anti-apoptotic proteins. One heavily studied family of apoptotic proteins is the B-cell lymphoma 2 (BCL-2) family of regulator proteins which determine cell fate by either inhibiting or inducing apoptosis. Members of this family possess the BCL-2 homology domain 3 (BH3) or the 'death domain' which is the active site in execution of the apoptotic function. Examples of genes in this family are the pro-apoptotic proteins BCL-2-like protein 11 (*BIM*), BCL-2-like protein 4 (*BAX*), BCL-2 associated agonist of cell death (*BAD*) and BCL-2 homologous antagonist/killer (*BAK*), and the anti-apoptotic proteins B-cell lymphoma-extra-large (BCL-xL), BCL-2 like 2 (BCL-w) and BCL-2 homolog Bfl-1/A1 (*BFL-1/A1*) (Kale et al., 2018). Between pro- and anti-apoptotic proteins, substances suspected to cause apoptosis are arguably best investigated for pro-apoptotic gene and protein expression, and of the many pro-apoptotic genes and proteins, the *BIM* and *BAD* genes have been featured flavonoid driven apoptosis.

#### 5.1.3.1. *BIM*

Whilst it has many other functions, the *BIM* gene is a primary mediator of apoptosis. Being a member of the BCL-2 family, it functions in a tightly regulated milieu of other factors which either exacerbate or ameliorate apoptosis progression. When a cytotoxic signal is initiated, expression of *BIM* gene increases and the resultant protein blocks anti apoptotic proteins such as BCL-xL and BCL-w whilst activating other pro-apoptotic proteins such as BAX and BAK. These will in turn trigger cytochrome C proteins which downstream invoke caspase proteins ultimately resulting in classic apoptotic cascades involving cell shrinkage and formation of membrane-bound apoptotic bodies (Hübner et al., 2008). Regulation of the *BIM* protein, besides the action of transcription factors which either increase or decrease the expression, can involve phosphorylation. However, because *BIM* has multiple phosphorylation sites which are utilised by members of the MAP kinase family, including ERK, JNK, and p38 isoforms, phosphorylation alone cannot decide whether *BIM* is activated or deactivated (Ley et al., 2005). In adipocytes, the *BIM* gene is generally downregulated in white adipose tissue during obesity but is downregulated in the brown or beige phenotype. Wang et al. (2020) proposed that the transcriptional coactivators YAP and TAZ are responsible for suppressing the *BIM* gene. Interestingly, Pulito et al. (2019) goes on to suggest that flavonoids, especially quercetin reduces the presence of YAP and TAZ, and this will, by default, suggest that flavonoids can increase apoptosis by increasing the presence of the *BIM* protein. Whilst literature on the effect of the *BIM* gene on cancer cells abound, there is still a scarcity of the same on adipocytes.

#### 5.1.3.2. *BAD*

The *BAD* protein is known more for arresting the effects of anti-apoptotic genes than actively inducing apoptosis itself. It actively drives cell apoptosis by the formation of heterodimers with BCL-xL, BCL-W and BCL-2, thus reducing their death repressor function. When *BAD* dimerises with the anti-apoptotic proteins, it competitively precludes the heterodimerization of these proteins with BAK and BAX, pro apoptotic proteins which function by causing the release of cytochrome c downstream of the apoptotic cascade. As a member of the BCL2 family, *BAD* engages the intracellular death-ligand, that is the BH3 domain to affect its pro-apoptotic function. This function is enabled if the cell membrane is chemically permeabilised (Ryan and Letai, 2013; Letai et al., 2002). Whether flavonoids invoke cell membrane

permeability or not is yet to be investigated. However there has been some studies around the effect of a selection of some flavonoids on 3T3-L1 cells which suggest that flavonoids can trigger the intrinsic apoptotic cascade. Work by Kim et al. (2018) showed that red paper extract which is rich in flavonoids upregulated *BAK*, *BAD* and *BAX* expression whilst silencing the presence of the anti-apoptotic proteins, *BCL-2* and inhibiting the phosphorylation of *BAD*. These findings have increased interest in finding the effect of quercetin and chrysin on the *BAD* gene expression on SGBS cells.

#### 5.1.4. Differentiation

Whilst proliferation is a process resulting in the increase of cell numbers, differentiation, on the other hand is the process which alters the morphology and function of cells. The age-old debate on whether proliferation and differentiation are mutually exclusive processes, can best be addressed if the focus is streamlined to either single cells or cell populations. Xia et al. (2006) explains this issue by asserting that within individual cells, there are a module of genes of proliferation that get repressed when the switch to differentiation takes place. They uphold the notion that proliferation is poorly compatible with differentiation (Garcia et al., 1999). For adipocytes, the module of genes involved in differentiation contains different genes depending on the organism from which the cells were derived. However, there are a number of genes and transcription factors which are ubiquitously present in many species. Ntambi and Young-Cheul, (2000) described the adipocyte moving from proliferation to differentiation, they indicated that after differentiation is initiated by exogenous promoters, the cell abandons the cell cycle and growth is arrested. This happens concurrently with the induction of the first transcriptional factors CCAAT/enhancer binding protein beta (*C/EBP beta*) and CCAAT/enhancer binding proteins delta (*C/EBP delta*) which promote the expression of peroxisome proliferator-activated receptor gamma (*PPAR gamma*) and *C/EBP alpha*.

Once activated, *PPAR gamma* and *C/EBP alpha* cross-regulate each other to maintain their gene expression despite a reduction in the expression of *C/EBP beta* and *C/EBP delta*. Expression of these genes peak during differentiation but stabilise when the cell is fully differentiated after which differentiated phase specific genes such as Leptin, Glucose transporter type 4 (*GLUT4*), fatty acid binding protein 4 (*FABP4*), Adiponectin, fatty acid synthase (*FAS*) and Uncoupling protein 1 (*UCP1*) are seen to increase. *GLUT4*, Leptin and

Adiponectin have been heavily studied in white adipose tissue (Stern et al., 2016), whereas UCP1 has featured in many brown or beige fat studies (Shinde et al., 2021). Most of the genes highly expressed in fully differentiated adipocytes have a function related to insulin governance, glucose uptake and general energy equilibrium. Whilst studies of these genes in adipocytes exists, there is a scarcity of the same in adipocytes, both white and brown, in the presence of flavonoids. Moreover, SGBS cells which possess both white and brown phenotype characteristics, would warrant a study to map out the pathway by which flavonoids affect adipogenesis.

#### 5.1.4.1. PPAR gamma

Peroxisome proliferator- activated receptor gamma (PPAR gamma), also known as the glitazone reverse insulin resistance receptor, is a transcriptional factor encoded by the *PPAR gamma* gene. There are two isoforms of this receptor, *PPAR gamma 1* and 2. In humans, PPAR gamma 1 is typically found in all tissues except muscle whereas adipose tissue and the intestines are the source of *PPAR gamma 2*. As a regulator of adipocyte differentiation, PPAR gamma is itself regulated via phosphorylation through the MEK/ERK pathway. Reduction of *PPAR gamma* expression in vitro causes partial insulin insensitivity, reduction in fatty acid storage and changes in glucose metabolism (Suwaki et al., 2007; Ahmadian et al., 2013). Increased *PPAR gamma* transcript expression is positively related to increased adiponectin release from adipocytes and subsequent increase in cholesterol production. Besides synthetic molecules such as thiazolidinediones (TZDs), there are many natural substances that act as PPAR gamma agonists by directly binding to the receptor, examples are polyunsaturated fatty acids and phytochemicals such as phytocannabinoids (O'Sullivan et al., 2005) or extracts from curcuma, lemongrass, and pomegranate (Ciavarella et al., 2020). Agonists which reduce the expression of PPAR gamma in adipocytes have been associated with positive health outcomes, however, synthetic agonists have been seen, in many studies to have other unfavourable side effects. There therefore is some merit in investigating the effects of flavonoids on the expression of *PPAR gamma* and related genes on human adipocytes.

#### 5.1.4.2. GLUT4

Glucose is needed in cells for metabolism. Its cellular uptake is facilitated by the *GLUT4* transporter which is an insulin-regulated protein found primarily in adipose tissues and striated muscle (Govers, 2014). The uptake is achieved through facilitated diffusion of

circulating glucose down its concentration gradient. Without activation, *GLUT4* is sequestered intracellularly but after insulin secretion increases because of rising blood glucose, there are more insulin and receptor bindings which, through second messengers, promotes the translocation of *GLUT4* from intracellular compartments to the cell surface. Increased GLUT4 presence is correlated to accumulation of triglycerides and cell hypertrophy. The gene that codes for the GLUT4 protein is regulated by endogenous transcription factors and other exogenous molecules. An example of a transcription factor that mediates the transcription of GLUT4 is SREBP-1c (Im et al., 2006). Post translational modifications of GLUT4 are largely dependent on insulin homeostasis but many pathways especially the PI3K-AKT pathway play a role in the regulation of the gene and its protein stages. Many studies have shown that flavonoids can affect the behaviour of the GLUT4 protein both prior to its position on the membrane and when it is fully function as a transporter (Gonzalez-Menendez et al., 2014) but not much is known on the direct effect of the same flavonoids on gene transcription. It is therefore important to investigate the effect of flavonoids on the expression of *GLUT4* transcripts in SGBS cells.

#### 5.1.4.3. *Leptin*

Leptin, an adipokine, is a peptide hormone encoded by the *LEP* (leptin) gene which plays a major role in the regulation of energy homeostasis and is generally expressed in differentiated adipocytes but not in the precursor preadipocytes. Cell culture experiments to assess the expression of this gene and its protein are possible but the effect of the secreted gene is difficult to measure in vitro because leptin primarily attaches to leptin receptors in the brain which influence levels of satiety. Whilst adipocytes have leptin receptors, they have little effect on cell metabolism. However, indirectly, leptin modifies fat cell sensitivity to insulin and thereby inhibiting triglyceride accumulation. In animal models, leptin is also known to stop adipocyte hyperplasia and hypertrophy through the inhibition of circulating growth factors (Harris, 2014). Therefore, leptin impacts on adipogenesis during both the proliferation and differentiation stages. A review by Rufino et al. (2021) gives a wide exposition of how several flavonoids affect leptin expression and resultant effect of obesity. They showed that different flavonoids reduce obesity by either decreasing the expression of leptin transcripts, modification of the resultant protein or reduction of leptin resistance. These studies were conducted on either 3T3-L1 cells, HepG2 cells, Huh7 hepatic cells, HT-29 cancer cells,

adipocytes derived from human MSCs, adipocytes isolated from male Wistar rats and various mice/rat models. This thus indicates a void in knowledge on how the leptin gene and protein are expressed in SGBS cells under the treatment of chrysin and quercetin.

#### 5.1.4.4. *Adiponectin*

*Adiponectin* is a homeostatic adipokine with metabolic properties like leptin, it is a multimeric protein encoded by the *Adipo Q* gene and released predominantly by adipocytes. *Adiponectin* is not expressed by human preadipocytes but starts presenting as soon as the differentiation process begins (Yang et al., 2017; Achari and Jain, 2017). Unlike leptin, low levels of *adiponectin* are associated to negative health outcomes which include insulin insensitivity, obesity, and cardiovascular disease. Increase of *adiponectin* expression correlate to an increasing expression of adipocyte differentiation markers. There have been some studies that looked at the expression of *adiponectin* after flavonoid treatment treat. Li et al. (2021) for example looked at the effect of flavonoid-rich Smilax China L. extract on obesity in mice. They found that the extract reduced obesity by, amongst other things, increasing the plasma *adiponectin* levels and upregulating the *adiponectin*-receptor/AMPK signalling pathway. Another study by Yin et al. (2017) looked at the effect of grape seed procyanidin B2 in mice, they showed an upregulation of the *adiponectin*, and a downregulation of the leptin mRNA levels. Whether the flavonoids quercetin and chrysin have similar effects on human adipocytes is yet to be elucidated.

#### 5.1.4.5. *UCP1*

Humans have three types of adipocytes, white, brown, and beige. The brown and beige types are thermogenic, they express high levels of uncoupling protein 1 (UCP1) that dissipates heat by uncoupling the mitochondrial proton gradient from mitochondrial respiration (Ikeda and Yamada, 2020). There exist other UCP1 independent thermogenesis mechanisms in brown and beige adipocytes, but these are not well characterised. These alternative mechanisms are thought to involve creatine substrate cycling and Ca<sup>2+</sup> cycling (Ikeda and Yamada, 2020). SGBS cells have both brown and brite characteristics and therefore they express UCP1 whose abundance is associated with positive health outcomes. UCP1 is poorly expressed in preadipocytes but increases in presence as differentiation progresses. The conversion of white adipocytes to their brown/beige phenotype and the engagement of brown/brite cells to dissipates heat by uncoupling the mitochondrial proton gradient is both genetically

predisposed and environmentally triggered. It is known that low temperatures above the shivering point can trigger this process but not much is known on whether exogenous molecules can achieve the same. Studies on effects of flavonoids on expression of UCP1 in adipocytes exist but they are haunted by the paradoxical challenge that the same flavonoids reduce differentiation and UCP1 is expressed in differentiated cells. However, some studies have shown increased UCP1 expression in animal models after feeding with flavonoid rich foods or supplements. Lee et al. (2020) for example showed that sesamol, a flavonoid mimetic, increased the expression of the UCP1 gene and protein in white adipocytes with the result of better health outcomes for obese mice. In another study, Choi et al. (2019) showed that in obese mice, quercetin supplements upregulate UCP1 in adipose tissue using the AMPK/PPAR $\gamma$  pathway through sympathetic stimulation. Since cells in culture do not benefit from the nervous system, it is yet to be seen whether flavonoids increase UCP1 expression on human adipocytes in culture.

#### 5.1.5. Transcription factors and cellular pathways

Transcription factors are proteins involved in the nuclear process of transcribing RNA from DNA. They initiate and regulate the transcription of genes, that is, stimulating or repressing them to complete the transcription translation cascade. To achieve the transcription function, they employ DNA-binding domains which avails the ability to bind to specific enhancer or promoter sequences of DNA. In adipogenesis, like many other biochemical processes, there are many transcriptional factors that regulate the expression of specific genes. Identifying these transcription factors and how they are affected by test substances helps in elucidating the pathways by which these substances effect their function. For many adipogenesis studies, the C/EBPs and SREBPs transcription factors have been investigated. Armed with genes and transcription factors, it is easier to establish the pathway by which an agent affects cellular processes. Many cellular pathways exist but for adipogenesis, and these are mediated by cellular kinases which modifies other proteins by covalently adding or removing phosphates (phosphorylation/dephosphorylation). Of interest in adipogenesis are the ERK and AKT pathways

##### 5.1.5.1. C/EBPs

CCAAT/enhancer-binding proteins (C/EBPs) are a family of basic region-leucine zipper (b-ZIP) transcription factors that bind to consensus CCAAT sequence found within the regulatory

regions of target genes. Within this family, there 6 variants C/EBP alpha, beta, gamma, delta, epsilon, and zeta which share a common carboxyl-terminal (C-terminal) domains but vary in amino-terminal (N-terminal) transactivation domains. In adipocyte differentiation the 2 variants, C/EBP beta and C/EBP delta increase in expression in the first 24 hours, this increase is driven by exogenous additives such as dexamethasone (DEX) and methylisobutylxantine (MIX) in the differentiation media. Without these additives, in vitro differentiation is not achievable. Presence of C/EBP beta and C/EBP delta in turn trigger the expression of differentiation specific genes, *PPAR gamma* and C/EBP alpha. C/EBP beta decays first, in the first 48 hours but C/EBP delta gradually reduces in expression for up to 8 days (Erickson et al., 2000; Lane et al., 1999) and by this time, C/EBP alpha expression will be mounting. C/EBP alpha is the limiting gene in white adipose tissue, cells with knocked out C/EBP alpha will not differentiate even in the presence of *PPAR gamma*. C/EBP alpha presence leads to the direct transactivation of adipose specific genes such as *GLUT4*, leptin and *adiponectin*. However, in brown adipose tissue, it is *PPAR gamma*, the parallel transcription factor, which is the deciding option, in the presence of *PPAR gamma*, brown/brite adipocyte cells devoid of C/EBP alpha can still differentiate. For SGBS, which show a high level of the brown/brite phenotype, it is more meaningful to investigate the effect of test substance on the expression of *PPAR gamma* than of C/EBP alpha. There have been some studies which have looked at the effect of flavonoids on the expression of C/EBPs in adipocytes, Hadrich and Sayadi (2018) for example saw reduced expression *PPAR gamma* and CEBP alpha in 3T3-L1 cells treated with the flavonoid apigenin. It is not yet known whether quercetin and chrysin has the same effect on SGBS cells. Besides C/EBPs, another transcription factor which mediate the process of adipogenesis exist, worth mentioning is SREBP-1c.

#### 5.1.5.2. *SREBP1c*

Adipocytes function in maintaining the homeostatic balance of fatty acid synthesis and glucose utilisation amongst other things. Insulin is a major core regulatory molecule in that process. Sterol regulatory element binding protein-1c (SREBP-1c) is an example of a transcription factor which is activated by insulin. SREBP-1c is synthesised in its inactive form in the endoplasmic reticulum membranes, it then requires post-translational changes to produce its transcriptionally active form which functions in the nucleus. This modification to produce proteolytic mature SREBP-1c proteins is achieved by insulin. Once active, SREBP-1c



is able to induce key genes of adipogenesis which include C/EBPs, PPARs, *adiponectin* and *GLUT4*. SREBP-1c is functional both in preadipocytes and mature adipocytes. Reduction in its expression produces the lean phenotype which is associated with positive health outcomes. Flavonoids have been shown to reduce the rate of expression of SREBP-1 in animal models, Al-Maamari et al. (2021) showed that the flavonol quercetin inhibited SREBP-1c expression and improved the life of mice with liver disease. In another study on the 3T3-L1 cell line, Ha et al. (2016) found that extracts from the purple gromwell (*Lithospermum erythrorhizon*) caused an increase in phosphorylation of AMP-activated protein kinase (AMPK) and precursor SREBP-1c and thus reduced the presence of active SREBP-1c protein. This had an overall effect of the reduction of inhibition of adipogenesis. Whether the flavonoids quercetin and chrysin reduces adipogenesis in SGBS cells using the same pathway still needs to be investigated.

#### 5.1.5.3. *Erk pathway*

The extracellular-signal-regulated kinase (ERK) pathway is one of the various cellular pathways by which genes are expressed and cells function in their roles. It forms part of a bigger network, the mitogen activated protein kinase (MAPK) signalling pathway. Extracellular molecules such as growth factors, hormones, synthetic and natural agents can activate the ERK cascade mostly initiated at membrane receptors, but from within, cellular stresses can begin the process. The ERK cascade is regulated by competing actions of upstream kinases and inhibitory phosphatases. Level of activity can therefore be simplified to either the phosphorylated or the dephosphorylated status of components within the cascade. Adipogenesis is one of the processes that depend on the MAPK/ERK pathway, both proliferation and differentiation depends on the cascade. Many studies looking at effects of flavonoids on adipogenesis, implicate the MAPK/ERK pathway (Oh et al., 2020; Liu et al., 2018; Prusty et al., 2002). Most of these studies are either on animal models or 3T3-L1 cell lines. There is still a void in knowledge on how flavonoids harness the ERK pathway in human adipocytes.

#### 4.1.5.4 *Akt pathway*

Protein kinase B (PKB), generally known as Akt, is a set of serine/threonine-specific protein kinases involved in many cellular processes which include proliferation, apoptosis, differentiation and glucose metabolism. There are 3 isoforms of Akt, whose genes are referred to as Akt1, Akt2, and Akt3. Of interest to the adipogenesis story are the first 2, Akt1

and Akt2 because they are involved in apoptosis, proliferation, differentiation, and glucose metabolism (Yang et al., 2004; Garofalo et al., 2003; Chen et al., 2001). For gene transcript experiment purposes, homologous gene sequences for all 3 isoforms are normally used and the transcript is only referred to simply as Akt. Studies involving flavonoids on adipogenesis have implicated Akt in their pathways, like Erk, most of these studies were on animal models and cell lines. An understanding of how Akt is involved in human adipocytes which have been treated with quercetin and chrysin will help in elucidating the pathway by which flavonoids influence adipogenesis in SGBS cells.

#### 5.1.6. Methods for elucidating molecular processes

Molecular processes and pathways have been a topic of interest when therapeutic agents have been investigated. The methodologies employed to understand these include RNA and DNA extraction and quantification, qPCR protocols, gel blots, protein extraction and quantification, Southern, Northern and Western blotting for RNA, DNA and protein analysis respectively. While the Northern blot technique on RNA analysis is easy and relatively fast, it has a lot of limitations such as lack of sensitivity, a large quantity of nucleic acids is needed for detection by blot hybridisation. In contrast, PCR techniques have the benefit of first amplifying single copies of DNA (or RNA after reverse transcription) to detectable levels before comparative quantifications. Another demerit of Northern blotting is the challenge of multiple probe analysis, there must be a stripping stage to remove the first probe before hybridisation with a second, progressive stripping reduces sensitivity. Southern blotting on the other hand is expensive and time consuming without much sensitivity. Being a semi-quantitative process, Southern blotting only provides DNA fragment size estimates. Whilst this suggests qPCR techniques as the more efficient approach, they have their limitations which include high costs and challenges of primer dimerisation. Primer dimerisations can be ruled out by running product gels and analysing melt curves. Although RNA transcripts are indicative of transcribed genes, not all transcriptions result in functional proteins. To address this need, Western blots, although cumbersome, can be used. Many studies on molecular processes for adipocytes and especially SGBS cells have been conducted and most of these have employed qPCR protocols together with Western blots (Fischer-Posovszky et al., 2008; Yeo et al., 2017; Klusóczyki et al., 2019).

### 5.1.7. Chapter aims.

The aim of this chapter therefore was to explore the effects of flavonoids on gene expression on a selection of proliferation, apoptosis, and differentiation marker genes as well as associated transcription factor genes using the qPCR protocol. A choice of proteins known to mediate the adipogenesis process were also investigated using the Western blot technique

## 5.2. Method

### 5.2.1. Cell culture

SGBS cells were grown in well plates as described in chapter 2.8. Wells treated with 100  $\mu$ M of flavonoid were produced in duplicate wells to maximise RNA harvest and match the other treatments. A volume of 500  $\mu$ l of phenol was shared across 3 wells of replicate conditions for all treatments except for the 100  $\mu$ M concentration which had 6 wells. RNA in phenol was harvested after every experiment and immediately frozen in  $-80^{\circ}\text{C}$ . All RNA purification, quantification, and conversion to cDNA were done as a complete experiment batch. Repeats were done on different days.

Proliferation experiment flavonoid treatments were done on day 0, 12 hours after seeding when cells were adhered. Treatment of cells with flavonoids in differentiation experiments were seeded as shown in figure 5.2.1 below

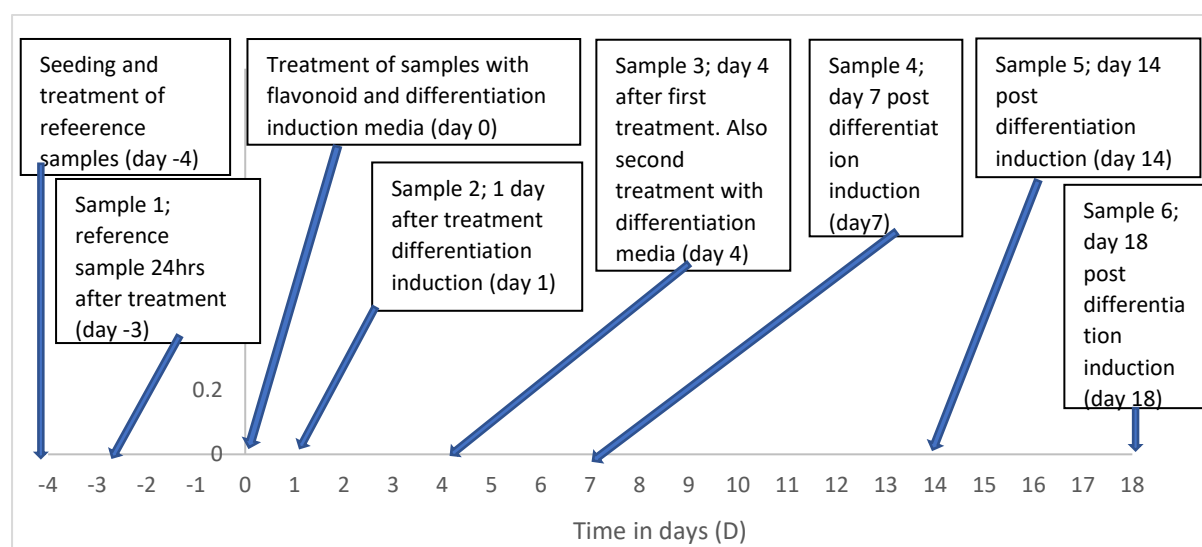


Figure 5.2.1 An illustration of treatment and RNA extraction regime for cells treated with quercetin and chrysin during differentiation.

### 5.2.2. RNA extraction and quantification.

RNA was extracted using the universal DNA/RNA extraction kit from Primerdesign™ Ltd. The serine protease, Proteinase K, was used to degrade proteins and other nucleases that could degrade the RNA. A volume of 50 µl of elution buffer was used to maximise RNA concentration.

RNA quantification was achieved using a Qubit fluorometer (Quant-it Assay). The results were confirmed using a nanodrop spectrophotometer, (Genova Nano spectrophotometer). Calibration of the Quant-it Assay and use of the Qubit fluorometer followed the Invitrogen experimental protocol and instruction manual. Assay working solution was made by a 1:200 dilution from the concentrate. Tubes were made in duplicate. The volumes used are shown in the table below.

Table 5.1: Preparation of assay tube for quantification of standards and samples using the Quant-it Assay.

	<b>Standard Assay Tube</b>	<b>Sample Assay Tube</b>
<b>Volume of working solution to add</b>	190 µl	190-199 µl
<b>Volume of Standard to add</b>	10 µl	---
<b>Volume of User sample to add</b>	----	1-10 µl
<b>Total volume in each Assay Tube</b>	200 µl	200 µl

The nanodrop spectrophotometer was used according to manufacturer's specifications micro-volume life science spectrophotometer. The absorbance ratios (A260/A280 and A260/A230) were used to estimate the nucleic acids purity.

Presence of RNA was confirmed with gel electrophoresis. A 0.8% agarose gel was prepared using DEPC treated 1X TAE buffer and 0.01% ethidium bromide. The test samples were prepared by adding 1 µl of 6X loading buffer to each 5 µl RNA sample. A volume of 15 µl of each sample, including the lambda/100 bp ladder for calibration purposes, were loaded into the relevant wells and run using a setting of 90 volts for approximately 90 minutes. Upon completion, the RNA bands were visualised using an ultraviolet transilluminator.

### 5.2.3. cDNA synthesis

Primers for cDNA conversion were designed and supplied by Primerdesign™ Ltd. The primers

used were an equal volume combination of oligo-dT and random primers. All nucleic acid work was carried out on ice. RNA templates of 1 µg and a nanoScript2 enzyme volume of 1 µl were used for RNA to cDNA conversion. The temperature settings for the conversion to cDNA are shown on the table below.

Table 5.2: cDNA synthesis cycle temperatures and duration.

Condition	Temperature	Time
Random primer settling	25°C (Room temperature)	5 minutes
Incubation	42°C	20 minutes
Heat Inactivation	75°C	10 minutes
Storage	-20°C	Indefinitely

The newly synthesised cDNA was run on an agarose gel treatment with RNase to show presence of double stranded nucleic acid. The absorbance ratios (A260/A280 and A260/A230) were used to estimate the nucleic acids purity.

#### 5.2.4. qPCR procedure

All qPCR experiments were done on an Applied Biosystems StepOne™ Plus PCR machine. All the primers for qPCR were designed and supplied by Primerdesign™ Ltd. The reference gene tested against in all the reactions was the Hypoxanthine Phosphoribosyl transferase (HPRT) gene. The following primers were used are listed in the table below.

Table 5.3: List of primers used for qPCR gene analysis

Gene of interest	Primerdesign™ code
Ki-67	ENSG00000148773
<i>TPX2TPX2</i>	ENSG00000088325
<i>Adiponectin</i>	ENSG00000181092
<i>BIM</i>	ENSG00000153094
<i>BAD</i>	ENSG00000002330
<i>GLUT4</i>	ENSG00000181856
PPARγ	ENSG00000132170
HPRT reference gene	HK-SY-hu-900

The qPCR analysis was carried out following the Primerdesign™ standard protocol. The protocol was set to capture melt and amplification curves. A sample of the qPCR products were run on gel electrophoresis to rule out primer dimers. The delta-delta Ct method ( $2^{-\Delta\Delta Ct}$ )

was used to calculate the relative fold gene expression. All reactions for the three repeats were done in duplicate. Statistical significance between the values was calculated using a one-way ANOVA and the appropriate post hoc test for multiple comparisons, while paired observations were analysed using students' t test.

#### 5.2.5. Protein analysis

The bicinchoninic acid (BCA) assay was used to show and quantify the presence of proteins. The concentration of the protein was measured using spectrometry at a peak absorbance of 562 nm. Known values for bovine serum albumin (BSA) standards were used to produce a calibration graph and a straight-line equation was used to determine the concentration of protein in the test samples. BSA protein standards were firstly prepared at concentrations of 0, 0.05, 0.1, 0.2, 0.4, 0.6, 0.8, and 1 mg/ml from a stock solution of 10 mg/ml of BSA prepared in 0.9% NaCl.

Cell lysates were made on ice by scrapping cells in lysis buffer after a 10-minute incubation. A small aliquot of cell lysate was diluted to 1 in 10 in 0.9% NaCl. A volume of 10 µl of each sample was added in duplicate to a 96-well plate along with 200 µl of freshly prepared BCA working reagent (BCA with 2% Copper Sulphate ( $\text{CuSO}_4$ )) was also added to each well. The plate was incubated at 37 °C with gentle agitation for 30 minutes. The absorbance was subsequently read at 562 nm using a Thermo plate reader (MultiSkan<sup>®</sup> Spectrum and SkanIt<sup>®</sup> software version 2.2). A final concentration (mg/ml) of samples was determined using the equation of the calibration curve and factoring in of the dilution factor.

The western blotting process was carried out following the Bio-Rad protocol using a Bio-Rad mini-protein II electrophoresis unit. Pre-made sodium Dodecyl Sulphate Polyacrylamide Gel Electrophoresis (SDS-PAGE) were used to separate proteins according to their size and charge. Kaleidoscope pre stained molecular weight markers (BioRad) were loaded on to each gel to monitor the migration of proteins. Equal amounts of protein lysate were added to each lane and then resolved by electrophoresis on a 10% (w/v) polyacrylamide resolving gel and 4% stacking gel immersed in running buffer for less than 90 minutes (until the leading marker arrives at the bottom) at 40mA.

Proteins that were separated by gel electrophoresis were transferred to a nitrocellulose membrane by the semi-dry blotting procedure. Blotting papers as well as the SDS gel were

pre-soaked in blotting buffer before transferring onto a blotting stack on the Invitrogen™ iBlot™ 2 Gel Transfer device. Electroblothing was performed by administering 100 mA/blotted gel at 120 V and 50 W for 1 hour. After transfer, membranes were blocked in 4% w/v non-fat dry milk powder (Marvel) dissolved in TBS-Tween. This involved incubation for 30 minutes at room temperature with gentle agitation on a rocker.

A range of antibodies were used to interrogate the proteins on the blot. Primary antibodies were diluted in 2 % non-fat dry milk powder dissolved in TBS-Tween. The range of primary antibodies and dilution factors are given in Table 4.4. Blots were incubated at room temperature for 1 hour on a or overnight at 4 °C on a gentle rocker. TBS-Tween was used to wash the membranes several times after incubation to remove unbound antibodies. Species-specific secondary antibodies diluted in 2 % non-fat dry milk powder dissolved in TBS-Tween were used to incubate the membranes for 1 hour at room temperature. Residual unbound secondary antibody was removed by washing several times in TBS-Tween.

Table 5.4. Primary antibodies used and dilutions levels.

<b>Antibody</b>	<b>Supplier</b>	<b>Dilution factor</b>
pAkt	Cell signal technology	1:1000
pErk	Cell signal technology	1:500
Akt	Cell signal technology	1:1000
Erk	Cell signal technology	1:2000
UCP1	Abcam	1:1000
Leptin	Abcam	1:300
SREBP1c	Invitrogen (Thermo Fisher Scientific)	1:500
CEBP beta	Invitrogen (Thermo Fisher Scientific)	1:500
β-actin	Sigma	1:10000
PPAR gamma	Sigma	1:1000

Washed membranes were stored in TBS-Tween at 4 °C ready for quantification. For reading and quantification, membranes were air dried and covered in enhanced chemiluminescence (ECL) solution and incubated for 1 minute in room temperature. Blotted membranes were

placed on photographic Amersham Hyperfilm ECL™ film in a darkroom. The films were developed using a CAWO Cawomat 2000 IR® film processor and scanned and saved as jpg. files at 300 dots per inch (dpi). Signals were quantified with ImageJ (U. S. National Institutes of Health, Bethesda, Maryland, USA) software.

The house keeping protein  $\beta$  actin was used to standardise protein loading. The blotted membrane was stripped of all the bound antibodies with a stripping solution (ReBlot Plus®) for 30mins. After removal of the stripping solution, the blot was washed in TBS-Tween and blocked using 4 % non-fat dry milk powder for 1.5 hours at room temperature. The membranes were then washed twice with TBS-Tween for 1 minute and the  $\beta$  actin (1:10 000 antibody dilution) prepared in 4% w/v non-fat milk powder in TBS-Tween overnight on a gentle shaker at 4°C. A secondary antibody was applied as described above.

#### 5.2.6. Statistical analysis

Results are expressed as the mean  $\pm$  SD for the number of assays indicated. Where necessary, geometrical means were taken instead of arithmetic mean. For all gene expressions, the results were mean of 3 independent experiments, with 2 duplicates (n=6). For relative gene expression, the  $2^{-\Delta\Delta CT}$  method was used. This was calculated by finding the difference between the ct values of the gene of interest and endogenous control for both the experimental sample as well as the control sample. Relative protein quantification was determined by first subtracting background densities from the protein of interest (PI) and the normalising control (NC). This was followed by identifying the NC that had the least density value. All the NC values were divided by that least NC density value. The least density value will thus a value of 1. Finally, all PI values were divided by the relative NC values in respective lanes. For multiple comparisons of groups, statistical significance was calculated and evaluated by one-way ANOVA followed by Tukey post-hoc test. To compare two groups, two-tailed paired Student's t-test was used.



### 5.3. Results

#### 5.3.1. Gene expression; general.

Melt curves analysis were used to assess whether the qPCR assays had produced single, specific products. Figure 4.1 is an example of a melt curve which was used to determine whether the amplified double-stranded DNA products were a single discrete species.

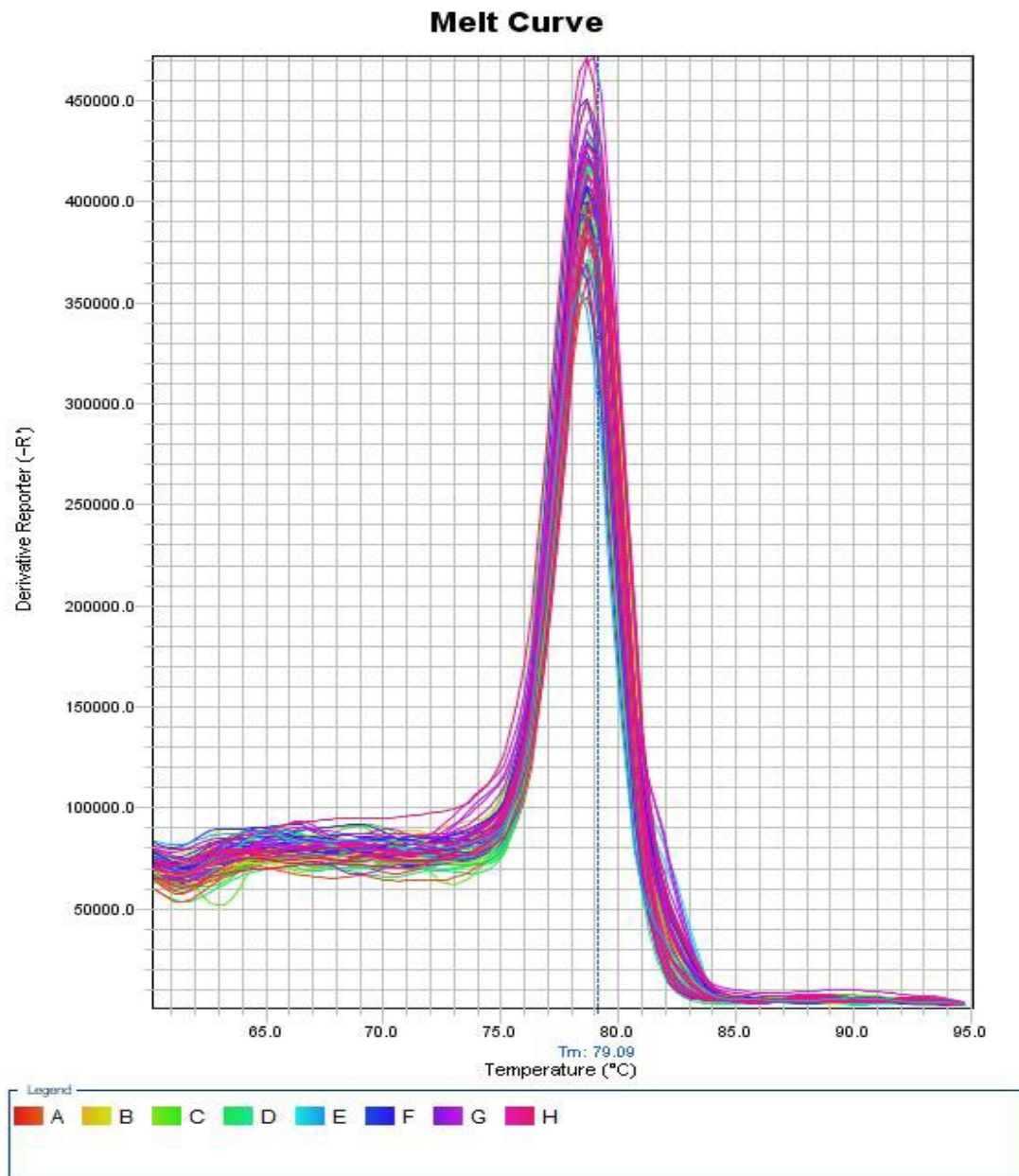


Figure 5.1. *BIM* gene on a chrysin melt curve, a typical denaturation curve performed after qPCR cycling showing a single peak suggesting a single discrete species of amplicon. The primer melting temperature was between 76 and 80 °C and the primer efficiency was high.

DNA products run through a gel produced single bands indicating single amplicons. Figure 4.2 shows a typical gel run with the final qPCR products to ascertain primer specificity.

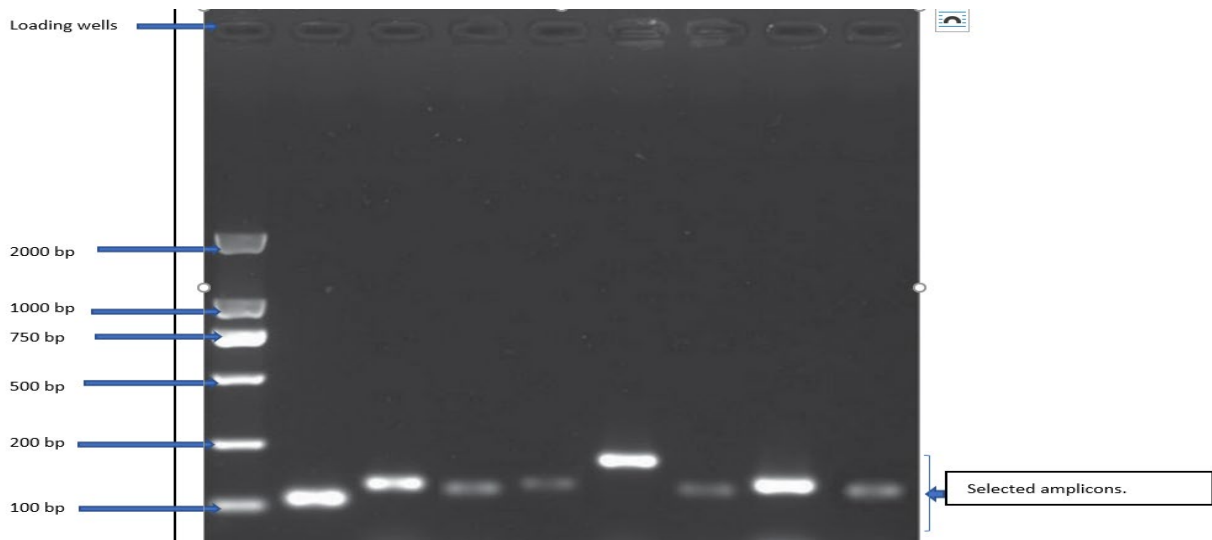


Figure 5.2 A typical gel electrophoresis run of qPCR products showing single bands. The first lane is the size marker and the rest are gene products.

Specific primers produced cycle threshold ( $C_T$ ) values above 40 (undetermined). Standard deviations ( $C_T$  SD) of less than 0.5 were deemed as acceptable as illustrated in in figure 4.2

#	Well	Omit	Flag	Sample N...	Target Na...	Task	Dyes	$C_T$	$C_T$ Mean	$C_T$ SD	$\Delta C_T$
1	A1	<input type="checkbox"/>			PPARGam...	NTC	SYBR-None	Undetermi...			
2	A2	<input type="checkbox"/>			PPARGam...	NTC	SYBR-None	Undetermi...			
3	A3	<input type="checkbox"/>		C1	PPARGam...	UNKNOWN	SYBR-None	29.222	29.308	0.121	
4	A4	<input type="checkbox"/>		C1	PPARGam...	UNKNOWN	SYBR-None	29.393	29.308	0.121	
5	A5	<input type="checkbox"/>		C2	PPARGam...	UNKNOWN	SYBR-None	29.491	29.573	0.116	
6	A6	<input type="checkbox"/>		C2	PPARGam...	UNKNOWN	SYBR-None	29.655	29.573	0.116	
7	A7	<input type="checkbox"/>		C3	PPARGam...	UNKNOWN	SYBR-None	29.909	29.799	0.156	
8	A8	<input type="checkbox"/>		C3	PPARGam...	UNKNOWN	SYBR-None	29.688	29.799	0.156	
9	A9	<input type="checkbox"/>		C4	PPARGam...	UNKNOWN	SYBR-None	30.357	30.428	0.101	
10	A10	<input type="checkbox"/>		C4	PPARGam...	UNKNOWN	SYBR-None	30.499	30.428	0.101	
11	A11	<input type="checkbox"/>		C5	PPARGam...	UNKNOWN	SYBR-None	30.323	30.43	0.151	
12	A12	<input type="checkbox"/>		C5	PPARGam...	UNKNOWN	SYBR-None	30.536	30.43	0.151	
13	B1	<input type="checkbox"/>		C6	PPARGam...	UNKNOWN	SYBR-None	30.708	30.832	0.176	
14	B2	<input type="checkbox"/>		C6	PPARGam...	UNKNOWN	SYBR-None	30.956	30.832	0.176	
15	B3	<input type="checkbox"/>		C7	PPARGam...	UNKNOWN	SYBR-None	31.316	31.371	0.078	
16	B4	<input type="checkbox"/>		C7	PPARGam...	UNKNOWN	SYBR-None	31.426	31.371	0.078	
17	B5	<input type="checkbox"/>		C8	PPARGam...	UNKNOWN	SYBR-None	31.796	31.736	0.084	
18	B6	<input type="checkbox"/>		C8	PPARGam...	UNKNOWN	SYBR-None	31.677	31.736	0.084	
19	B7	<input type="checkbox"/>		C9	PPARGam...	UNKNOWN	SYBR-None	29.433	29.459	0.036	
20	B8	<input type="checkbox"/>		C9	PPARGam...	UNKNOWN	SYBR-None	29.485	29.459	0.036	
21	B9	<input type="checkbox"/>		C10	PPARGam...	UNKNOWN	SYBR-None	29.017	29.026	0.013	
22	B10	<input type="checkbox"/>		C10	PPARGam...	UNKNOWN	SYBR-None	29.035	29.026	0.013	
23	B11	<input type="checkbox"/>		C11	PPARGam...	UNKNOWN	SYBR-None	29.402	29.531	0.182	
24	B12	<input type="checkbox"/>		C11	PPARGam...	UNKNOWN	SYBR-None	29.660	29.531	0.182	
25	C1	<input type="checkbox"/>		C12	PPARGam...	UNKNOWN	SYBR-None	31.646	31.817	0.242	
26	C2	<input type="checkbox"/>		C12	PPARGam...	UNKNOWN	SYBR-None	31.988	31.817	0.242	
27	C3	<input type="checkbox"/>		C13	PPARGam...	UNKNOWN	SYBR-None	29.149	29.196	0.067	
28	C4	<input type="checkbox"/>		C13	PPARGam...	UNKNOWN	SYBR-None	29.243	29.196	0.067	

Figure 5.3 A screen shot of a typical qPCR run of the *PPAR gamma* gene expressed on chrysin treated SGBS cells showing primer specificity by having indeterminate  $C_T$  values for the no template control and  $C_T$  SD values of less than 0.5.

### 5.3.2. Gene expression; Proliferation

The following genes: *TPX2*, *Ki67*, *BIM*, *BAD*, *PPAR gamma*, *adiponectin*, *GLUT4*, *SREBP1c* and *CEBP- $\beta$*  across a range of concentrations of quercetin and chrysin. Figures 5.3.1a to 5.3.7b below show the dose and time impact of the flavonoids on gene expression. For all gene expressions, the results are a mean of 3 independent experiments, each with 2 duplicates, therefore n=6.

#### 5.3.2.1. *Ki67* gene

There was a general reduction in *Ki67* gene expression on SGBS cells treated with either quercetin or chrysin over a 3-day period.

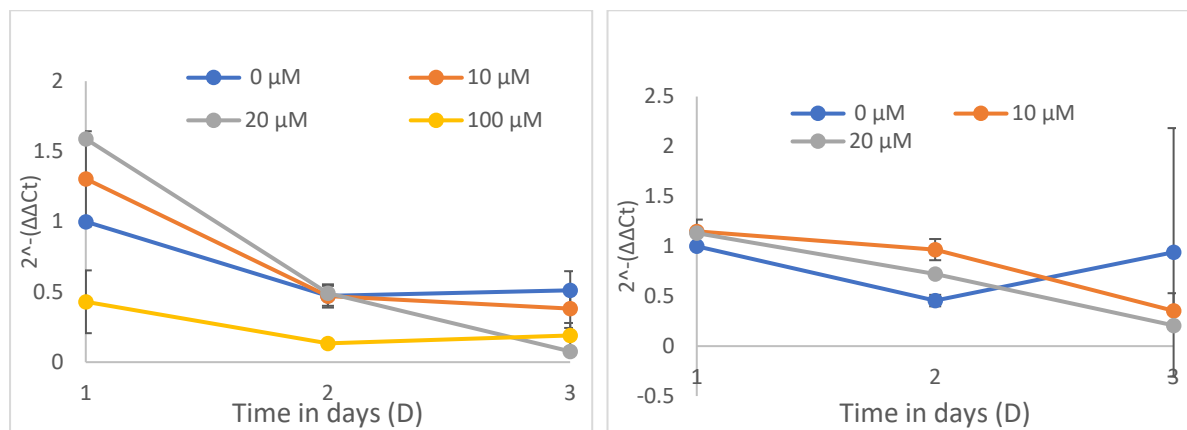


Figure 5.3.1a and b. Effect of concentration on the relative expression of the *Ki67* gene in quercetin and chrysin treated SGBS cells over 3 days. There was a general decrease in gene expression across the 3 days. This decrease was significant in cells treated by 20 and 100  $\mu$ M of quercetin and 10 and 20  $\mu$ M after 3 days ( $p < 0.05$ ). The concentration of 100  $\mu$ M was omitted as it proved to be toxic.

#### 5.3.2.2. *TPX2* gene

*TPX2* gene was generally suppressed in SGBS cells treated with quercetin over a 3-day period. There was no significant difference in *TPX2* gene expression for chrysin treated SGBS cells relative to the control. There was a gradual decrease in expression over the 3 days, however.

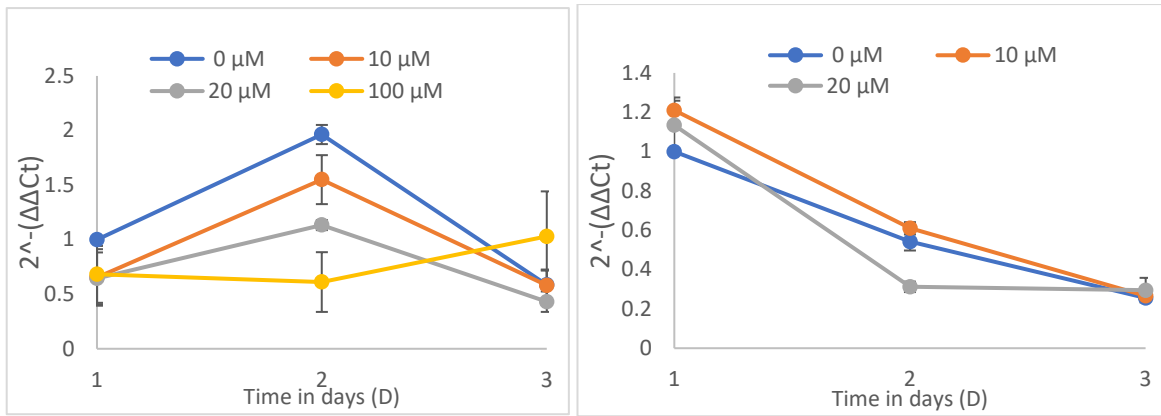


Figure 5.3.2a and b. Effect of concentration on the relative expression of the *TPX2* gene in quercetin and chrysin treated SGBS cells over 3 days. There was a significant decrease in expression in cells treated by all concentrations of quercetin after day 2 ( $p < 0.05$ ). This decrease appear to wane away by the third day except for the 100 μM concentration which showed a significant recovery ( $p < 0.05$ ). There was general decrease in expression of *TPX2* for all chrysin treatments with a significantly lower expression for the 20 μM treatment after day 1 ( $p < 0.05$ ). The chrysin concentration of 100 μM was omitted as it proved to be toxic.

### 5.3.2.3. *BIM* gene

The *BIM* gene generally increases over the 3 days of culture. All quercetin treatments had elevated *BIM* expression relative to the control by day 3. Chrysin treated cells had suppressed *BIM* expression over the same period of time.

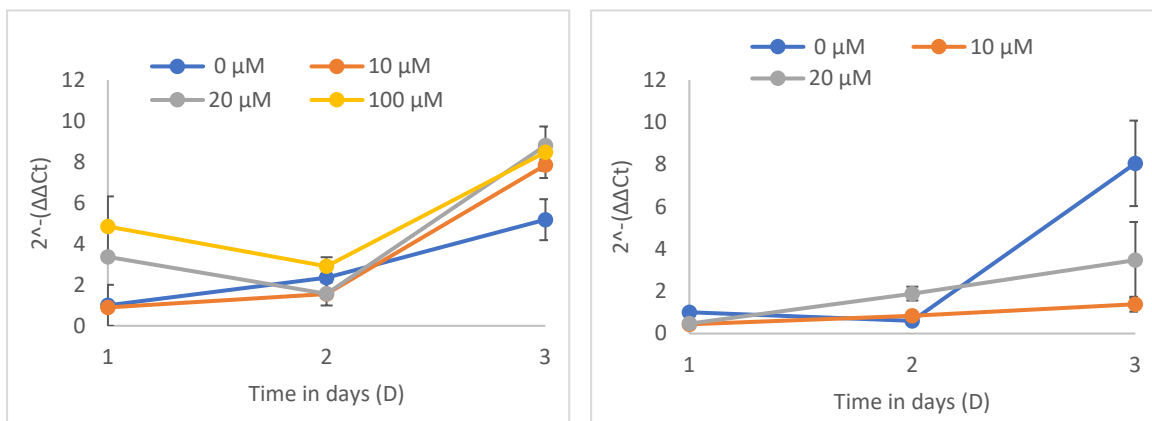


Figure 5.3.3a and b. Effect of flavonoid concentration on the relative expression of the *BIM* gene in quercetin and chrysin treated SGBS cells over 3 days. There was a general increase in gene expression across the 3 days. This increase was significant in cells treated with all concentrations of quercetin ( $p < 0.05$ ). Whilst chrysin treated cells marginally increased in expression, they were significantly lower

compared to the control ( $p < 0.05$ ) for the 10 and 20  $\mu\text{M}$  concentrations. The concentration of 100  $\mu\text{M}$  of chrysin was omitted as it proved to be toxic.

#### 5.3.2.4. *BAD* gene

The *BAD* gene marginally increases over the 3 days of culture.

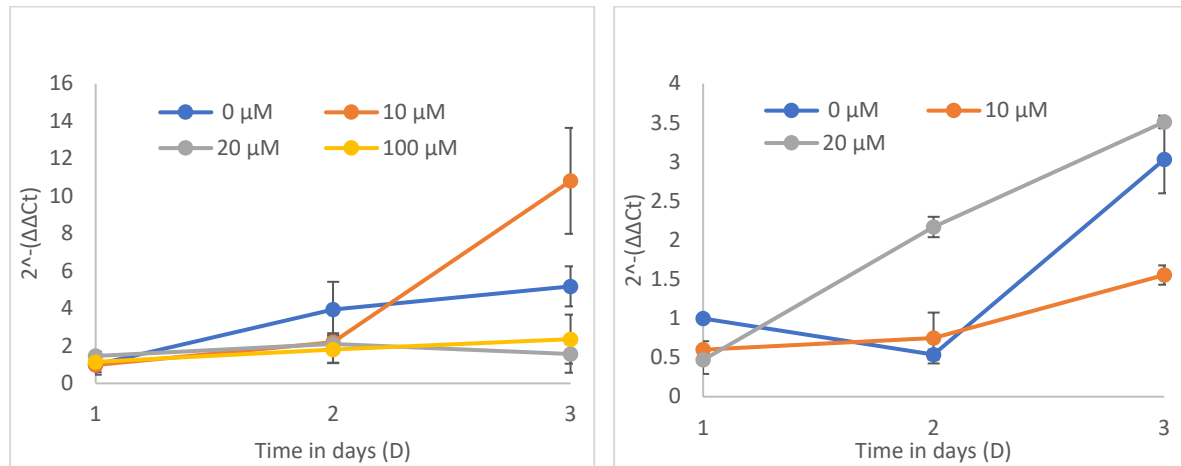


Figure 5.3.4a and b. Effect of flavonoid concentration on the relative expression of the *BIMBAD* gene in quercetin and chrysin treated SGBS cells over 3 days. There was a general increase in gene expression across the 3 days. This increase was suppressed significantly in cells treated with concentrations of 20 and 100  $\mu\text{M}$  but elevated in 10  $\mu\text{M}$  of quercetin ( $p < 0.05$ ) by the third day. In chrysin treated cells, the 20  $\mu\text{M}$  concentration significantly increased in expression on day 2 ( $p < 0.05$ ). However, the significance was absent by day 3. The 10  $\mu\text{M}$  concentration was significantly reduced by day 3 ( $p < 0.05$ ) relative to the control. The concentration of 100  $\mu\text{M}$  of chrysin was omitted as it proved to be toxic.

#### 5.3.2.5. *Adiponectin* gene

The *adiponectin* gene did not show much change in expression during the first three days of preadipocyte incubation. There was a positive gradient across the three days.

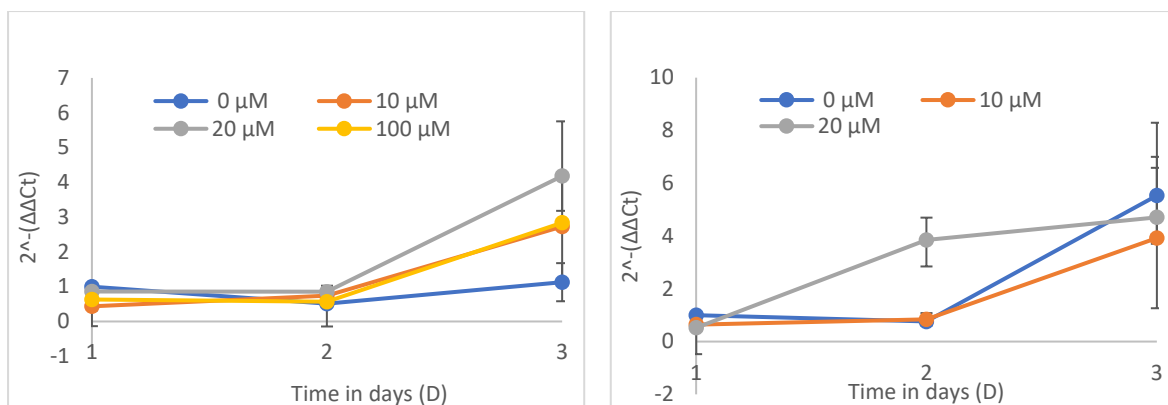


Figure 5.3.5a and b. Effect of concentration on the relative expression of the *adiponectin* gene in quercetin and chrysin treated SGBS cells over 3 days. There was a general but marginal increase in gene expression ( $p>0.05$ ) across the 3 days for both quercetin and chrysin. However, the 20  $\mu\text{M}$  quercetin treatment had a 4-fold increase after 2 days when compared to the control. On day 3, quercetin treated cells appear to have a slight increase of *adiponectin* expression relative to the control whereas chrysin showed the opposite. These patterns are however not statistically significant ( $p>0.05$ ). Chrysin concentration of 100  $\mu\text{M}$  was omitted as it proved to be toxic.

#### 5.3.2.6. GLUT4 gene

The *GLUT4* gene did not show much change in expression during the first three days of preadipocyte incubation. However, there was a general upward trend (increase) in gene expression across time.

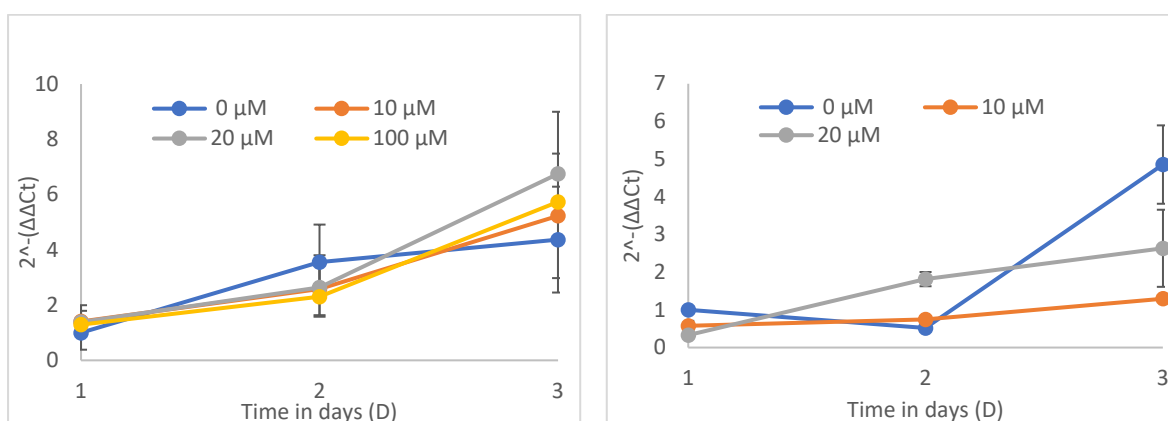


Figure 5.3.6a and b. Effect of concentration on the relative expression of the *GLUT4* gene in quercetin and chrysin treated SGBS cells over 3 days. There was a general but marginal increase in gene expression ( $p>0.05$ ) across the 3 days for both quercetin and chrysin. On day 3, quercetin treated cells appear to have a slight increase of *GLUT4* expression relative to the control whereas chrysin showed the opposite. These patterns are however not statistically significant ( $p>0.05$ ). Chrysin concentration of 100  $\mu\text{M}$  was omitted as it proved to be toxic.

### 5.3.2.7. PPAR $\gamma$ gene

The PPAR $\gamma$  gene did not show much change in expression during the first three days of preadipocyte incubation. Gene expression marginally increased with time across all treatments.

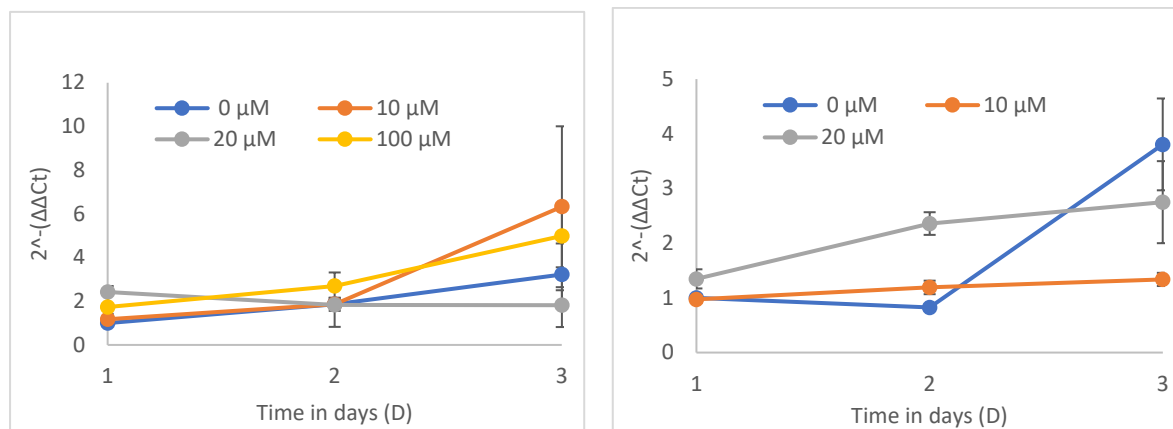


Figure 5.3.7a and b. Effect of concentration on the relative expression of the PPAR $\gamma$  gene in quercetin and chrysin treated SGBS cells over 3 days. There was a general but marginal increase in gene expression ( $p > 0.05$ ) across the 3 days which was positive for quercetin and negative for chrysin. The 10  $\mu$ M concentration was significantly suppressed relative to the control ( $p > 0.05$ ) for chrysin after day 3 whereas, quercetin had the opposite trend. These patterns are however not statistically significant ( $p > 0.05$ ). Chrysin concentration of 100  $\mu$ M was omitted as it proved to be toxic.

### 5.3.2.8. SREBP1c gene on quercetin

The SREBP1c gene was tested across a larger range of concentrations for SGBS preadipocytes treated with quercetin after 24 hours. Expressions were shown relative to day 0 samples. SREBP1c had a 9-fold increase on the untreated cells after 4 hours, however, all other treatments had a reduced gene expression over the same period of time.

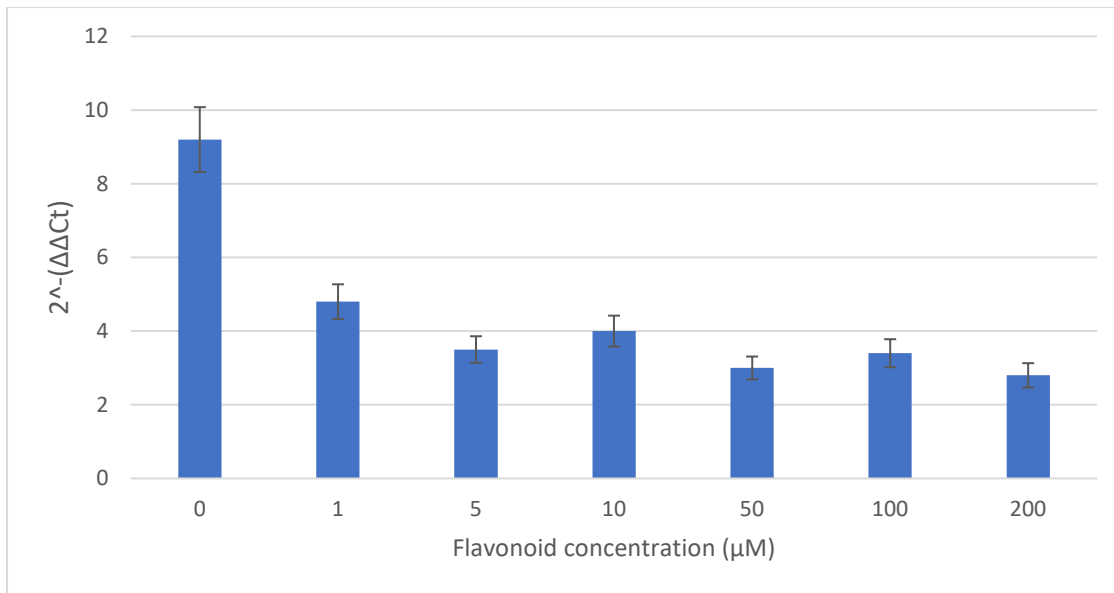


Figure 5.3.8. All treatments significantly reduced the expression of *SREBP1c* ( $p < 0.05$ ) after 24 hours of incubation. The reduction was more pronounced as the concentrations increased although there were no significant differences between quercetin doses.

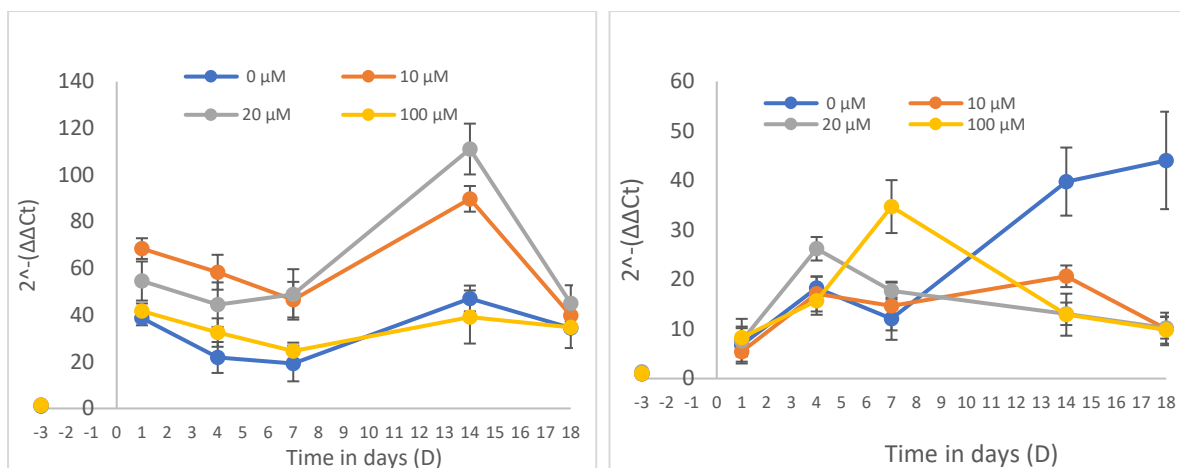
### 5.3.3. Gene expression; Differentiation.

The following genes: *PPAR gamma*, *adiponectin*, *GLUT4*, *UCP1*, *TPX2*, *Ki67Ki67*, *BIM*, *BAD*, *SREBP1c* and *CEBP-β* across a range of concentrations of quercetin and a selection of chrysin samples. Figures 5.3.9 to 5.3.26 below show the dose and time impact of the flavonoids on gene expression.

#### 5.3.3.1. PPAR $\gamma$ gene

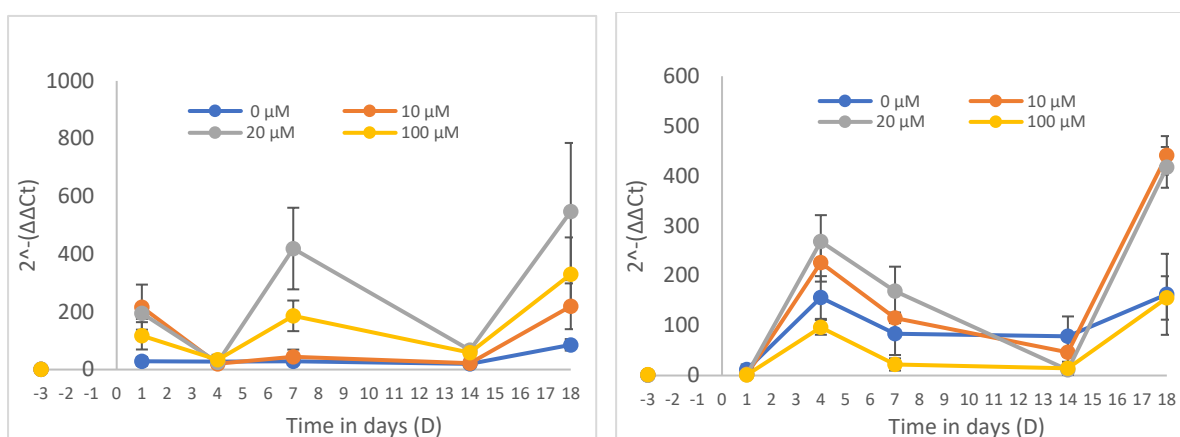
The *PPAR gamma* gene was elevated in expression for cells treated with peri-physiological concentrations of the quercetin across the time range. However, this was not evident in chrysin where gene expression was suppressed relative to the control after two weeks of incubation.





### 5.3.3.2. *Adiponectin* gene

Expression of the *adiponectin* gene did not vary across the time of incubation for the untreated controls. Higher concentrations (20  $\mu\text{M}$  and 100  $\mu\text{M}$ ) of quercetin produced higher levels of *adiponectin* gene expression on day 7. All flavonoid treatments had elevated *adiponectin* gene expression after day 18 except for chrysin at 100  $\mu\text{M}$ .



### 5.3.3.3. GLUT4 gene

*GLUT4* gene expression was constant in reference samples across time. However, treated cells increased in relative expression as the incubation time approached 18 days. Chrysin concentrations of 20  $\mu\text{M}$  had spikes of increased relative expression on day 1 and 14, quercetin treatments of 10  $\mu\text{M}$  spiked at day 14.

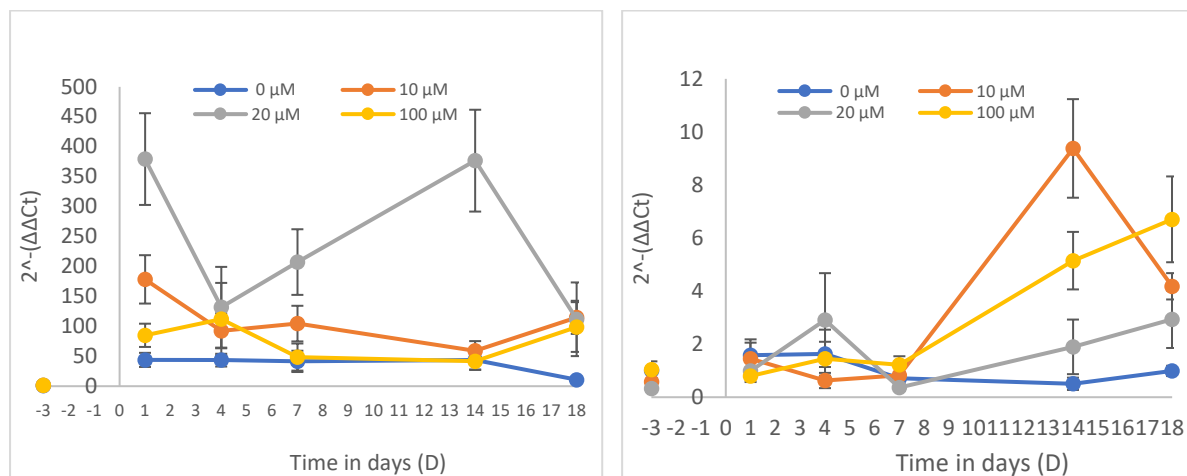


Figure 5.3.11 a and b. Effect of concentration on the relative expression of the *GLUT4* gene in quercetin and chrysin treated SGBS cells over 18 days. Cells treated with 20  $\mu\text{M}$  concentrations of quercetin significantly increased gene expression ( $p < 0.05$ ) throughout the incubation time. All concentrations were significantly upregulated ( $p < 0.05$ ) by day 14 for chrysin and 18 for quercetin.

The effect of quercetin on the expression of *GLUT4* gene on cells treated twice, at day 0 and day 4 with concentrations of 0, 1, 10 and 100  $\mu\text{M}$ . There was a gradual increase in expression of the gene on cells treated with physiological concentrations of quercetin.

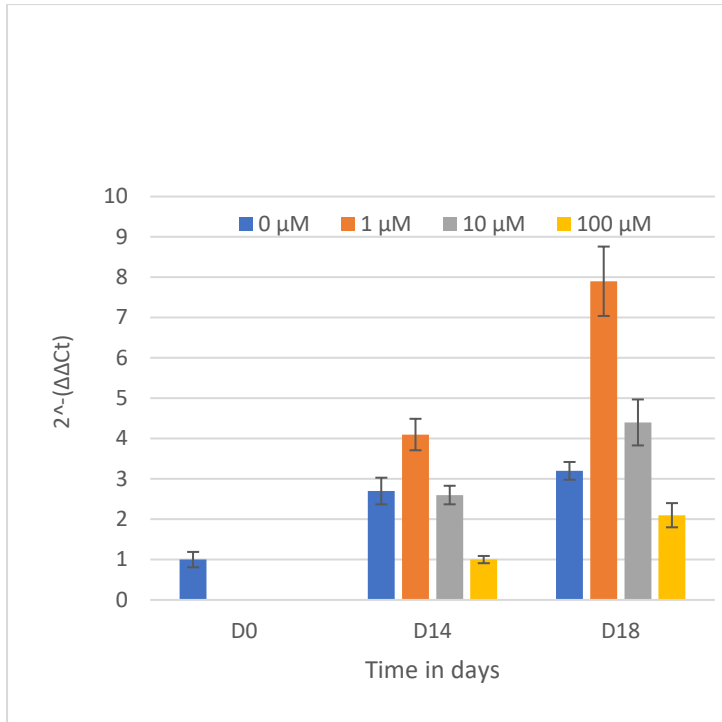


Figure 5.3.12 Effect of concentration on the relative expression of the GLUT4 gene in quercetin treated SGBS cells over 18 days. GLUT4 expression increase over time even on the untreated cells as more cells reverted from preadipocytes to differentiated adipocytes. Cells treated with 1 μM concentrations of quercetin significantly increased gene expression ( $p < 0.05$ ) for day 14 and 18. The relative downregulation of the gene in cells treated with 100 μM appear to wane away over time.

#### 5.3.3.4. *SREBP1c* gene

Expression of the *SREBP1c* gene increased as the cells morphed from preadipocytes to the differentiated form. All quercetin concentration treatments were elevated relative to the control with the 10 μM concentration having the highest increase.

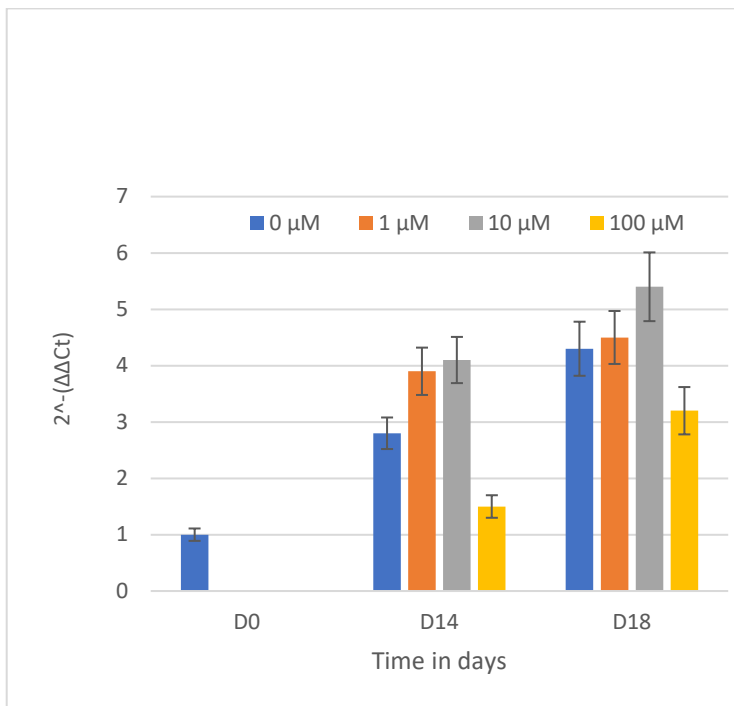


Figure 5.3.13. Effect of concentration on the relative expression of the SREBP1c gene in quercetin treated SGBS cells over 18 days. All treatments had a significant increase of expression compared to day 0 control; treatments of 1 and 10 μM were significantly elevated ( $p < 0.05$ ) relative to their vehicle controls. The greatest increase was in the 10 μM treatment.

### 5.3.3.5. *UCP1* gene

Expression of the *UCP1* gene increased in untreated cells as they morphed from preadipocytes to the differentiated form. This was downregulated in treatments of quercetin of 10 and 100  $\mu\text{M}$ . Infra-physiological concentration of quercetin (1  $\mu\text{M}$ ) however, had increased expression relative to the vehicle control over the test period.

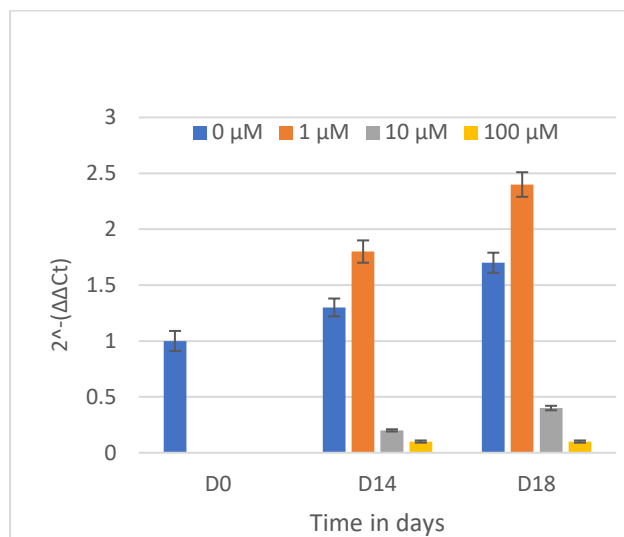


Figure 5.3.14. Effect of concentration on the relative expression of the *UCP1* gene in quercetin treated SGBS cells over 18 days. Treatments of 10 and 100  $\mu\text{M}$  were significantly downregulated relative to both the reference and vehicle controls ( $p < 0.05$ ) across the test times. The 1  $\mu\text{M}$  treatment however showed significant upregulation ( $p < 0.05$ ) over the 18 days relative to the controls. *UCP1* expression increased with time on the untreated controls.

### 5.3.3.6. *C/EBP-beta* gene

There was a gradual increase of *C/EBP $\beta$*  gene expression in untreated cells during the course of differentiation. The 100  $\mu\text{M}$  concentration increased the expression of the gene 15-fold on day 14 relative to the untreated sample. This increase, although still present, waned away by day 18. Treatments of 1 and 10  $\mu\text{M}$  concentrations were suppressed relative to the vehicle control on day 18.

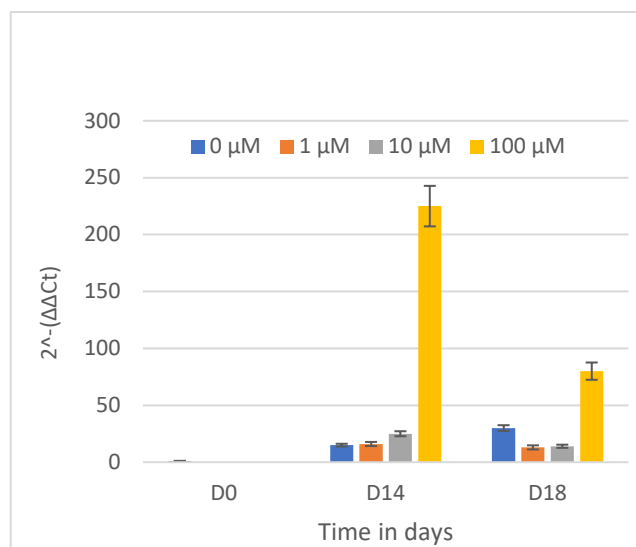


Figure 5.3.15 Effect of concentration on the relative expression of the *C/EBP $\beta$*  gene in quercetin treated SGBS cells over 18 days. Treatments of 10 and 100  $\mu\text{M}$  were significantly downregulated relative to both the reference and vehicle controls ( $p < 0.05$ ) across the test times. The 1  $\mu\text{M}$  treatment however showed significant upregulation ( $p < 0.05$ ) over the 18 days relative to the controls. *C/EBP $\beta$*  expression increased significantly with time on the untreated controls ( $p < 0.05$ ).

### 5.3.4. Protein expression; Proliferation.

Cells were treated as described in chapter 2. The following proteins were investigated; *SREBP1c*, C/EBP $\beta$ , Erk, pErk, Akt, pErk and leptin after 48 and 72 hours of incubation. The following bar charts representative examples of quantified blots for each protein (n=1).

#### 5.3.4.1. *SREBP1c* protein

Expression of the *SREBP1c* had doubled by day 2 of incubation on the untreated samples which increased slightly by the third day. All quercetin treatments, while greater than day 0 control, were relatively lower than the daily control in inverse concentration order.

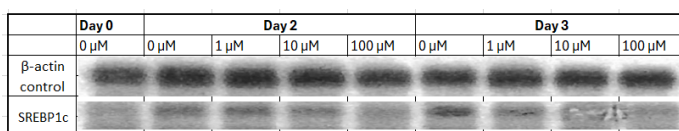
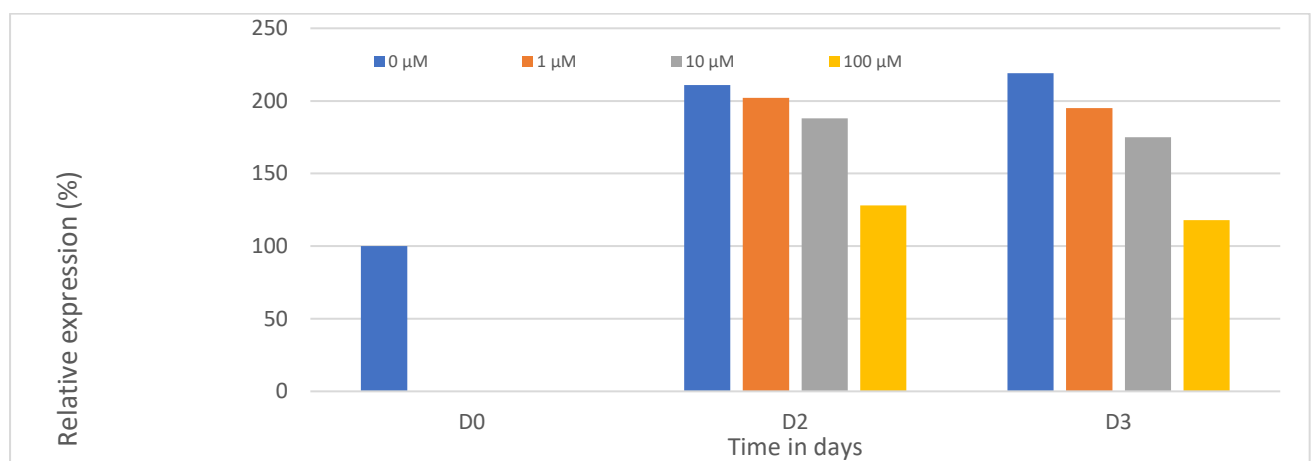


Figure 5.3.16a. Effect of concentration on the relative expression of the SREBP1c protein in quercetin treated SGBS preadipocytes over 3 days of incubation. SREBP1c protein production increased with incubation time to a 2-fold increase by day 2 and 3. The presence of flavonoids reduced the protein abundance in a dose and time dependant pattern, but all the flavonoid treatments had a protein presence greater than that of day 0 control. The associated Western blots are shown below the figure.

### 5.3.4.2. C/EBP $\beta$ protein

Expression of the C/EBP $\beta$  increased linearly on the untreated samples over the 3 days of incubation. The 1  $\mu$ M concentration lagged slightly behind the controls but the 10 and 100  $\mu$ M concentrations were suppressed below the day 0 reference control. The suppression marginally increased from day 2 to 3.

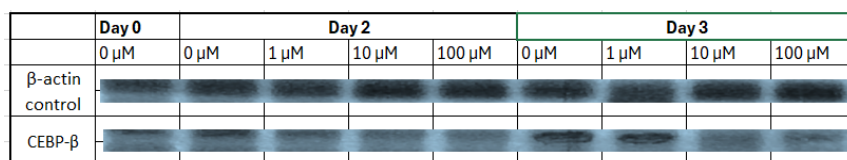
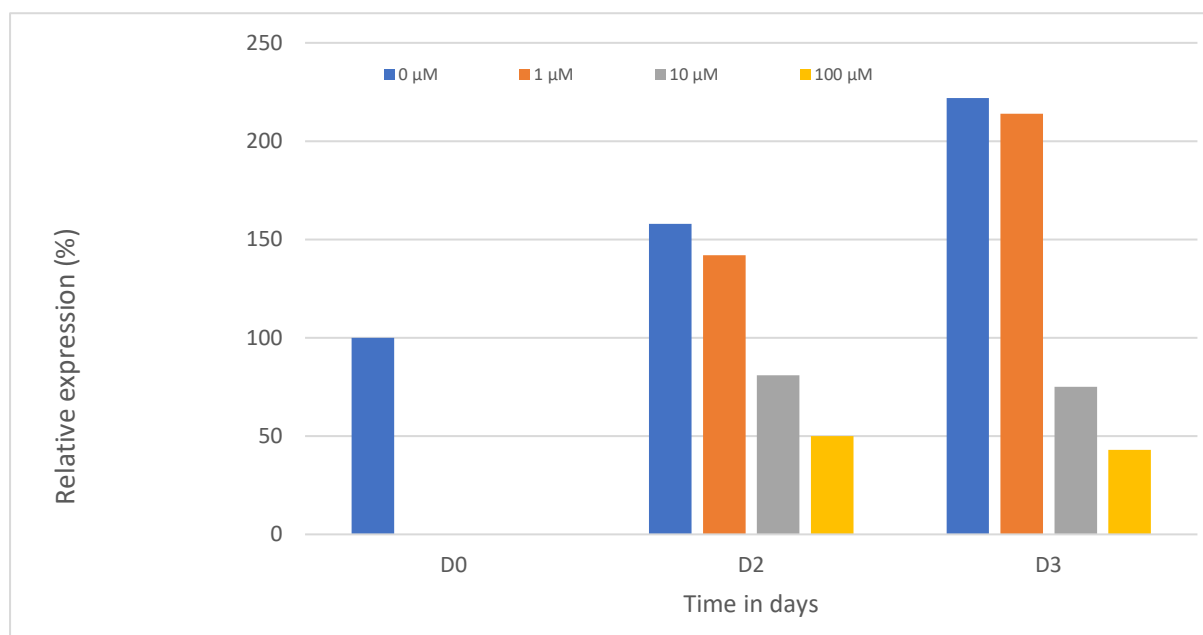


Figure 5.3.16. Effect of concentration on the relative expression of the C/EBP $\beta$  protein in quercetin treated SGBS preadipocytes over 3 days of incubation. C/EBP $\beta$  protein production increased with incubation time to more than double the initial value by day 3 in untreated cells. The presence of higher concentrations flavonoids reduced the protein abundance in a dose and time dependant pattern. The 1  $\mu$ M concentration, whilst higher than the day 0 reference control, closely lagged the untreated vehicle control. The associated Western blots are shown.

### 5.3.4.3. Erk and pErk

Both Erk and pErk appear to increase in expression with time. However, all concentrations of quercetin showed a proportional decrease in Erk protein presence to concentration. The protein pErk was elevated in treatments of 1 and 10  $\mu\text{M}$  concentrations for the 2 test days, the 100  $\mu\text{M}$  concentration, however, reduced the protein presence.

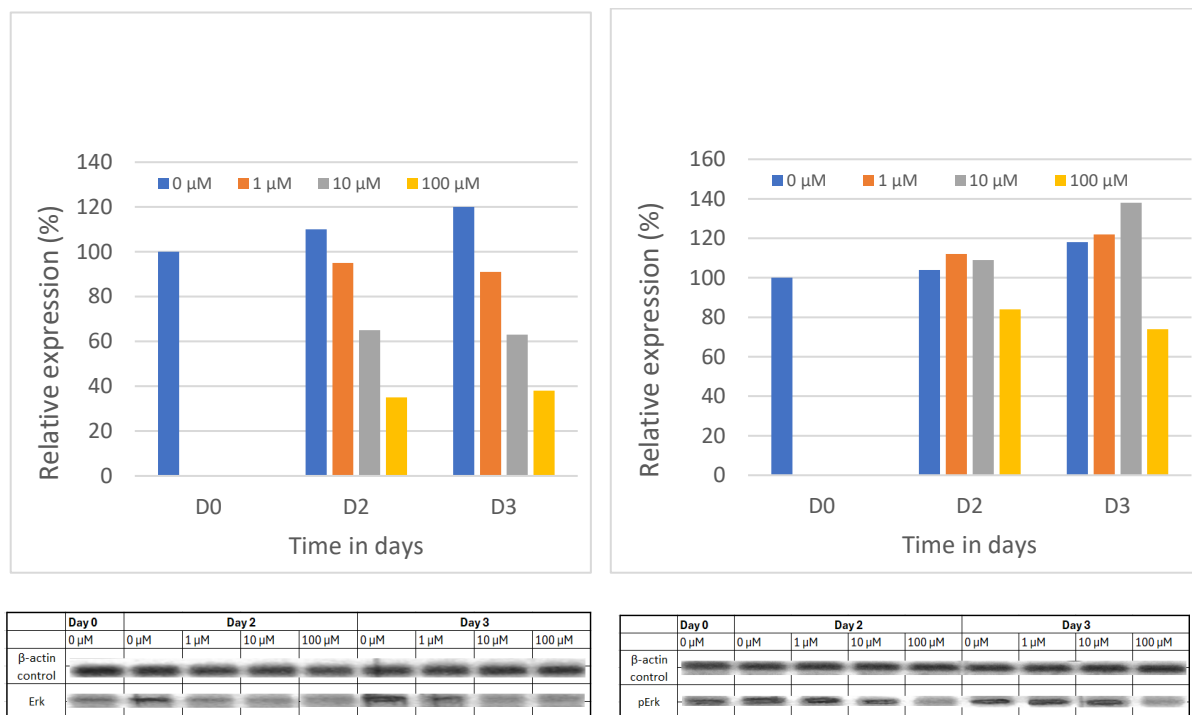


Figure 5.3.17 a and b. Effect of concentration on the relative expression of the Erk and pErk proteins in quercetin treated SGBS preadipocytes over 3 days of incubation. Erk protein increased lineally in the 2 test days to 20% more by day 3 on the untreated controls. The treatment concentrations of 1, 10 and 100  $\mu\text{M}$  reduced expression by 10%, 35% and 65% respectively after the three days of incubation. The difference in reduction between day 2 and 3 was negligible. The protein pErk showed increased expression for the 1 and 10  $\mu\text{M}$  concentrations up to 22% and 38% more respectively by day 3 relative to the day 0 control. The 100  $\mu\text{M}$  concentration showed a reduction of 26% by the same time. The associated Western blots are shown below the figure.

#### 5.3.4.4. Leptin protein

Presence of the leptin protein in the untreated samples was gradually reduced over the 2 test days relative to day 0 expression. There was barely any change on the 1 and 10  $\mu\text{M}$  treatments on day 2 with a slight decrease on day 3. However, the 100  $\mu\text{M}$  concentration increased leptin presence in the 2 test days.

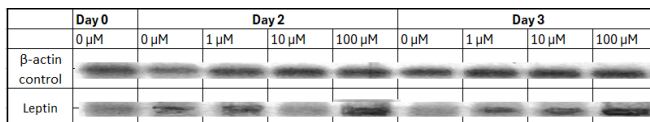
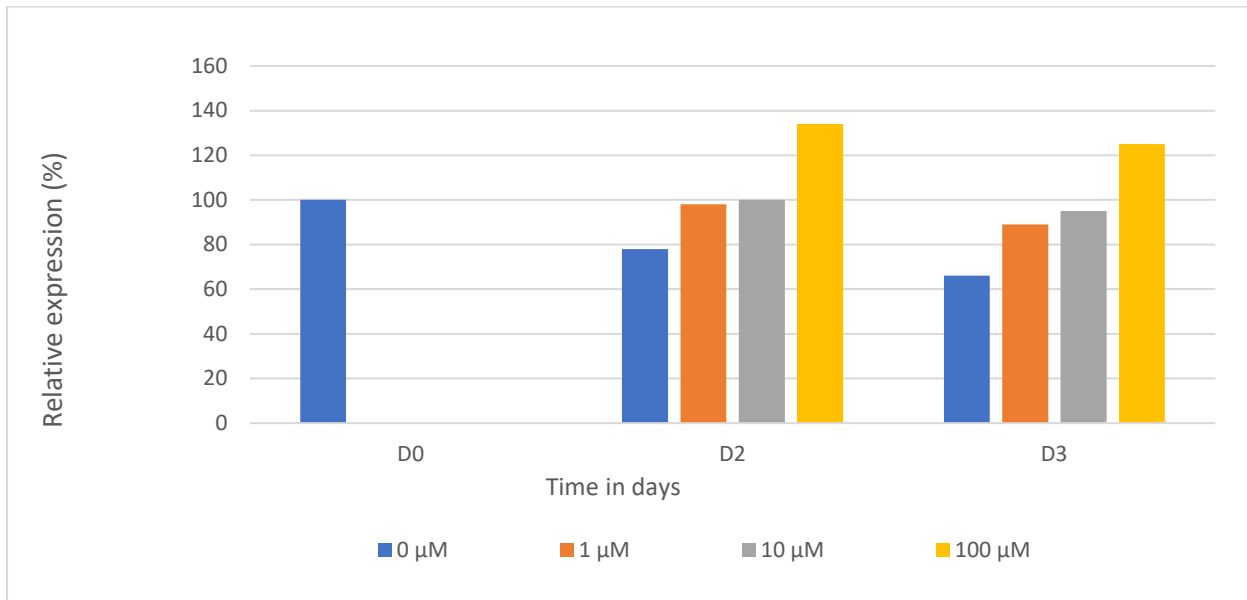


Figure 5.3.18. Effect of concentration on the relative expression of the leptin protein in quercetin treated SGBS preadipocytes over 3 days of incubation. The leptin protein production decreased with incubation time to 34% by day 3. The presence of 100  $\mu\text{M}$  quercetin increased the protein abundance to 34 and 25 % in day 2 and 3 respectively. The 1 and 10  $\mu\text{M}$  concentration, whilst higher than the daily untreated controls by up to 29% for the 10  $\mu\text{M}$  concentration on day 3, there was not much difference to the day 0 reference sample over the 2 days. The associated Western blots are shown below the figure.



### 5.3.4.5. Akt and pAkt proteins

The Akt protein increased linearly over the duration of incubation for the untreated controls. However, all the quercetin treatments reduced protein presence for both test days. The protein pAkt had increased expression on the treated samples than the daily controls. Day 3 values were slightly lower than day 2 values across the treatments.

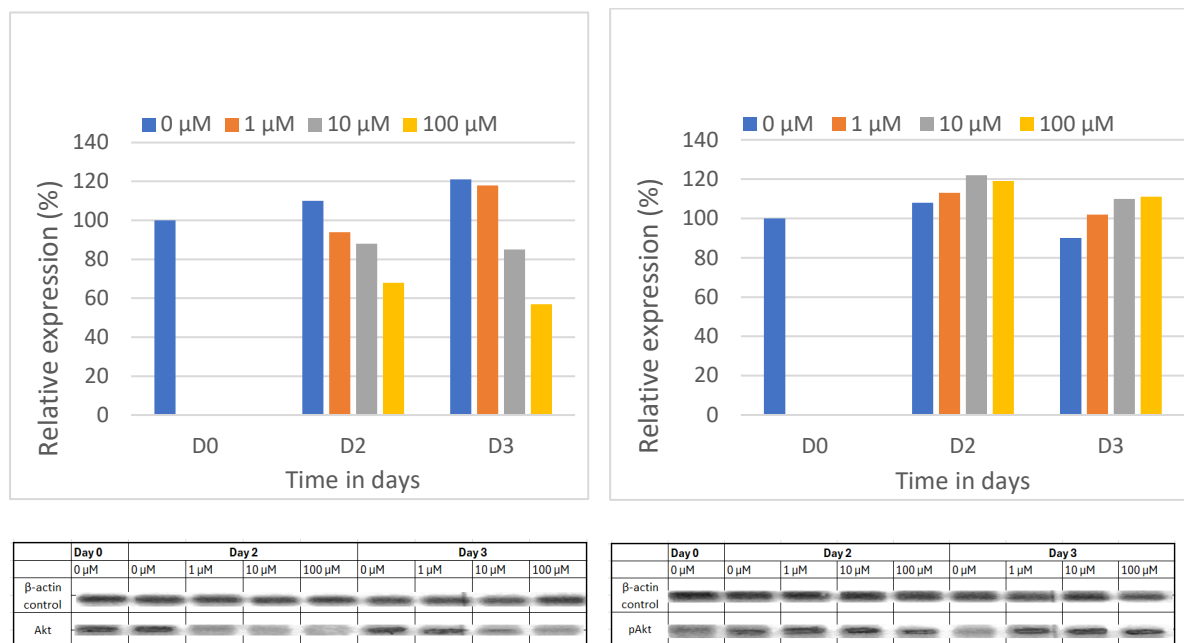


Figure 5.3.19 a and b. Effect of concentration on the relative expression of the Akt and pAkt proteins in quercetin treated SGBS preadipocytes over 3 days of incubation. The Akt protein increased linearly in the 2 test days to greater than 20% more by day 3 on the untreated controls. The greatest reduction was on the 100 μM which had a 42 and 64% reduction after day 2 and 3 of incubation respectively. The protein, pAkt showed a general increase in expression on the treated samples relative to the daily controls. Day 3 readings had all the treatment conditions having a value greater than the day 0 untreated control except for the day 3 untreated sample which was lower than the reference control by 10%. The associated Western blots are shown below the figure.

### 5.3.5. Protein expression; Differentiation.

Cells were treated and incubated as described in chapter 2. Cells were treated with flavonoid added differentiation initiation media (F0) on day 0 and flavonoid added differentiation media (F1) on day 4. Treated cells were incubated for 18 days with experimental samples taken on day 14 and day 18.

#### 5.3.5.1. SREBP1c protein

Expression of the SREBP1c increased to 2 and 2.7-fold by day 14 and 18 respectively on the untreated controls. All quercetin treatments, while greater than day 0 control, were relatively lower than the daily control in inverse concentration order.

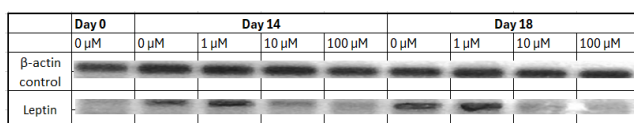
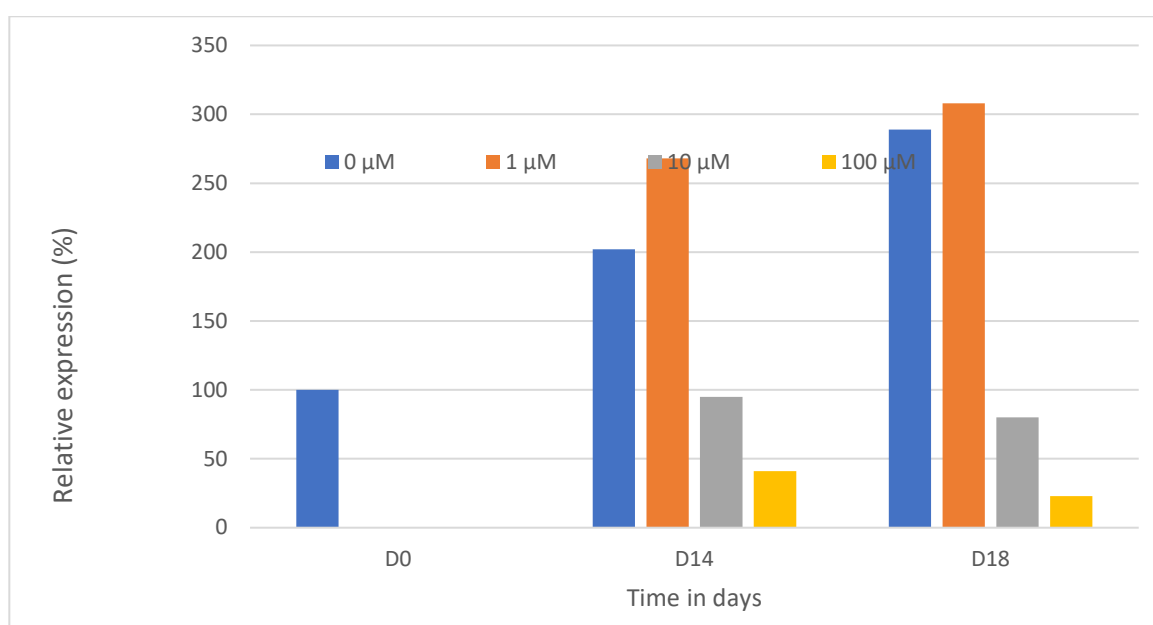
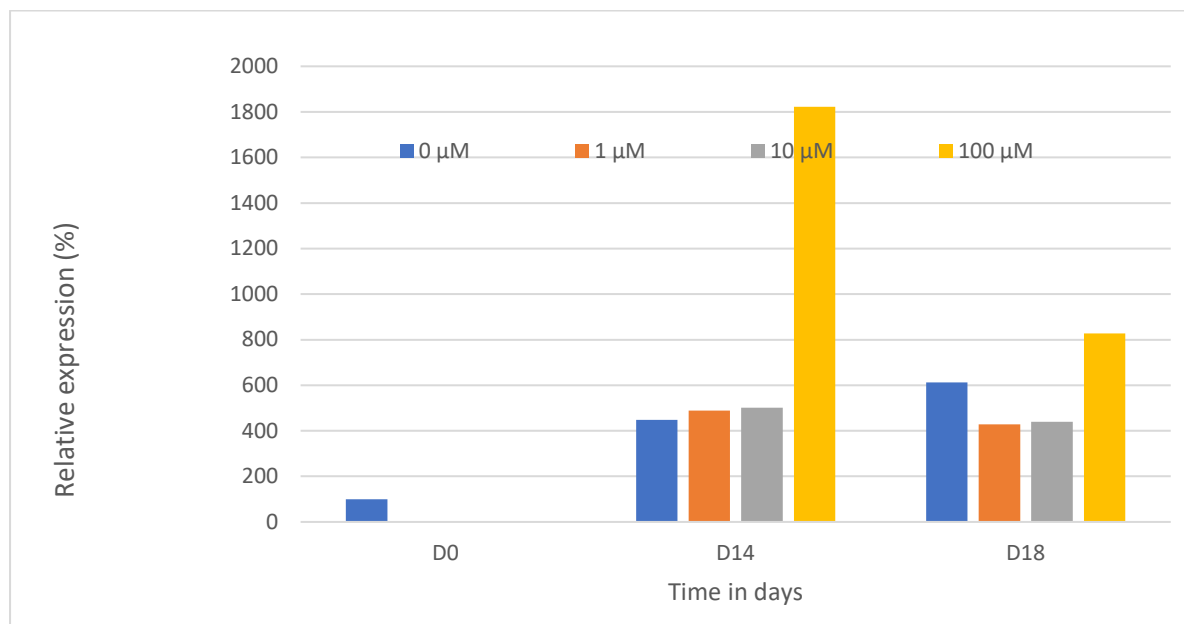


Figure 5.3.20. Effect of concentration on the relative expression of the SREBP1c protein in quercetin treated SGBS preadipocytes over 18 days of incubation. SREBP1c protein production increased with incubation time. The presence of flavonoids reduced the protein abundance in a dose and time dependant pattern for the 10 and 100 μM concentrations to levels lower than the day 0 absolute control. The 1 μM concentration however increased protein abundance by 32 and 6% for day 14 and day 18 respectively. The associated Western blots are shown below the figure.

### 5.3.5.2. C/EBP $\beta$ protein

Expression of the C/EBP $\beta$  had a marked increase in 100  $\mu$ M treated cells which rose to 18-fold levels in day 14. All other treatments were within the same range with a small increase of protein presence in day 14 on the 1 and 10  $\mu$ M treatments and a small decrease the same concentrations on day 18 relative to the daily controls.

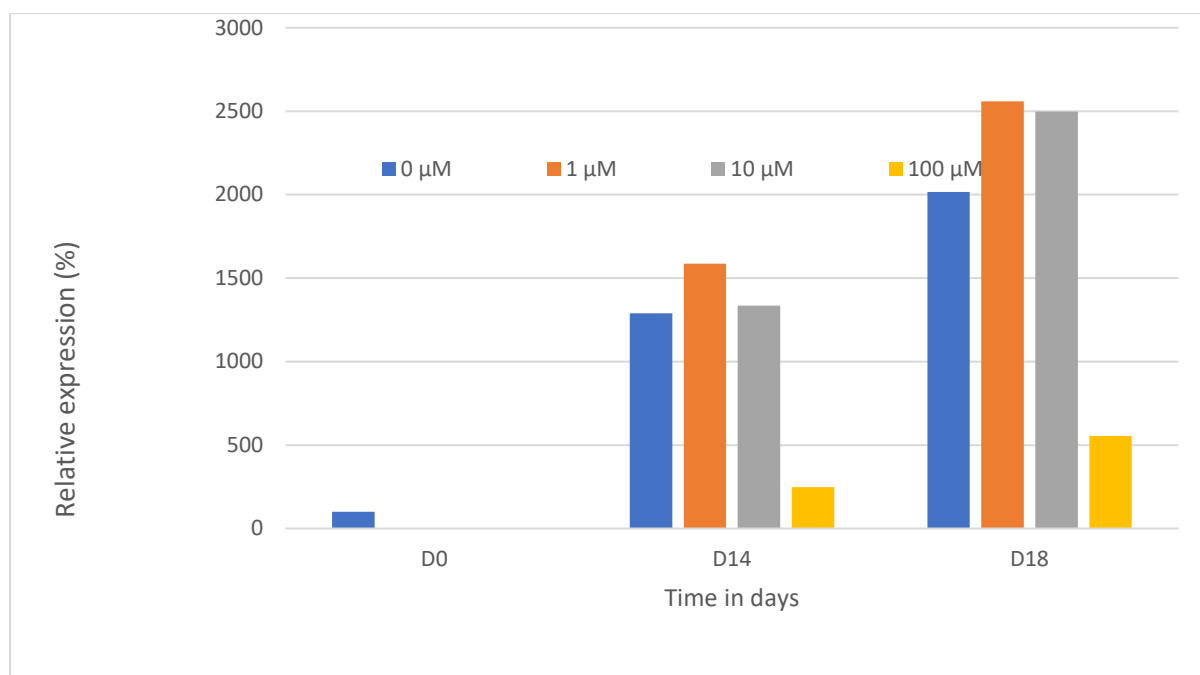


	Day 0		Day 14				Day 18			
	0 $\mu$ M	0 $\mu$ M	1 $\mu$ M	10 $\mu$ M	100 $\mu$ M	0 $\mu$ M	1 $\mu$ M	10 $\mu$ M	100 $\mu$ M	
$\beta$ -actin control	[Western blot bands for $\beta$ -actin control]									
C/EBP- $\beta$	[Western blot bands for C/EBP- $\beta$ ]									

Figure 5.3.21. Effect of concentration on the relative expression of the C/EBP $\beta$  protein in quercetin treated SGBS preadipocytes over 18 days of incubation. C/EBP $\beta$  protein production increased with incubation time to more than 6 times the initial value by day 18 in untreated cells. There was not much difference between the daily controls and the 1 and 10  $\mu$ M concentrations. The 100  $\mu$ M concentration was significantly higher, up to 18 and 8-fold for day 14 and 18 respectively. The associated Western blots are shown below the figure.

### 5.3.5.3. PPAR $\gamma$ protein

Expression of the PPAR $\gamma$  increased up to 25-fold on the untreated samples over the 3 days of incubation. Peri-physiological concentrations of the flavonoid were greater than the vehicle control on the 14<sup>th</sup> and 18<sup>th</sup> days with a greater increase on day 18. The concentration of 100  $\mu$ M whilst greater than day 0 reference point was markedly lower than the daily untreated controls.

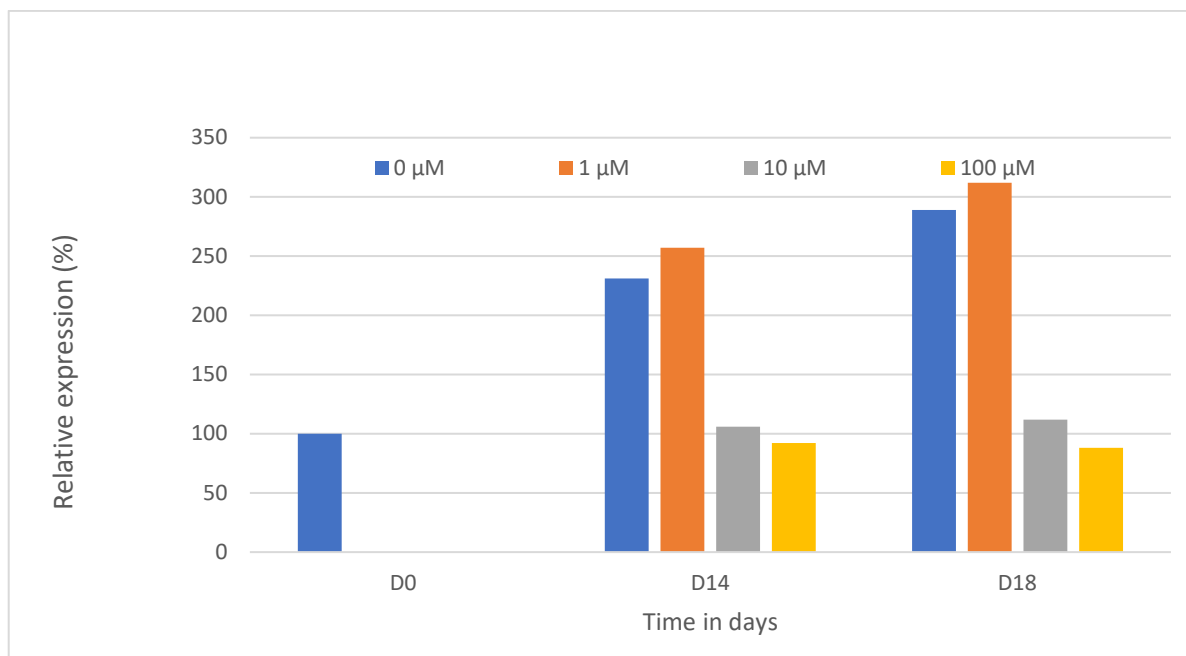


	Day 0	Day 14				Day 18			
	0 $\mu$ M	0 $\mu$ M	1 $\mu$ M	10 $\mu$ M	100 $\mu$ M	0 $\mu$ M	1 $\mu$ M	10 $\mu$ M	100 $\mu$ M
$\beta$ -actin control	[band]	[band]	[band]	[band]	[band]	[band]	[band]	[band]	[band]
PPAR $\gamma$	[band]	[band]	[band]	[band]	[band]	[band]	[band]	[band]	[band]

Figure 5.3.22. Effect of concentration on the relative expression of the PPAR $\gamma$  protein in quercetin treated SGBS preadipocytes over 18 days of incubation. PPAR $\gamma$  protein production increased with incubation time in untreated cells to greater than 12 and 20-fold for day 14 and 18 respectively. The 1  $\mu$ M concentration increased protein expression by 23 and 26% relative to the daily untreated controls for day 14 and 18 respectively. The 10  $\mu$ M whilst elevated had a lower impact than the 1  $\mu$ M. There was relative downregulation of protein expression in cells treated with 100  $\mu$ M quercetin of 80 and 72% respectively for day 14 and 18 although these values were greater than the absolute day 0 controls.

#### 5.3.5.4. UCP1 protein

Expression of the UCP1 increased on the untreated samples over the 18 days of incubation. The 1  $\mu\text{M}$  concentration had a slightly greater value than the daily controls but the 10 and 100  $\mu\text{M}$  concentrations had similar readings to the day 0 control.



	Day 0		Day 14				Day 18			
	0 $\mu\text{M}$	0 $\mu\text{M}$	1 $\mu\text{M}$	10 $\mu\text{M}$	100 $\mu\text{M}$	0 $\mu\text{M}$	1 $\mu\text{M}$	10 $\mu\text{M}$	100 $\mu\text{M}$	
$\beta$ -actin control										
UCP1										

Figure 5.3.23. Effect of concentration on the relative expression of the UCP1 protein in quercetin treated SGBS preadipocytes over 3 days of incubation. UCP1 protein production increased with incubation time to more than double the initial value by day 18 in untreated cells. The 1  $\mu\text{M}$  concentration of quercetin had a 10 and 7 % increase relative to the untreated daily control for day 14 and 18 respectively. All other concentrations were not dissimilar in protein expression to the reference control value. The associated Western blots are shown below the figure.

### 5.3.5.5. Akt and pAkt proteins

The Akt protein expression was suppressed in all treatment conditions. The suppression increased with increase in concentration. The pAkt protein presence was marginally raised in the untreated controls on day 2 and 3. The 1 and 10  $\mu\text{M}$  concentrations had higher levels of expression relative to the daily controls whereas the 100  $\mu\text{M}$  treatment produced less protein in day 14 of the experiment.

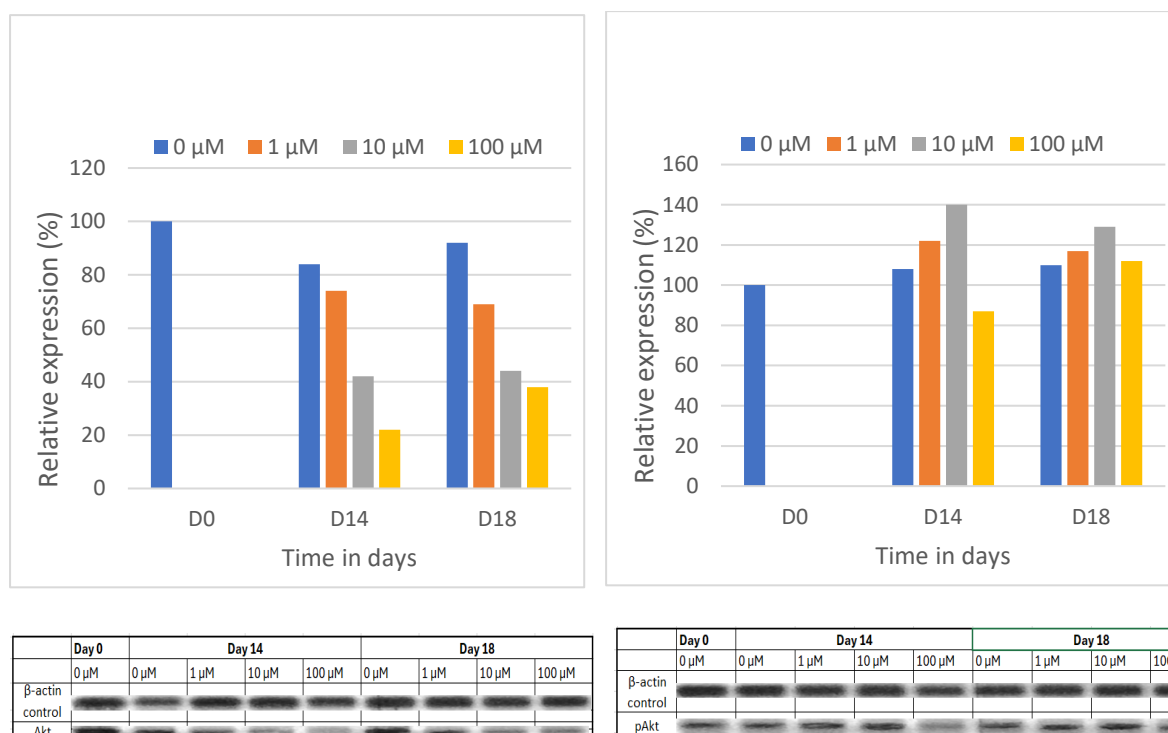
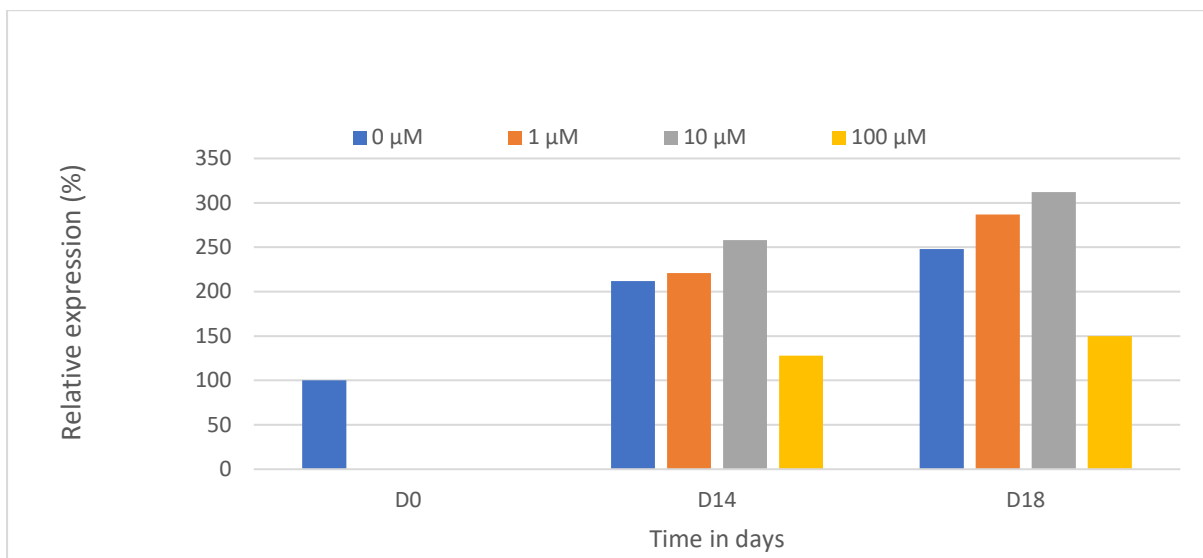


Figure 5.3.24 a and b. Effect of concentration on the relative expression of the Akt and pAkt proteins in quercetin treated SGBS preadipocytes over 18 days of incubation. The Akt protein was reduced in expression over time. The decrease was dependant on the concentration. There appears to be a recovery of expression for all treatments between day 14 and day 18 except for the 1  $\mu\text{M}$  treatment. However, this trend was minimal as it averaged below 10%. The protein, pAkt showed a general increase in expression on the daily controls. All the quercetin treatments increased the protein presence except for the 100  $\mu\text{M}$  concentration which was reduced by 20% on day 14. The increase was minimal averaging 16% with a high of 29% for the 10  $\mu\text{M}$  concentrations on day 14. The associated Western blots are shown below the figure.

### 5.3.5.6. Leptin protein

Presence of the leptin protein in the untreated samples was increased over the 2 test days relative to day 0 expression. The 1 and 10  $\mu\text{M}$  treatments showed greater protein presence in day 14 and 18 relative to the daily control. However, the 100  $\mu\text{M}$  concentration reduced leptin presence in day 14 and even more on day 18 although the values were greater than the absolute day 0 control.



	Day 0		Day 14			Day 18			
	0 $\mu\text{M}$	0 $\mu\text{M}$	1 $\mu\text{M}$	10 $\mu\text{M}$	100 $\mu\text{M}$	0 $\mu\text{M}$	1 $\mu\text{M}$	10 $\mu\text{M}$	100 $\mu\text{M}$
$\beta$ -actin control	[Western blot bands for $\beta$ -actin control]								
Leptin	[Western blot bands for Leptin]								

Figure 5.3.25. The leptin protein production increased with incubation time to 100 and 150% on days 14 and 18 respectively relative to the absolute control. The 1 and 10  $\mu\text{M}$  treatments had increased protein presence which increase with increase in concentration up to 25% more on day 18 for the 10  $\mu\text{M}$  treatment. Whilst it was greater than the day 0 absolute control levels, the 100  $\mu\text{M}$  treatments were reduced by 40% on both day 14 and day 18. The associated Western blots are shown below the figure.

### 5.3.5.7. Erk and pErk

There was an increase in protein Erk expression relative to the day 0 control with the exception of the 100  $\mu\text{M}$  treatment on day 14 which was suppressed. The 1  $\mu\text{M}$  concentration had the highest increase in protein presence for both day 14 and day 18. Both the 10 and 100  $\mu\text{M}$  concentrations increased in expression from day 14 to day 18 values. The protein pErk had a general decrease in expression for day 14 and 18 relative to the day 0 absolute control. However, the 10  $\mu\text{M}$  concentration, however had increases of above 20% for both day 14 and 18 expressions relative to day 0 absolute control.

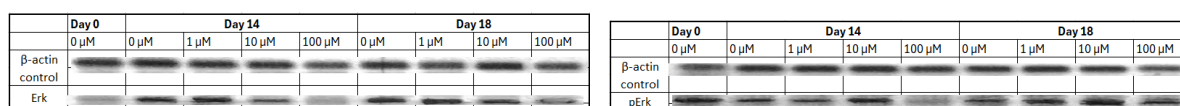
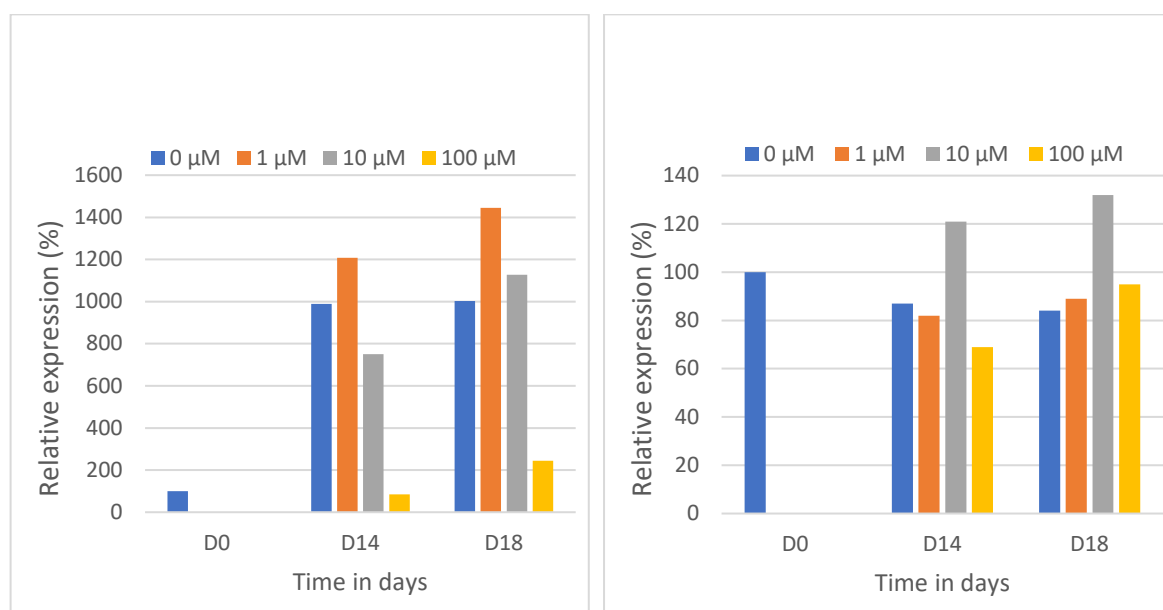


Figure 5.3.26 a and b. Effect of concentration on the relative expression of the Erk and pErk proteins in quercetin treated SGBS preadipocytes over 18 days of incubation. Erk protein increased in presence for all test conditions relative to the untreated controls except for the 100  $\mu\text{M}$  treatment which was 12% lower than the absolute control. The untreated daily controls did not vary between day 14 and 18. The treatment concentrations of 1  $\mu\text{M}$  had the greatest increase in expression of greater than 20 and 40% on day 14 and 18 respectively relative to the daily controls. The treatments of 10 and 100  $\mu\text{M}$  increased between day 14 and 18 by more than 40%. The protein pErk showed a general suppression in expression for all test conditions except for the  $\mu\text{M}$  concentrations which increased by 39 and 57% for day 14 and 18 respectively relative to the daily control. The associated Western blots are shown below the figure.



## 5.4. Discussion

### 5.4.1. Context

The aim of this chapter was to explore the effects of flavonoids on gene expression. The flavonoids quercetin and chrysin representing flavanols and flavones respectively were used to investigate genes associated with proliferation, apoptosis, differentiation, and insulin regulation pathways. Quercetin was additionally used to elucidate the signal pathways and protein expression involved in adipogenesis. The following genes were investigated; *PPAR gamma*, *adiponectin*, *GLUT4*, *UCP1*, *TPX2*, *Ki67*, *BIM*, *BAD*, *SREBP1c* and *CEBP- $\beta$*  whereas the proteins which were investigated are UCP1, PPAR gamma, SREBP1c, C/EBP beta, Erk, pErk, Akt, pErk and leptin.

### 5.4.2. Gene expression during preadipocyte proliferation

Preadipocyte growth was investigated over a period of 3 days to see whether flavonoids had any effect on genes associated with proliferation, cell death or insulin regulation pathways. The genes *Ki67* and *TPX2* were probed to assess changes in proliferation in cells treated with different concentrations of flavonoids. *BAD* and *BIM* genes were probed to identify changes in the apoptotic pathways during the growth phase of cells treated with flavonoids. Finally, the *PPAR gamma*, *adiponectin*, *GLUT4* genes which are associated with adipocyte differentiation and insulin regulation were also probed in the preadipocyte growth phase.

#### 5.4.2.1. *Ki67*

The *Ki67* gene encodes a nuclear protein linked to cellular proliferation through heterochromatin organisation (Sobecki et al., 2016). The gene codes for the nuclear protein p*Ki67* which is only produced in actively dividing cells. Proliferating cells have a relatively higher gene expression index for the *Ki67* gene compared to non-dividing cells and for this reason, *Ki67* is a recognised marker for proliferation (Li et al., 2015). There was a general reduction of up to 80% in *Ki67* gene expression on SGBS cells treated with either quercetin or chrysin over a 3-day period. The reduction seen in the expression of the *Ki67* gene in both the physiological and supra-physiological concentrations of both chrysin and quercetin treated cells show the potential that flavonoids possess the ability to reduce the rate of proliferation and ultimately viability of preadipocytes. These results concur with the viability assays carried out on the same cells in similar conditions except for peri-physiological flavonoid concentrations which appear to show increased proliferation relative to the controls. This

unexpected result appears to resonate with Sobecki et al. (2016) who showed that Ki-67 depletion caused the disruption of nucleogenesis without the inhibition of pre-rRNA processing. Therefore, in certain circumstances, proliferation can continue to take place in the presence of downregulated *Ki67* gene. It was also interesting to note that after 24 hrs, the expression of *Ki67* in cells treated with 10 and 20  $\mu\text{M}$  of both quercetin and chrysin were marginally higher than the running control. The same concentrations translated to the increased cell viability observed after 72 hours of incubation in viability assays conducted earlier. Gene expression change precedes phenotypic presentation. It can therefore be concluded that flavonoids are associated with the reduction of the viability or rate of proliferation of preadipocytes using a pathway that implicates the *Ki67* gene expression.

#### 5.4.2.2. *TPX2*

*TPX2* is a gene associated with microtubule nucleation spindle assembly which is required for normal assembly of mitotic spindles (King and Petry, 2020). Whilst this is necessary for cell division, viability and proliferation, microtubule assembly is also needed in apoptosis. Absence of change in *TPX2* expression may therefore be a result of self-cancellation of apoptotic and mitotic pathways (Viais et al., 2021). *TPX2* gene was generally suppressed in SGBS cells treated with quercetin over 3 days of culture (Figure 5.4.2a and b). There was no significant difference in *TPX2* gene expression for chrysin treated SGBS cells relative to the control. There was, however, a gradual decrease in expression of the *TPX2* gene over the 3 days for all test conditions. The trend of general downregulation of the *TPX2* gene with time in both treated and control cells suggests that as preadipocytes move towards differentiation, genes associated with proliferation diminish (Wang et al., 2018). The significant downregulation of quercetin treated cells relative to the control after 48 hours suggests that flavonoids reduce preadipocyte viability by downregulating the *TPX2* gene responsible for microtubule assembly during mitosis thus reduce proliferation or viability.

#### 5.4.2.3. Proliferation markers summary

There are many genetic markers for cell proliferation. In this study, *Ki67* and *TPX2* were investigated after treating SGBS preadipocytes with a range of concentrations of the flavonoids quercetin and chrysin. There was a general trend of transcript downregulation in treated cells suggesting that flavonoids are associated with reduction in the expression of cell proliferation markers. The most likely part of the cell cycle where *TPX2* is implicated is the

DNA synthesis (S) and cell growth 2 (G2) phases where greater microtubule activity is expected (Neumayer et al., 2014). Whereas *Ki67* is most likely implicated in the G1 and G0 phase crossover (Miller et al., 201). Whilst this is apparent, further studies are warranted to show the pathway by which these genes are involved and how flavonoids alter the pathway.

#### 5.4.2.4. *BIM* gene

The *BIM* (BCL2-interacting mediator of cell death) gene is a primary proapoptotic mediator although it has other cellular functions (O'Connor et al., 1998). It is a member of the evolutionally conserved *BCL2* gene family which is notable for regulation of apoptosis. Cells in culture grow through the distinct phases of lag, exponential (log), stationary, and death (Naciri, 2008). As the phases progress and more cells exit the cell cycle through apoptosis and other pathways (Grilo and Mantalaris, 2019), proapoptotic genes increase in expression. This view is supported by our findings which show a general increase in the *BIM* gene expression across the incubation time.

The *BIM* gene was seen to increase over the 3 days of culture (Figure 5.4.3a and b). All quercetin treatments had elevated *BIM* expression relative to the control by day 3. Chrysin treated cells had suppressed *BIM* expression over the same period of time although there was a general increase in expression when compared to the 24-hour measures. Predictably, cells treated with quercetin had a higher expression of the *BIM* gene (Figure 5.4.3a), suggesting increased proapoptotic activity. However, 10  $\mu\text{M}$  quercetin concentration would have been expected to reduce *BIM* expression to match the proliferation observed in viability assays earlier (chapter 2). The discordance between the gene expression and the phenotypic presentation could be explained by time lag, the genes expressed after 72 hours could manifest physical traits 2 or 3 days later. Furthermore, the *BIM* gene is not the only gene that trigger apoptosis; the process is complex and involves many genes acting at the same time. Examples of other genes feeding into the apoptotic cascade are caspases, other BCL2 family and tumor necrosis factor (TNF) receptor genes, and the p53 gene (Kiraz et al., 2016).

In our study, cells treated with chrysin at 100  $\mu\text{M}$  were excluded from the data because the concentration was found to be toxic for the reference gene. The relative *BIM* expression for the remaining concentrations was lower than those of the control which supports the previously described viability experiments which showed MTT, and cell counts at these

concentrations higher than the control (Figure 5.4.3b). It can therefore be concluded that flavonoids reduce the viability of preadipocytes at supra physiological concentrations by upregulating the *BIM* gene. However, at physiological concentrations flavonoids encourage cell proliferation by downregulating the *BIM* gene. Whilst there is a scarcity of literature involving preadipocytes and a range of chrysin concentrations, parallels can be drawn from work on breast cancer. Dalasanur-Nagaprashantha et al. (2018) for example, showed that chrysin and naringin increased apoptotic activity at super-physiological concentrations.

#### 5.4.2.5. *BAD* Gene

The *BAD* gene is another member of the BCL2 family known to be a regulator of programmed cell death. The gene codes for a protein which mediates apoptosis by forming heterodimers with BCLxL (B-cell lymphoma-extra-large) and BCL2. This dimerization negates the anti-apoptotic activity of BCLxL and BCL-2. As shown with the *BIM* gene, it is expected that as preadipocytes move along the growth curve, apoptotic activity increases and therefore genes associated with apoptosis will have a higher level of expression. In our study (Figure 4.4.3a and b), the *BAD* gene was elevated in expression over the 72 hours of incubation for the controls. Concentrations of 10  $\mu$ M quercetin and 20  $\mu$ M chrysin had a higher level of expression when compared to the controls after 72 hours, all other concentrations had suppressed gene expression levels relative to the daily controls. It is interesting that concentrations of 10  $\mu$ M quercetin and 20  $\mu$ M chrysin showed notable increase in the expression of *BAD*; these were the same concentrations seen to increase proliferation relative to untreated controls. Microscopic views of wells treated with similar peri-physiological concentrations of these flavonoids showed greater than 80% confluence. Confluency leads to contact inhibition and apoptotic pathways, and therefore the increased expression of *BAD* at these concentrations is expected (Brezden and Rauth, 1996). However, higher flavonoid concentrations lead to sparse growth and therefore lower apoptosis. Hence, the downregulated expression of the *BAD* gene after 72 hours. It is known that all genes associated with proliferation are not linear and simplistic, they form a complex matrix of action to regulate apoptosis. For example, the genes ERK1/2, AKT, PKA, and PKC induce cell survival by phosphorylating *BAD* (Sastry et al., 2020).

#### 5.4.2.6. Apoptotic markers summary

The *BAD* and *BIM* genes were chosen as they are frequently used markers of cell death through apoptosis amongst many others. The choice was informed by literature on SGBS cells (Wabitsch et al., 2001; Melzner et al., 2002; Fischer-Posovszky et al., 2008). There was a general pattern of increased apoptotic gene expressions with increased flavonoid concentrations. However, there were many results which were different from expectations, and this was accounted for by either the hormetic effect of physiological concentrations of flavonoids, the nonlinear and complex function of genes and the magnitude of confluency of cells growing in wells. Both genes, most likely reduce cell proliferation by delaying the G0/G1 to S phase cell cycle phase transition (Du et al., 2017). Further work is needed to identify the transcriptional factors that help map the pathway by which flavonoids induce apoptosis

#### 5.4.2.7. *Adiponectin* gene

The *adiponectin* gene is exclusively expressed in adipose tissue, it is associated with cellular metabolic and hormonal processes. It is especially involved in energy homeostasis and in lipid and glucose metabolism (Liu et al., 2003). The *adiponectin* protein promotes preadipocyte differentiation into committed adipocytes via the *PPAR gamma* pathway (Yang et al., 2018) and preadipocytes scarcely express the *adiponectin* gene. The *adiponectin* gene showed a non-significant ( $p>0.05$ ) increase in expression for the control and the flavonoid treated cells during the first three days of preadipocyte incubation (Figure 4.4.5a and b). Quercetin treated cells had the highest increase of up to 4-fold at 20  $\mu$ M. There was no significant difference in gene expression ( $p>0.05$ ) for chrysin treated cells after 72 hours although after 48 hours, the 20  $\mu$ M concentration had a significant increase of 300% ( $p<0.05$ ). Within the first 72 hours of culture, the wells contain precursor cells of adipocytes (preadipocytes) so there is little change in *adiponectin* gene expression until the induction of differentiation which is not spontaneous in culture. The insignificant increase of the gene as shown in the results support this notion. While transient surges in RT-qPCR are often experimental artefacts, the sustained trend of upregulation seen in quercetin treatments may indicate the potential merits of flavonoids in modifying lipid and glucose metabolism (Jung et al., 2006).

#### 5.4.2.8. *GLUT4*

The *GLUT4* gene, a member of the solute carrier family, encodes a protein that functions as an insulin-regulated facilitative glucose transporter (Holman, 2020). It is expressed in adipose

tissue and in cardiac and skeletal muscles (Yokomori et al., 1999). Like the *adiponectin* gene, the *GLUT4* gene showed little change in expression during the first three days of preadipocyte incubation. However, there was a general upward trend of up to 300% increase in gene expression during this time (Figure 5.4.6a and b). After 72 hours, quercetin treated cells appear to have a slight increase (50%) in *GLUT4* expression relative to the control whereas chrysin showed a reduction of up to 100%. Although the percentage differences were large, these patterns were not statistically significant ( $p > 0.05$ ). Yokomori et al. (1999) showed that the *GLUT4* gene in 3T3-L1 cells is marginally expressed in preadipocytes and is significantly elevated during differentiation. During incubation, preadipocytes gradually move towards the differentiation initiation stage and therefore *GLUT4* is expected to rise in expression. Preadipocytes in culture do not readily differentiate without a special induction media, therefore any gene expression increase, if any, will be minimal. This can explain the observed small increase of expression with time. All quercetin treatments had a marginal relative increase in expression. The same was observed on chrysin treated cells after 48 hours. From these findings, flavonoids can be loosely associated with the potential of increased glucose transportation in preadipocytes. If this is confirmed, this can translate to better health outcomes seeing that efficient glucose transportation is needed to reduce incidence of diabetes and other metabolic syndrome disorders.

#### 5.4.2.9. *PPAR gamma* gene

The *PPAR gamma* (peroxisome proliferator activated receptor gamma) gene encodes a protein which regulates fatty acid metabolism and can induce adipocyte differentiation (Chawla et al., 1994). The protein *PPAR gamma* is a necessary component for differentiation and one of the key ingredients of differentiation initiation media. The *PPAR $\gamma$*  gene did not show much change in expression during the first three days of preadipocyte incubation. Gene expression marginally increased during the incubation time for all flavonoid treatments. The expression patterns were similar to those of the *adiponectin* and *GLUT4* genes which are associated with differentiation. Chawla et al. (1994) demonstrated that 3T3-L1 preadipocytes express very low levels of the gene. It is however significantly upregulated upon the induction of differentiation. Chrysin treatments of 10  $\mu$ M and 20  $\mu$ M treatments of quercetin at 72 hours showed relatively lower gene expression. Interestingly, the same treatments had significantly reduced differentiation ratios as shown in microscopic differentiation assays

(chapter 3). This may imply that flavonoids can reduce the potential of preadipocytes to differentiate to committed adipocytes.

#### 5.4.2.10. Differentiation markers summary

*GLUT4*, *PPAR gamma* and *adiponectin* genes were investigated on preadipocytes, all three genes appear to have no significant difference in expression ( $p > 0.05$ ) over the 3 days of incubation. However, there was a general pattern of increased expression of the genes in cells treated with quercetin but not those treated in chrysin. This observation is important in that, these genes are not only associated with differentiation of adipocytes, but they are also implicated in insulin sensitivity, glucose uptake and energy homeostasis. Further work is needed to map out the pathways in which these flavonoids achieve their functions.

#### 5.4.2.11. *SREBF1* gene

*SREBP1c* (Sterol regulatory element-binding transcription factor 1 also known as sterol regulatory element-binding protein 1) is a protein that is encoded by the *SREBF1* gene (Kobayashi et al., 2018). The encoded protein mediates insulin-induced fatty acid synthesis, lipogenesis and mediates a pivotal role in adipogenesis including the induction of *PPAR gamma* (Payne et al., 2009). Having seen the behaviour of the three genes associated with differentiation on quercetin treated adipocytes, it was deemed necessary to probe whether *SREBP1c* was involved in the pathway. The *SREBP1c* gene was tested using a larger range of quercetin concentrations in SGBS preadipocytes treated with quercetin after 24 hours. Expressions were shown relative to day 0 samples. *SREBP1c* had a 9-fold increase on the untreated cells after 24 hours, however, all other treatments had a reduced gene expression of at least 50% relative to the 24-hour control although each treated sample had at least a 2-fold increase relative to the absolute day 0 control. Downregulated *SREBP1c* expression translates to lower levels of *PPAR gamma* expression and/or utilisation and ultimately reduced differentiation of preadipocytes. This mirrors the differentiation assay result observed earlier (chapter 3). These findings concur with Eberlé et al. (2004) who found a significant reduction in the expressions of *SREBP1c* gene in cells treated with a naphthoquinone compound which is a flavonoid homologue. It is also important to note that *SREBP1c* is expressed a lot earlier in the maturation of adipocytes and the presence of the translated protein will affect differentiation genes downstream (Fajas et al., 1999). As a result,

the reduction of abundance of differentiation associated genes will be seen much later in differentiation.

#### 5.4.3. Adipocyte differentiation

Whilst it is intuitive to investigate the behaviour of differentiation associated genes during the differentiation stage of SGBS cells that have been treated with a range of flavonoid concentrations, it was also deemed necessary to investigate the behaviour of proliferation genes and genes that are known to code for transcription factors associated to both differentiation and proliferation. To that effect, the following genes were probed using the qPCR technique; *PPAR gamma*, *adiponectin*, *GLUT4*, *SREBP1c*, *UCP1*, *TPX2*, *Ki67*, *BIM*, *BAD* and *CEBP-beta* for a range of concentrations of quercetin and a selection of chrysin samples.

##### 5.4.3.1. *PPAR gamma*

*PPAR gamma* gene encodes a protein which regulate fatty acid metabolism as well as inducing adipocyte differentiation (Chawla et al., 1994). Differentiation is primarily regulated by two main genes, *CEBP-alpha* and *PPAR gamma* alongside many other transcription factors (Madsen et al., 2014). However, of the 2 parallel genes, *PPAR gamma* has the limiting factor, that is, differentiation is possible with *PPAR gamma* and without *CEBP-alpha* but *CEBP-alpha* alone will not complete differentiation without *PPAR gamma* (Rosen et al., 2002). Within the constraints of resources, a decision was therefore made to investigate *PPAR gamma*. In our study, *PPAR gamma* transcript increased in expression gradually (up to 300% for chrysin and 125% for quercetin) in untreated cell controls for both quercetin and chrysin over the incubation period to peak at day 14 before the gradient of increase declined. This pattern of gene expression where an increase is followed by a reduction towards 100% differentiation rate has also been noted by Sue et al. (2021), Fischer-Posovszky (2008) and Wabitsch (2001). Chawla et al. (2008) went on to show that *PPAR gamma* is expressed at high levels in adipose tissue in contrast to a variety of other tissues or to pre adipocytes. Interestingly, *PPAR gamma* protein is needed to induce adipose differentiation, and, in the process, the adipose tissue expresses more *PPAR gamma* mRNA in a typical positive feedback loop (Wafer et al., 2017). There was a slight depression in expression of the transcript from day 4 to day 7 on the control samples before the general increase for both flavonoids. This is expected because the treatment on day 0 included a *PPAR gamma* agonist as part of the differentiation cocktail. Through positive feedback and autocrine cellular communication, the *PPAR gamma* agonist



in the media primes the gene expression cascade. On day 4, the media was changed to a mix which did not contain *PPAR gamma* agonist and therefore the positive feedback was disrupted and any increase that was observed thereafter was a result of increased differentiation. The expression of *PPAR gamma* transcript is insulin dependent (Rieusset, 1999). In culture, insulin is added to the differentiation media. In these experiments, the last media change was made on day 4, thereafter, the cells thrive on existing media. The insulin therefore gets expended and hence the decline in *PPAR gamma* transcript expression.

*PPAR gamma* transcript expression was significantly elevated ( $p < 0.05$ ) in expression to greater than 100% for cells treated with peri-physiological concentrations of quercetin across the time range until day 14. There was no significant difference ( $p > 0.05$ ) in expression on day 18. However, this was not evident in chrysin where gene expression was suppressed relative to the control ( $p < 0.05$ ) for all treatments by day 14 of incubation. Concentrations of 20  $\mu\text{M}$  and 100  $\mu\text{M}$  were significantly elevated ( $p < 0.05$ ) on day 4 and 7 respectively for chrysin treated cells after which all concentrations were significantly downregulated. The findings are supported by Swick (2011) who observed that quercetin, at high concentrations, inhibits adipogenesis. They concluded that quercetin reduces preadipocyte differentiation through the regulation of early cell cycle events. The same can be extrapolated to chrysin which was seen to significantly reduce gene expression ( $p < 0.05$ ) for all concentrations by day 18. Swick (2011) focused their work on L3T3-L1 cell lines. There is a scarcity of literature on flavonoids on SGBS cells to the same extent. Feng et al. (2016) produced results that support the findings of increased expression of *PPAR gamma* on 3T3-L1 cells treated with the flavonoid apigenin. They demonstrated that apigenin acted as a modulator by binding and activating *PPAR gamma*. They went on to conclude that activation of *PPAR gamma* by the flavonoid blocks the transcription factor p65, one of the five components that form the NF- $\kappa\text{B}$  (nuclear factor kappa-light-chain-enhancer of activated B cells) translocation into nuclei. This is achieved by the inhibition of p65/*PPAR gamma* complex translocation into nuclei a move that reduces NF- $\kappa\text{B}$  activation a prerequisite in macrophage polarisation. Here again, the positive feedback loop is seen to be involved.

The role of *PPAR gamma* in adipogenesis is therefore complex, the impact of flavonoids in the process is dependent on the flavonoid type, duration of exposure and the concentration. Chrysin in this instance appears to be associated with small decrease of *PPAR gamma*

transcript expression on all concentrations tested (treatments had higher transcript presence relative to the control although the difference was insignificant at  $p>0.05$ ) after 7 days or when experimental cells reached 50% differentiation as shown in relative differentiation experiments. Quercetin on the other hand behaved this way only on high concentrations. According to Swick (2011), physiological concentrations appear to be associated with reduction of inflammation whereas higher concentrations have an association with reduction in the rate of differentiation.

#### 5.4.3.2. *Adiponectin*

The *adiponectin* gene which is associated with cellular metabolic and hormonal processes is highly expressed in adipose tissue. The gene transcript is responsible for energy homeostasis and lipid and glucose metabolism (Liu et al., 2003). Like *PPAR gamma*, *adiponectin* is a marker for differentiation. It is involved in autocrine regulation of insulin sensitivity and modulation of both glucose and lipid metabolism (Fu et al., 2005). For this reason, *adiponectin* was investigated to see whether flavonoids affect its expression in reducing adipogenesis. Figure 5.4.11a of our study results show that peri-physiological concentrations of quercetin significantly increased gene expression up to 20-fold for the 20  $\mu\text{M}$  concentration ( $p<0.05$ ) over the incubation time except for day 4 and day 14. Chrysin treatment with concentrations of 10  $\mu\text{M}$  and 20  $\mu\text{M}$  significantly elevated transcript expression up to 20-fold on day 18 ( $p<0.05$ ) over the incubation time except for day 1 and 14. Untreated controls increased transcript expression significantly after the 18 days of incubation up to 10-fold compared to the seeding control cells. For both flavonoids, all concentrations, except 100  $\mu\text{M}$  of chrysin, caused significant (up to a 100-fold) increase in *adiponectin* transcript expression. Chrysin concentrations of 100  $\mu\text{M}$  were seen to be toxic in earlier proliferation and differentiation experiments (chapters 3 and 4). It is paradoxical however, that the flavonoid concentrations that caused an increase in *adiponectin* transcript, a gene that correlates positively with differentiation, did not actually cause increased differentiation as seen of differentiation assays (chapter 4). Fu et al. (2005) observed that cells with overexpressed *adiponectin* differentiated into mature adipocytes more rapidly in the abundance of other transcriptional factors such as *C/EBP $\alpha$* , *SREBP1c*, adipocyte lipid binding protein (ALBP/aP2) and *PPAR gamma coactivator-1 $\alpha$*  (*PGC-1 $\alpha$* ). Therefore, there are other limiting factors that stop increases in *adiponectin* expression translating into higher levels of differentiation. This

observation highlights the limitations of *in vitro* studies as whole organism experiments would benefit from overall homeostasis feedback loops.

#### 5.4.3.3. *GLUT4*

Results from *adiponectin* and *PPAR gamma* experiments appear to suggest activity of other genes and proteins such as insulin. For that reason, gene transcripts such as *GLUT4* generates interest. This is because *GLUT4* gene, encodes a protein that functions as an insulin-regulated facilitative glucose transporter (Holman, 2020). It is expressed predominantly in adipose tissue but can also be seen in cardiac and skeletal muscles (Yokomori et al., 1999). Cells treated with 10 and 20  $\mu$ M concentrations of quercetin significantly increased *GLUT4* transcript expression by up to 8-fold ( $p < 0.05$ ) throughout the incubation time compared to untreated cells. All concentrations were significantly upregulated ( $p < 0.05$ ) by day 14 for chrysin and day 18 for quercetin. There was no significant change in transcript expression for the untreated controls across the incubation time ( $p > 0.05$ ). Increase in *GLUT4* expression is positively correlated with increase in differentiation (Weems and Olson, 2011), this was not so for cells treated with all concentrations of the test flavonoids because earlier experiments (chapter 4) show the opposite, the increase in *GLUT4* expression did not reflect the reduction in differentiation of cells treated with flavonoids which was observed in earlier experiments. The apparent increase in transcript expression in the first 4 days is likely to be a result of Rosiglitazone which was part of the media components added on day 0. Rosiglitazone increases cell surface *GLUT4* levels by increasing endosomal recycling (Martinez et al., 2010). *GLUT4*, being an insulin-regulated glucose transporter abundant in adipose tissues, is associated with glucose homeostasis and the removal of glucose from circulation (Huang and Czech, 2007; Shepherd and Kahn, 1999). Another pertinent observation related to proliferation and differentiation results (chapter 2 and 4) is that whilst flavonoid treated cells show reduced proliferation and differentiation rates, they appear to recover when incubated for a longer time. The increased *GLUT4* transcript expression can possibly be the driver for recovery mode of the treated cells. Increase in *GLUT4* transcript seen at the end of incubation can also be associated with the possibility of efficient glucose transportation and insulin sensitivity. This assertion would need further experimental validation.

On the parallel experiment where SGBS cells were treated with quercetin during the course of differentiation and not at the inception of differentiation, time points of 0, 14 and 18 days

were investigated for concentrations of 0, 1, 10 and 100  $\mu\text{M}$ . *GLUT4* transcript expression increased over time even on the untreated cells as more cells reverted from preadipocytes to differentiated adipocytes. Cells treated with 1  $\mu\text{M}$  concentrations of quercetin significantly increased gene expression ( $p < 0.05$ ) for day 14 and 18. The relative downregulation of the gene in cells treated with 100  $\mu\text{M}$  appear to wane away over time. The increase in expression observed on the 1  $\mu\text{M}$  treated cells mirrored the differentiation results observed in chapter 4. There is a scarcity of literature which show the impact of treating cells part way through the differentiation of adipocytes, however, work by Nakao et al. (2016) bear similarities to the current study. They show that cells treated with the flavonoid Baicalein at the early stages of adipogenesis (0-2 days) showed a reduction in *GLUT4* expression. Their work however focused on 6-day adipogenesis studies and so do not show what would have happened after 18 days. They attributed the decrease of the intracellular lipid accumulation of 3T3-L1 cells by down-regulation of glucose uptake via repression of Akt-C/EBP $\alpha$ -*GLUT4* signalling in the very early stage of adipogenesis, as early as the first hour of incubation. *GLUT4* expression is dependent on insulin. Since insulin is part of the media composition, and that the last media change was done on day 4, subsequent days may suffer from insulin depletion, and this could affect the results.

#### 5.4.3.4. *SREBP1c*

*SREBP1c* is a known transcription factor which is initially assembled in the membranes of the endoplasmic reticulum and has to undergo post-translational modification through phosphorylation to achieve its role as a functional transcription factor (Ferre and Fofelle, 2007). The post-translational modification is tightly regulated by insulin (Ducluzeau et al., 2001). *SREBP1c*, a gene that promotes efficient energy metabolism, is responsible for the expression of many other genes associated with glucose and lipid control. *SREBP1c* is also known for early adipocyte differentiation initiation through the induction of the expression of *PPAR gamma* whilst facilitating fatty acid accumulation and metabolism (Khalilpourfarshbafi et al., 2018). SGBS cells were treated with 0, 1, 10 and 100  $\mu\text{M}$  of quercetin on day 4 of differentiation which was tested for the expression of the *SREBP1c* transcript on days 14 and 18. Most treatments had a significant increase of expression compared to day 0 control which was greater than 2 fold (Figure 5.4.13) with exceptions of 100  $\mu\text{M}$  which had no significant difference; treatments of 1 and 10  $\mu\text{M}$  were significantly

elevated ( $p < 0.05$ ) relative to their vehicle controls up to 8-fold increase for 1  $\mu\text{M}$  on day 18 for 10  $\mu\text{M}$ . Physiological concentrations of quercetin showed increase in the expression of *SREBP1c* transcript in the same manner as the same concentrations were seen to increase proliferation (chapter 3) but not as seen in differentiation experiments (chapter 4). High concentrations of quercetin had reduced transcript levels which mirrored proliferation and differentiation outcomes. Ha et al. (2016) aptly confirms these results in that they demonstrate that reduction in differentiation by a flavonoid mimetic,  $\beta$ -hydroxyisovalerylshikonin, is affected post translationally. Whilst an increase in *SREBP1c* may be apparent, it is the phosphorylation thereof that determines its downstream action on other genes associated with differentiation. They went on to demonstrate that  $\beta$ -hydroxyisovalerylshikonin causes phosphorylation of *SREBP1c* which in turn reduces the expression of triglyceride synthesis enzymes, acetyl-CoA carboxylase (ACC)1, fatty acid synthase (FAS) and stearoyl-CoA desaturase (SCD)1 and thereby reducing intracellular triglyceride accumulation. Therefore, it can be argued that the reduction of differentiation by high concentrations of quercetin is correlated to *SREBP1c* expression whereas physiological concentrations may affect the posttranslational form of *SREBP1c* and not its precursor form.

#### 5.4.3.5. *UCP1*

Uncoupling protein 1 (*UCP1*) or thermogenic, is one of many mitochondrial inner membrane proteins that act as proton channels. *UCP1* is unique in that it is devoted to adaptive thermogenesis which is a specialised function performed by brown adipocytes. Other *UCPs* are responsible for the pumping of protons from the mitochondrial intermembrane space to the mitochondrial matrix and in the process of produce ATP using the reduced form of the coenzyme nicotinamide adenine dinucleotide (NADH). With *UCP1* however, the crossing of the proton results in heat generation and therefore it is a regulator of thermogenesis.

In this study *UCP1* transcript was probed to see the effect of flavonoids on thermogenic activity which has a direct correlation to the browning of adipocytes. The brown phenotype in adipocytes has a higher level of *UCP1* expression. *UCP1* expression increased with time on the untreated controls. Treatments of 10 and 100  $\mu\text{M}$  were significantly downregulated by greater than 50% relative to both the reference and vehicle controls ( $p < 0.05$ ) over the test times (Figure 5.4.15). The 1  $\mu\text{M}$  treatment however showed significant upregulation ( $p < 0.05$ ) over the 18 days relative to the controls.

It is known that *UCP1* expression increases with differentiation (Carey et al., 2014), in fact, many studies show that white preadipocytes barely express *UCP1* (Wabitch et al., 2001; Tews et al., 2019) but the expression increases significantly by day 14 of cells treated with differentiation media (Yeo et al., 2017). Expression of *UCP1* in SGBS cells was correlated to the rate of differentiation or accumulation of lipid droplets and not duration of differentiation (Fischer-Posovszky., 2008). Results from the current study confirm these findings in that, concentrations of quercetin which cause a reduction in triglyceride accumulation (10 and 100  $\mu$ M) translated to reduced *UCP1* transcript expression. Interestingly, 1  $\mu$ M concentration significantly ( $p < 0.05$ ) increased expression by at least 10%. This increase in expression by low flavonoid concentrations could be the result of either increase in the quantity of mitochondria per cell, a feature in browning of adipocytes or by increased activity and size of the mitochondria. The same trend was observed in work by Arias et al. (2017) who found an increase in *UCP1* expression and the browning in rats fed with quercetin and resveratrol rich food. It is also interesting to note that their findings showed no increase in weight for rats fed with the flavonoid diet yet the *UCP1* transcript was significantly increased. The current findings concur with these in vivo studies in that, concentrations of quercetin known to show no significant increase in differentiation were seen to increase *UCP1* transcript expression. Zhang et al. (2019) in their review, concluded that flavonoids increased *UCP1* expression, increased the conversion of white adipose tissue to their brown phenotype and reduced the risk of metabolic function disorders which include obesity. In explaining the pathway in which flavonoids increase *UCP1* expression, Zhang et al. (2019) showed that AMPK-PGC-1 $\alpha$ /Sirt1 and PPAR signalling pathways were involved. Other authors observed similar outcomes using different flavonoids and animal models. Kamiya et al. (2019) described an increase in *UCP1* in brown adipose tissue in mice which were fed with Puerariae flower extract isoflavone and they concluded that the isoflavone increased *UCP1* and browning through the Cyclic-AMP and the Cyclic adenosine monophosphate Response Element Binding protein (CREB) pathways. Similarly, Takahashi and Ide (2008) found an increase in *UCP1* in rats fed with the isoflavone from soya which was directly linked to increase in *PPAR gamma* expression increase. In spite of the many existing studies on mice and animal cell lines, there is so far, a scarcity in work that looked at flavanols on human adipocytes as covered in this study.

#### 5.4.3.6. C/EBP beta

The transcript C/EBP beta was investigated in cells treated with flavonoids because of the known association with *PPAR gamma* (Lefterova et al., 2008), *adiponectin* (Park et al., 2004) and *GLUT4* (Wu et al., 1998) which were already seen to be affected by quercetin treatment. C/EBP beta is a member of the transcription factor family associated with the regulation of cellular proliferation and differentiation. Furthermore, most genes responsible for adipocyte differentiation in many cases employ a pathway which involve C/EBP proteins of which C/EBP beta is one.

In this study, C/EBP beta expression increased significantly with time on the untreated controls ( $p < 0.05$ ). This sustained increase during differentiation is similar to that observed by Yeh et al. (1995) who showed a correlation in C/EBP beta presence to the ability and the rate of differentiation. Treatments of 1 and 10  $\mu\text{M}$  were significantly downregulated by over 50% relative to the vehicle controls ( $p < 0.05$ ) on day 18. Reduction of *C/EBP beta* after treatment by flavonoids is consistent with other work, for example, similar studies such as work by (Khalilpourfarshbafi et al., 2019) showed suppression of key adipogenic transcription factors that include *C/EBP beta*. They concluded that flavonoids were linked to the activation of AMPK and Wnt pathways which are upstream of *C/EBP beta* transcript expression. They further postulated that the reduction of *C/EBP beta* expression resulted in inhibition of clonal cell expansion, and cell-cycle arrest features that reduce proliferation and encourage differentiation. Nerlov (2007) confirmed these findings and further showed that *C/EBP beta* is a downstream function of the Ras and MAPK pathways. They also showed that cyclinD1 alleviated the repressor activity of *C/EBP beta*.

Figure 5.4.16. shows the 100  $\mu\text{M}$  quercetin treatment producing significant upregulation ( $p < 0.05$ ) over the 18 days relative to the controls with a fold difference of 22 and 3 for day 14 and 18 respectively. Whilst this phenomenon has not been recorded elsewhere, it is important to mention that the majority of cells treated with high concentrations of quercetin die but a small fraction remains dormant and then start to recover exponentially within the first seven days. Since C/EBP beta is a member of transcription factor family associated with the regulation of cellular proliferation (Tolomeo and Grimaudo, 2020), the upregulation could be indicative of the rapid recovery of the cells that have survived the cytotoxic effects of high concentrations of quercetin.

#### 5.4.4. Protein analysis

While gene transcript level analysis provides valuable data for cellular activity in cells treated with test substances, protein analysis is equally valuable because proteins are more direct mediators of cellular processes (Powers and Palecek, 2012). Besides the classic transcription translation processes for protein synthesis, there are some post translational modifications that proteins undergo which dictate the ultimate action of the protein in the cellular process. Some proteins exist transiently in the cell, but some continue to bioaccumulate, and their impact is dependent on the level of abundance. Gene transcripts seen to be impacted by flavonoids were investigated for subsequent protein quantities. Other proteins which were predicted to belong to the pathway in which the flavonoids exert their effect were also probed. The following proteins were blotted and quantified: Erk, pErk, Akt, pAkt, Leptin, UCP1, PPAR gamma, SREBP1c and C/EBP beta, they were drawn from proliferation and differentiation experiments.

##### 5.4.4.1. C/EBP beta during proliferation

It has been stated that C/EBP beta is a member of a transcription factor family associated with the regulation of cellular proliferation and an upstream driver for the expression of several genes that promote cell proliferation. The resultant protein contains a basic leucine zipper (bZIP) domain which is also found in many DNA binding eukaryotic proteins. Its function is to mediate sequence specific DNA binding properties by employing the leucine zipper to hold together (dimerise) two DNA binding regions (Ellenberger, 1994) giving it its transcription factor property.

In this study, C/EBP beta protein production increased with incubation time to more than double the initial value by day 3 in untreated cells. This observation is supported by Nerlov (2007) who indicated that expression of C/EBP beta increases when preadipocytes approach differentiation. In this study, preadipocytes were cultured for 4 days before induction of differentiation when they were deemed confluent enough for contact inhibition to start the gene cascade that change cell populations from proliferating to differentiation. The steady rise in expression of C/EBP beta towards the differentiation start can be expected and is supported by literature. Guo and Tang (2015) made the same argument but further instigate that C/EBP beta has to undergo post-translational modifications which makes it suitable for its role as a transcription factor. C/EBP beta, according to Guo and Tang (2015), activates the



expression of *PPAR gamma* and *C/EBP alpha* by directly binding to their promoters in the process of adipocyte differentiation. They further show that *C/EBP beta* for differentiation is expressed earlier than *PPAR gamma* and *C/EBP alpha* are expressed which is necessary because *PPAR gamma* and *C/EBP alpha* are both anti-mitotic, and their premature expression would otherwise prevent the cells from re-entering the cell cycle through mitotic clonal expansion (MCE), a prerequisite to adipocyte differentiation (Yeh et al., 1995). This accounts for the observed early expression of *C/EBP beta* for cells that were later seen to have a higher differentiation ratio.

The presence of higher concentrations of flavonoids on the other hand reduced the protein abundance in a dose and time dependant pattern. If abundance of *C/EBP beta* translate to a greater level of differentiation, then flavonoid treated cells would less readily start to differentiate compared to untreated cells (Rupasinghe, 2020). In line with this, it has been shown that quercetin binds to *C/EBP beta* in cells and represses the transcriptional activity of *C/EBP beta* and thereby reduce both proliferation and differentiation (Shimizu et al., 2015). This was confirmed by previous differentiation experiments in this study. The 1  $\mu$ M concentration, whilst higher than the day 0 reference control, closely lagged the untreated vehicle control, there was no significant difference in reduction between the 1  $\mu$ M quercetin concentration and the vehicle control. It can be concluded therefore that at very low concentrations, the flavonoid quercetin has no significant impact on *C/EBP beta* expression on cells in the first three days of growth.

#### 5.4.5. SREBP1c during proliferation

Like *C/EBP beta*, sterol-regulatory-element-binding protein 1c (SREBP1c) is another transcription factor associated with adipogenesis and other biological processes. Having found that *PPAR gamma*, *Adiponectin* and *GLUT4* were implicated in the flavonoid treated SGBS cells proliferation and differentiation processes, it was necessary to probe the proteins that are known to be transcription factors to elucidate the pathway with which the flavonoids affect adipocyte proliferation and differentiation. This is more so because *SREBP1c* is known to respond to insulin and is essential for glucose carbon utilization and storage qualities related to adipogenesis (Ferre and Fofelle, 2007).

In this study, SREBP1c protein production increased with incubation time to a 2-fold increase by day 14 and 18 in the untreated cells. This is supported by literature (Ferre and Fofelle,

2007; Payne et al., 2009). The increase in the protein presence is related to increase in insulin utilisation for proliferation and preparation for differentiation (Kim et al., 1998). The presence of flavonoids reduced the protein abundance in a dose and time dependant pattern, but all the flavonoid treatments had a protein presence greater than that of day 0 control. The fact that the presence of flavonoids bears an association with abundance *SREBP1c* protein suggests that flavonoids reduce the adipogenesis process by affecting a pathway involving *SREBP1c*. *SREBP1c* is a membrane resident protein, it needs to be cleaved by proteases and undergo nuclear translocation for it to execute its role as a transcription factor for genes involved in adipocyte proliferation and differentiation (Gathercole et al., 2013). When the protein is not cleaved, its presence continues to subsist with time hence there was a cumulative increase across the 3 days for cells treated with flavonoids to a level greater than the day 1 control but less than the running controls. Some of the processes that repress the proteolytic cleavage of *SREBP1c* include phosphorylation by AMP-activated protein kinase (AMPK) or attachment by other ligands which competitively take the place of the protein cofactors. It is possible that flavonoids may be acting as alternative or competitive ligands, or they encourage the phosphorylation of the *SREBP1c* protein. Further experiments to identify the exact pathway are needed. However, it still stands that, *SREBP1c*, whose presence increases expression of enzymes that generate NADPH, malic enzyme (ME), glucose 6-phosphate dehydrogenase (G6PD), and phosphogluconate dehydrogenase (6PDG), and other molecules of energy storage (Gathercole et al., 2013), is seen to decrease in the presence of flavonoids.

#### 5.4.5.1. Erk and pErk during proliferation

Extracellular signal-regulated kinases (Erks) are cellular proteins that communicate signals from receptors on the cell surface to nuclear DNA. They occur as 2 subtypes which form the mitogen-activated protein kinases (MAPK)/ERK pathway; Erk 1 and 2 which are very similar in size (molecular weights of 44 and 42 kDa respectively) and function and are generally located in the cytoplasm (Guo et al., 2020). Erks can self-phosphorylate their C transcription activation domain (TAD) to get activated and be able to directly control their own gene transcription (Morimoto et al., 2007). In their non-phosphorylated form, ERKs are inactive, their N- and C-terminal domains are interconnected in the cytoplasm. Erks, together with classical MAPKs play an important role in many cellular processes which include cell proliferation and

differentiation. Increase in expression of Erk proteins is often linked to increase in proliferation especially in cancerous cells (Mader and Pantel, 2017). It is with this understanding that it was necessary to find the protein levels of Erk and its phosphorylated form pErk to elucidate the pathway by which flavonoids affect adipogenesis.

In this study, proliferation experiments were conducted to see the effect of concentration on the relative expression and phosphorylation status of the Erk proteins in quercetin treated SGBS preadipocytes over 3 days of incubation. Erk protein increased linearly in the 3 test days to 20% more by day 3 of the untreated controls. This observation is confirmed by (Prusty et al., 2002) who found an increase in Erk protein in the first 3 days of preadipocyte incubation on 3T3 cells. Day 3 marked the day of optimal proliferation before the cells underwent contact inhibition as the cells approached full confluence past day 3. The increase in Erk presence in the untreated cells can be related to increase in proliferation as seen in parallel experiments. The quercetin treatment concentrations of 1, 10 and 100  $\mu\text{M}$  reduced expression by 10%, 35% and 65% respectively after the three days of incubation. The difference in reduction between day 2 and 3 was negligible. This finding resonates with Ahn et al. (2008) who found that quercetin increased proliferation in adipocytes in a dose and time dependant manner which was inversely proportional to Erk protein activity. Their work on 3T3 cells showed that when higher quercetin concentrations were used to treat cells, Erk protein activity was reduced, and cell proliferation decreased whilst apoptosis increased. The Erk protein is involved in many antiproliferative pathways which include apoptosis, autophagy and senescence (Cagnol and Chambard, 2010). However, Erk activity is not limited to a negative correlation with antiproliferative events, Sun et al. (2015) showed that hyperactivity of Erk proteins can be seen in apoptosis in a pathway involving p38–mitogen-activated protein kinase (MAPK) and caspases 8 and 3, or induction of mitochondrial cytochrome c release (Cagnol and Chambard, 2010). In their review, Sun et al. (2015) showed that for preadipocytes, reduction in proliferation was correlated to reduction of Erk expression when antiproliferative agents were introduced. In this study, Erk can be assumed to be associated with the reduction in the expression of *Ki67* and *TPX2* which were also seen to reduce within the same time frames of 1 to 3 days of preadipocyte incubation. However, Erk presence alone does not give conclusive pathway elucidation of adipogenesis in cells treated with flavonoids, phosphorylated Erk on the other hand can provide more information.

The phosphorylation of Erk showed no significant change for the 1 and 10  $\mu\text{M}$  quercetin concentrations which was less than 5% but the 100  $\mu\text{M}$  quercetin concentration showed a reduction of 26% over the 3 days of incubation. Furthermore, presence of quercetin reduced relative phosphorylation at higher concentrations. Erk is activated by phosphorylation, and it can either be translocated to the nucleus to work as a signal kinase on adipogenic genes or it can promote other cytoplasmic proteins to be phosphorylated thereby regulate the activity of other kinases (Guo et al., 2020). Our work is suggesting that quercetin is either the direct or indirect signal or stimulus triggering the chain of these events as seen by the correlation between the quercetin concentrations and the reduction of proliferation genes *Ki67* and *TPX2* and the increase in apoptotic gene activity of *BIM* and *BAD* genes as seen on the qPCR experiments. These proliferation and apoptotic genes are known to be enabled by the transcription effect of Erk and pErk (Cagnol and Chambard, 2010; Min et al., 2018; Sun et al., 2015; Ghemrawi et al., 2018; Guo et al., 2007). However, there is a scarcity of literature on the pathway of these genes on SGBS cells that have been treated with quercetin. Most of the studies have been conducted on cancer cells and the closest studies to this work are experiments on 3T3-L1 cells.

#### 5.4.5.2. Leptin during proliferation

Leptin is a protein produced by adipose tissue; in whole organisms, it controls the homeostatic balance of hunger and satiety. Whilst it is known that differentiated adipocytes do produce leptin, many studies claim that preadipocytes do not express the gene that encodes the leptin protein under normal conditions (Maffei et al., 1995; Leroy et al., 1996; Melzner et al., 2002; Wang et al., 2005). However, Wang et al. (2008) proposed that preadipocytes under stress can express the protein leptin. The presence of leptin early on the process of adipogenesis has also been associated with browning and reduction of triglycerides accumulation after differentiation (Wang et al., 2008; Wang et al., 2019). Whilst Wang et al. (2019) demonstrated hypoxia as one stressor able to allow preadipocytes to prematurely produce leptin, it is necessary to see whether flavonoids can exert such an effect and whether the result has any relationship with reduction in triglycerides and increase browning after quercetin treatment.

In this study, preadipocytes had leptin protein production which decreased with incubation time to 34% by day 3 in untreated controls. This resonates with other studies which show

transient leptin transcription in the first few hours after seeding and sharply reducing in the following hours. The spike is potentially a result of the trypsinisation, centrifugation and seeding stress. The presence of 100  $\mu\text{M}$  quercetin increased the protein abundance to 34 and 25 % in day 2 and 3 respectively. The 1 and 10  $\mu\text{M}$  concentration, whilst higher than the daily untreated controls by up to 29% for the 10  $\mu\text{M}$  concentration on day 3, had little difference (less than 5%) compared to the day 0 reference sample over the 2 days. Here it was shown that presence of quercetin induced an increase in the protein leptin that was dependant on the dose level. In experiments where exogenous leptin was introduced in preadipocytes, the result was a decrease in proliferation (Wagoner et al., 2006). These experiments were however on animal models and used supraphysiological doses of the protein, leptin. There is a scarcity of literature on how flavonoids impact the expression of leptin in preadipocytes. In their work, they concluded that leptin inhibited preadipocyte proliferation by modifying the release of factors from other tissues which are not adipocytes.

#### 5.4.5.3. Akt and pAkt during proliferation

The protein kinase B (PKB) or Akt is a protein involved in metabolism, survival, and growth signal transduction pathways (Manning and Cantley, 2007). Akt function involves 2 steps, recruitment to the cell membrane and phosphorylation once docked at the membrane. Increased levels of phosphorylated Akt alone are not conclusive as many biological functions use the same process of phosphorylation and what may appear to be glucose metabolism signal could be an apoptotic process. Furthermore, many genes related to adipogenesis are transduced through the Akt pathway. Having seen the reduction of proliferation in earlier growth experiments and having seen a downregulation of proliferation specific genes and upregulation of apoptotic genes, it became necessary to investigate the Akt protein and its phosphorylated state to elucidate the pathway by which flavonoids and especially quercetin exert their effect on human SGBS cells.

The Akt protein increased linearly in the 2 test days to greater than 20% more by day 3 in the untreated controls. Treated cells showed a reduction in the presence of the protein at high concentrations where the greatest reduction was on the 100  $\mu\text{M}$  quercetin concentration which had a 42 and 64% reduction after day 2 and 3 of incubation, respectively. The protein, pAkt showed no meaningful change over the concentrations range and times with variations of 5% or less. Flavonoids are known to reduce PI3-K/Akt and mechanistic target of rapamycin

(mTOR) pathway activities in cancerous cells (Syed et al., 2013). Like Akt, mTOR is a protein kinase regulating cell growth, survival, metabolism, and immunity. In their work Syed et al. (2013) showed that Akt and pAkt were downregulated after flavonoid treatments and high concentrations. Zhang et al. (2018) collaborates these findings with work across many cell lines and many flavonoids. Whilst their work was again on cancer cell lines, they concluded that flavonoids reduced Akt/pAkt pathway activity in concentrations above 20  $\mu$ M. This study, whilst not looking at cancer cells, has also shown that Akt production is reduced in a dose dependant manner in preadipocytes. However, the insignificant change in pAkt could be a result of other competing cellular processes that use same pathway. For example, a reduction in proliferation would reduce Akt phosphorylation whilst a contemporaneous increase in apoptosis will demand a rise in pAkt. This situation may present a self-cancelling diagnosis. Shearin et al. (2016) whose work investigated Akt in adipocytes demonstrated that Akt was necessary for the insulin-signalling cascade, and absence of Akt through gene knockouts would result in lipodystrophy. Their work however focused more on differentiated adipocytes *in vitro*, except when they worked on animal models, then the adipose tissue would be the whole range from nascent preadipocytes to fully differentiated cells. As in other proteins mentioned earlier, there is still a scarcity of literature on Akt expression in preadipocytes, especially SGBS cells, under the treatment of flavonoids.

#### 5.4.5.4. SREBP1c protein during differentiation

It is known that SREBP-1c is a transcription factor involved in adipocyte differentiation (Gathercole et al., 2013). Its effect downstream controls differentiation associated genes such as *GLUT4*, *Adiponectin*, *UCP1*, *PPAR gamma* and *C/EBP $\alpha$* , genes that have already been seen to reduce when adipocytes are treated with flavonoids. As a membrane bound member of the basic helix–loop–helix-leucine zipper family of transcription factors, *SREBP1c* needs to be cleaved and translocated to the nucleus where it executes its transcription role. For cleavage to take place, a transduction molecule is needed. This can be SREBP cleavage-activating protein (SCAP) or insulin-induced gene 1 protein (INSIG1) or any mimetic resembling one of these. Exogenous biomolecules are also known to trigger the signal transduction cascade (Lee and Yaffe, 2016). Nevertheless, little is known about changes in activity of *SREBP1c* across the differentiation stages of adipocytes, especially those under the influence of different concentrations of the flavonoid quercetin.

In this study, SREBP1c protein production increased with incubation time on untreated cells and cells treated with quercetin concentrations within the physiological range. The 1  $\mu$ M concentration actually increased protein abundance by 32 and 6% for day 14 and day 18 respectively compared to the vehicle controls. These findings of increased SREBP1c protein associated with increase in lipid accumulation have been reported before (Ferre and Fofelle, 2007). However, the element of sub-physiological concentrations eliciting increased protein expression is new. Seo et al., (2015) for example showed reduction of SREBP1c in OP9 cells treated with quercetin. However, the lowest concentration used was 5  $\mu$ M and there are very few equivalent studies that explored quercetin at concentrations below 5  $\mu$ M. The presence of 10 and 100  $\mu$ M concentrations of quercetin reduced the protein abundance in a dose and time dependant pattern to levels lower than the day 0 absolute control up to 14-fold reduction. This reduction resonated with the expression of UCP1 protein and *GLUT4* gene across the same concentrations and time frames. Although focusing on OP9 cells, Seo et al. (2015) concluded that quercetin reduces the expression of transcription factors such as *C/EBP $\alpha$* , *PPAR gamma* and *SREBP-1c* for both RNA transcript and protein levels.

#### 5.4.5.5. *C/EBP beta* protein during differentiation

*C/EBP beta* plays a crucial role during adipocyte differentiation because it induces the expression of *C/EBP alpha* and *PPAR gamma* genes known for enabling differentiation (Guo et al., 2015). *C/EBP beta* achieves this by binding to the promoter region of these genes and thus induce their expression. In culture, *C/EBP beta* is itself induced by dexamethasone a synthetic glucocorticoid which is added to the differentiation media. *In vivo*, glucagon acts as the induction agent for *C/EBP beta* (Matsuno et al., 1996). Inhibitors to *C/EBP beta* exist, examples are synthetic chemicals and natural plant products such as helenalin (Jakobs et al., 2016) and emodin (Choudhari et al., 2020). Helenalin acetate, for example, was shown to inhibit *C/EBP beta* by a direct binding mechanism. Having seen a reduction in adipocyte differentiation when cells were treated with quercetin, it is possible that the flavonoid may be acting as a direct repressor to the action of *C/EBP beta*. Investigating the effect of flavonoids on *C/EBP beta* will therefore help elucidate the pathway by which flavonoids exerts their effect on adipogenesis and in this case, the effect of quercetin on SGBS cell differentiation.

In this study, C/EBP beta protein production increased with incubation time to more than 6 times the initial value by day 18 in untreated cells. There was barely any difference between day 14 and day 18 protein levels on untreated controls (less than 5%). Similar studies have shown a spike in C/EBP beta protein expression immediately after the induction of differentiation which waned gradually with further incubation (Rosen et al., 2002; Guo and Tang, 2015). In their work, Rosen et al. (2002) demonstrated that *C/EBP beta* rapidly increases in expression in the first 24 hours of differentiation induction and thereafter drift downwards as the expression of *C/EBP alpha* and *PPAR gamma* rise. Because cultured cells that are made to differentiate are grown in dexamethasone enriched media, it will be expected that *C/EBP beta* increases and gradually decrease as the dexamethasone is being expended. There was not much difference between the daily controls and the 1 and 10  $\mu$ M concentrations at day 14 and 18. If the spike in increase of *C/EBP beta* happens at the beginning of differentiation induction which is day 1 (day 4 of incubation), and it drifts downwards, then by day 14, the differences may have been lost. Ushijima et al. (2014) described the same observations, they noted maximum *C/EBP beta* expression on day 4, by day 7 the expression was below half and almost insignificant by day 18. Their work looked at the effect of Indian hedgehog protein during chondrocyte differentiation. Cao et al. (1991) also looked at the expression of three C/EBP isoforms during adipose conversion of 3T3-L1 cells, they concluded that C/EBP beta and C/EBP delta are expressed at the early stages of differentiation hitting a peak by day 2. C/EBP alpha would then be expressed incrementally until maximum differentiation. Therefore, for cells which have started differentiating after 4 days of incubation, presence of C/EBP beta is seen to peak earlier on and by day 14 and 18, there is barely any meaningful expression to be noted.

Contrary to the findings from the 1 and 10  $\mu$ M quercetin concentrations, the 100  $\mu$ M concentration had significantly higher levels of C/EBP beta presence, up to 18 and 8-fold for day 14 and 18 respectively. Whilst this is counter-intuitive, it can be explained by the fact that at high concentrations, quercetin kills most cells and those that remain viable go into senescence until presence of quercetin, whose bioavailability is limited, is expended. At which point cells recover, start to proliferate and because differentiation factors in the media are present, they start to differentiate. Therefore, quercetin in this instance, delayed the differentiation process and the spike of C/EBP beta presence is seen much later. This result



supports the argument of cell recovery after flavonoid treatment and the challenges of flavonoid bioavailability (Joshi et al., 2022). From this observation, it stands to be argued that if flavonoids are to succeed as a dietary supplement, they need to be taken consistently.

#### 5.4.5.6. PPAR gamma protein during differentiation

Peroxisome proliferator- activated receptor gamma (PPAR gamma), also known as the glitazone reverse insulin resistance receptor, is a transcription factor that regulates adipocyte differentiation. It is an upstream regulator of such genes as *adiponectin* and *GLUT4* which directly mediates adipocyte differentiation. Reduction of the presence of the PPAR gamma protein for example, inhibits adipogenesis, reduces *adiponectin* abundance and impairs insulin stimulated glucose uptake through GLUT4 proteins (Liao et al., 2007). PPAR gamma itself is regulated by phosphorylation of the Ras/Raf/Mitogen-activated protein kinase/ERK kinase (MEK)/extracellular-signal-regulated kinase (ERK) cascade pathway (Suwaki et al., 2007). Having seen that quercetin affects the expression of *adiponectin* and *GLUT4* transcripts and that ERK and pERK presence is also affected by the same flavonoid, it was necessary to investigate the presence of PPAR gamma protein to elucidate the pathway by which quercetin achieves its role of reducing adipogenesis.

PPAR gamma protein production increased with incubation time in untreated control cells up to 20-fold on 18 respectively (Figure 5.4.23). The correlation between PPAR gamma presence and level of differentiation has also been observed in other studies (Rosen et al., 1999; Sue et al., 2021; Fischer-Posovszky, 2008; Wabitsch, 2001). However, not many studies have carried out *in vitro* experiments of adipocytes past day 14 to show whether the presence of the protein keeps increasing. Gene expression experiments conducted earlier, showed that the protein level decreased after day 14 by more than 25% to day 18 (Figure 5.4.10a). This may suggest that, whilst levels of RNA transcript reduce, the available protein is bioaccumulated. This is also typical of cells which produce protein molecules that become cell membrane receptors. Accumulation of PPAR gamma membrane receptors alone is not enough to induce greater levels of differentiation, there has to be corresponding availability of PPAR gamma agonists to initiate the transduction cascade (Yang et al., 2009). It is yet to be shown whether flavonoids can act as such agonists.

Treatment of SGBS cells with quercetin showed a reduction in the presence of PPAR gamma at high concentrations whilst showing what appears to be hormetic effects at very low

concentrations. The 1  $\mu$ M concentration increased protein expression by 23 and 26% relative to the daily untreated controls for day 14 and 18 respectively (Figure 5.4.23). PPAR gamma presence is not only associated with differentiation, but it also has a direct correlation with browning of fat cells (Zhang et al., 2019). Zhang et al. (2019) work on animal models showed that flavonoids prevent adipogenic differentiation but induce white adipose tissue browning and beiging through the AMPK and PPAR signalling pathways. The 10  $\mu$ M did not have any meaningful difference from the control (under 5%). Seeing that the PPAR gamma pathway is involved in 2 conflicting processes, browning and adipogenic differentiation reduction, absence of a change may mean self-cancelling effects. Further pathway analysis downstream is needed to qualify this. There was significant downregulation of protein expression in cells treated with 100  $\mu$ M quercetin of 80 and 72% for day 14 and 18 respectively but interestingly, this was higher than the absolute day 0 controls. The fact that the values were higher than the day 0 absolute control confirms that differentiation is still taking place, albeit at a very low level. Many studies on animal models have made the observation linking flavonoids to the reduction of steatosis (abnormal retention of lipids within a cell or organ). Feng et al. (2016) for example demonstrated that the flavonoid apigenin was a direct modulator of PPAR gamma which reduced fat accumulation. They concluded that unlike other synthetic ligands such as rosiglitazone, apigenin significantly reduced adipocyte differentiation without side effects. They went on to propose that, by virtue of the apigenin having the capacity to reduce fat accumulation, flavonoids had the potential to ameliorate metabolic disorders. Even more interesting is the fact that a study by Salam et al., (2008) identified at least 6 flavonoids as *PPAR gamma* direct agonists, they stimulated PPAR gamma transcriptional activity in transcriptional factor assays. The identified flavonoids were flavone apigenin and chrysin, which are flavones; psi-baptigenin, biochanin-A and genistein, which are isoflavones and hesperidin, which is a flavanone glycoside. Whilst a negative correlation between quercetin and PPAR gamma protein abundance has been established, there is still needed to investigate other pathway proteins to establish the full mechanism by which flavonoids impair adipogenesis.

#### 5.4.5.7. UCP1 protein during differentiation

UCP1 protein has been associated with adipocyte browning and beiging. Presence of UCP1 is also heavily associated with such other proteins as PPAR gamma coactivator 1 $\alpha$  (PGC-1 $\alpha$ ),

PPAR gamma, PPAR gamma agonists such as rosiglitazone (Zhang et al., 2019) and leptin (Scarpace and Matheny, 1998). Having seen the relationship between PPAR gamma proteins, UCP1 gene transcript and leptin gene transcript with quercetin, it was imperative to investigate UCP1 protein presence in order to elucidate the pathway by which flavonoids exert their effect on adipogenesis and whether browning can be correlated to flavonoid presence.

UCP1 protein presence increased with incubation time in untreated controls, this was expected because UCP1 is produced more by differentiated adipocytes with cellular lipid droplets (Tews et al., 2019; Wabitch et al., 2001; Carey et al., 2014). When cells were treated with a 1  $\mu$ M concentration of quercetin (Figure 5.4.23), which is at the low end of the physiological concentration range, UCP1 protein presence increased up to 10%. Because increase in UCP1 presence is related to browning, this is suggestive that quercetin, in this case may, amongst other things, helped in the beiging or browning differentiating adipocytes. This position is supported by Zhang et al. (2019) who argued that flavonoids are able to induce beiging of white adipose tissue and thermogenesis. Although the literature cited in their work did not use human SGBS cells, they suggested the mechanism of flavonoids in increasing the brown phenotype as using the AMP-activated protein kinase (AMPK)- Peroxisome proliferator-activated receptor-gamma coactivator (PGC)-1alpha/Sirtuin 1 (SIRT1) and PPAR signalling pathways. Treatment with quercetin concentrations of 10 and 100  $\mu$ M resulted in UCP1 protein production by greater than 60%. Since UCP1 protein is expressed in abundance in differentiated adipocytes and flavonoids at 10 and 100  $\mu$ M concentrations reduce adipocyte differentiation, it would be expected that UCP1 protein presence will be greatly reduced at these concentrations. These findings are similar to those by Pei et al. (2021) whose work on mice showed that, within physiological concentrations, quercetin increased browning of white adipose tissue with a correlated increase in UCP1 presence. They concluded that quercetin is able to prevent adipogenic differentiation whilst also inducing the beiging of white adipocytes through AMPK and PPAR gamma pathways. Other authors arriving at the same conclusion albeit with different cell models include Zhang et al. (2016), Bae et al. (2014) and Moon et al. (2013), they concur in asserting that quercetin possessed anti-differentiation properties whilst encouraging brown phenotype abundance. There is still scarcity of literature on the complete pathway of this flavonoid on SGBS cells.

#### 5.4.5.8. Akt phosphorylation during differentiation

It has been established that Akt is a protein involved in metabolism, survival, and growth signal transduction pathways (Manning and Cantley, 2007). Activation of Akt is dependent on the phosphorylation status, therefore the levels of pAkt are relevant in elucidating the pathway by which Akt is involved. Having seen the effect of quercetin on PPAR gamma, Leptin, UCP1, C/EBP beta and SREBP1c proteins as well as the RNA transcript coding for *PPAR gamma*, *adiponectin*, *GLUT4*, *UCP1*, *TPX2*, *Ki67*, *BIM*, *BAD*, *SREBP1c* and *CEBP-β* during differentiation and that Akt and pAkt are implicated in the mechanisms of genes coding for these transcripts, it is necessary to investigate Akt and pAkt levels during differentiation during quercetin treatment.

In untreated cells, there was a slight decrease in Akt expression, the decrease was only around 10% of the preadipocyte control (Figure 5.4.24). The phosphorylated Akt presence had an even lower difference in day 14 and 18 results compared to the preadipocyte control although the difference was a gradual increase. This variation in protein expression in untreated controls could be the sum effect of a complex mixture of mechanisms because Akt and pAkt are a common currency in many cellular processes (Adlung et al., 2017; Song et al., 2007). Treatment with quercetin reduced Akt abundance by up to 70% by day 14 for treatments of 100 μM. The reduction in Akt protein presence was positively dependant on the concentration of quercetin. These findings are similar to those by Kim et al. (2012) who observed flavonoids inhibiting adipogenesis by a mechanism involving the Akt signalling pathway. Their work used 3T3-L1 cells which were treated by citrus aurantium flavonoids. Akt levels were at their lowest on day 14 for treated cells, there appeared to be a recovery of expression for all treatments between day 14 and day 18 except for the 1 μM treatment. Apparently, many studies looking at adipocyte differentiation rarely go up to or over 14 days of incubation (. Most RNA transcript and protein levels max around 6 and 8 days of incubation. What appear to continue increasing is rate of differentiation, triglyceride levels and lipid droplet size Fischer-Posovszky, 2008; Wabitsch, 2001).

Phosphorylated Akt, (pAkt) presence in cells treated with quercetin was increased except for the 100 μM concentration which was reduced by 20% on day 14. The increase was minimal averaging 16% with a high of 29% for the 10 μM concentrations on day 14. It would have been expected to see pAkt values diminishing at the same rate as Akt seeing that the active form

of Akt is pAkt in adipogenesis and other pathways. However, these values under comparison are not absolute quantities but relative measures. Moreover, pAkt being a ubiquitous molecule involved in other pathways such that, when differentiation is being reduced, proliferation for example could be increasing. This will demand an increase in pAkt presence. Finally, the half-life of pAkt in the cell is higher than that of Akt, and changes in cellular microenvironments may alter this half-life (Fan et al., 2013). More research out of the scope of this study is needed to establish the dynamics and bioavailability of Akt and pAkt in different cellular conditions.

#### 5.4.5.9. Leptin protein during differentiation

Leptin is known for the regulation of energy balance in adipocytes using the negative feedback signalling loop (Harris et al., 2014). Adipocytes possess leptin receptors on the cell membrane whilst concurrently producing the hormone leptin thus making the leptin signal transduction cascade autocrine. Leptin effects its antiadipogenic function by directly reducing the size of white fat depots and indirectly modifying adipocyte sensitivity to insulin to inhibit lipid accumulation. Having seen the reduction of adipocyte size in cells treated with quercetin and the changes in insulin regulating genes after cells were treated with flavonoids, it was necessary to investigate whether quercetin achieves adipogenesis reduction by modulating the leptin protein.

Figure 5.4.26. shows that leptin protein production increased with incubation time to 100 and 150% on days 14 and 18 respectively relative to the absolute control for the untreated cells. This pattern was also observed by Melzner et al. (2002) who asserted that leptin is generally abundant in mature adipocytes but not in preadipocytes. Treatment with 1 and 10  $\mu\text{M}$  concentrations of quercetin caused a small increase in leptin presence of less than 5% for the 1  $\mu\text{M}$  treatment on day 14 and up to 25% more on day 18 for the 10  $\mu\text{M}$  treatment. The 100  $\mu\text{M}$  quercetin treatment however, had a significant decrease in leptin presence down to 40% on both day 14 and day 18. It is worth noting however that although there was a significant decrease in expression on 100  $\mu\text{M}$  treated cells, the protein presence was higher than the preadipocyte control.

The reduction in quercetin abundance with high concentrations of quercetin was expected because it is similar to the findings of Khalilpourfarshbafi et al. (2019) and Forney et al. (2018). Although these comparison results were based on animal models, they provide a clear

explanation on how quercetin reduces fat accumulation. Melzner et al. (2002) demonstrated that quercetin reduces adipogenesis through the methylation of cytosine-phosphate-guanine islands (CpGs) within the CCAAT/enhancer-binding protein  $\alpha$  (or C/EBPs) a process that resonates with the current findings of our *C/EBP* gene expression results. The fact that 100  $\mu$ M treatments of quercetin still produced significantly higher levels of the protein leptin compared to the preadipocyte controls is also not surprising, quercetin presence does not stop preadipocyte differentiation but reduces the rate of differentiation and the size of fat droplets produced.

The increased presence of the protein leptin in low doses of quercetin was not expected. Having seen a reduction at the rate of differentiation at 10  $\mu$ M concentrations in earlier experiments, it would have been expected to see leptin levels decreasing if the leptin is associated with decreased accumulation of fat mass as literature prescribes. Considering the fact that the flavonoid was given at the beginning of differentiation induction, it is possible that the molar presence of the flavonoid wanes with time to a point that by day 14 and 18, the concentration of will be below physiological levels. Earlier pilot studies on glucuronidation of quercetin showed that, whilst minimal, quercetin converts to its glucuronides in a time dependant manner. Besides glucuronides, quercetin can morph into any of its many metabolites (Hai et al., 2020) with time, suggesting that the bioavailability of quercetin is time dependant. Work by Gugler et al. (1975) gives an insight on the bioavailability of quercetin. They demonstrated that in humans, quercetin has a mean half-life of less than 3 hours and of the absorbed quantity, a high proportion is converted into quercetin metabolites. Whilst most studies are on animal and human models, parallels can be drawn with cell strains. An interesting spin on this observation can be construed from work by Arias et al. (2014), they showed that at peri physiological concentrations, quercetin can reduce insulin resistance through the leptin pathway without decreasing adipose tissue and skeletal muscle fat accumulation. This meant that leptin could increase without a corresponding increase in rate of differentiation. It can therefore be concluded that Leptin presence is associated with reduction in adipogenesis either directly through the CEBP pathway or indirectly through insulin sensitivity as Harris et al. (2014) proposes.

#### 5.4.5.10. Erk phosphorylation during differentiation

Erk and pErk, key downstream elements of the RAF/MEK/ERK transduction pathway have been implicated in adipogenesis processes that include PPAR gamma and CEBPs (Prusty et al., 2002) and GLUT4 and adiponectin (Ciao et al., 2020). Having observed that quercetin affects the expression of *PPAR gamma*, *CEBP beta*, *GLUT4* and *adiponectin*, it was necessary to investigate how Erk and its phosphorylated form vary when SGBS cells are treated with quercetin to map the pathway by which the flavonoid achieves its adipogenesis reduction role.

Our study showed Erk protein increased in presence for all test conditions relative to the untreated controls except for the 100  $\mu$ M quercetin treatment which was 12% lower than the absolute control (Figure 5.4.27 a). The untreated daily controls did not vary between day 14 and 18. The treatment concentrations of 1 $\mu$ M had the greatest increase in expression of greater than 20% on day 14 and 40% on day 18 relative to the daily controls. The treatments of 10 and 100  $\mu$ M increased between day 14 and 18 by more than 40%. Phosphorylated Erk presence showed a general suppression in expression for all test conditions except for the 10  $\mu$ M concentrations which increased by 39 and 57% for day 14 and 18 respectively relative to the daily control. Erk is activated when it is phosphorylated (Prusty et al., 2002). Presence of Erk alone is not indicative of a process because many cellular processes employ this kinase. The fact that phosphorylation was reduced in the presence of flavonoids may suggest that adipogenesis is reduced by flavonoids by stopping the Erk kinase from phosphorylating and thus shutting the MEK/ERK pathway. The perceived increase in the presence of Erk may signal activity in another biological process, for example, the preadipocytes that fail to differentiate will start recovering and proliferating when differentiation enhancers have been spent. This notion of recovery was observed in earlier chapters.

#### 5.4.6. Conclusion

It has been shown that the flavonoids are associated with the reduction of the expression of proliferation associated genes, increase in expression of apoptosis associated genes and downregulation of genes associated with differentiation in SGBS cells. The effects were evident at peri-physiological concentrations of below 10  $\mu$ M. The transcriptional factors and the kinases affected suggests that the MAPK/ERK and the PI3K-AKT-mTOR pathways are involved in how flavonoids affect adipogenesis. Of greatest interest is the apparent browning

of the adipocytes as seen by the increase in *UCP1* expression at physiological concentrations. This suggests a great potential for flavonoids having positive health outcomes.



## 6. Discussion

Obesity is a persistent health concern whose burden has increased over the last decade (Wong et al., 2022). In 2021, the world health organisation claimed that since 1975, global obesity has more than trebled (WHO, 2021) and it is no longer a challenge of the affluent society but the greater world population with sharp rises from the third world countries. With obesity, many comorbidities such as loss of insulin sensitivity, high blood pressure, dyslipidemia, type 2 diabetes, cardiovascular disorders, and other organ diseases emerge. This will obviously bring massive health and socioeconomic burdens. Management of obesity has been driven chiefly by lifestyle changes and exercise, but this too has limits and cannot apply to everyone. Pharmaceutical medications are also on the market, some of these work by suppressing hunger and increasing satiety after a small meal in a bid to cut calorie intake (Prillaman, 2023). Some of these drugs work by slowing metabolism and substrate absorption, while others affect insulin sensitisation and glucagon activity among other things (Zhong et al., 2022). Whichever mechanism of function, pharmaceutical drugs have always had concerning side effects such as high blood pressure or liver disorders.

Interest has recently shifted to herbal medicines and other natural plant products. Indeed, the French paradox, though often challenged, has brought some insights into the correlation between the consumption of plant phytochemicals and general reduction of cardiovascular diseases and obesity (Biagi and Bertelli, 2015). Particularly, flavonoids have been implicated in the fight of obesity as seen by body weight reduction, fat mass and plasma triglyceride reduction and the lowering of cholesterol (Rufino et al., 2021), but not much is known about their structure function relationship or their specific mechanism in the transition of the fat cell between the preadipocyte stage to the fully committed adipocyte.

The work from this thesis has addressed the following questions: Do flavonoids affect adipogenesis in a cell model? Does this effect occur during SGBS preadipocyte growth and proliferation? Or does the effect of the flavonoids on adipogenesis occur during differentiation? Is there a hierarchical order of effect of the flavonoids on the proliferation and differentiation of fat cells? Do flavonoid combinations from different classes enhance their effect on adipogenesis? What are the molecular pathways that are involved in the process? These questions were investigated using a variety of tools which included MTT assays for cell viability, microscopic cell counts, Oil red o staining, triglyceride quantification,

protein extraction and quantification using the western blot protocols and gene expression quantifications using RT-qPCR protocols. Flavonoid and flavonoid combination rankings were made using IC50 values generated from microscopic cell counts and oil red O stain absorbance readings.

#### 6.1. Preadipocyte proliferation.

Adipose tissue comprises of adipocytes, preadipocytes, fibroblasts, vascular endothelial cells, and some immune cells. Preadipocytes, being derived from mesenchymal cells are themselves adipocyte (fat cell) precursors but play a pivotal role in lipid metabolism in their own right. Whilst the average lifespan of an adipocyte is known to be about 10 years (Arner et al., 2011), not much is known about that of the preadipocyte. However, like other cells, the preadipocyte goes through the cell cycle stages of G1, S, G2 and M stages and it is believed to be arrested at the G1 stage upon the induction of differentiation or when antiproliferation stressors are introduced. The same is also evident in human adipose tissue-derived stem cells (hASCs) where more than 80% of the cells in a clone go to G0/G1 phase arrest when anti proliferation stressors are introduced (Marcon et al., 2019). Some cells will stay in the phase until enough growth factors are available and they continue in the cell cycle, but others go into one form or the other of cell death depending on the induced transcription factors.

This study showed that flavonoids, at adequate concentrations ( $>25 \mu\text{M}$ ) reduce the proliferation of preadipocytes, however, when left in culture, even those cells treated with very high concentrations ( $\geq 100 \mu\text{M}$ ) of flavonoid and had a big reduction in proliferation ( $>75\%$ ) still recovered. Flavonoids therefore can be thought to reduce cell viability and thus reducing proliferation by reversibly arresting the cell cycle. This has 2 implications; to certify that flavonoids are not toxic and their presence in cells does not cause catastrophic damage as well indicate that benefits from flavonoids cannot rely on a single dose but will need continuous consumption so that the bioavailability of the flavonoids can be maintained, and the benefits sustained. The notion of flavonoid inducing cell cycle arrest, however, does not preclude the possibility of reduction of proliferation by apoptosis, autophagy, or cell death programmes. Molecular gene analysis assays are therefore useful in elucidating this other possibility.

Both flavones and flavonols reduced the rate of proliferation of preadipocytes. Flavones reduced effectiveness with increase in number of hydroxyl groups on the phenyl carbon ring B whereas flavonols increased effectiveness with increase in B phenyl ring hydroxyl groups. It is known that functional hydroxyl groups in flavonoids effect antioxidant properties by mopping away reactive oxygen (and other element) species or by the chelation of metal ions (Marcon et al., 2019). Whether it will be chelating metal ions or scavenging free radicals, will be determined by the side groups on the heterocyclic C ring (fig 6.1). Flavones have no hydroxyl group on position 3 of the C ring, this skews the molecular polarity and lends it to depend more on its chelating capacity. Presence of hydroxyl groups in that case does not help in the chelating drive but hinder. Therefore, the findings of reduced effectiveness of flavones with the increase in hydroxyl groups on the B carbon ring.

The absence of the hydroxyl group on position 3 of the C ring makes flavones more lipophilic, they easily ingress the lipid membrane of the cell. This will suggest that flavones will become more bioavailable in the cell and exert their efficacy better than similar size flavonols and this is what this study showed.

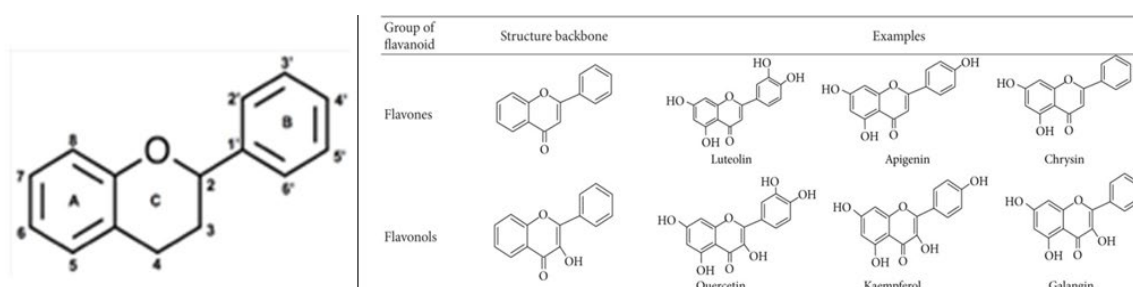


Figure 6.1 Chemical Structures of the generic flavonoid, the flavones luteolin, apigenin and chrysin, and the flavonols quercetin, kaempferol and galangin showing letter designation and variation in hydroxyl groups on the B and C rings. Adopted from Kumar and Pandey (2013).

Flavonols on the other hand have a hydroxyl group on position 3 of the C ring. This hydroxyl group reduces lipophilicity for flavonols because they form weak hydrogen bonds with the outside hydrophilic heads of the preadipocyte cell membrane. Even more, this C ring hydroxyl group is known to get glycosylated which changes the biochemical characteristics of the flavonoid (Panche et al., 2016). Flavonols effectiveness, however, is dependent on the hydroxyl groups on the B carbon ring because the mechanism of action is associated with

the hydrogen bonds that are formed at the surface of the cell and the secondary lattice structures that emerge. Once inside the cell, the hydroxyl groups have a different function, they modulate the stability of RNA (Pradhan et al., 2018). The more the B ring hydroxyl groups, the more the effects and therefore quercetin with two B ring hydroxyl groups will be expected to be more effective than kaempferol with one hydroxyl group. Kaempferol will in turn be more effective than galangin which does not have any hydroxyl groups on the B ring. The hierarchy of the flavonoids was therefore predictable, and this was revealed by the results of this study.

Combined flavonoids, in general, were more effective than single doses at similar concentrations. Whilst this exists in literature for some combinations. There is scarcity of studies pitting flavones and flavonols as experimented in this work. For those who investigated combined flavonoids and found synergy, they attributed it to emerging lattice structures which exponentiates the free radical buffering system (Qin et al., 2018). Too many hydroxyl groups per unit molecule gives cell stress which may force it to enter the G1 phase arrest. Many studies on the synergistic effects were shown on differentiating adipocytes. These findings on proliferating preadipocytes are novel. The synergy in flavonoid combination finding is attractive and can translate to meaningful applications. For example, flavonoids being natural plant products exist in nature being a mixture of many flavonoid classes. Consuming these natural products will present different types of flavonoids available for combinations. The synergistic effects will therefore help in the war against obesity.

This study also found that at physiological concentrations, flavonoids confer hormesis to preadipocytes. Single flavonoids had more hormetic effects than combined doses. Whilst in some of the cases, the level of a low-dose stimulation has no statistical significance when compared to the untreated control, it was consistent enough to warrant observation. Although exciting, this phenomenon is not unique to flavonoids but present in situations, where a stressor, be it a poison, pharmaceutical drug or toxin will some over compensatory behaviour to the cell function (Chirumbolo, 2011). Hormesis, in this case, is therefore only an evolutionary adaptive response to stressors which is a more general behaviour of cell towards low doses. What could not be known from the proliferation experiments is whether the hyper proliferating cells that were subjected to low and physiological concentration

doses would translate to greater or less differentiation. This was addressed in the differentiation experiments.

## 6.2. Adipocyte differentiation.

Differentiation experiments showed that the flavanols quercetin, kaempferol and galangin, and the flavones chrysin, apigenin and luteolin at all concentrations reduce the rate of differentiation of human adipocytes in a dose dependant manner. It is exciting that even the low and physiological concentration doses which induced hormesis during proliferation did not translate to higher levels of differentiation. Cells which were treated with low doses of flavonoids during proliferations (and showed hormetic hyperproliferation) and were induced for differentiation without further flavonoid treatment also showed significantly lower rates of differentiation compared to the untreated controls. The apparent counterintuitive hyperproliferation drive by low doses therefore does negate the function of flavonoids in the control of adipogenesis. This finding is both relevant and meaningful because of the limited bioavailability of flavonoids in blood and body fluids, the organismal working concentrations are low (Thilakarathna and Rupasinghe, 2013). Physiological concentrations of quercetin can be as low as 2  $\mu$ M and concentrations of even 10  $\mu$ M are often referred to as supraphysiological (Winterbone et al., 2009). Therefore naturally available concentrations are enough to manage adipogenesis and arguably the hope towards the fight against obesity and its comorbidities.

When flavonoids effectiveness was ranked by their IC<sub>50</sub> values which were derived from oil red O assays, the effectiveness of flavones was directly proportional to the absence of hydroxyl groups on the third and determinant carbon ring (B) whilst for flavanols, the relationship was inverse. This is the same pattern which was observed on proliferation experiments suggesting that the role of hydroxyl groups is pertinent to the effect of flavonoids on adipogenesis both during proliferation and during differentiation. Whilst synergy between flavonoid combination was clear with the exception of one pair on proliferation experiments, it was not so on differentiation studies. It appeared that combined flavonoids exhibited additive attributes, the combined IC<sub>50</sub> values were not far from the arithmetic mean IC<sub>50</sub> of the single flavonoids. Few studies show this additive outcome from flavonoid combinations however, flavonoids when added with other compounds can evidence this outcome. An example is work by Harmon and Harp (2001) on

3T3-L1 cells which saw additive effects between the flavonoid genistein and epinephrine but not between genistein and naringenin, a structurally similar flavonoid. Additive effects from 2 flavonoids are as good as the single flavonoids themselves, they still work towards reducing adipogenesis. Antagonism would have been a worrying outcome.

Oil red O results were confirmed by microscopic differential counts together with triglyceride assays. This combination did not only confer validity to the methodology but also opened ways in the understanding of possible mechanisms by which flavonoids exert their effect. For example, lower concentrations of flavonoids had a relatively higher value of differentiation counts but a lower value of oil red O reading; morphology microscopic views showed that the differentiated cells contained fewer and smaller lipid droplets. This means many cells could have started the differentiation process, but they did not necessarily accumulate as many lipid droplets as would an untreated cell. Besides reduction in differentiation this finding is also a feature that is associated with browning of adipocytes. It is therefore possible that flavonoids reduce the differentiation of adipocytes whilst increasing the brown phenotype. Zhang et al. (2019) came to the same conclusion after reviewing many studies working on different flavonoids. Their work however, focused on in vivo studies where measures of the function of the sympathetic nervous system (SNS) could be assessed. This finding is exciting in that there is scarcity of literature on the browning of SGBS cells after chrysin and quercetin treatment. Confirmatory molecular tests for the current results would be used to qualify this assertion.

Reduction of differentiation by the presence of flavonoids occurred irrespective of the treatment timing, whether it was done before (a), during (b) or after (c) differentiation induction. However, those that were treated in all phases (a, b and c) had the greatest impact. This observation has attractive applications. The increased reduction after repeated treatment would suggest more benefits from a sustained consumption of flavonoids as opposed to infrequent uptakes. The fact that adipocyte differentiation reduced yet viability of cells was maintained that the flavonoids at physiological and even supra physiological concentrations do not have toxic implications on the cells when accumulated. This finding from SGBS cells is new. Another relevant application of the findings is the fact that flavonoids are effective on reducing adipogenesis irrespective of the timing of treatment (consumption). Adipose tissue contains a dynamic presence of cells at different stages of

maturation. Consuming flavonoids will affect all stages and as the finding suggest, the flavonoids continue to be useful irrespective of what stage they have been applied. This finding is supported by Shishtar et al. (2020) who looked cognitive markers in longitudinal study. However similar findings in SGBS cells are not available.

After differentiation was induced, the number of differentiated and undifferentiated cells continued to rise with the number of differentiated cells rising faster post differentiation induction except for the 100  $\mu$ M concentration treatment after 14 days. It was clear from the results that differentiation and proliferation were happening at the same time. This finding brings to play the question of whether proliferation and differentiation are mutually exclusive. In vivo proliferation and differentiation exist in a continuum, they do not conform to an on off switch (Ruijtenberg and van den Heuvel, 2016). Cell cycle regulators and cell type-specific gene transcription factors share a dynamic inverse but sustained presence.

### 6.3. Gene expressions and molecular pathways

Flavonoids are known to affect gene expression on test cells. The genes affected vary between cell type, flavonoid type, and treatment regime. Results from the proliferation experiments suggested that there is a form of reduction in preadipocyte viability which could either be caused by reversible cell cycle arrest, cell death or both. Similarly, the observed reduction in adipocyte differentiation could have resulted from the modulation of one or more of the differentiation associated genes. Even more interesting is the need to find whether proliferation associated genes are still affected during differentiation and whether differentiation specific genes are modulated before the induction of differentiation in preadipocytes.

In addressing these questions, the flavonoids quercetin and chrysin which represents flavonols and flavones respectively were used to investigate genes associated with proliferation, apoptosis, differentiation, insulin regulation pathways and browning. These genes were interrogated in proliferating preadipocytes and in differentiation induced adipocytes. To map out potential pathways by which these genes are regulated, quercetin alone was additionally used to elucidate the signal pathways and protein expression involved in adipogenesis. The following genes were investigated; *PPAR gamma*, *adiponectin*, *GLUT4* and *UCP1* as related to differentiation; *TPX2* and *Ki67* as related to proliferation; *BIM* and *BAD* as related to apoptosis; *SREBP1c* and *CEBP- $\beta$*  as related to major pathways

implicated in adipogenesis in general. Furthermore, the proteins UCP1, PPAR gamma, SREBP1c, C/EBP beta, Erk, pErk, Akt, pErk and leptin were investigated to qualify the gene expression results and to further elucidate possible pathways involved.

Preadipocytes treated with either quercetin or chrysin and investigated for the proliferation markers *Ki67* and *TPX2* showed a general trend of transcript downregulation in treated cells suggesting that flavonoids are associated with reduction in the expression of cell proliferation markers. *TPX2* is associated with microtubule assembly (Neumayer et al., 2014) in the S and G2 phases of the cell cycle, failure of microtubule arrangement often leads to deleterious cell forms which in turn triggers cell death pathways. *Ki67* on the other hand is implicated in the interface between G1 and G0 (Miller et al., 2011). This is the phase where cells can reversibly get into the quiescent stage that is the resting stage outside of the replicative cell cycle. Worse still it can get into the irreversible senescent phase which often associated with the induction of differentiation (Baserga, 2008). Interestingly, periphysiological concentrations which in earlier experiments showed hormetic effects did not show any *Ki67* or *TPX2* gene expression spikes. It can therefore be concluded that flavonoids can either force the cells into a cell death route or a reversible resting pathway. MTT and cell count proliferation experiments earlier indicated the possibility of cell viability recovery in a dose dependant manner. Therefore, it is possible that both these pathways are happening concurrently.

The choice of the *BIM* and *BAD* genes as possible pathway routes for cell death on SGBS cells were informed by literature (Wabitsch et al., 2001; Melzner et al., 2002; Fischer-Posovszky et al., 2008). As expected, at high concentrations, the apoptosis associated genes were upregulated, at physiological concentrations they pattern had many variations suggesting multiple pathways converging at such concentrations. Both genes, most likely complemented the reduction of cell proliferation by delaying the G0/G1 to S phase cell cycle phase transition (Du et al., 2017) and concurrently coding for apoptosis. Further work is needed to identify the transcriptional factors that help map the pathway by which flavonoids induce apoptosis.

Differentiation associated genes had no meaningful difference from the control during proliferation. This was expected because SGBS do not spontaneously proliferate but would need differentiation inducing media. However, quercetin levels of expression were slightly



elevated to those of chrysin. This variation may be because these genes are not exclusively limited to differentiation but have crossovers with proliferation and other cellular functions. They are known, for example to be involved in insulin sensitivity, glucose uptake and energy homeostasis (McNay and Pearson-Leary, 2020).

The gene transcript results gave a good indication of the potential pathways that are affected by the flavonoids; however, protein analysis was equally important to pursue because proteins are more direct mediators of cellular processes (Powers and Palecek, 2012). Besides the classic transcription translation processes for protein synthesis, there are some post translational modifications that proteins undergo which dictate the ultimate action of the protein in the cellular process. Some proteins exist transiently in the cell, but some continue to bioaccumulate, and their impact is dependent on the level of abundance. The western blot results showed that the Erk and Akt pathways are modulated by the flavonoids, they also confirmed the gene transcript results of *SREBP1c*, *CEBP-β*, *PPAR gamma*, *adiponectin*, *GLUT4* and *UCP1*.

The UCP1 results were encouraging, they support the oil red O and microscopic differential counts differentiation results which suggested the potential of the browning of adipocytes after treatment by flavonoids. Besides reducing the quantity and size of white adipocytes, consuming flavonoids could actually help convert some white adipocytes to the healthier phenotype of beige cells. Recently, Pei et al. (2021) investigated the effect of quercetin on non-shivering thermogenesis of brown adipose tissue in high-fat diet-induced obese mice. Their results were not conclusive, but it would have been more interesting if their focus was on the beige phenotype. However, Arias et al. (2017) found that a combination of the flavonoids resveratrol and quercetin induces browning in white adipose tissue of rats fed an obesogenic diet. The genetic signature of their findings mirrored those of beige adipocytes.

Overall, I have shown that flavonoids quercetin and chrysin are associated with the reduction of the expression of proliferation associated genes, increase in expression of apoptosis associated genes at supra-physiological concentrations and downregulation of genes associated with differentiation. The transcriptional factors and the kinases affected suggests that the MAPK/ERK and the PI3K-AKT-mTOR pathways are involved in how flavonoids affect adipogenesis. Of greatest interest is the apparent browning of the adipocytes as seen by the increase in UCP1 expression at physiological concentrations.

Quercetin and chrysin when consumed consistently are therefore potential ingredients of both fat reduction and conversion to a healthier form.

#### 6.4. Future work

At the beginning of this study, it was hoped that besides pure flavonoids, flavonoid metabolites would be generated by growing SGBS cells in media containing metabolised flavonoids after passing them through Caco-2/TC-7 human colon adenocarcinoma cells that mimic the gut. Although the method was developed and optimised, the yield of metabolites was small but resonated with literature. There was no merit in trying to feed the low yields which were generally lower than normal physiological concentrations. The study was therefore limited in the sense that it could not be shown whether flavonoid metabolites had the same effect as the flavonoids themselves as originally designed.

The study established that the MTT assay had limitations when it came to investigating proliferation in cells treated with combined flavonoids. Although the cell count parallel was enough to answer the question, it would have been better to have an independent confirmatory test alongside the counts. In the same manner, resources limited the diversity of flavonoids that could be investigated for molecular to all the 6 that were taken through proliferation and differentiation experiments. A more complete picture would have engaged all the flavonoid combinations for gene expression and protein analysis.

Finally, a complete map of the pathway by which the flavonoids exert their effect on adipogenesis would have been better achieved by investigating many more genes and transcription factors. For example, in elucidating the exact apoptotic pathway the cells could have gone through, a whole panel of *BcXL*, *BCL*, *BAK*, *caspases*, *FSL* and such other genes would need to be investigated. The same can be said about the complete panel of antibodies that would have been needed for a broader picture using western blots.

This work could be developed in two areas. The first is that of dedifferentiating cells that have been treated with low doses of flavonoids and see whether they more readily dedifferentiate compared to the wild type. The emerging preadipocytes would redifferentiate using media designed to differentiate into adipocytes, osteoblasts, or muscle cells. This could answer the question of why nature allows proliferation of

preadipocytes at low flavonoid concentrations, is it to allow a pool of more preadipocytes that can be redifferentiated to other cells that confer better health?

The second area that this work could benefit from is focusing on the browning of white adipocytes. Whilst UCP1 is a well-studied defining transcript, putative beige cells after would benefit from further qualifiers for example, by using flow cytometry to ascertain relevant CD markers which definitively define beige cells. Furthermore, quantifying the “beigeness” would be more interesting, can some cells be more beige than the others after flavonoid or flavonoid combination treatment?

### 6.5. Conclusion

This thesis has looked at the effects of flavonoids on adipogenesis. It investigated how the flavonoid classes of flavones and flavonols in singles and in cross class combinations affect the rate of proliferation of preadipocytes and the differentiation of the preadipocytes into fully committed adipocytes. Proliferation work used MTT assays and microscopic cell counts to evaluate the effect of flavonoid concentration which ranged from very low, physiological, supra-physiological and very high concentrations. Differential microscopic cell counts oil red O assays and triglyceride quantification assays were used to quantify the effects of the flavonoid classes and their combinations on differentiation. Gene transcript analysis using RT-qPCR and protein analysis using western blots was used to map out putative mechanism by which the flavonoids effected preadipocytes and differentiated adipocytes.

Flavonoids and their combinations reduced preadipocyte proliferation at and above supra-physiological concentrations. At low concentrations, the flavonoid treatment exhibited hormesis in that proliferation was generally increased compared to the untreated controls. Flavonoid combinations appeared to be synergistic with a few exceptions, whilst flavones were comparatively more effective than flavonols. Effectiveness of flavonols increased with the number of hydroxyl groups on the determinant (B) carbon ring whereas flavones were the opposite. It was suggested that lipophilicity in flavones and hydroxyl group hydrogen bonding with hydrophilic outer end of the cell membrane in flavonols could, amongst other things, be responsible for their effectiveness. Combined flavonoid classed were thought to benefit from a combination of the merits of the separate flavones and flavonols as well as the putative formation of cocrystals. Preadipocytes treated once with a range of the concentrations recovered and continued to grow when incubated for 7 days. This suggested

that the bioavailability of flavonoids, if not replenished would decay suggesting the importance of continually consuming the flavonoids.

All flavonoid concentrations, single or in combinations, caused reduction in preadipocyte differentiation, that included the low concentrations that increased proliferation in preadipocyte growth experiments. Combining flavonoids appeared to have an additive effect in most combinations with a few that were less effective than the individual constituents. Treatment timing during the differentiation stages did not matter as treating before, during and after differentiation induction all reduced the rate of differentiation. However, treating at all 3 stages resulted in the highest decrease of the rate of differentiation. This again has application relevance in the consumption of the flavonoids. A small disparity between oil red O results and cell counts opened up the fact that not only does the rate of differentiation get reduced, but the sizes of the oil droplets per cell are smaller and fewer. This finding suggested that white adipocytes could be converting to their beige phenotype.

Transcript expression assays and western blots on a selected few flavonoids indicated suggested that the effectiveness of the flavonoids could be driven by reduction in the expression of proliferation genes and higher concentrations, increased expression of apoptotic genes and modulation of genes related to differentiation, insulin sensitivity, glucose uptake and browning. This all presents an attractive suggestion that flavones and flavonols can reduce the level of adipocyte differentiation whilst converting white adipocytes into healthier phenotypes. Confirmatory experiments on the putative emerging beige cells still need to be robustly carried out.

## 7 References:

- Abdallah, H.M., Hassan, N.A., El-Halawany, A.M., Mohamed, G.A., Safo, M.K. and El-Bassossy, H.M., (2020). Major flavonoids from *Psiadia punctulata* produce vasodilation via activation of endothelial dependent NO signaling. *Journal of Advanced Research*, 24, pp.273-279.
- Abotaleb, M., Samuel, S. M., Varghese, E., Varghese, S., Kubatka, P., Liskova, A., & Büsselberg, D. (2018). Flavonoids in Cancer and Apoptosis. *Cancers*, 11(1).
- Achari, A.E. and Jain, S.K., (2017). AdiponectinAdiponectin, a therapeutic target for obesity, diabetes, and endothelial dysfunction. *International Journal of Molecular Sciences*, 18(6).
- Adlung, L., Kar, S., Wagner, M.C., She, B., Chakraborty, S., Bao, J., Lattermann, S., Boerries, M., Busch, H., Wuchter, P. and Ho, A.D., (2017). Protein abundance of AKT and ERK pathway components governs cell type-specific regulation of proliferation. *Molecular Systems Biology*, 13(1).
- Agouni, A., Lagrue-Lak-Hal, A.H., Mostefai, H.A., Tesse, A., Mulder, P., Rouet, P., Desmoulin, F., Heymes, C., Martinez, M.C., Andriantsitohaina, R. (2009). Red wine polyphenols prevent metabolic and cardiovascular alterations associated with obesity in Zucker fatty rats (Fa/Fa) *PLoS One*. 214; pp 67-78
- Ahmadian, M., Suh, J.M., Hah, N., Liddle, C., Atkins, A.R., Downes, M. and Evans, R.M., (2013). PPAR $\gamma$  signaling and metabolism: the good, the badBADbad and the future. *Nature Medicine*, 19(5).
- Ahn, J., Lee, H., Kim, S., Park, J., & Ha, T. (2008). The anti-obesity effect of quercetin is mediated by the AMPK and MAPK signaling pathways. *Biochemical and Biophysical Research Communications*, 373(4).
- Al-Maamari, J.N.S., Rahmadi, M., Panggono, S.M., Prameswari, D.A., Pratiwi, E.D., Ardianto, C., Balan, S.S. and Suprapti, B., (2021). The effects of quercetin on the expression of SREBP-1c mRNA in high-fat diet-induced NAFLD in mice. *Journal of Basic and Clinical Physiology and Pharmacology*, 32(4).

Al-Odat, O.S., Guirguis, D.A., Schmalbach, N.K., Yao, G., Budak-Alpdogan, T., Jonnalagadda, S.C. and Pandey, M.K., (2022). Autophagy and Apoptosis: Current Challenges of Treatment and Drug Resistance in Multiple Myeloma. *International Journal of Molecular Sciences*, 24(1), p.644.

Amin, M.U., Khurram, M., Khattak, B. and Khan, J., (2015). Antibiotic additive and synergistic action of rutin, morin and quercetin against methicillin resistant *Staphylococcus aureus*. *BMC Complementary and Alternative Medicine*, 15(1), pp.1-12.

Anari, L., Mehrabani, D., Nasiri, M., Zare, S., Jamhiri, I. and Acker, J., (2022). in Vitro Effect of Methamphetamine on Proliferation, Differentiation and Apoptosis of Adipose Tissue Stem Cells: In vitro Effect of Methamphetamine. *Journal of Pharmacy & Pharmaceutical Sciences*, 25.

Andrea, G., & Enrique, S. (2021). Isolation and differentiation of primary white and brown preadipocytes from newborn mice. *JoVE (Journal of Visualized Experiments)*,

Apovian, C.M., 2016. Obesity: definition, comorbidities, causes, and burden. *The American journal of managed care*, 22(7 Suppl), pp.s176-85.

Arias, N., Macarulla, M.T., Aguirre, L., Martínez-Castaño, M.G. and Portillo, M.P., (2014). Quercetin can reduce insulin resistance without decreasing adipose tissue and skeletal muscle fat accumulation. *Genes & nutrition*, 9(1),1-9.

Arias, N., Picó, C., Teresa Macarulla, M., Oliver, P., Miranda, J., Palou, A., & Portillo, M. P. (2017). A combination of resveratrol and quercetin induces browning in white adipose tissue of rats fed an obesogenic diet. *Obesity*, 25(1).

Arias, N., Picó, C., Teresa Macarulla, M., Oliver, P., Miranda, J., Palou, A. and Portillo, M.P., (2017). A combination of resveratrol and quercetin induces browning in white adipose tissue of rats fed an obesogenic diet. *Obesity*, 25(1), pp.111-121.

Arimochi, H., Sasaki, Y., Kitamura, A., & Yasutomo, K. (2016). Differentiation of preadipocytes and mature adipocytes requires PSMB8. *Scientific reports*, 6(1), 1-8.

Arner, P., Bernard, S., Salehpour, M., Possnert, G., Liebl, J., Steier, P., Buchholz, B.A., Eriksson, M., Arner, E., Hauner, H., Skurk, T., Rydén, M., Frayn, K.N. and Spalding, K.L. (2011). Dynamics

of human adipose lipid turnover in health and metabolic disease. *Nature*. 25;478(7367):110-3.

Artaud-Wild, S.M., Connor, S.L., Sexton, G. and Connor, W.E., 1993. Differences in coronary mortality can be explained by differences in cholesterol and saturated fat intakes in 40 countries but not in France and Finland. A paradox. *Circulation*, 88(6), pp.2771-2779.

Audano, M., Pedretti, S., Caruso, D., Crestani, M., De Fabiani, E. and Mitro, N., (2022). Regulatory mechanisms of the early phase of white adipocyte differentiation: An overview. *Cellular and Molecular Life Sciences*, 79(3), pp.1-14.

Bae, C.R., Park, Y.K. and Cha, Y.S., (2014). Quercetin-rich onion peel extract suppresses adipogenesis by down-regulating adipogenic transcription factors and gene expression in 3T3-L1 adipocytes. *Journal of the Science of Food and Agriculture*, 94(13).

Baserga, R. (2008). "Biochemistry of the Cell Cycle: A Review". *Cell Proliferation*. 1 (2): 167–191

Batsis, J.A., Mackenzie, T.A., Bartels, S.J., Sahakyan, K.R., Somers, V.K. and Lopez-Jimenez, F., 2016. Diagnostic accuracy of body mass index to identify obesity in older adults: NHANES 1999–2004. *International journal of obesity*, 40(5), pp.761-767.

Biagi, M. and Bertelli, A.A., (2015). Wine, alcohol and pills: What future for the French paradox? *Life sciences*, 131, pp.19-22.

Bosdou, J.K., Kolibianakis, E.M., Tarlatzis, B.C. and Fatemi, H.M., (2016). Sociocultural influences on fertility in the Middle East: the role of parental consanguinity, obesity and vitamin D deficiency. *Fertility and sterility*, 106(2), pp.259-260.

Bouraoui, L., Gutiérrez, J. and Navarro, I., (2008). Regulation of proliferation and differentiation of adipocyte precursor cells in rainbow trout (*Oncorhynchus mykiss*). *Journal of Endocrinology*, 198(3), pp.459-469.

Branco, J.C., Motta, J., Wiener, C., Oses, J.P., Pedrotti Moreira, F., Spessato, B., Dias, L. and da Silva, R., (2017). Association between obesity and suicide in woman, but not in man: a population-based study of young adults. *Psychology, health & medicine*, 22(3), pp.275-281.

BrdU Assay, EdU Assay, MTT Assay, XTT Assay, WST-1 Assay, Luminescent ATP Assay, Ki67/Ki67, CFSE, Live/Dead Assays, Trypan Blue

Brezden, C.B. and Rauth, A.M. (1996). Differential cell death in immortalized and non-immortalized cells at confluency. *Oncogene*. 12(1).

Briggs, M.R., Yokoyama, C., Wang, X., Brown, M.S., Goldstein, J.L. (1993). Nuclear protein that binds sterol regulatory element of low-density lipoprotein receptor promoter. I. Identification of the protein and delineation of its target nucleotide sequence. *J Biol Chem*. 268(19).

Brooks, R. F. (2021). Cell cycle commitment and the origins of cell cycle variability. *Frontiers in Cell and Developmental Biology*, 9. 12-14.

Cagnol, S., & Chambard, J. C. (2010). ERK and cell death: mechanisms of ERK-induced cell death—apoptosis, autophagy and senescence. *The FEBS Journal*, 277(1).

Calabrese, E.J., (2001). Overcompensation stimulation: a mechanism for hormetic effects. *Critical Reviews in Toxicology*, 31(4-5), pp.425-470.

Calabrese, E.J., Agathokleous, E., Kapoor, R., Dhawan, G. and Calabrese, V., (2021). Luteolin and hormesis. *Mechanisms of Ageing and Development*, 199, p.111559.

Cao, Z., Umek, R.M. and McKnight, S.L., (1991). Regulated expression of three C/EBP isoforms during adipose conversion of 3T3-L1 cells. *Genes & Development*, 5(9) 2.

*Cardiodiabetes* (2023) *What are Triglycerides?* Available at: <https://clinidiabet.com/en/infodiabetes/cardiodiabetes/15.htm> (Accessed: February 22, 2023).

Carey, A.L., Vorlander, C., Reddy-Luthmoodoo, M., Natoli, A.K., Formosa, M.F., Bertovic, D.A., Anderson, M.J., Duffy, S.J. and Kingwell, B.A., (2014). Reduced UCP-1 content in in vitro differentiated beige/brite adipocytes derived from preadipocytes of human subcutaneous white adipose tissues in obesity. *PloS one*, 9(3).

Casado-Díaz, A., Rodríguez-Ramos, Á., Torrecillas-Baena, B., Dorado, G., Quesada-Gómez, J.M. and Gálvez-Moreno, M.Á., (2021). Flavonoid phloretin Inhibits adipogenesis and Increases OPG expression in adipocytes derived from human bone-marrow mesenchymal stromal-cells. *Nutrients*, 13(11), p.4185.



CDC (2022). *Defining adult overweight & obesity Centers for Disease Control and Prevention*. Centers for Disease Control and Prevention. Available at: <https://www.cdc.gov/obesity/basics/adult-defining.html> (Accessed: May8, 2022).

Chait, A. and Den Hartigh, L.J., (2020). Adipose tissue distribution, inflammation and its metabolic consequences, including diabetes and cardiovascular disease. *Frontiers in cardiovascular medicine*, 7, p.22-46.

Chan, P.C. and Hsieh, P.S., (2017). The role of adipocyte hypertrophy and hypoxia in the development of obesity-associated adipose tissue inflammation and insulin resistance. *Adiposity Omics Mol. Underst.* Online accessed at [www.intechopen.com/chapters/52454](http://www.intechopen.com/chapters/52454) on 12 November 2022.

Chawla, A., Schwarz, E.J., Dimaculangan, D.D. and Lazar, M.A., (1994). Peroxisome proliferator-activated receptor (PPAR) gamma: adipose-predominant expression and induction early in adipocyte differentiation. *Endocrinology*, 135(2).

Chen, W.S., Xu, P.Z., Gottlob, K., Chen, M.L., Sokol, K., Shiyanova, T., Roninson, I., Weng, W., Suzuki, R., Tobe, K. and Kadowaki, T., (2001). Growth retardation and increased apoptosis in mice with homozygous disruption of the Akt1 gene. *Genes & Development*, 15(17).

Chen, Y., McMillan-Ward, E., Kong, J., Israels, S.J. and Gibson, S.B., (2008). Oxidative stress induces autophagic cell death independent of apoptosis in transformed and cancer cells. *Cell Death & Differentiation*, 15(1), pp.171-182.

Chirumbolo, S., (2011). Hormesis, resveratrol and plant-derived polyphenols: some comments. *Human & experimental toxicology*, 30(12), pp.2027-2030.

Choi, H., Kim, C.S. and Yu, R., (2019). Quercetin Upregulates Uncoupling Protein 1 in White/Brown Adipose Tissues through Sympathetic Stimulation. *Journal of Obesity & Metabolic Syndrome*, 28(1).

Choudhari, A.S., Mandave, P.C., Deshpande, M., Ranjekar, P. and Prakash, O., (2020). Phytochemicals in cancer treatment: From preclinical studies to clinical practice. *Frontiers in Pharmacology*, 1614.

Ciavarella, C., Motta, I., Valente, S. and Pasquinelli, G., (2020). Pharmacological (or synthetic) and nutritional agonists of PPAR- $\gamma$  as candidates for cytokine storm modulation in COVID-19 disease. *Molecules*, 25(9).

Cinti, S. (2005). The adipose organ. *Prostaglandins Leukot Essent Fatty Acids* 73:9–15.

Dalasanur-Nagaprashantha, L., Adhikari, R., Singhal, J., Chikara, S., Awasthi, S., Horne, D., & Singhal, S. S. (2018). Translational opportunities for broad-spectrum natural phytochemicals and targeted agent combinations in breast cancer. *International Journal of Cancer*, 142(4).

D'amato, F. (1989). Polyploidy in cell differentiation. *Caryologia*, 42(3-4), 183-211.

DeFuria J., Bennett G., Strissel K.J., Perfield J.W., 2nd, Milbury P.E., Greenberg A.S., Obin M.S. (2009). Dietary blueberry attenuates whole-body insulin resistance in high fat-fed mice by reducing adipocyte death and its inflammatory sequelae. *J. Nutr.* 139:1510–1516.

Dias, M.C., Pinto, D.C. and Silva, A.M., (2021). Plant flavonoids: Chemical characteristics and biological activity. *Molecules*, 26(17), p.5377.

Du, X., Fu, X., Yao, K., Lan, Z., Xu, H., Cui, Q. and Yang, E., (2017). Bcl-2 delays cell cycle through mitochondrial ATP and ROS. *Cell Cycle*, 16(7), 707-713.

Ducluzeau, P. H., Perretti, N., Laville, M., Andreelli, F., Vega, N., Riou, J. P., & Vidal, H. (2001). Regulation by insulin of gene expression in human skeletal muscle and adipose tissue: evidence for specific defects in type 2 diabetes. *Diabetes*, 50(5).

Duronio, R. J., & Xiong, Y. (2013). Signaling pathways that control cell proliferation. *Cold Spring Harbor perspectives in biology*, 5(3), a008904.

Eberlé D, Hegarty B, Bossard P, Ferré P and Foufelle, F. (2004). SREBP transcription factors: master regulators of lipid homeostasis. *Biochimie*. 86.

Eckel, J., (2018). *The cellular secretome and organ crosstalk*. Academic Press. New York

Ellenberger, T. (1994). "Getting a grip in DNA recognition: structures of the basic region leucine zipper, and the basic region helix-loop-helix DNA-binding domains". *Current Opinion in Structural Biology*. 4 (1).

Elmegerhi, S., Su, C., Buglewicz, D.J., Aizawa, Y. and Kato, T.A., (2018). Effect of hydroxyl group position in flavonoids on inducing single-stranded DNA damage mediated by cupric ions. *International Journal of Molecular Medicine*, 42(1), pp.658-664.

Erickson, R. L., Longo, K. A., Ross, S. E., Hemati, N. & MacDougald, O. A. (2000) Structure and function of C/EBP $\alpha$ . Ntambi, J. M. eds. *Adipocyte Biology and Hormone Signalling*. IOS Press, Inc Burke, VA.

Eseberri, I., Miranda, J., Lasa, A., Mosqueda-Solís, A., González-Manzano, S., Santos-Buelga, C. and Portillo, M.P., (2019). Effects of quercetin metabolites on triglyceride metabolism of 3T3-L1 preadipocytes and mature adipocytes. *International journal of molecular sciences*, 20(2), 264.

Fajas, L., Schoonjans, K., Gelman, L., Kim, J.B., Najib, J., Martin, G., Fruchart, J.C., Briggs, M., Spiegelman, B.M. and Auwerx, J., (1999). Regulation of peroxisome proliferator-activated receptor  $\gamma$  expression by adipocyte differentiation and determination factor 1/sterol regulatory element binding protein 1: implications for adipocyte differentiation and metabolism. *Molecular and Cellular Biology*, 19(8).

Fan, C.D., Lum, M.A., Xu, C., Black, J.D. and Wang, X., (2013). Ubiquitin-dependent regulation of phospho-AKT dynamics by the ubiquitin E3 ligase, NEDD4-1, in the insulin-like growth factor-1 response. *Journal of Biological Chemistry*, 288(3).

Fan, J. Y., Carpentier, J. L., Van Obberghen, E., Grunfeld, C., Gorden, P., and Orci, L. (1983). Morphological changes of the 3T3-L1 fibroblast plasma membrane upon differentiation to the adipocyte form. *Journal of Cell Science*, 61(1), 219-230.

Feng, X., Weng, D., Zhou, F., Owen, Y.D., Qin, H., Zhao, J., Huang, Y., Chen, J., Fu, H., Yang, N. and Chen, D., (2016). Activation of PPAR gamma by a natural flavonoid modulator, apigenin ameliorates obesity-related inflammation via regulation of macrophage polarization. *EBioMedicine*, 9.

Fernández, A., Ordóñez, R., Reiter, R.J., González-Gallego, J. and Mauriz, J.L., (2015). Melatonin and endoplasmic reticulum stress: relation to autophagy and apoptosis. *Journal of pineal research*, 59(3), pp.292-307.

Ferre, P., & Foufelle, F. (2007). SREBP-1c transcription factor and lipid homeostasis: clinical perspective. *Hormone Research in Paediatrics*, 68(2).

Ferrières, J. (2004). The French paradox: lessons for other countries. *Heart*, 90(1), 107–111.

Fève, B. (2005). Adipogenesis: cellular and molecular aspects. *Best Practice & Research Clinical Endocrinology & Metabolism*, 19(4), 483-499.

Finkelstein, E.A., Khavjou, O.A., Thompson, H., Trogon, J.G., Pan, L., Sherry, B. and Dietz, W., (2012). Obesity and severe obesity forecasts through 2030. *American journal of preventive medicine*, 42(6), pp.563-570.

Fischer-Posovszky, P., Newell, F.S., Wabitsch, M. and Tornqvist, H.E., (2008). Human SGBS cells—a unique tool for studies of human fat cell biology. *Obesity facts*, 1(4), 184-189.

Forney, L. A., Lenard, N. R., Stewart, L. K., & Henagan, T. M. (2018). Dietary Quercetin Attenuates Adipose Tissue Expansion and Inflammation and Alters Adipocyte Morphology in a Tissue-Specific Manner. *International journal of molecular sciences*, 19(3).

Freedman, D.S., Butte, N.F., Taveras, E.M., Lundeen, E.A., Blanck, H.M., Goodman, A.B. and Ogden, C.L., 2017. BMI z-Scores are a poor indicator of adiposity among 2-to 19-year-olds with very high BMIs, NHANES 1999-2000 to 2013-2014. *Obesity*, 25(4), pp.739-746.

Fu, Y., Luo, N., Klein, R. L., & Garvey, W. T. (2005). Adiponectin promotes adipocyte differentiation, insulin sensitivity, and lipid accumulation. *Journal of Lipid Research*, 46(7) 9.

Galmozzi, A., Kok, B. P., & Saez, E. (2021). Isolation and differentiation of primary white and brown preadipocytes from newborn mice. *JoVE (Journal of Visualized Experiments)*, (167), e62005.

Garcia, A.J., Vega, M.D. and Boettiger, D., (1999). Modulation of cell proliferation and differentiation through substrate-dependent changes in fibronectin conformation. *Molecular Biology of the Cell*, 10(3).

García-Barrado, M.J., Iglesias-Osma, M.C., Pérez-García, E., Carrero, S., Blanco, E.J., Carretero-Hernández, M. and Carretero, J., (2020). Role of flavonoids in the interactions among obesity, inflammation, and autophagy. *Pharmaceuticals*, 13(11), p.342.

Garofalo, R.S., Orena, S.J., Rafidi, K., Torchia, A.J., Stock, J.L., Hildebrandt, A.L., Coskran, T., Black, S.C., Brees, D.J., Wicks, J.R. and McNeish, J.D., (2003). Severe diabetes, age-dependent loss of adipose tissue, and mild growth deficiency in mice lacking Akt2/PKB $\beta$ . *The Journal of Clinical Investigation*, 112(2).

Garrow, J.S. (1988) Obesity and related diseases. London: Churchill Livingstone.

Gathercole, L. L., Morgan, S. A., & Tomlinson, J. W. (2013). Hormonal regulation of lipogenesis. *Vitamins & Hormones*, 91.

Ghaben, A.L. and Scherer, P.E., (2019). Adipogenesis and metabolic health. *Nature reviews Molecular cell biology*, 20(4), pp.242-258.

Ghahremani, H. and Salami, S., 2021. French Paradox, Alcohol, and Health Related Concerns. *International Journal of Cancer Management*, 14(7).

Ghemrawi, R., Battaglia-Hsu, S. F., & Arnold, C. (2018). Endoplasmic reticulum stress in metabolic disorders. *Cells*, 7(6).

Ghoniem, A. A., Ail, Y., Wiltfang, J., & Gierloff, M. (2015). Improved adipogenic in vitro differentiation: comparison of different adipogenic cell culture media on human fat and bone stroma cells for fat tissue engineering. *Anatomy & cell biology*, 48(2), 85-94.

Giroud, M., Jodeleit, H., Prentice, K.J. and Bartelt, A., (2022). Adipocyte function and the development of cardiometabolic disease. *The Journal of Physiology*, 600(5), pp.1189-1208.

Gonzalez-Menendez, P., Hevia, D., Rodriguez-Garcia, A., Mayo, J.C. and Sainz, R.M., (2014). Regulation of GLUT transporters by flavonoids in androgen-sensitive and-insensitive prostate cancer cells. *Endocrinology*, 155(9).

Goossens, C., Vander Perre, S., Van den Berghe, G., & Langouche, L. (2017). Proliferation and differentiation of adipose tissue in prolonged lean and obese critically ill patients. *Intensive care medicine experimental*, 5(1), 1-15.

Goossens, G.H., (2017). The metabolic phenotype in obesity: fat mass, body fat distribution, and adipose tissue function. *Obesity facts*, 10(3), pp.207-215.

Govers, R., (2014). Molecular mechanisms of GLUT4GLUT4 regulation in adipocytes. *Diabetes & Metabolism*, 40(6).

- Granada, A. E., Jiménez, A., Stewart-Ornstein, J., Blüthgen, N., Reber, S., Jambhekar, A., and Lahav, G. (2020). The effects of proliferation status and cell cycle phase on the responses of single cells to chemotherapy. *Molecular biology of the cell*, 31(8), 845-857.
- Green, D. R., & Llambi, F. (2015). Cell Death Signaling. *Cold Spring Harbor Perspectives in Biology*, 7(12).
- Green, H., and Kehinde, O. (1974). Sublines of mouse 3T3 cells that accumulate lipid. *Cell*, 1(3), 113-116.
- Gregoire, F. M., Smas, C. M., and Sul, H. S. (1998). Understanding adipocyte differentiation. *Physiological reviews*, 78(3), 783-809.
- Grijalva-Guiza, R.E., Jiménez-Garduño, A.M. and Hernández, L.R., (2021). Potential Benefits of Flavonoids on the Progression of Atherosclerosis by Their Effect on Vascular Smooth Muscle Excitability. *Molecules*, 26(12), p.3557.
- Grilo, A. L., & Mantalaris, A. (2019). Apoptosis: A mammalian cell bioprocessing perspective. *Biotechnology Advances*, 37(3) 5.
- Gryniewicz, G., Zegrocka-Stendel, O., Pucko, W., Ramza, J., Kościelecka, A., Kołodziejki, W. and Woźniak, K., (2004). X-ray and <sup>13</sup>C CP MAS investigations of structure of two genistein derivatives. *Journal of molecular structure*, 694(1-3), pp.121-129.
- Gugler, R., Leschik, M. and Dengler, H.J., (1975). Disposition of quercetin in man after single oral and intravenous doses. *European journal of clinical pharmacology*, 9(2).
- Guo, L., Li, X. and Tang, Q.Q., (2015). Transcriptional regulation of adipocyte differentiation: a central role for CCAAT/enhancer-binding protein (C/EBP)  $\beta$ . *Journal of Biological Chemistry*, 290(2).
- Guo, W., Wong, S., Xie, W., Lei, T., & Luo, Z. (2007). Palmitate modulates intracellular signalling, induces endoplasmic reticulum stress, and causes apoptosis in mouse 3T3-L1 and rat primary preadipocytes. *American Journal of Physiology-Endocrinology and Metabolism*, 293(2).

Guo, X., Liu, J., Cai, S., Wang, O. and Ji, B., (2016). Synergistic interactions of apigenin, naringin, quercetin and emodin on inhibition of 3T3-L1 preadipocyte differentiation and pancreas lipase activity. *Obesity Research & Clinical Practice*, 10(3), pp.327-339.

Guo, Y. J., Pan, W. W., Liu, S. B., Shen, Z. F., Xu, Y., & Hu, L. L. (2020). ERK/MAPK signalling pathway and tumorigenesis. *Experimental and Therapeutic Medicine*, 19(3).

Ha, J.H., Jang, J., Chung, S.I. and Yoon, Y., (2016). AMPK and SREBP-1c mediate the anti-adipogenic effect of  $\beta$ -hydroxyisovalerylshikonin. *International Journal of Molecular Medicine*, 37(3).

Hadrich, F. and Sayadi, S., (2018). Apigenin inhibits adipogenesis in 3T3-L1 cells by downregulating PPAR $\gamma$  and CEBP- $\alpha$ . *Lipids in Health and Disease*, 17(1).

Hai, Y., Zhang, Y., Liang, Y., Ma, X., Qi, X., Xiao, J., Xue, W., Luo, Y. and Yue, T., (2020). Advance on the absorption, metabolism, and efficacy exertion of quercetin and its important derivatives: Absorption, metabolism and function of quercetin. *Food Frontiers*, 1(4), 420-434.

Harasstani, O.A., Moin, S., Tham, C.L., Liew, C.Y., Ismail, N., Rajajendram, R., Harith, H.H., Zakaria, Z.A., Mohamad, A.S., Sulaiman, M.R. and Israf, D.A., (2010). Flavonoid combinations cause synergistic inhibition of proinflammatory mediator secretion from lipopolysaccharide-induced RAW 264.7 cells. *Inflammation research*, 59, pp.711-721.

Hardcastle, S., Taylor, A., Bailey, M. and Castle, R., (2008). A randomised controlled trial on the effectiveness of a primary health care-based counselling intervention on physical activity, diet and CHD risk factors. *Patient education and counseling*, 70(1), pp.31-39.

Harmon, A.W. and Harp, J.B., (2001). Differential effects of flavonoids on 3T3-L1 adipogenesis and lipolysis. *American Journal of Physiology-cell physiology*, 280(4), pp.C807-C813

Harris, R.B., (2014). Direct and indirect effects of leptin on adipocyte metabolism. *Biochimica et Biophysica Acta (BBA)-Molecular Basis of Disease*, 1842(3).

Heenan, K.A., Carrillo, A.E., Fulton, J.L., Ryan, E.J., Edsall, J.R., Rigopoulos, D., Markofski, M.M., Flouris, A.D. and Dinas, P.C., (2020). Effects of nutrition/diet on brown adipose tissue in humans: A systematic review and meta-analysis. *Nutrients*, 12(9), p.2752.

Hojjat, T.A. and Hojatt, R., (2021). *Economics of obesity*. Springer International Publishing.

Hollman, P.C., Van Trijp, J.M., Buysman, M.N., vd Gaag, M.S., Mengelers, M.J., De Vries, J.H. and Katan, M.B., (1997). Relative bioavailability of the antioxidant flavonoid quercetin from various foods in man. *FEBS letters*, 418(1-2), pp.152-156.

Holman, G. D. (2020). Structure, function and regulation of mammalian glucose transporters of the SLC2 family. *Pflügers Archiv-European Journal of Physiology*, 472(9).

Hostetler, G.L., Ralston, R.A. and Schwartz, S.J., (2017). Flavones: Food sources, bioavailability, metabolism, and bioactivity. *Advances in Nutrition*, 8(3), pp.423-435.

Huang, S. and Czech, M.P. (2007). The GLUT4GLUT4 glucose transporter. *Cell Metabolism*. 5(4).

Huang, S., Xue, Q., Xu, J., Ruan, S. and Cai, T., (2019). Simultaneously improving the physicochemical properties, dissolution performance, and bioavailability of apigenin and daidzein by co-crystallization with theophylline. *Journal of Pharmaceutical Sciences*, 108(9), pp.2982-2993.

Hübner, A., Barrett, T., Flavell, R. A., & Davis, R. J. (2008). Multisite phosphorylation regulates BIM/BIM stability and apoptotic activity. *Molecular Cell*, 30(4).

Iannaccone, M., D'Olimpio, F., Cella, S. and Cotrufo, P., (2016). Self-esteem, body shame and eating disorder risk in obese and normal weight adolescents: A mediation model. *Eating behaviors*, 21, pp.80-83.

Ikeda, K. and Yamada, T., (2020). UCP1UCP1 dependent and independent thermogenesis in brown and beige adipocytes. *Frontiers in Endocrinology*, 11.

Im, S.S., Kwon, S.K., Kang, S.Y., Kim, T.H., Kim, H.I., Hur, M.W., Kim, K.S. and Ahn, Y.H., (2006). Regulation of GLUT4GLUT4 gene expression by SREBP-1c in adipocytes. *Biochemical Journal*, 399(1).

Iqbal, H. M. N., & Keshavarz, T. (2017). The challenge of biocompatibility evaluation of biocomposites. In *Biomedical Composites* (pp. 303-334). Woodhead Publishing.

Isika, D.K., Özkömeç, F.N., Çeşme, M. and Sadik, O.A., (2022). Synthesis, biological and computational studies of flavonoid acetamide derivatives. *RSC Advances*, 12(16), pp.10037-10050.



Ivey, K.L., Jensen, M.K., Hodgson, J.M., Eliassen, A.H., Cassidy, A. and Rimm, E.B., (2017). Association of flavonoid-rich foods and flavonoids with risk of all-cause mortality. *British Journal of Nutrition*, 117(10), pp.1470-1477.

Jakobs, A., Steinmann, S., Henrich, S.M., Schmidt, T.J. and Klempnauer, K.H., (2016). Helenalin acetate, a natural sesquiterpene lactone with anti-inflammatory and anti-cancer activity, disrupts the cooperation of CCAAT box/enhancer-binding protein  $\beta$  (C/EBP beta) and co-activator p300. *Journal of Biological Chemistry*, 291(50).

Jeong, S., Davis, J., Rodriguez, J. and Han, Y., (2016). What makes them more vulnerable than others? Obesity, negative emotions, and peer bullying victimization. *International journal of offender therapy and comparative criminology*, 60(14), pp.1690-1705.

Jiang, L., Rong, J., Wang, Y., Hu, F., Bao, C., Li, X. and Zhao, Y. (2011). The relationship between body mass index and hip osteoarthritis: a systematic review and meta-analysis. *Joint Bone Spine*, 78(2), pp.150-155.

Jiao, H., Shen, W., Ohe, Y., Miura, K., Tamura, T., & Saijo, N. (1992). A new 3-(4, 5-dimethylthiazol-2-yl)-2, 5-diphenyltetrazolium bromide (MTT) assay for testing macrophage cytotoxicity to L1210 and its drug-resistant cell lines in vitro. *Cancer Immunology, Immunotherapy*, 35(6), 412-416.

Jimenez-Giron, A., Queipo-Ortuño, M.I., Boto-Ordóñez, M., Muñoz-González, I., Sánchez-Patan, F., Monagas, M., Martín-Alvarez, P.J., Murri, M., Tinahones, F.J., Andrés-Lacueva, C. and Bartolomé, B., (2013). Comparative study of microbial-derived phenolic metabolites in human feces after intake of gin, red wine, and dealcoholized red wine. *Journal of Agricultural and Food Chemistry*, 61(16), pp.3909-3915.

Joshi, M., Pathak, K. and Dhaneshwa, S., (2022). Nanotechnology-based strategies for effective delivery of phytoconstituents for the management of rheumatoid arthritis. *Pharmacological Research-Modern Chinese Medicine*, 100061.

Jung, S.M., Sanchez-Gurmaches, J. and Guertin, D.A. (2019). Brown Adipose Tissue Development and Metabolism. *Handb Exp Pharmacol*. 251:3-36. doi: 10.1007/164-168.

Jung, U.J., Lee, M.K., Park, Y.B., Kang, M.A. and Choi, M.S., 2006. Effect of citrus flavonoids on lipid metabolism and glucose-regulating enzyme mRNA levels in type-2 diabetic mice. *The International Journal of Biochemistry & Cell Biology*, 38(7).

Jurasekova, Z., Domingo, C., García-Ramos, J.V. and Sánchez-Cortés, S., (2014). Effect of pH on the chemical modification of quercetin and structurally related flavonoids characterized by optical (UV-visible and Raman) spectroscopy. *Physical Chemistry Chemical Physics*, 16(25), pp.12802-12811.

Kale, J., Osterlund, E.J. and Andrews, D.W., (2018). BCL-2 family proteins: changing partners in the dance towards death. *Cell Death & Differentiation*, 25(1).

Kamiya, T., Nagamine, R., Sameshima-Kamiya, M., Tsubata, M., Ikeguchi, M. and Takagaki, K., (2012). The isoflavone-rich fraction of the crude extract of the Puerariae flower increases oxygen consumption and BAT UCP1/UCP1 expression in high-fat diet-fed mice. *Global Journal of Health Science*, 4(5).

Keaver, L., Xu, B., Jaccard, A. and Webber, L., (2020). Morbid obesity in the UK: A modelling projection study to 2035. *Scandinavian Journal of Public Health*, 48(4), pp.422-427.

Kelly, G.L. and Strasser, A., (2020). "Toward Targeting Antiapoptotic MCL-1 for Cancer Therapy". *Annual Review of Cancer Biology*. 4.

Khalilpourfarshbafi, M., Gholami, K., Murugan, D. D., Abdul Sattar, M. Z., & Abdullah, N. A. (2019). Differential effects of dietary flavonoids on adipogenesis. *European Journal of Nutrition*, 58(1).

Khan, A.W., Kotta, S., Ansari, S.H., Sharma, R.K. and Ali, J., (2015). Enhanced dissolution and bioavailability of grapefruit flavonoid Naringenin by solid dispersion utilizing fourth generation carrier. *Drug development and industrial pharmacy*, 41(5), pp.772-779.

Khanna, D., Peltzer, C., Kahar, P. and Parmar, M.S., 2022. Body mass index (BMI): a screening tool analysis. *Cureus*, 14(2).

Khaodhiar, L., McCowen, K.C. and Blackburn, G.L., (1999). Obesity and its comorbid conditions. *Clinical cornerstone*, 2(3), pp.17-31.

Kim, G.S., Park, H.J., Woo, J.H., Kim, M.K., Koh, P.O., Min, W., Ko, Y.G., Kim, C.H., Won, C.K. and Cho, J.H., (2012). Citrus aurantium flavonoids inhibit adipogenesis through the Akt signaling pathway in 3T3-L1 cells. *BMC Complementary and Alternative Medicine*, 12(1).

Kim, H.J., You, M.K., Lee, Y.H., Kim, H.J., Adhikari, D. and Kim, H.A., (2018). Red pepper seed water extract inhibits preadipocyte differentiation and induces mature adipocyte apoptosis in 3T3-L1 cells. *Nutrition Research and Practice*, 12(6).

Kim, J. H., Lee, S., and Cho, E. J. (2020). Flavonoids from *Acer okamotoanum* inhibit adipocyte differentiation and promote lipolysis in the 3T3-L1 cells. *Molecules*, 25(8), 1920.

Kim, J.B., Sarraf, P., Wright, M., Yao, K.M., Mueller, E., Solanes, G., Lowell, B.B. and Spiegelman, B.M., (1998). Nutritional and insulin regulation of fatty acid synthetase and leptin gene expression through ADD1/SREBP1. *The Journal of Clinical Investigation*, 101(1).

Kim, J.B., Wright, H.M., Wright, M., Spiegelman, B.M. (1998). ADD1/SREBP1 activates PPARgamma through the production of endogenous ligand. *Proc Natl Acad Sci USA*. 1998;95(8).

Kim, J.Y., 2021. Optimal diet strategies for weight loss and weight loss maintenance. *Journal of obesity & metabolic syndrome*, 30(1), p.20.

King, M.R., Petry, S. (2020). Phase separation of TPX2TPX2 enhances and spatially coordinates microtubule nucleation. *Nature Communication*. 11.

Kiraz, Y., Adan, A., Kartal Yandim, M., Baran, Y. (2016). Major apoptotic mechanisms and genes involved in apoptosis. *Tumour Biology*. 37(7).

Kling, B., Bücherl, D., Palatzky, P., Matysik, F.M., Decker, M., Wegener, J. and Heilmann, J., (2014). Flavonoids, flavonoid metabolites, and phenolic acids inhibit oxidative stress in the neuronal cell line HT-22 monitored by ECIS and MTT assay: a comparative study. *Journal of Natural Products*, 77(3), pp.446-454.

Kobayashi, M., Fujii, N., Narita, T., & Higami, Y. (2018). SREBP-1c-Dependent Metabolic Remodeling of White Adipose Tissue by Caloric Restriction. *International Journal of Molecular Sciences*, 19(11).

Kraus, N. A., Ehebauer, F., Zapp, B., Rudolphi, B., Kraus, B. J., and Kraus, D. (2016). Quantitative assessment of adipocyte differentiation in cell culture. *Adipocyte*, 5(4), 351-358.

Kroemer, G., Marino, G., and Levine, B. (2010). Autophagy and the integrated stress response. *Molecular Cell* 40

Kuipers, E.N., Dam, A.D.V., Held, N.M., Mol, I.M., Houtkooper, R.H., Rensen, P.C. and Boon, M.R., (2018). Quercetin lowers plasma triglycerides accompanied by white adipose tissue browning in diet-induced obese mice. *International Journal of Molecular Sciences*, 19(6), p.1786.

Kumar, S. and Pandey, A.K., (2013). Chemistry and biological activities of flavonoids: an overview. *The scientific world journal*, 16(1). pp.147-152.

Kumari, A., Yadav, S.K., Pakade, Y.B., Singh, B. and Yadav, S.C., (2010). Development of biodegradable nanoparticles for delivery of quercetin. *Colloids and Surfaces B: Biointerfaces*, 80(2), pp.184-192.

Lajous, M., Bijon, A., Fagherazzi, G., Boutron-Ruault, M.C., Balkau, B., Clavel-Chapelon, F. and Hernán, M.A., 2014. Body mass index, diabetes, and mortality in French women: explaining away a “paradox”. *Epidemiology (Cambridge, Mass.)*, 25(1), p.10.

Lane, M. D., Tang, Q. & Jiang, M. (1999). Role of the CCAAT enhancer binding proteins (C/EBPs) in adipocyte differentiation. *Biochemical and Biophysical Research Communications*.266

Lee, D.H., Chang, S.H., Yang, D.K., Song, N.J., Yun, U.J. and Park, K.W., (2020). Sesamol increases Ucp1/UCP1 expression in white adipose tissues and stimulates energy expenditure in high-fat diet-fed obese mice. *Nutrients*, 12(5).

Lee, J. E., Schmidt, H., Lai, B., & Ge, K. (2019). Transcriptional and epigenomic regulation of adipogenesis. *Molecular and Cellular Biology*, 39(11), e00601-18.

Lee, M. J., & Yaffe, M. B. (2016). Protein regulation in signal transduction. *Cold Spring Harbor Perspectives in Biology*, 8(6).

Lee, S.H., Kim, Y.H., Yu, H.J., Cho, N.S., Kim, T.H., Kim, D.C., Chung, C.B., Hwang, Y.I. and Kim, K.H., (2007). Enhanced bioavailability of soy isoflavones by complexation with  $\beta$ -cyclodextrin in rats. *Bioscience, biotechnology, and biochemistry*, 71(12), pp.2927-2933.

Lefterova, M.I., Zhang, Y., Steger, D.J., Schupp, M., Schug, J., Cristancho, A., Feng, D., Zhuo, D., Stoeckert, C.J., Liu, X.S. and Lazar, M.A., (2008). PPAR gamma/PPAR gamma and C/EBP factors

orchestrate adipocyte biology via adjacent binding on a genome-wide scale. *Genes & development*, 22(21).

Lehane, A.M. and Saliba, K.J. (2008). Common dietary flavonoids inhibit the growth of the intraerythrocytic malaria parasite. *BMC Research Notes*, 1(1), pp.1-5.

Leroy, P., Dessolin, S., Villageois, P., Moon, B. C., Friedman, J. M., Ailhaud, G., & Dani, C. (1996). Expression of ob gene in adipose cells: regulation by insulin. *Journal of Biological Chemistry*, 271(5).

Letai, A., Bassik, M.C., Walensky, L.D., Sorcinelli, M.D., Weiler, S. and Korsmeyer, S.J., (2002). Distinct BH3 domains either sensitize or activate mitochondrial apoptosis, serving as prototype cancer therapeutics. *Cancer Cell*, 2(3).

Ley, R., Ewings, K.E., Hadfield, K. and Cook, S.J., (2005). Regulatory phosphorylation of BIMBIM: sorting out the ERK from the JNK. *Cell Death and Differentiation*, 12(8).

Li, L.T., Jiang, G., Chen, Q., & Zheng, J.N. (2015). Ki67Ki67 is a promising molecular target in the diagnosis of cancer (Review). *Molecular Medicine Reports*, 11.

Li, S., Bouzar, C., Cottet-Rousselle, C., Zagotta, I., Lamarche, F., Wabitsch, M., Tokarska-Schlattner, M., Fischer-Posovszky, P., Schlattner, U. and Rousseau, D., (2016). Resveratrol inhibits lipogenesis of 3T3-L1 and SGBS cells by inhibition of insulin signaling and mitochondrial mass increase. *Biochimica et Biophysica Acta (BBA)-Bioenergetics*, 1857(6), 643-652.

Li, X., Yang, L., Li, J., Lin, L. and Zheng, G., (2021). A flavonoid-rich *Smilax china* L. extract prevents obesity by upregulating the adiponectin/adiponectin-receptor/AMPK signalling pathway and modulating the gut microbiota in mice. *Food & Function*, 12(13).

Li, Y., Rong, Y., Bao, L., Nie, B., Ren, G., Zheng, C., Amin, R., Arnold, R.D., Jeganathan, R.B. and Huggins, K.W., (2017). Suppression of adipocyte differentiation and lipid accumulation by stearidonic acid (SDA) in 3T3-L1 cells. *Lipids in health and disease*, 16(1), 1-10.

Liao, W., Nguyen, M.A., Yoshizaki, T., Favellyukis, S., Patsouris, D., Imamura, T., Verma, I.M. and Olefsky, J.M., (2007). Suppression of PPAR- $\gamma$  attenuates insulin-stimulated glucose uptake

by affecting both GLUT1 and GLUT4 in 3T3-L1 adipocytes. *American Journal of Physiology-Endocrinology and Metabolism*, 293(1).

Lillie, R. D., and Ashburn, L. L. (1943). Supersaturated solutions of fat stains in dilute isopropanol for demonstration of acute fatty degeneration not shown by Herxheimer's technique. *Arch Pathol*, 36, 432-440.

Liu, L., Zhou, M., Lang, H., Zhou, Y. and Mi, M., (2018). Dihydromyricetin enhances glucose uptake by inhibition of MEK/ERK pathway and consequent down-regulation of phosphorylation of PPAR $\gamma$  in 3T3-L1 cells. *Journal of Cellular and Molecular Medicine*, 22(2).

Liu, R.H., (2003). Health benefits of fruit and vegetables are from additive and synergistic combinations of phytochemicals. *The American Journal of Clinical Nutrition*, 78(3), pp.517S-520S.

Liu, Y.M., Lacorte, J.M., Viguerie, N., Poitou, C., Pelloux, V., Guy-Grand, B., Coussieu, C., Langin, D., Basdevant, A. and Clément, K., (2003). Adiponectin gene expression in subcutaneous adipose tissue of obese women in response to short-term very low-calorie diet and refeeding. *The Journal of Clinical Endocrinology & Metabolism*, 88(12).

Ludwig, D.S. and Sørensen, T.I., (2022). An integrated model of obesity pathogenesis that revisits causal direction. *Nature Reviews Endocrinology*, 18(5), pp.261-262.

Luo, Z., Murray, B.S., Ross, A.L., Povey, M.J., Morgan, M.R. and Day, A.J. (2012). Effects of pH on the ability of flavonoids to act as Pickering emulsion stabilizers. *Colloids and Surfaces B: Biointerfaces*, 92, pp.84-90.

Ma, Q., Cui, Y., Xu, S., Zhao, Y., Yuan, H. and Piao, G., (2018). Synergistic inhibitory effects of acacetin and 11 other flavonoids isolated from *Artemisia sacrorum* on lipid accumulation in 3T3-L1 Cells. *Journal of Agricultural and Food Chemistry*, 66(49), pp.12931-12940.

Mader, S., & Pantel, K. (2017). Liquid biopsy: current status and future perspectives. *Oncology research and treatment*, 40(7-8).

Maffei, M., Fei, H., Lee, G.H., Dani, C., Leroy, P., Zhang, Y., Proenca, R., Negrel, R., Ailhaud, G. and Friedman, J.M., (1995). Increased expression in adipocytes of ob RNA in mice with lesions of the hypothalamus and with mutations at the db locus. *Proceedings of the National Academy of Sciences*, 92(15).

Manach, C. and Donovan, J.L., (2004). Pharmacokinetics and metabolism of dietary flavonoids in humans. *Free radical research*, 38(8), pp.771-786.

Manning, B. D., and Cantley, L. C. (2007). AKT/PKB signaling: navigating downstream. *Cell*, 129(7).

Marcon, B.H., Shigunov, P., Spangenberg, L., Pereira, I.T., de Aguiar, A.M., Amorín, R., Rebelatto, C.K., Correa, A. and Dallagiovanna, B., (2019). Cell cycle genes are downregulated after adipogenic triggering in human adipose tissue-derived stem cells by regulation of mRNA abundance. *Scientific Reports*, 9(1), p.5611.

Martinez, L., Berenguer, M., Bruce, M. C., Le Marchand-Brustel, Y., and Govers, R. (2010). Rosiglitazone increases cell surface GLUT4 $GLUT4$  levels in 3T3-L1 adipocytes through an enhancement of endosomal recycling. *Biochemical Pharmacology*, 79(9).

Matson, J. P., & Cook, J. G. (2017). Cell cycle proliferation decisions: the impact of single cell analyses. *The FEBS journal*, 284(3), 362–375.

Matsuno, F., Chowdhury, S., Gotoh, T., Iwase, K., Matsuzaki, H., Takatsuki, K., Mori, M. and Takiguchi, M., (1996). Induction of the C/EBP beta gene by dexamethasone and glucagon in primary-cultured rat hepatocytes. *The Journal of Biochemistry*, 119(3).

Maurer, S., Harms, M. and Boucher, J., (2021). The colorful versatility of adipocytes: white-to-brown transdifferentiation and its therapeutic potential in humans. *The FEBS Journal*, 288(12), pp.3628-3646.

McKinsey Global Institute (2014) How the world could better fight obesity <http://www.mckinsey.com/industries/healthcare-systems-and-services/our-insights/how-the-world-could-better-fight-obesity>. Accessed on 21 December 2022.

McNay, E.C. and Pearson-Leary, J., (2020). GluT4 $GLUT4$  : A central player in hippocampal memory and brain insulin resistance. *Experimental neurology*, 323, p.113076.

Melzner, I., Scott, V., Dorsch, K., Fischer, P., Wabitsch, M., Brüderlein, S., Hasel, C. and Möller, P., (2002). Leptin gene expression in human preadipocytes is switched on by maturation-induced demethylation of distinct CpGs in its proximal promoter. *Journal of Biological Chemistry*, 277(47).

Mertens-Talcott, S.U., Talcott, S.T. and Percival, S.S., (2003). Low concentrations of quercetin and ellagic acid synergistically influence proliferation, cytotoxicity and apoptosis in MOLT-4 human leukemia cells–. *The Journal of nutrition*, 133(8), pp.2669-2674.

Miller, I., Min, M., Yang, C., Tian, C., Gookin, S., Carter, D. and Spencer, S.L., (2018). Ki67Ki67 is a graded rather than a binary marker of proliferation versus quiescence. *Cell Reports*, 24(5).

Miller, R.T., (2005). Ki-67 clone K-2: A useful marker of fat cells and lipoblasts. *Immunohistochemistry ProPath*. 1

Min, W., Wu, M., Fang, P., Yu, M., Shi, M., Zhang, Z., & Bo, P. (2018). Effect of baicalein on GLUT4GLUT4 translocation in adipocytes of diet-induced obese mice. *Cellular Physiology and Biochemistry*, 50(2), 426-436.

Mittal, B., (2019). Subcutaneous adipose tissue & visceral adipose tissue. *The Indian journal of medical research*, 149(5), p.571-122.

Mohajan, D. and Mohajan, H.K., (2023). Obesity and its related diseases: a new escalating alarming in global health. *Journal of Innovations in Medical Research*, 2(3), pp.12-23.

Moon, J., Do, H.J., Kim, O.Y. and Shin, M.J., (2013). Antiobesity effects of quercetin-rich onion peel extract on the differentiation of 3T3-L1 preadipocytes and the adipogenesis in high fat-fed rats. *Food and Chemical Toxicology*, 58.

Morimoto, H., Kondoh, K., Nishimoto, S., Terasawa, K., & Nishida, E. (2007). Activation of a C-terminal transcriptional activation domain of ERK5 by autophosphorylation. *Journal of Biological Chemistry*, 282(49).

Moskot, M., Jakóbkiewicz-Banecka, J., Smolińska, E., Piotrowska, E., Węgrzyn, G. and Gabig-Cimińska, M., (2015). Effects of flavonoids on expression of genes involved in cell cycle regulation and DNA replication in human fibroblasts. *Molecular and Cellular Biochemistry*, 407(1).

Naciri, M., Kuystermans, D., & Al-Rubeai, M. (2008). Monitoring pH and dissolved oxygen in mammalian cell culture using optical sensors. *Cytotechnology*, 57(3), 245-250.

Nagai, S., Matsumoto, C., Shibano, M. and Fujimori, K., (2018). Suppression of fatty acid and triglyceride synthesis by the flavonoid orientin through decrease of C/EBP $\delta$  expression and inhibition of PI3K/Akt-FOXO1 signaling in adipocytes. *Nutrients*, 10(2), p.130.



Nakao, Y., Yoshihara, H., & Fujimori, K. (2016). Suppression of very early stage of adipogenesis by baicalein, a plant-derived flavonoid through reduced Akt-C/EBP $\alpha$ -GLUT4GLUT4 signaling-mediated glucose uptake in 3T3-L1 adipocytes. *PLoS One*, 11(9).

Nerlov, C., (2007). The C/EBP family of transcription factors: a paradigm for interaction between gene expression and proliferation control. *Trends in Cell Biology*, 17(7).

Neumayer, G., Belzil, C., Gruss, O.J. and Nguyen, M.D., (2014). TPX2TPX2: of spindle assembly, DNA damage response, and cancer. *Cellular and Molecular Life Sciences*, 71(16).

Niu, G., Yin, S., Xie, S., Li, Y., Nie, D., Ma, L., Wang, X. and Wu, Y., (2011). Quercetin induces apoptosis by activating caspase-3 and regulating Bcl-2 and cyclooxygenase-2 pathways in human HL-60 cells. *Acta Biochim Biophys Sin*, 43(1).

Ntambi, J.M. and Young-Cheul, K., (2000). Adipocyte differentiation and gene expression. *The Journal of Nutrition*, 130(12).

O'Sullivan, S.E., Tarling, E.J., Bennett, A.J., Kendall, D.A. and Randall, M.D., (2005). Novel time-dependent vascular actions of  $\Delta$ 9-tetrahydrocannabinol mediated by peroxisome proliferator-activated receptor gamma. *Biochemical and Biophysical Research Communications*, 337(3).

O'Connor L, Strasser A, O'Reilly LA, Hausmann G, Adams JM, Cory S, Huang DC (1998). ["BimBIM: a novel member of the Bcl-2 family that promotes apoptosis"](#). *EMBO J*. 17 (2).

Oh, J.H., Karadeniz, F., Lee, J.I., Seo, Y., Jang, M.S. and Kong, C.S., (2020). Effect and comparison of luteolin and its derivative sodium luteolin-4'-sulfonate on adipogenic differentiation of human bone marrow-derived mesenchymal stem cells through AMPK-mediated PPAR $\gamma$  signaling. *Evidence-Based Complementary and Alternative Medicine*, 20.

Ortega, F.B., Sui, X., Lavie, C.J. and Blair, S.N., 2016, April. Body mass index, the most widely used but also widely criticized index: would a criterion standard measure of total body fat be a better predictor of cardiovascular disease mortality?. In *Mayo Clinic Proceedings* (Vol. 91, No. 4, pp. 443-455). Elsevier.

- Oteiza, P.I., Erlejman, A.G., Verstraeten, S.V., Keen, C.L. and Fraga, C.G., (2005). Flavonoid-membrane interactions: a protective role of flavonoids at the membrane surface?. *Clinical and Developmental Immunology*, 12(1), pp.19-25.
- Panche, A.N., Diwan, A.D. and Chandra, S.R., (2016). Flavonoids: an overview. *Journal of nutritional science*, 5, p.e47.
- Pant, R., Firmal, P., Shah, V. K., Alam, A., & Chattopadhyay, S. (2021). Epigenetic regulation of adipogenesis in development of metabolic syndrome. *Frontiers in Cell and Developmental Biology*,8.
- Park, B.H., Qiang, L. and Farmer, S.R., (2004). Phosphorylation of C/EBP beta at a consensus extracellular signal-regulated kinase/glycogen synthase kinase 3 site is required for the induction of adiponectin *adiponectin* gene expression during the differentiation of mouse fibroblasts into adipocytes. *Molecular and cellular biology*, 24(19).
- Payne, V. A., Au, W. S., Lowe, C. E., Rahman, S. M., Friedman, J. E., O'Rahilly, S., & Rochford, J. J. (2009). C/EBP transcription factors regulate SREBP1c *SREBP1c* gene expression during adipogenesis. *The Biochemical journal*, 425(1).
- Pei, Y., Otieno, D., Gu, I., Lee, S.O., Parks, J.S., Schimmel, K. and Kang, H.W., (2021). Effect of quercetin on nonshivering thermogenesis of brown adipose tissue in high-fat diet-induced obese mice. *The Journal of Nutritional Biochemistry*, 88.
- Peng, L., Wang, B. and Ren, P., (2005). Reduction of MTT by flavonoids in the absence of cells. *Colloids and Surfaces B: Biointerfaces*, 45(2), pp.108-111.
- Perera, R.S., Chen, L., Hart, D.J., Spector, T.D., Arden, N.K., Ferreira, M.L. and Radojčić, M.R. (2022), February. Effects of body weight and fat mass on back pain—direct mechanical or indirect through inflammatory and metabolic parameters? In *Seminars in Arthritis and Rheumatism* (Vol. 52, p. 151935). WB Saunders.
- Powers, A. D., & Palecek, S. P. (2012). Protein analytical assays for diagnosing, monitoring, and choosing treatment for cancer patients. *Journal of Healthcare Engineering*, 3(4).
- Pradhan, A.B., Bhuiya, S., Haque, L. and Das, S., (2018). Role of hydroxyl groups in the B-ring of flavonoids in stabilization of the Hoogsteen paired third strand of Poly (U). Poly (A)\* Poly (U) triplex. *Archives of biochemistry and biophysics*, 637, pp.9-20.

Premathilaka, R., Rashidinejad, A., Golding, M. and Singh, J., (2022). Oral delivery of hydrophobic flavonoids and their incorporation into functional foods: Opportunities and challenges. *Food Hydrocolloids*, p.107567.

Prillaman, M. (2023). The 'breakthrough' obesity drugs that have stunned researchers. *Nature*, 613(7942), pp.16-18.

Prusty, D., Park, B. H., Davis, K. E., & Farmer, S. R. (2002). Activation of MEK/ERK signaling promotes adipogenesis by enhancing peroxisome proliferator-activated receptor  $\gamma$  (PPAR $\gamma$ ) and C/EBP alpha gene expression during the differentiation of 3T3-L1 preadipocytes. *Journal of Biological Chemistry*, 277(48).

Pulito, C., Korita, E., Sacconi, A., Valerio, M., Casadei, L., Lo Sardo, F., Mori, F., Ferraiuolo, M., Grasso, G., Maidecchi, A., Lucci, J., Sudol, M., Muti, P., Blandino, G., & Strano, S. (2019). Dropwort-induced metabolic reprogramming restrains YAP/TAZ/TEAD oncogenic axis in mesothelioma. *Journal of Experimental & Clinical Cancer Research: CR*, 38(1).

Qin, X., Lu, Y., Peng, Z., Fan, S. and Yao, Y., (2018). Systematic chemical analysis approach reveals superior antioxidant capacity via the synergistic effect of flavonoid compounds in red vegetative tissues. *Frontiers in chemistry*, 6, p.9.

Rieusset, J., Andreelli, F., Auboeuf, D., Roques, M., Vallier, P., Riou, J.P., Auwerx, J., Laville, M. and Vidal, H., (1999). Insulin acutely regulates the expression of the peroxisome proliferator-activated receptor-gamma in human adipocytes. *Diabetes*, 48(4).

Riss, T. L., Moravec, R. A., Niles, A. L., Duellman, S., Benink, H. A., Worzella, T. J., and Minor, L. (2016). Cell viability assays. *Assay Guidance Manual [Internet]*.

Roberts, L. D., Virtue, S., Vidal-Puig, A., Nicholls, A. W., and Griffin, J. L. (2009). Metabolic phenotyping of a model of adipocyte differentiation. *Physiological Genomics*, 39(2), 109-119.

Roesler, A. and Kazak, L., (2020). UCP1-independent thermogenesis. *Biochemical Journal*, 477(3), pp.709-725.

Roffey, D.M., Ashdown, L.C., Dornan, H.D., Creech, M.J., Dagenais, S., Dent, R.M. and Wai, E.K. (2011). Pilot evaluation of a multidisciplinary, medically supervised, nonsurgical weight loss program on the severity of low back pain in obese adults. *The Spine Journal*, 11(3), pp.197-204.

Rohrberg, J., Corella, A., Taileb, M., Kilinc, S., Jokisch, M.L., Camarda, R., Zhou, A., Balakrishnan, S., Chang, A.N. and Goga, A., (2018). MYC dysregulates mitotic spindle function creating a dependency on TPX2/TPX2. Available at SSRN 3189389. Accessed on 10 February 2022

Romieu, I., Dossus, L., Barquera, S., Blottière, H.M., Franks, P.W., Gunter, M., Hwalla, N., Hursting, S.D., Leitzmann, M., Margetts, B. and Nishida, C., 2017. Energy balance and obesity: what are the main drivers?. *Cancer Causes & Control*, 28(3), pp.247-258.

Rosen, E.D., Hsu, C.H., Wang, X., Sakai, S., Freeman, M.W., Gonzalez, F.J. and Spiegelman, B.M., (2002). C/EBP alpha induces adipogenesis through PPAR $\gamma$ : a unified pathway. *Genes & Development*, 16(1).

Rosen, E.D., Sarraf, P., Troy, A.E., Bradwin, G., Moore, K., Milstone, D.S., Spiegelman, B.M. and Mortensen, R.M., (1999). PPAR gamma/PPAR *gamma* is required for the differentiation of adipose tissue in vivo and in vitro. *Molecular Cell*, 4(4).

Rosenwald, M. and Wolfrum, C., (2014). The origin and definition of brite versus white and classical brown adipocytes. *Adipocyte*, 3(1), pp.4-9.

Rufino, A.T., Costa, V.M., Carvalho, F. and Fernandes, E., 2021. Flavonoids as antiobesity agents: A review. *Medicinal Research Reviews*, 41(1).

Ruijtenberg, S. and van den Heuvel, S., (2016). Coordinating cell proliferation and differentiation: Antagonism between cell cycle regulators and cell type-specific gene expression. *Cell cycle*, 15(2), pp.196-212

Ruijtenberg, S. and van den Heuvel, S., (2016). Coordinating cell proliferation and differentiation: Antagonism between cell cycle regulators and cell type-specific gene expression. *Cell cycle*, 15(2), pp.196-212.

Rupasinghe, H.P., (2020). Special Issue "flavonoids and their disease prevention and treatment potential": Recent advances and future perspectives. *Molecules*, 25(20).

Ryan, D., Barquera, S., Barata Cavalcanti, O. and Ralston, J., (2021). The global pandemic of overweight and obesity: addressing a twenty-first century multifactorial disease. In *Handbook of global health* (pp. 739-773). Cham: Springer International Publishing.

Ryan, J. and Letai, A., (2013). BH3 profiling in whole cells by fluorimeter or FACS. *Methods*, 61(2).

Saely, C.H., Geiger, K. and Drexel, H., (2012). Brown versus white adipose tissue: a mini-review. *Gerontology*, 58(1), pp.15-23.

Sahu, A.K. and Mishra, A.K., (2022). Photophysical Behavior of Plant Flavonols Galangin, Kaempferol, Quercetin, and Myricetin in Homogeneous Media and the DMPC Model Membrane: Unveiling the Influence of the B-Ring Hydroxylation of Flavonols. *The Journal of Physical Chemistry B*, 126(15), pp.2863-2875.

Salam, N.K., Huang, T.H.W., Kota, B.P., Kim, M.S., Li, Y. and Hibbs, D.E., (2008). Novel PPAR-gamma agonists identified from a natural product library: A virtual screening, induced-fit docking and biological assay study. *Chemical Biology & Drug Design*, 71(1).

Sarantopoulos, C.N., Banyard, D.A., Ziegler, M.E., Sun, B., Shaterian, A. and Widgerow, A.D., (2018). Elucidating the preadipocyte and its role in adipocyte formation: a comprehensive review. *Stem Cell Reviews and Reports*, 14, pp.27-42.

Sarjeant, K. and Stephens, J.M., 2012. Adipogenesis. *Cold Spring Harbor perspectives in biology*, 4(9), p.a008417.

Sastry, K.S., Ibrahim, W.N. and Chouchane, A.I. (2020). Multiple signaling pathways converge on proapoptotic protein BADBAD to promote survival of melanocytes. *FASEB J.* 34(11).

Scarpace, P.J. and Matheny, M., (1998). Leptin induction of UCP1/UCP1 gene expression is dependent on sympathetic innervation. *American Journal of Physiology-Endocrinology and Metabolism*, 275(2).

Schwingshackl, L., Zähringer, J., Beyerbach, J., Werner, S.S., Nagavci, B., Hesecker, H., Koletzko, B., Meerpohl, J.J. and International Union of Nutritional Sciences (IUNS) Task force on Dietary Fat Quality, (2021). A scoping review of current guidelines on dietary fat and fat quality. *Annals of Nutrition and Metabolism*, 77(2), pp.65-82.

Scott, M. A., Nguyen, V. T., Levi, B., & James, A. W. (2011). Current methods of adipogenic differentiation of mesenchymal stem cells. *Stem cells and development*, 20(10), 1793-1804.

Seidell, J.C. and Halberstadt, J., (2015). The global burden of obesity and the challenges of prevention. *Annals of Nutrition and Metabolism*, 66(Suppl. 2), pp.7-12.

Seo, Y.S., Kang, O.H., Kim, S.B., Mun, S.H., Kang, D.H., Yang, D.W., Choi, J.G., Lee, Y.M., Kang, D.K., Lee, H.S. and Kwon, D.Y., (2015). Quercetin prevents adipogenesis by regulation of

transcriptional factors and lipases in OP9 cells. *International Journal of Molecular Medicine*, 35(6).

Shearin, A.L., Monks, B.R., Seale, P. and Birnbaum, M.J., (2016). Lack of AKT in adipocytes causes severe lipodystrophy. *Molecular metabolism*, 5(7).

Shepherd, P.R. and Kahn, B.B. (1999). Glucose transporters and insulin action--implications for insulin resistance and diabetes mellitus. *N Engl J Med*. 341(4).

Shimizu, M., Li, J., Inoue, J., & Sato, R. (2015). Quercetin represses apolipoprotein B expression by inhibiting the transcriptional activity of C/EBP beta. *PloS one*, 10(4).

Shinde, A.B., Song, A. and Wang, Q.A., (2021). Brown adipose tissue heterogeneity, energy metabolism, and beyond. *Frontiers in Endocrinology*, 12.

Shipp, S.L., Cline, M.A. and Gilbert, E.R., (2016). Promotion of adipogenesis by neuropeptide Y during the later stages of chicken preadipocyte differentiation. *Physiological Reports*, 4(21).

Shishtar, E., Rogers, G.T., Blumberg, J.B., Au, R. and Jacques, P.F., (2020). Long-term dietary flavonoid intake and change in cognitive function in the Framingham Offspring cohort. *Public health nutrition*, 23(9), pp.1576-1588.

Siao, A.C., Lin, Y.Y., Shih, L.J., Tsuei, Y.W., Chuu, C.P., Kuo, Y.C. and Kao, Y.H., (2020). Endothelin-1 stimulates preadipocyte growth via the PKC, STAT3, AMPK, c-JUN, ERK, sphingosine kinase, and sphingomyelinase pathways. *American Journal of Physiology-Cell Physiology*, 319(5).

Sobecki, M., Mrouj, K., Camasses, A., Parisis, N., Nicolas, E., Llères, D., Gerbe, F., Prieto, S., Krasinska, L., David, A., Eguren, M., Birling, M. C., Urbach, S., Hem, S., Déjardin, J., Malumbres, M., Jay, P., Dulic, V., Lafontaine, D., Feil, R. and Fisher, D. (2016). The cell proliferation antigen Ki-67 organises heterochromatin. *eLife*, 5.

Son, T.G., Camandola, S. and Mattson, M.P., (2008). Hormetic dietary phytochemicals. *Neuromolecular medicine*, 10, pp.236-246.

Song, D., Cheng, L., Zhang, X., Wu, Z. and Zheng, X., (2019). The modulatory effect and the mechanism of flavonoids on obesity. *Journal of Food Biochemistry*, 43(8),12954.

- Song, G., Ouyang, G. and Bao, S., (2005). The activation of Akt/PKB signalling pathway and cell survival. *Journal of Cellular and Molecular Medicine*, 9(1), 59-71.
- Song, Z., Xiaoli, A.M. and Yang, F., (2018). Regulation and metabolic significance of de novo lipogenesis in adipose tissues. *Nutrients*, 10(10), p.1383.
- Sperelakis, N. (Ed.). (2001). *Cell physiology sourcebook: a molecular approach*. Elsevier, London.
- Stark, G.R. and Taylor, W.R., (2004). Analyzing the G2/M checkpoint. *Checkpoint Controls and Cancer: Volume 1: Reviews and Model Systems*, pp.51-82.
- Stern, J.H., Rutkowski, J.M. and Scherer, P.E., (2016). Adiponectin, leptin, and fatty acids in the maintenance of metabolic homeostasis through adipose tissue crosstalk. *Cell Metabolism*, 23(5).
- Strable, M. S., & Ntambi, J. M. (2010). Genetic control of de novo lipogenesis: role in diet-induced obesity. *Critical Reviews in Biochemistry and Molecular Biology*, 45(3), 199–214.
- Su, S.C., Chiang, C.F., Hsieh, C.H., Lu, G.H., Liu, J.S., Shieh, Y.S., Hung, Y.J. and Lee, C.H., (2021). Growth arrest-specific 6 modulates adiponectin expression and insulin resistance in adipose tissue. *Journal of Diabetes Investigation*, 12(4).
- Sun, Y., Liu, W. Z., Liu, T., Feng, X., Yang, N., & Zhou, H. F. (2015). Signaling pathway of MAPK/ERK in cell proliferation, differentiation, migration, senescence and apoptosis. *Journal of Receptors and Signal Transduction*, 35(6).
- Suwaki, N., Masuyama, H., Masumoto, A., Takamoto, N. and Hiramatsu, Y., (2007). Expression and potential role of peroxisome proliferator-activated receptor  $\gamma$  in the placenta of diabetic pregnancy. *Placenta*, 28(4).
- Swick, J.C., (2011). *Effect of the flavonoid quercetin on adipocytes*. scholarworks.umass.edu
- Syed, N.D., M Adhami, V., Imran Khan, M., & Mukhtar, H. (2013). Inhibition of Akt/mTOR signaling by the dietary flavonoid fisetin. *Anti-Cancer Agents in Medicinal Chemistry (Formerly Current Medicinal Chemistry-Anti-Cancer Agents)*, 13(7).

Takahashi, Y. and Ide, T. (2008). Effects of soy protein and isoflavone on hepatic fatty acid synthesis and oxidation and mRNA expression of uncoupling proteins and peroxisome proliferator-activated receptor gamma in adipose tissues of rats. *J Nutr Biochem*. 10.1016

Talorete, T.P., Bouaziz, M., Sayadi, S. and Isoda, H., (2006). Influence of medium type and serum on MTT reduction by flavonoids in the absence of cells. *Cytotechnology*, 52, pp.189-198.

Teixeira, A., Eiras-Dias, J., Castellarin, S.D. and Gerós, H., (2013). Berry phenolics of grapevine under challenging environments. *International journal of molecular sciences*, 14(9), pp.18711-18739.

Tews, D., Brenner, R. E., Siebert, R., Debatin, K. M., Fischer-Posovszky, P., & Wabitsch, M. (2022). 20 Years with SGBS cells—a versatile in vitro model of human adipocyte biology. *International Journal of Obesity*, 46(11), pp.1939-1947.

Tews, D., Pula, T., Funcke, J.B., Jastroch, M., Keuper, M. and Debatin, K.M., (2019). Elevated UCP1/UCP1 levels are sufficient to improve glucose uptake in human white adipocytes. *Redox Biology* 26:101286.

Thilakarathna, S.H. and Rupasinghe, H.V., (2013). Flavonoid bioavailability and attempts for bioavailability enhancement. *Nutrients*, 5(9), pp.3367-3387.

Tolomeo, M., & Grimaudo, S. (2020). The "Janus" Role of C/EBPs Family Members in Cancer Progression. *International Journal of Molecular Sciences*, 21(12).

Trayhurn, P., (2022). Adipokines: inflammation and the pleiotropic role of white adipose tissue. *British Journal of Nutrition*, 127(2), pp.161-164.

Tzeng, C.W., Yen, F.L., Wu, T.H., Ko, H.H., Lee, C.W., Tzeng, W.S. and Lin, C.C., (2011). Enhancement of dissolution and antioxidant activity of kaempferol using a nanoparticle engineering process. *Journal of agricultural and food chemistry*, 59(9), pp.5073-5080.

Ushijima, T., Okazaki, K., Tsushima, H., Ishihara, K., Doi, T. and Iwamoto, Y., (2014). CCAAT/enhancer binding protein  $\beta$  regulates expression of indian hedgehog during chondrocytes differentiation. *PloS one*, 9(8).



Van Marken Lichtenbelt, W.D., Vanhomerig, J.W., Smulders, N.M., Drossaerts, J.M., Kemerink, G.J., Bouvy, N.D., Schrauwen, P., Teule, G.J. (2009). Cold-activated brown adipose tissue in healthy men. *N. Engl. J. Med.* 360:1500–1508.

Van Tonder, A., Joubert, A.M. and Cromarty, A.D., (2015). Limitations of the 3-(4, 5-dimethylthiazol-2-yl)-2, 5-diphenyl-2H-tetrazolium bromide (MTT) assay when compared to three commonly used cell enumeration assays. *BMC research notes*, 8, pp.1-10.

Varinli, H., Osmond-McLeod, M. J., Molloy, P. L., & Vallotton, P. (2015). LipiD-Quant: a novel method to quantify lipid accumulation in live cells [S]. *Journal of lipid research*, 56(11), 2206-2216.

Vernarelli, J. A., & Lambert, J. D. (2017). Flavonoid intake is inversely associated with obesity and C-reactive protein, a marker for inflammation, in US adults. *Nutrition & Diabetes*, 7(5), e276–.

Viais, R., Fariña-Mosquera, M., Villamor-Payà, M., Watanabe, S., Palenzuela, L., Lacasa, C., & Lüders, J. (2021). Augmin deficiency in neural stem cells causes p53-dependent apoptosis and aborts brain development. *Elife*, 10, e67989.

Victor, I. A., Andem, A. B., Archibong, I. A., & Iwok, E. O. (2020). Interplay between cell proliferation and cellular differentiation: A mutually exclusive paradigm. *Global Scientific Journals GSJ*, 8(1).

Vidal-Puig, A.J., Considine, R.V., Jimenez-Liñan, M., Werman, A., Pories, W.J., Caro, J.F. and Flier, J.S., (1997). Peroxisome proliferator-activated receptor gene expression in human tissues. Effects of obesity, weight loss, and regulation by insulin and glucocorticoids. *The Journal of clinical investigation*, 99(10).

Wabitsch, M., Brenner, R.E., Melzner, I., Braun, M., Möller, P., Heinze, E., Debatin, K.M. and Hauner, H., (2001). Characterization of a human preadipocyte cell strain with high capacity for adipose differentiation. *International Journal of Obesity*, 25(1).

Wafer, R., Tandon, P. and Minchin, J.E., (2017). The role of peroxisome proliferator-activated receptor gamma (PPARG) in adipogenesis: Applying knowledge from the fish aquaculture industry to biomedical research. *Frontiers in Endocrinology*, 8, 102.

- Wagoner, B., Hausman, D. B., & Harris, R. B. (2006). Direct and indirect effects of leptin on preadipocyte proliferation and differentiation. *American Journal of Physiology-Regulatory, Integrative and Comparative Physiology*, 290(6).
- Waldén, T.B., Hansen, I.R., Timmons, J.A., Cannon, B. and Nedergaard, J., (2012). Recruited vs. nonrecruited molecular signatures of brown, “brite,” and white adipose tissues. *American journal of physiology-endocrinology and metabolism*, 302(1), pp.E19-E31.
- Wali, J.A., Jarzebska, N., Raubenheimer, D., Simpson, S.J., Rodionov, R.N. and O’Sullivan, J.F., (2020). Cardio-metabolic effects of high-fat diets and their underlying mechanisms—a narrative review. *Nutrients*, 12(5), p.1505.
- Wang, B., Jenkins, J. R., & Trayhurn, P. (2005). Expression and secretion of inflammation-related adipokines by human adipocytes differentiated in culture: integrated response to TNF- $\alpha$ . *American Journal of Physiology-Endocrinology and Metabolism*. 12.
- Wang, B., Wood, I. S., & Trayhurn, P. (2008). Hypoxia induces leptin gene expression and secretion in human preadipocytes: differential effects of hypoxia on adipokine expression by preadipocytes. *Journal of Endocrinology*, 198(1).
- Wang, J., Ge, J., Cao, H., Zhang, X., Guo, Y., Li, X., Xia, B. and Shi, X. E. (2019). Leptin promotes white adipocyte browning by inhibiting the Hh signaling pathway. *Cells*, 8(4).
- Wang, L., Wang, S., Shi, Y., Li, R., Günther, S., Ong, Y.T., Potente, M., Yuan, Z., Liu, E. and Offermanns, S., (2020). YAP and TAZ protect against white adipocyte cell death during obesity. *Nature Communications*, 11(1).
- Wang, P., Henning, S. M., & Heber, D. (2010). Limitations of MTT and MTS-based assays for measurement of antiproliferative activity of green tea polyphenols. *PloS one*, 5(4), e10202.
- Wang, S., Zhang, Y., Xu, Q., Yuan, X., Dai, W., Shen, X., (2018). The differentiation of preadipocytes and gene expression related to adipogenesis in ducks. *Anasplatyrhynchos. PLoS ONE* 13(5)
- Wang, X.X., Liu, G.Y., Yang, Y.F., Wu, X.W., Xu, W. and Yang, X.W., (2017). Intestinal absorption of triterpenoids and flavonoids from *Glycyrrhizae radix et rhizoma* in the human Caco-2 monolayer cell model. *Molecules*, 22(10), p.1627.

Weems, J., & Olson, A. L. (2011). Class II histone deacetylases limit GLUT4GLUT4 gene expression during adipocyte differentiation. *Journal of Biological Chemistry*, 286(1).

WHO, (2022). *Obesity causes cancer and is major determinant of disability and death, warns New who report* (no date) World Health Organization. World Health Organization. Available at: <https://www.who.int/europe/news/item/03-05-2022-obesity-causes-cancer-and-is-major-determinant-of-disability-and-death--warns-new-who-report> (Accessed: June17, 2022).

Willett, W.C., (1998). Is dietary fat a major determinant of body fat?. *The American journal of clinical nutrition*, 67(3), pp.556S-562S.

Willett, W.C., Sacks, F., Trichopoulou, A., Drescher, G., Ferro-Luzzi, A., Helsing, E. and Trichopoulos, D., (1995). Mediterranean diet pyramid: a cultural model for healthy eating. *The American journal of clinical nutrition*, 61(6), pp.1402S-1406S.

Windmueller, R., Leach, J.P., Babu, A., Zhou, S., Morley, M.P., Wakabayashi, A., Petrenko, N.B., Viatour, P. and Morrissey, E.E., (2020). Direct comparison of mononucleated and binucleated cardiomyocytes reveals molecular mechanisms underlying distinct proliferative competencies. *Cell reports*, 30(9), pp.3105-3116.

Winterbone, M.S., Tribolo, S., Needs, P.W., Kroon, P.A. and Hughes, D.A., (2009). Physiologically relevant metabolites of quercetin have no effect on adhesion molecule or chemokine expression in human vascular smooth muscle cells. *Atherosclerosis*, 202(2), pp.431-438.

Withrow, D. and Alter, D.A., 2011. The economic burden of obesity worldwide: a systematic review of the direct costs of obesity. *Obesity reviews*, 12(2), pp.131-141.

Wong, C. P., Kaneda, T., and Morita, H. (2014). Plant natural products as an anti-lipid droplets accumulation agent. *Journal of natural medicines*, 68(2), 253-266.

Wong, M.C., McCarthy, C., Fearnbach, N., Yang, S., Shepherd, J. and Heymsfield, S.B., (2022). Emergence of the obesity epidemic: 6-decade visualization with humanoid avatars. *The American journal of clinical nutrition*, 115(4), pp.1189-1193.

Wong, S.P., Li, J., Shen, P., Gong, Y., Yap, S.P. and Yong, E.L., (2007). Ultrasensitive cell-based bioassay for the measurement of global estrogenic activity of flavonoid mixtures revealing additive, restrictive, and enhanced actions in binary and higher order combinations. *Assay and Drug Development Technologies*, 5(3), pp.355-362.

Wu, X., Sakharkar, M.K., Wabitsch, M. and Yang, J., (2020). Effects of sphingosine-1-phosphate on cell viability, differentiation, and gene expression of adipocytes. *International Journal of Molecular Sciences*, 21(23), p.9284.

Wu, Z., Xie, Y., Morrison, R.F., Bucher, N.L. and Farmer, S.R., (1998). PPARgamma induces the insulin-dependent glucose transporter GLUT4GLUT4 in the absence of C/EBPalpha during the conversion of 3T3 fibroblasts into adipocytes. *The Journal of clinical investigation*, 101(1).

Xia, K., Xue, H., Dong, D., Zhu, S., Wang, J., Zhang, Q., Hou, L., Chen, H., Tao, R., Huang, Z., Fu, Z., Chen, Y. G., & Han, J. D. (2006). Identification of the proliferation/differentiation switch in the cellular network of multicellular organisms. *PLoS Computational Biology*, 2(11).

Xia, Y., Xu, R. and Jiang, C., (2022). The Research Progress on Cocrystals of Flavonoids. *Open Access Library Journal*, 9(1), pp.1-18.

Xu, Z., You, W., Liu, J., Wang, Y. and Shan, T., (2020). Elucidating the regulatory role of melatonin in brown, white, and beige adipocytes. *Advances in Nutrition*, 11(2), pp.447-460.

Yadav, B.K., Khursheed, A.T.I.F. and Singh, R.D., (2019). Cocrystals: A complete review on conventional and novel methods of its formation and its evaluation. *Asian J. Pharm. Clin. Res*, 12(7), pp.68-74.

Yang, H.C., Deleuze, S., Zuo, Y., Potthoff, S.A., Ma, L.J. and Fogo, A.B., (2009). The PPAR gammaPPAR gamma agonist pioglitazone ameliorates aging-related progressive renal injury. *Journal of the American Society of Nephrology*, 20(11).

Yang, W., Yang, C., Luo, J., Wei, Y., Wang, W., & Zhong, Y. (2018). AdiponectinAdiponectin promotes preadipocyte differentiation via the PPAR gammaPPAR gamma pathway. *Molecular Medicine Reports*, 17(1).

Yang, Z.Z., Tschopp, O., Baudry, A., Duemmler, B., Hynx, D. and Hemmings, B.A., (2004). Physiological functions of protein kinase B/Akt. *Biochemical Society Transactions*, 32(2).

Yeh, W. C., Cao, Z., Classon, M., & McKnight, S. L. (1995). Cascade regulation of terminal adipocyte differentiation by three members of the C/EBP family of leucine zipper proteins. *Genes & Development*, 9(2).

Yeo, C.R., Agrawal, M., Hoon, S., Shabbir, A., Shrivastava, M.K., Huang, S., Khoo, C.M., Chhay, V., Yassin, M.S., Tai, E.S. and Vidal-Puig, A., (2017). SGBS cells as a model of human adipocyte browning: A comprehensive comparative study with primary human white subcutaneous adipocytes. *Scientific reports*, 7(1), 1-12.

Yin, M., Zhang, P., Yu, F., Zhang, Z., Cai, Q., Lu, W., Li, B., Qin, W., Cheng, M., Wang, H. and Gao, H., (2017). Grape seed procyanidin B2 ameliorates hepatic lipid metabolism disorders in db/db mice. *Molecular Medicine Reports*, 16(3).

Ying, T. and Simmons, R.A., (2021). The role of adipocyte precursors in development and obesity. *Frontiers in Endocrinology*, 11, p.613606.

Yokomori, N., Tawata, M., & Onaya, T. (1999). DNA demethylation during the differentiation of 3T3-L1 cells affects the expression of the mouse GLUT4 *GLUT4* gene. *Diabetes*, 48(4).

Yuan, J, and Kroemer, G. (2010). Alternative cell death mechanisms in development and beyond. *Genes Dev* 24.

Zhang, H.W., Hu, J.J., Fu, R.Q., Liu, X., Zhang, Y.H., Li, J., Liu, L., Li, Y.N., Deng, Q., Luo, Q.S. and Ouyang, Q., (2018). Flavonoids inhibit cell proliferation and induce apoptosis and autophagy through downregulation of PI3K mediated PI3K/AKT/mTOR/p70S6K/ULK signaling pathway in human breast cancer cells. *Scientific Reports*, 8(1).

Zhang, S., Yang, X. and Morris, M.E., (2004). Combined effects of multiple flavonoids on breast cancer resistance protein (ABCG2)-mediated transport. *Pharmaceutical Research*, 21(7), pp.1263-1273.

Zhang, X., Heckmann, B. L., and Liu, J. (2013). Studying lipolysis in adipocytes by combining siRNA knockdown and adenovirus-mediated overexpression approaches. In *Methods in cell biology* (Vol. 116, pp. 83-105). Academic Press.

Zhang, X., Li, X., Fang, H., Guo, F., Li, F., Chen, A. and Huang, S. (2019). Flavonoids as inducers of white adipose tissue browning and thermogenesis: signalling pathways and molecular triggers. *Nutrition & Metabolism*, 16(1).

Zhang, X., Li, X., Fang, H., Guo, F., Li, F., Chen, A. and Huang, S., (2019). Flavonoids as inducers of white adipose tissue browning and thermogenesis: signalling pathways and molecular triggers. *Nutrition & metabolism*, 16, pp.1-15.

Zhang, Z., Li, D., Luo, C., Huang, C., Qiu, R., Deng, Z. and Zhang, H., (2019). Cocrystals of natural products: Improving the dissolution performance of flavonoids using betaine. *Crystal Growth & Design*, 19(7), pp.3851-3859.

Zhao, L., Zheng, M., Cai, H., Chen, J., Lin, Y., Wang, F., Wang, L., Zhang, X. and Liu, J., (2023). The activity comparison of six dietary flavonoids identifies that luteolin inhibits 3T3-L1 adipocyte differentiation through reducing ROS generation. *The Journal of Nutritional Biochemistry*, 112, p.109208.

Zhong, P., Zeng, H., Huang, M., Fu, W. and Chen, Z., (2022). Efficacy and safety of once-weekly semaglutide in adults with overweight or obesity: A meta-analysis. *Endocrine*, 75(3), pp.718-724.

Zhu, L., Ma, J., Mu, R., Zhu, R., Chen, F., Wei, X., Shi, X., Zang, S. and Jin, L., (2018). Bone morphogenetic protein 7 promotes odontogenic differentiation of dental pulp stem cells in vitro. *Life Sciences*, 202, pp.175-181.

Zirlin, A. (1974). *Prevention of crystallization of sparingly soluble flavonoids in food systems*. FOR IND RES CIR Ltd CENTRE. U.S. Patent 3,832,475.